

# THE LINAC4 PROJECT

A. M. Lombardi for the LINAC4 team , CERN, Geneva, Switzerland

## Abstract

Linac4 is a normal conducting, 160 MeV H<sup>-</sup> ion accelerator that is being constructed within the scope of the LHC injectors upgrade project. Linac4 will be connected to the Proton Synchrotron Booster (PSB) during the next long LHC shut-down and it will replace the current 50 MeV hadron linac, Linac2. Linac4 is presently being commissioned, with the aim of achieving the final energy at the end of the year. A test of the injection chicane and a reliability run will follow. The beam commissioning, in steps of increasing energy, has been prepared by an extended series of studies and interlaced with phases of installation. In this paper we will detail the beam dynamics challenges and we will report on the commissioning results.

ject. A sketch of Linac4 and a detailed description of the layout and beam dynamics can be found in [1,2].

The pre-injector includes a source followed by a Low Energy Beam Transport at 45 keV, a Radio Frequency Quadrupole which accelerates the beam to 3MeV and a Medium Energy Beam Transport line (MEBT). The MEBT, 3.6 m in length, houses a fast chopper with the purpose of removing selected micro-bunches in the 352 MHz sequence and therefore avoid losses at capture in the CERN PSB (1MHz). Presently the preferred scheme envisages to chop out 133 bunches over 352 with a resulting average current reduced by 40%. The beam is then further accelerated to 50 MeV by a conventional Drift Tube Linac (DTL) equipped with Permanent Magnet Quadrupoles (PMQ), to 100 MeV by a Cell-Coupled Drift Tube Linac (CCDTL) and to 160 MeV by a  $\pi$ -mode structure (PIMS). The focusing after 100 MeV is provided by Electromagnetic Quadrupoles (EMQ) whereas between 50 and 100 MeV by a combination of PMQs and EMQs. The nominal beam delivered by Linac4 consist of an H-pulse 400 $\mu$ sec in duration and with peak current during

## INTRODUCTION

Linac4 is a 160 MeV H<sup>-</sup> linear accelerator presently under construction at CERN. It will replace the present 50 MeV proton Linac2 as injector of the CERN PS Booster, as a first step of the LHC Injector Upgrade pro-

| LINAC4 machine layout- 352MHz |                 |                    |               |                    |                         |
|-------------------------------|-----------------|--------------------|---------------|--------------------|-------------------------|
| Pre-injector (9m)             |                 | DTL (19m)          |               | CCDTL (25m)        | II-mode (23m)           |
| 3MeV                          |                 | 50 MeV             |               | 100 MeV            | 160 MeV                 |
| SOURCE                        | RFQ             | 3 Tanks            |               | <u>7 Modules</u>   | 12 Modules              |
| Plasma Generator              | CHOPPER LINE    | 3 Klystrons : 5 MW |               | 7 Klystrons : 7 MW | 8 Klystrons: 12MW       |
| Extraction                    | 11 EMQ          | 1 EMQ              |               | 7 EMQ + 14 PMQ     | 12 EMQ                  |
| e-Dump                        | 3 Cavities      | 114 PMQ            |               | 7 EMQ + 14 PMQ     | 12 steerers             |
| LEBT                          | 2 Chopper units | 2 steerers         |               | 7 steerers         |                         |
| 2 solenoids                   | In-line dump    |                    |               |                    |                         |
| Pre chopper                   |                 |                    |               |                    |                         |
| Beam Commissioning stages     |                 |                    |               |                    |                         |
| 45 keV                        | 3 MeV           | 12 MeV             | 50 MeV        | 105 MeV            | 160 MeV                 |
| Not yet the final source      | Octobre2013     | August 2014        | November 2015 | June 2016          | Octobre 2016 (foreseen) |

Figure 1: Layout of Linac4 and key stages of the beam commissioning.

## THE ESS ACCELERATOR

Håkan Danared, Mohammad Eshraqi and Morten Jensen,  
European Spallation Source, Lund, Sweden

### *Abstract*

The European Spallation Source, ESS, is now in construction in Lund, Sweden. It will be a long-pulse spallation source, using a 2 GeV superconducting proton linac to deliver a 5 MW beam onto a rotating, helium-gas-cooled tungsten target. ESS is a partnership between, at present, 11 European nations. According to current planning, the accelerator will be ready for beam in 2019, and by 2023 ESS will start operating as a user facility. This paper reviews the current status of the accelerator project.

### INTRODUCTION

Construction work at the ESS site started in the summer of 2014, and now, two years later, the accelerator tunnel is cast, the front-end building, klystron gallery and cold-box building are nearing completion, and piling for the target building is in progress. Work on instrument halls and laboratory and office buildings has begun or will begin in the near future.

At the same time, accelerator, target and neutron-instrument hardware is being designed, prototyped and built at the more than 100 partner institutions around Europe that will deliver in-kind contributions to ESS.

One of the top-level parameters of the ESS project [1] is the 5 MW average beam power. This will be achieved with a 62.5 mA peak beam current at 2 GeV energy, a 14 Hz pulse-repetition rate and a 2.86 ms pulse length.

This beam will hit a spallation target made from tungsten. It is a wheel with 36 sectors, rotating so that consecutive beam pulses will hit adjacent sectors. The wheel is cooled by gaseous helium.

The design of moderators and reflectors is essential for the performance of the neutron source. This design has gone through successive generations. An optimized configuration together with the long-pulse concept gives an unprecedented neutron brightness, and ESS will in total be up to 100 times more powerful than existing neutron sources.

There will be 16 neutron instruments built within the 1,843 M€ construction budget of ESS (plus another 90 M€ from the Swedish government for infrastructure), and another six instruments are included in the complete facility.

Before all instruments are built, however, ESS is expected to start operating as a user facility in 2023.

### IN-KIND

A major fraction of the linac hardware is provided as in-kind contributions from accelerator laboratories across Europe or in collaboration with institutions in the host countries Sweden and Denmark that have agreed to provide all their funding as cash. Exceptions are mainly expensive, purely commercial equipment such as cryo

plants and RF sources, where there is little academic interest for a potential in-kind partner but a substantial economic risk.

In this in-kind model, ESS in Lund is responsible for the overall design of the accelerator, largely expressed as requirement documents in several levels down to individual work packages. Detailed design, prototyping and manufacturing are then made at the partner laboratories, while ESS in Lund monitors progress through earned-value management and runs regular reviews of work packages and work units. When components arrive to the site, also a substantial fraction of the installation work will be done by in-kind labour. Continuous knowledge transfer during the course of the project is evidently important, since ESS will eventually take full ownership and responsibility of the facility.

Currently, work on the accelerator is under way at 23 partner institutions in 10 countries. The value of this work represents a little above 50% of the 510 M€ accelerator construction budget.

In-kind partners and their main contributions are: Aarhus University: Beam delivery system; Atomki, Debrecen: RF local protection system; University of Bergen: Ion source expertise; CEA Saclay: RFQ, elliptical cavities, cryomodules, beam diagnostics; Cockcroft Institute, Daresbury: Target imaging; DESY, Hamburg: Beam diagnostics; Elettra, Trieste: Spoke RF power, beam diagnostics, magnets, magnet power converters; ESS-Bilbao: MEBT, warm-linac RF, beam diagnostics; University of Huddersfield: RF distribution; IFJ PAN, Krakow: Manpower for installation and tests; INFN Catania: Ion source, LEBT; INFN Legnaro: DTL; INFN Milan: Medium-beta cavities; IPN Orsay: Spoke cavities, cryomodules, cryo distribution; Lodz University of Technology: LLRF; Lund University: LLRF, test stand; NCBJ, Swierk: LLRF, gamma blockers; University of Oslo: Beam diagnostics; STFC Daresbury Laboratory: High-beta cavities, vacuum; Tallinn University of Technology: Power converters; Uppsala University: Test stand; Warsaw University of Technology: LLRF, phase reference line; Wrocław University of Technology: Cryo distribution.

Since no institution has expressed interest in either the accelerator cryo plant or the test stand and instruments cryo plant, the project schedule has forced ESS in Lund to procure these. (The cryo plant cooling the moderators will however be an in-kind contribution to the target.)

Also, there are no partners for klystrons, IOTs or the modulator production yet. Prototypes have been procured or built by ESS, but the series production is still open for in-kind contributions.

# A FIFTEEN YEAR PERSPECTIVE ON THE DESIGN AND PERFORMANCE OF THE SNS ACCELERATOR

S. M. Cousineau, Oak Ridge National Laboratory, Oak Ridge, TN

## Abstract

Construction of the Spallation Neutron Source (SNS) accelerator began approximately fifteen years ago. Since this time, the accelerator has broken new technological ground with the operation of the world’s first superconducting H<sup>-</sup> linac, the first liquid mercury target, and 1.4 MW of beam power. This talk will reflect on the issues and concerns that drove key decisions during the design phase, and will consider those decisions in the context of the actual performance of the accelerator. Noteworthy successes will be highlighted and lessons-learned will be discussed. Finally, a look forward toward the challenges associated with a higher power future at SNS will be presented.

## INTRODUCTION

The SNS accelerator was designed as a short pulse, high power proton driver for neutron production. The top levels goals of the accelerator are to provide 1.4 MW of proton beam power with 90% reliability. The final proton beam exiting the accelerator is composed of 1 us pulses of 1 GeV protons operating at a repetition rate of 60 Hz. A third goal, related to the reliability metric, is to maintain beam loss levels to the order of < 1 W/m, corresponding to approximately 100 mrem/hr residual radiation at 30 cm distance, throughout the accelerator in order to allow for routine, hands on maintenance of system components.

To obtain the short pulse structure of the beam, an H<sup>-</sup> linac and accumulator ring combination was chosen. From there, the design decisions for the subsystems were driven by the high power, high reliability, low loss goals stated previously. These decisions and their impact on accelerator performance will be discussed in the forthcoming sections, following a brief summary of the accelerator performance to date.

## PERFORMANCE METRICS

The accelerator was commissioned beginning in 2002, and the first neutrons were produced in 2006. The power ramp up took longer than planned due to difficulties in the target systems [1]. The accelerator was operated in production mode with 1.4 MW of beam power for the first time in the fall of 2015. After this production cycle resulted in a premature target failure, the beam power was reduced to 1.1 MW in a move to prioritize reliability for the neutron users. The power will be ramped back up in to 1.4 MW in a stepwise fashion over the course of the next few years in a controlled study of target cavitation damage versus beam power. Fig. 1 shows the beam power evolution of the SNS accelerator since the beginning of operations in 2006.

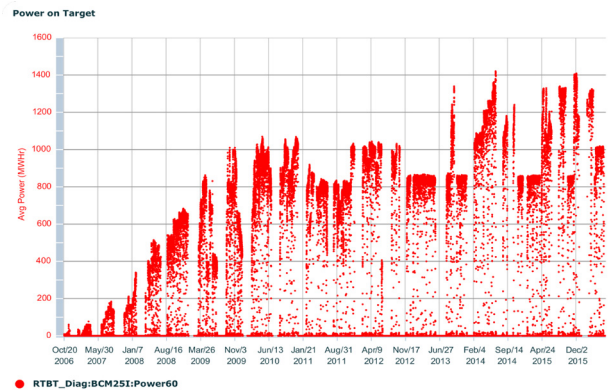


Figure 1: SNS beam power evolution.

The accelerator reliability metric is defined as the number of hours of delivered neutron production divided by the number of hours scheduled. Catastrophic equipment failures such as target failures that result in long downtimes have major impact on the reliability metric. The SNS has suffered seven premature target failures, as well as one equipment failure in the MEBT with comparable downtime. Target failures have progress from early life failures due to manufacturing details to failures due to cavitation damage at high power. Aside from these single event failures, the remainder of the accelerator systems are operating with very high reliability, as demonstrated in Fig. 2, which shows the historical reliability metric with and without the target and MEBT failures.

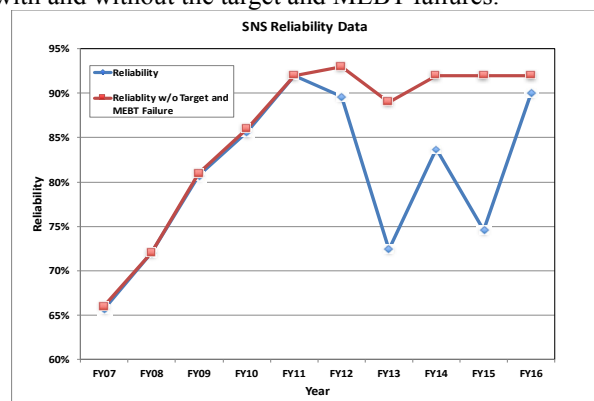


Figure 2: SNS accelerator reliability metric.

Finally, while reliability and beam power are the metrics relevant to the neutron user program, for the accelerator the level of residual radiation is top level consideration which determines how efficiently equipment maintenance can be performed. Table 1 below shows the activation levels throughout the accelerator following the 1.4 MW production run. With the exception of the ring injection area, which was always anticipated to be hot, the activation is well below the 1 W/m criterion.

## LHC RUN 2: RESULTS AND CHALLENGES

R. Bruce\*, G. Arduini, H. Bartosik, R. de Maria, M. Giovannozzi, G. Iadarola, J.M. Jowett, K. Li, M. Lamont, A. Lechner, E. Metral, D. Mirarchi, T. Pieloni, S. Redaelli, G. Rumolo, B. Salvant, R. Tomas, J. Wenninger, CERN, Geneva, Switzerland

### Abstract

The first proton run of the LHC was very successful and resulted in important physics discoveries. It was followed by a two-year shutdown where a large number of improvements were carried out. In 2015, the LHC was restarted and this second run aims at further exploring the physics of the standard model and beyond at an increased beam energy. This article gives a review of the performance achieved so far and the limitations encountered, as well as the future challenges for the CERN accelerators to maximize the data delivered to the LHC experiments in Run 2. Furthermore, the status of the 2016 LHC run and commissioning is discussed.

### INTRODUCTION

The CERN Large Hadron Collider (LHC) [1, 2] is built to collide 7 TeV protons or heavy ions of equivalent rigidity. Following the downtime after an incident in one of the main dipole circuits during the first commissioning in 2008 [3], the operation restarted at lower beam energy to minimize the risk. Therefore, the first proton run (2010–2013) [4–6] was carried out at 3.5 TeV–4 TeV. Furthermore, a bunch spacing of 50 ns was used instead of the nominal 25 ns. This implied fewer bunches with larger intensity and hence a high peak luminosity but larger than nominal pileup. Run 1 resulted in about  $30 \text{ fb}^{-1}$  of proton data and important physics results, most notably the discovery of the Higgs boson [7, 8].

Run 1 was followed by a long shutdown (LS1, 2013–2014) with a large number of consolidation and upgrade activities [9]. The bus-bar splices between the superconducting magnets were improved, in order to make sure that the LHC could operate at higher energy without risk of repeating the 2008 incident. Run 2 started in 2015 and is planned to continue until the end of 2018. The main accelerator goals of Run 2 are to produce more than  $100 \text{ fb}^{-1}$  of data at a higher energy and using the nominal 25 ns bunch spacing, but with lower bunch charge for lower pileup.

The parameters achieved so far in Run 1 and Run 2, together with the design values, are shown in Table 1. At the time of writing in end of June 2016, the LHC has entered its production phase with a luminosity that has just reached nominal, a stored beam energy of around 250 MJ, and a good machine availability after a few initial technical issues. This article gives a review of the achievements so far, as well as the issues encountered and the challenges ahead for reaching the goals of the LHC.

### BEAM FROM THE INJECTORS

The success of the LHC is highly dependent on the availability and the beam quality of the injector complex. Protons

are injected at 450 GeV into the LHC, after passing through a chain of 4 accelerators: LINAC 2, PSB, PS, and SPS [10]. The present limitations on bunch intensity  $N_B$  and normalized emittance  $\epsilon_n$  in the injector chain are summarized in Fig. 1 for the standard 25 ns LHC beam [11]. The brightness is limited by space charge effects in the PSB and the PS and the fact that, in the PSB, several injections are performed from LINAC 2 per PSB bunch. This means that in order to increase the intensity, more injections are needed, which occupy different phase-space areas and hence cause larger  $\epsilon_n$ . In the SPS, longitudinal instabilities occur if  $N_B \gtrsim 1.3 \times 10^{11}$  protons per bunch. The green dots in Fig. 1 show the actual achieved beams in 2015.

Figure 1 refers to the standard 25 ns LHC beams, which have been used so far in 2015–2016. Several different schemes exist [12], where the most interesting for LHC physics is the so-called BCMS beam (Batch compression, merging and splitting) [13, 14]. It has almost a factor 2 smaller  $\epsilon_n$ , since lower-intensity bunches with smaller  $\epsilon_n$  are taken from the PSB and merged in the PS to achieve about the same  $N_B$  as for the standard beam. However, fewer bunches per train can be achieved and hence a slightly smaller number of total bunches in the LHC.

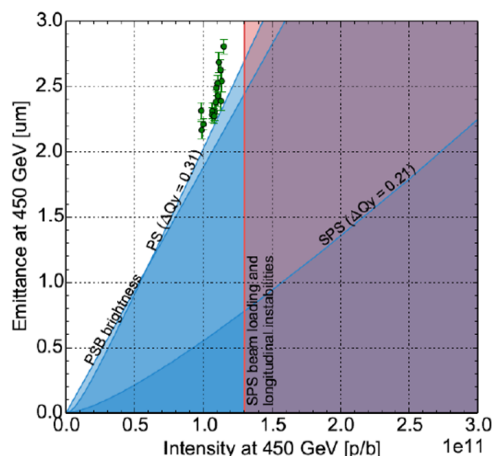


Figure 1: Limitations on the beam intensity and normalized emittance in the injector chain. The white area to the left represents the possible configuration space for the LHC beams and the green dots the beams used in 2015.

### THE 2015 PROTON RUN

Because of the large number of changes applied in LS1, a significant recommissioning period was needed. Therefore 2015 was considered to be a commissioning year, with the main goal to reestablish high-intensity operation with the new running parameters. A beam energy of 6.5 TeV was

\* roderik.bruce@cern.ch

# RECENT PROGRESS OF J-PARC MR BEAM COMMISSIONING AND OPERATION

S. Igarashi<sup>†</sup> for the J-PARC MR Beam Commissioning Group  
 KEK/J-PARC Center, Tsukuba, Ibaraki 305-0801 Japan

## Abstract

The main ring (MR) of the Japan Proton Accelerator Research Complex (J-PARC) has been providing 30-GeV proton beams for elementary particle and nuclear physics experiments since 2009. The beam power of 415 kW has been recently achieved with  $2.15 \times 10^{14}$  protons per pulse and the cycle time of 2.48 s for the neutrino oscillation experiment. Main efforts in the beam tuning are to minimize beam losses and to localize the losses at the collimator section. Recent improvements include the 2<sup>nd</sup> harmonic rf operation to reduce the space charge effect with a larger bunching factor and corrections of resonances near the operation setting of the betatron tune. Because the beam bunches were longer with the 2<sup>nd</sup> harmonic rf operation, the injection kicker system was improved to accommodate the long bunches. We plan to achieve the target beam power of 750 kW in JFY 2018 by making the cycle time faster to 1.3 s with new power supplies of main magnets, rf upgrade and improvement of injection and extraction devices. The possibility of the beam power beyond 750 kW is being explored with new settings of the betatron tune.

## INTRODUCTION

The Japan Proton Accelerator Research Complex (J-PARC) consists of the high intensity proton accelerators and the experimental facilities to make use of the proton beams [1]. It has three accelerators; a 400 MeV linear accelerator, 3 GeV rapid cycling synchrotron (RCS) and 30 GeV main ring (MR). MR is a synchrotron with the circumference of 1567.5 m and with three-fold symmetry as shown in Fig. 1. The first straight section is for injection devices and beam collimators. The proton beams from RCS are transported through a beam transport line (3-50BT) to MR. The second straight section is for slow extraction (SX) devices to deliver the beam to the hadron hall. The third straight section is for rf cavities and fast extraction (FX) devices to extract the beam to the neutrino beam-line or the beam abort line.

The cycle time is 2.48 s for the FX mode. The beam is extracted in one turn at the top energy to the neutrino oscillation experiment (T2K). For the SX mode the cycle time is 5.52 s with the flattop duration of 2.93 s. Beam spills of 2 s duration are then delivered to elementary particle and nuclear physics experiments in the hadron hall.

The T2K experiment observed the appearance of electron neutrinos from muon neutrinos made from the secondary particles of the high intensity protons [2]. High

intensity proton beams are further demanded for the precise measurements of neutrino mixing parameters.

The beam power has been steadily increased as shown in Fig. 2 in the last six years. It was mostly about 390 kW in the operation of Jan. ~ May of 2016 for FX with  $2 \times 10^{14}$  protons per pulse (ppp). The plan to achieve the target beam power of 750 kW is to make the cycle faster from 2.48 s to 1.3 s with  $2 \times 10^{14}$  ppp. A milestone for the number of accelerated protons was therefore reached. Further efforts are being made for higher intensity. The user operation of 415 kW was successful during the last three days.

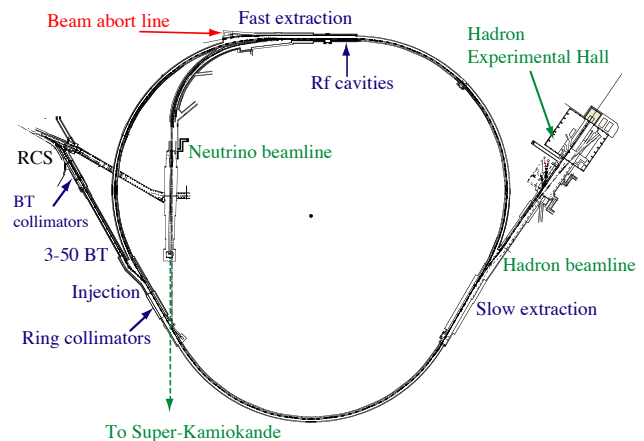


Figure 1: Layout of J-PARC MR.

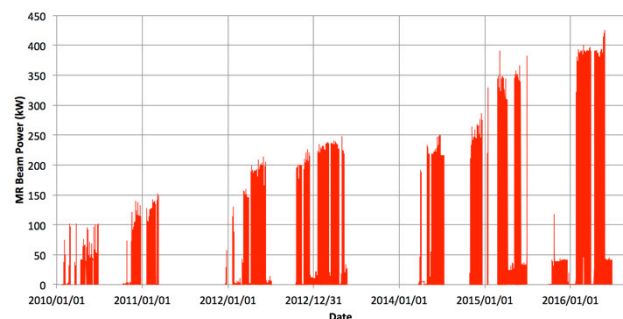


Figure 2: Beam Power Trend Graph.

## OPERATION STATUS FOR THE FAST EXTRACTION

Eight bunches of beams are injected to MR in 4 times during the injection period of 0.13 s. The acceleration takes 1.4 s and the accelerated protons are extracted in one turn. The recovery for the magnet currents takes 0.94 s and the total cycle is 2.48 s. Figure 3 shows the beam

<sup>†</sup> susumu.igarashi@kek.jp

# ACCELERATOR PHYSICS CHALLENGES IN FRIB DRIVER LINAC\*

M. Ikegami, K. Fukushima, Z. He, S. Lidia, Z. Liu, S. M. Lund, F. Marti, T. Maruta<sup>†</sup>, D. Maxwell, G. Shen, J. Wei, Y. Yamazaki, T. Yoshimoto, Q. Zhao  
 Facility for Rare Isotope Beams, Michigan State University, MI 48824, USA

## Abstract

FRIB (Facility for Rare Isotope Beams) is a heavy ion linac facility to accelerate all stable ions to the energy of 200 MeV/u with the beam power of 400 kW, which is under construction at Michigan State University in USA. FRIB driver linac is a beam power frontier accelerator aiming to realize two orders of magnitude higher beam power than existing facilities. It consists of more than 300 low-beta superconducting cavities with unique folded layout to fit into the existing campus with innovative features including multi charge state acceleration. In this talk, we overview accelerator physics challenges in FRIB driver linac with highlight on recent progresses and activities preparing for the coming beam commissioning.

## INTRODUCTION

The Facility for Rare Isotope Beams (FRIB) is a high-power heavy ion accelerator facility now under construction at Michigan State University under a cooperative agreement with the US DOE [1]. Its driver linac operates in CW (Continuous Wave) mode and accelerates all stable ions to kinetic energies above 200 MeV/u with the beam power on target up to 400 kW. This novel facility is designed to accelerate and control multiple ion species simultaneously to enhance beam power. The linac has a folded layout as shown in Fig. 1, which consists of a front-end, three Linac Segments (LSs) connected with two Folding Segments (FSs), and a Beam Delivery System (BDS) to deliver the accelerated beam to the production target. The front-end consists of two ECR (Electron Cyclotron Resonance) ion sources, a normal conducting CW RFQ (Radio Frequency Quadrupole), and beam transport lines to separate, collimate, and bunch the multiple ion charge states emerging from the ECR sources. Ion sources are located on the ground level and an extracted beam from one of two ion sources is delivered to the linac tunnel through a vertical beam drop. In the FRIB driver linac, superconducting RF cavities are extensively employed. After acceleration up to 0.5 MeV/u with a normal conducting RFQ, ions are accelerated with superconducting QWRs (Quarter Wave Resonators) and HWRs (Half Wave Resonators) to above 200 MeV/u. There are two types each of QWRs ( $\beta = 0.041$  and  $0.085$ ) and HWRs ( $\beta = 0.29$  and  $0.53$ ) with different geometrical beta. The frequency and aperture diameter for QWRs are 80.5 MHz and 36 mm respectively, and those

for HWRs are 322 MHz and 40 mm respectively. We have three  $\beta = 0.041$  cryomodules housing four cavities and 11  $\beta = 0.085$  cryomodules housing eight cavities in LS1 (Linac Segment 1). We have 12  $\beta = 0.29$  cryomodules housing six cavities and 12  $\beta = 0.53$  cryomodules housing eight cavities in LS2 (Linac Segment 2). There are 6  $\beta = 0.53$  cryomodules followed by a space to add cryomodules for future upgrade in LS3 (Linac Segment 3). The total number of superconducting RF cavities is 332 including those for longitudinal matching in the Folding Segments. Each superconducting RF cavity is driven by an independent solid state amplifier. Transverse focusing in the superconducting linac sections is provided by superconducting solenoids (8 Tesla, 20 mm bore radius). It is unique to have such large scale linac sections with low- $\beta$  superconducting RF cavities together with multi charge state acceleration at high CW power. This poses accelerator physics challenges specific to the FRIB driver linac.

We reported beam physics challenges in FRIB at the previous series of this workshop [2]. Here, we don't repeat the challenges we identified at the previous workshop while we have been continuously pursuing those areas. As general accelerator challenges for high power linacs were summarized at the previous workshop [3], we try to focus in this paper on challenges specific to FRIB and/or those for

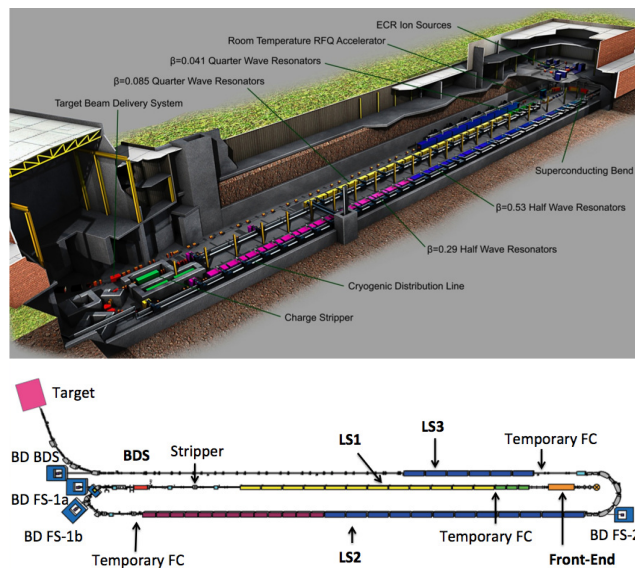


Figure 1: Layout of FRIB driver linac. Top: Cut view of FRIB driver linac building. Bottom: Schematic layout for the FRIB driver linac (top view).

\* Work supported by the U.S. Department of Energy Office of Science under Cooperative Agreement DE-SC0000661

<sup>†</sup> On leave from KEK/J-PARC

Copyright © 2016 CC-BY-3.0 and by the respective authors

# BEAM OPTICS SIMULATION STUDY ON THE PRE-STRIPPER LINAC FOR RARE ISOTOPE SCIENCE PROJECT\*

J. W. Kim<sup>†</sup>, J. H. Jang, H. C. Jin, Institute for Basic Science, Daejeon, Korea  
P. N. Ostroumov, B. Mustapha, J. A. Conway, Argonne National Laboratory, Argonne IL, USA

## Abstract

The rare isotope science project (RISP) under development in Korea aims to provide various heavy-ion beams for nuclear and applied science users. A pre-stripper linac is the first superconducting section to be constructed for the acceleration of both stable and radioisotope beams to the energy of 18.5 MeV/u with a DC equivalent voltage of 160 MV. The current baseline design consists of an ECR ion source, an RFQ, cryomodules with QWR and HWR cavities and quadrupole focusing magnets in the warm sections between cryomodules. Recently we have developed an alternative design in collaboration with Argonne's Linac Development Group to layout the linac based on state-of-the-art ANL's QWR operating at 81.25 MHz and multi-cavity cryomodules of the type used for the ATLAS upgrade and Fermilab PIP-II projects. End-to-end beam dynamics calculations have been performed to ensure an optimized design with no beam losses. The numbers of required cavities and cryomodules are significantly reduced in the alternative design. The results of beam optics simulations and error sensitivity studies are discussed.

## INTRODUCTION

A next-generation rare isotope science facility using the in-flight fragment (IF) separation technique requires a high-current heavy-ion accelerator capable of delivering  $^{238}\text{U}$  beam with a few hundred kW power to a thin production target [1]. First, high currents of highly charged ions are needed to efficiently produce such high-power heavy ion beams. An ECR ion source operating at 28 GHz [2] has been developed, but for the heaviest ions, the beam current in a single charge state is still lower than required for a next generation IF facility.

To fully utilize the available accelerating voltage of a heavy-ion linac, charge strippers are employed in the process of multi-step acceleration. To accelerate a uranium beam to 200 MeV/u, charge stripping at 18 MeV/u was determined to be optimal. A significant merit of a superconducting linac is that its longitudinal acceptance is large enough to simultaneously accelerate multiple charge states of uranium produced at the charge stripper. Therefore, a large fraction of the beam is accelerated after the stripper and beam losses in the charge state selection section are significantly reduced resulting in lower radiation levels in that region.

\*Work supported by National Research Foundation Grant No. 20110018946 and the Rare Isotope Science Project.  
†jwkim@ibs.re.kr

The layout of the pre-stripper linac of the Rare Isotope Science Project (RISP) ongoing in Korea [3] is shown in Fig 1. The linac is designed to accelerate either radioisotope beams from the ISOL target or stable beams from the ECR. In fact, a plan is to accelerate both radioisotope and stable beams simultaneously when their charge-to-mass ratios are within 2%. For instance,  $^{132}\text{Sn}^{18+}$  can be accelerated together with  $^{238}\text{U}^{33+}$ . The isotope beam from ISOL is charge-bred before being injected into the pre-stripper linac. The charge breeding takes tens of ms in EBIS, which is under development at RISP [4], and stable ions can be accelerated during charge-breeding. Since the time duration for injection and extraction of isotope beams is much shorter than 1 ms and the breeding takes tens of ms, the fraction of stable beam can be over 90%. The simultaneous acceleration scheme of stable and radioisotope beams was devised for the proposed multi-user upgrade of the ATLAS linac at Argonne [5].

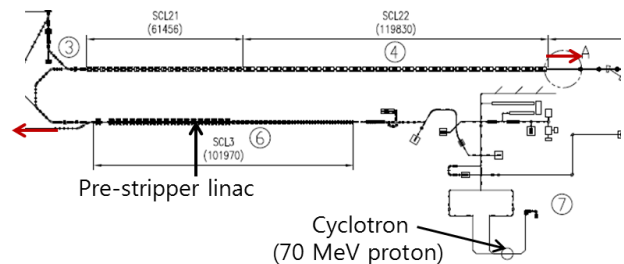


Figure 1: Layout of the pre-stripper linac of the RISP baseline design.

The injector includes an RFQ and the beam energy to the first cavity is 500 keV/u. The pulsing of stable ions according to the time structure of the charge-bred radioisotope beam is formed by an electric chopper. At the end of pre-stripper linac the two beams are switched by a kicker magnet either to low energy experimental area or to the achromatic 180° bending section after charge stripping.

## CURRENT BEAM OPTICS DESIGN

The current design of the pre-stripper linac is based on the use of two kinds of superconducting cavities: QWR ( $\beta_{\text{opt}}=0.047$ ) and HWR ( $\beta_{\text{opt}}=0.12$ ) operating at 81.25 and 162.5 MHz, respectively [6]. Transverse focusing components were decided to be quadrupole doublets based on the thought that superconducting solenoids located inside cryomodule can affect the cavity

# CHALLENGES AND PERFORMANCE OF THE C-ADS INJECTOR SYSTEM\*

Y. Chi<sup>†</sup>, Institute of High Energy Phys, Beijing, China

## Abstract

Along with the rapid development of nuclear power plants in China, treatment of the nuclear waste has become a crucial issue. Supported by the "Strategic Priority Research Program" of the Chinese Academy of Sciences (CAS), the Chinese Accelerator-Driven System (C-ADS) project is now on-going. The accelerator of C-ADS is a superconducting (SC) Continuous Wave (CW) proton linear accelerator (linac) with 1.5 GeV energy and 10 mA beam current. In the injector part many challenges to developing technologies including Radio Frequency Quadrupole (RFQ) and low  $\beta$  SC cavities and related hardware's. This paper presents the progress of development of C-ADS injectors and related hardware.

## ROADMAP OF C-ADS

In January 2011, a special program of nuclear energy promoted by the CAS - Advanced Fission Energy Program - was launched. This program is a strategic plan with its long-term planning until 2032 (see Figure 1). The R&D of the first phase has been funded by the "Strategic Priority Research Program" of CAS.

### (i) Phase I (R&D Facility)

- Accelerator goal: 10 mA  $\times$  250 MeV
- Reactor goal: 10 MWth
- Schedule goal: Before the end of the decade
- Short term goals: 5 MeV by 2015; 25 MeV by 2016

### (ii) Phase II (Experimental Facility)

- Accelerator goal: 10 mA  $\times$  1 GeV
- Reactor goal: 100 MWth
- Schedule goal: Approximately 2032

### (iii) Phase III (Demonstration Facility)

- Accelerator goal: 10 mA  $\times$  1.5 GeV
- Reactor goal: 1000 MWth

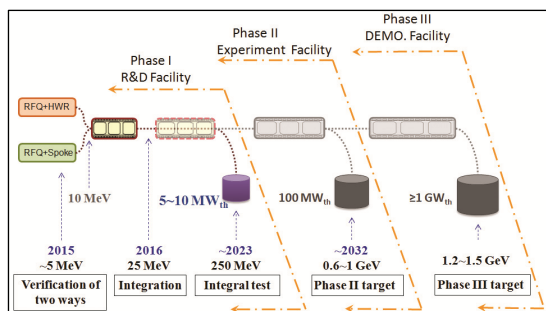


Figure 1: Road map of C-ADS project.

## DESIGN OF C-ADS LINAC

### Proton Beam Requirements for C-ADS

C-ADS are anticipated as a demonstration facility for transmutation of nuclear waste on an industrial scale, and would require a beam power of at least 10 MW. Besides the high beam power, the reliability of the machine should be very high. The design specification of the proton beam for C-ADS is shown in Table 1.

Table 1: Specifications of the Required Proton Beams of C-ADS

| Parameters          | Value         | Unit     |
|---------------------|---------------|----------|
| Particle            | Proton        |          |
| Energy              | 1.5           | GeV      |
| Current             | 10            | mA       |
| Beam power          | 15            | MW       |
| RF frequency        | 162.5/325/650 | MHz      |
| Beam loss           | <1            | W/m      |
| Duty factor         | 100%(CW)      |          |
|                     | <2500*        | 1s<t<10s |
| Beam trips per year | <2500         | 10s<t<5m |
|                     | <25           | t>5m     |

### Design Philosophy of the C-ADS Linac

The C-ADS linac is an extremely challenging accelerator, and there is no existing model in the world yet. The concept may share features in common with several other high power accelerators being developed in the U.S. and Europe, such as Project-X, MYRRHA, IFMIF and EURISOL.

With the approved SC Radio Frequency (RF) technology, especially the positive test results of low  $\beta$  Spoke resonators and Half Wave Resonators (HWR) at FNAL and ANL, and the success of the medium  $\beta$  Elliptical cavities at SNS, it is believed that an all superconducting proton linac except the RFQ is possible and favored due to the difficulty to deal with huge heat deposit in a CW room-temperature acceleration structure. Another advantage of using superconducting cavities is that one can use independently phased resonators to make local compensation when some cavities fail during operation. This is very important to achieve the very strict demands for the reliability of the ADS driving accelerator. So, C-ADS linac uses SC acceleration structures except the RFQs, and works in CW mode.

The RF frequencies for the main linac have been selected as 325 MHz for the Spoke cavity section and 650 MHz for the Elliptical cavity section. However, two different designs employing different RF frequencies are

\* Work supported by Chinese Academy of Sciences (CAS)

<sup>†</sup> chiyl@ihep.ac.cn

# FIGURE-8 STORAGE RING – INVESTIGATION OF THE SCALED DOWN INJECTION SYSTEM

H. Niebuhr\*, A. Ates, M. Droba, O. Meusel, D. Noll, U. Ratzinger, J.F. Wagner  
 Institute for Applied Physics, Goethe-University, Frankfurt am Main, Germany

## Abstract

To store high current ion beams up to 10 A, a superconducting storage ring (F8SR) is planned at Frankfurt university. For the realisation, a scaled down experimental setup with normalconducting magnets is being built. Investigations of beam transport in solenoidal and toroidal guiding fields are in progress. At the moment, a new kind of injection system consisting of a solenoidal injection coil and a special vacuum vessel is under development. It is used to inject a hydrogen beam sideways between two toroidal magnets. In parallel operation, a second hydrogen beam is transported through both magnets to represent the circulating beam. In a second stage, an ExB-Kicker will be used as a septum to combine both beams into one. The current status of the experimental setup will be shown. For the design of the experiments, computer simulations using the 3D simulation code bender were performed. Different input parameters were checked to find the optimal injection and transport channel for the experiment. The results will be presented.

charged ion species can be stored with higher energies. In order to focus the high current beams, toroidal magnets (called toroids) and solenoids are used around the whole ring. The twisted Figure-8 geometry is necessary because of the  $R \times B$  drift of beams transported through the toroidal magnetic fields. An additional advantage of this structure is the possibility to transport two different beams independently, one in each direction, and to perform interaction experiments at two areas of the ring where the beams cross. The F8SR is shown in Fig. 1.

## SIMULATIONS USING THE PARTICLE-IN-CELL CODE BENDER

To investigate the dynamics of ion beams in solenoidal and toroidal magnetic field systems and for the development of the scaled down injection experiment, simulations using the Particle-in-Cell code bender [1] were performed. For this purpose, the external fields of the magnets used in the experiment were calculated using CST (M-Static Solver) on a mesh of  $1 \times 1 \times 1$  mm resolution and the beam tube geometry was included (required for losses calculations). Different geometries, injection coils and magnetic field strengths were used to investigate the beam behavior and to find a working and realizable injection system with a high acceptance and transmission.

To get a look on the beam path and behavior from different points of view, the tracking results of the ring beam and the injection beam are plotted together with the magnetic field strength  $B_z$ . One result is shown in Fig. 2. In this figure the upper picture shows a top view on the drift of the two beams, the ring beam moves from left to right and the injection beam from above to right. The lower picture shows the side view.

Using this view the basic idea of the injection system can be seen and how it works. The injected beam drifts from the injection channel to the transport channel and then gets transported through the second toroid. Using the plotted parameters, the injected beam is matched perfectly, so no gyration occurs and the beam adjustment does not change. In this process, the beam also drifts down to the level of the ring beam. The possibility of using a kicker system to merge the two beams is available. In this simulation, the ring beam was not matched perfectly and so the beam adjustment – visible by the different gyration inside the first and the second toroid – changed. By using different parameters for the ring beam, this effect can be reduced.

For the characterization of an injection system, a set of simulations with different parameters were necessary. To compare the results, a method to figure out how large the

## F8SR – FIGURE-8 STORAGE RING

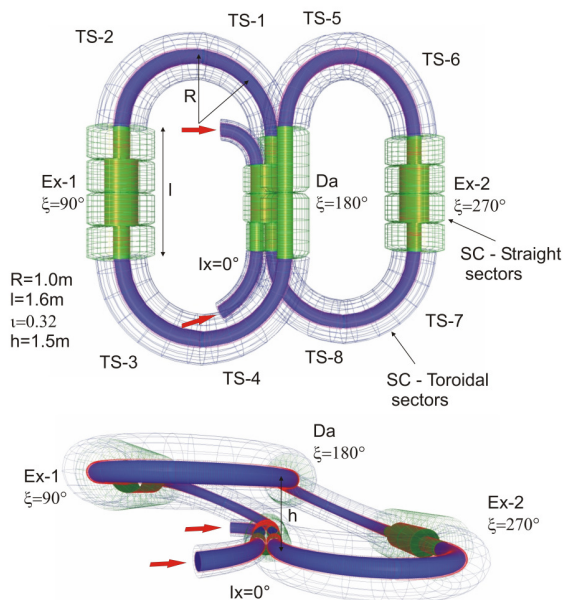


Figure 1: F8SR – Low-Energy Superconducting Magneto-static Storage Ring.

The F8SR is a low-energy superconducting magnetostatic storage ring for high current beams, for example proton beams up to 10 A with an energy of up to 150 keV. Higher

\* niebuhr@iap.uni-frankfurt.de

# STUDY ON THE MAGNETIC MEASUREMENT RESULTS OF THE INJECTION SYSTEM FOR CSNS/RCS\*

M.Y. Huang<sup>1,2#</sup>, S.N. Fu<sup>1,2</sup>, N. Huang<sup>1</sup>, L.H. Huo<sup>1</sup>, H.F. Ji<sup>1,2</sup>, W. Kang<sup>1,2</sup>, Y.Q. Liu<sup>1,2</sup>, J. Peng<sup>1,2</sup>, J. Qiu<sup>1,2</sup>, L. Shen<sup>1,2</sup>, S. Wang<sup>1,2</sup>, X. Wu<sup>1,2</sup>, S.Y. Xu<sup>1,2</sup>, J. Zhang<sup>1,2</sup>, G.Z. Zhou<sup>1,2</sup>

1: Institute of High Energy Physics, Chinese Academy of Sciences, Beijing, China

2: Dongguan Institute of Neutron Science, Dongguan, China

## Abstract

A combination of the H<sup>-</sup> stripping and phase space painting method is used to accumulate a high intensity beam in the Rapid Cycling Synchrotron (RCS) of the China Spallation Neutron Source (CSNS). The injection system for CSNS/RCS consists of three kinds of magnets: four direct current magnets (BC1-BC4), eight alternating current magnets (BH1-BH4 and BV1-BV4), two septum magnets (ISEP1 and ISEP2). In this paper, the magnetic measurements of the injection system were introduced and the data analysis was processed. The field uniformity and magnetizing curves of these magnets were given, and then the magnetizing fitting equations were obtained.

## INTRODUCTION

The China Spallation Neutron Source (CSNS) is a high power proton accelerator-based facility [1]. It consists of an 80 MeV H<sup>-</sup> linac (upgradable to 250 MeV for CSNS-II), a 1.6 GeV Rapid Cycling Synchrotron (RCS), a solid tungsten target station, and some instruments for neutron applications [2]. With a repetition rate of 25 Hz, the RCS, which accumulates an 80 MeV injection beam, accelerates the beam to the designed energy of 1.6 GeV and extracts the high energy beam to the target. The design goal of beam power for CSNS is 100 kW and can be upgradable to 500 kW [3].

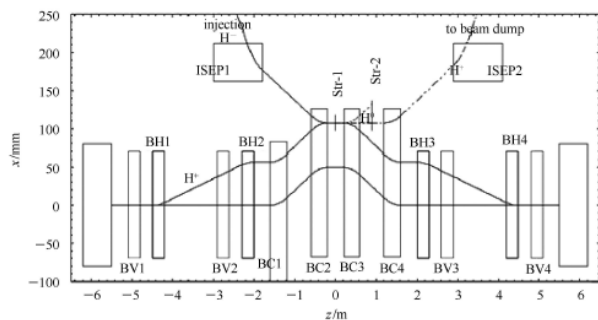


Figure 1: Layout of the RCS injection system.

For the high intensity proton accelerators, the injection with H<sup>-</sup> stripping and phase space painting is actually a practical method [4] which is used for CSNS/RCS. Figure 1 shows the layout of the RCS injection system. It consists of a fixed horizontal bump (four direct current (DC) dipole magnets, BC1-BC4), a horizontal painting

bump (four alternating current (AC) dipole magnets, BH1-BH4), a vertical painting bump (four AC dipole magnets, BV1-BV4), two septum magnets (ISEP1, ISEP2), and two stripping foils (Str-1, Str-2) [5].

In order to obtain the field uniformity and magnetizing curves of different kinds of magnets in the injection system for CSNS/RCS, the magnetic measurements need to be done. By using some codes of numerical analysis, the measurement results can be processed. Then the field uniformity and magnetizing curves can be given and the magnetizing equations can be fitted.

## MEASUREMENTS OF BC MAGNETS

For the injection system of CSNS/RCS, four DC dipole magnets, BC1-BC4, give a fixed horizontal bump in the middle for an additional closed-orbit shift of 60 mm. The physics design parameters of the four BC magnets are the same and they share only one power supply.

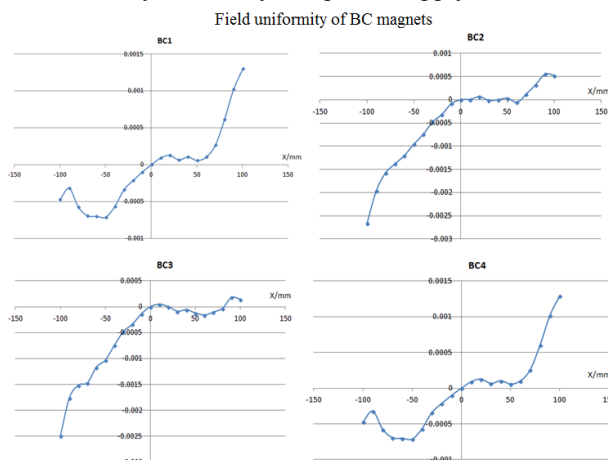


Figure 2: Field uniformity of the four BC magnets.

After the measurements of the four BC magnets, their field uniformity can be obtained, as shown in Fig. 2. It can be known that the field uniformity of any one BC magnet is smaller than  $\pm 0.3\%$  which meets the physics design requirement ( $< \pm 0.5\%$ ). In addition, it can be found that there are some differences between the four BC magnets although they are the same in the physics design.

The magnetizing curves of the four BC magnets and their auxiliary coils also can be given after the magnetic measurements. By using some codes of numerical analysis, the magnetizing curves can be fitted. After the analysis of fitting errors, it can be known that the linear of

\*Work supported by National Natural Science Foundation of China (Project Nos. 11205185)

#huangmy@ihep.ac.cn

# H<sup>-</sup> CHARGE EXCHANGE INJECTION FOR XiPAF SYNCHROTRON

H. J. Yao<sup>†</sup>, S. X. Zheng, G. R. Li, X. L. Guan, X. W. Wang, Q. Z. Xing, Key Laboratory of Particle & Radiation Imaging (Tsinghua University), Ministry of Education, Beijing 100084, China  
 also at Laboratory for Advanced Radiation Sources and Application, Tsinghua University, Beijing 100084, China  
 also at Department of Engineering Physics, Tsinghua University, Beijing 100084, China

## Abstract

The physics design of the H<sup>-</sup> charge exchange injection system for Xi'an Proton Application Facility (XiPAF) synchrotron with the missing dipole lattice is discussed. The injection scheme is composed of one septum magnet, three chicane dipoles, two bump magnets and one carbon stripping foil. A 7 μg/cm<sup>2</sup> carbon foil is chosen for 7 MeV H<sup>-</sup> beam for high stripping efficiency and low coulomb scattering effect. The simulation results of the horizontal and vertical phase space painting finished by two bumper magnets and mismatching respectively are presented.

## INTRODUCTION

Xi'an Proton Application Facility (XiPAF) is under construction in Xi'an, China, to fulfil the need of the experimental simulation of the space radiation environment, especially for the research of the single event effect (SEE). XiPAF is mainly composed of a 7 MeV linac injector, a synchrotron (60~230 MeV) and two experimental stations. The synchrotron [1] has a 6-fold "Missing-dipole" FODO lattice with its circumference of 30.9 m, the focusing structure consists of 6 dipoles and 12 quadrupoles, and six 2.21 m long drift space is left for accommodation of injection, extraction and acceleration system etc. The stripping injection method is chosen to achieve higher beam intensity of  $2 \times 10^{11}$  proton per pulse (PPP). And the phase space painting is chosen to control the space charge effect. The parameters from the linac injector are shown in Table 1.

Table 1: Injection Parameters for XiPAF Synchrotron

| Parameter                | Value              | Unit      |
|--------------------------|--------------------|-----------|
| Injection ion type       | H <sup>-</sup>     |           |
| Beam energy              | 7                  | MeV       |
| Peak current             | 5                  | mA        |
| Maximum repetition rate  | 0.5                | Hz        |
| Beam pulse width         | 10~40              | μs        |
| Normalized RMS emittance | ~0.25              | π mm·mrad |
| Injection period         | 0.85               | μs        |
| Number of particles      | $2 \times 10^{11}$ |           |

## INJECTION LAYOUT

The layout of injection system for XiPAF synchrotron is shown in Fig.1, a carbon strip foil near the center of the injection section and three DC chicane dipoles (CH1, CH2, CH3), are arranged in the injection section; and two

bumper magnets (Bump1, Bump2) located in the two sections adjacent to the injection section.

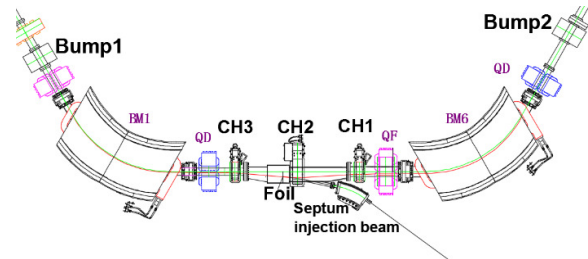


Figure 1: Injection Layout of XiPAF synchrotron.

In order to inject the beam properly, the closed orbit need to be bumped to the position of the strip foil during the beam injection. Three DC Chicane dipoles produce a fixed bump in the closed orbit near the strip foil. Then two bumpers are switched on to bend the closed orbit an additional 2.4 cm outward, and to make the closed orbit passing through the strip foil so that the injected beam and circulating beams overlap. The closed orbit bump produced by three chicane dipoles and two bumpers is shown in Fig.2.

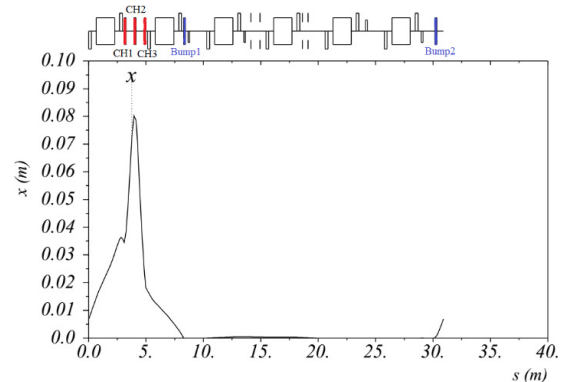


Figure 2: The closed orbit bump.

Table 2: Main Parameters of Chicanes and Bumpers

| Parameter            | CH1  | CH2  | Bump1 | Bump2 |
|----------------------|------|------|-------|-------|
| Kick angle (mrad)    | 70   | 140  | 10    | 7     |
| Magnetic field (T)   | 0.17 | 0.28 | 0.024 | 0.017 |
| Effective length(mm) | 150  | 200  | 160   | 160   |

The main parameters of three chicane dipoles and two bumpers are given in Table 2. The parameters of CH3 are same with the ones of CH1. During injection, 7 MeV H<sup>-</sup> beam is converted to protons by the strip foil. After the injection, the two bumpers are switched off to move the closed orbit off the strip foil completely.

<sup>†</sup> yaohongjuan@mail.tsinghua.edu.cn

# RF-KNOCKOUT SLOW EXTRACTION DESIGN FOR XiPAF SYNCHROTRON

H. J. Yao, G. R. Li, Q. Zhang, S. X. Zheng<sup>†</sup>, X. L. Guan, X. W. Wang

Key Laboratory of Particle & Radiation Imaging (Tsinghua University), Ministry of Education, Beijing 100084, China

also at Laboratory For Advanced Radiation Sources and Application, Tsinghua University, Beijing 100084, China

also at Department of Engineering Physics, Tsinghua University, Beijing 100084, China

## Abstract

The physics design of slow extraction for Xi'an Proton Application Facility (XiPAF) synchrotron is discussed. The extraction scheme is composed of two resonant sextupoles, one electrostatic septum (ES) and two septum magnets. The phase space diagram under the Hardt condition at the entrance of ES and the last three turn's trajectory before extraction are presented. A program is written with C++ to simulate slow extraction process by RF-knockout (RF-KO), the calculation results of dual frequency modulation (FM) and amplitude modulation (AM) are given, and the standard deviation of the fluctuation parameter  $R_1$  can be limited 0.2 with optimum parameters under a sampling frequency of about 10 kHz.

## INTRODUCTION

Xi'an Proton Application Facility (XiPAF) is under construction in Xi'an, China, to fulfil the need of the experimental simulation of the space radiation environment, especially for the research of the single event effect (SEE). XiPAF is mainly composed of a 7 MeV linac injector, a synchrotron (60~230 MeV) and two experimental stations. The synchrotron [1] has a 6-fold "Missing-dipole" FO-DO lattice with its circumference of 30.9 m. The irradiation experiments require 1~10 s proton beam, so the slow extraction system has been designed for XiPAF synchrotron. For this facility, the third-integer resonance and RF-KO (Radio Frequency Knock Out) technology are applied to accomplish slow extraction. The parameters of XiPAF synchrotron related to slow extraction system are listed in Table 1.

Table 1: The Parameters of XiPAF Synchrotron

| Parameter                 | Value       | Unit |
|---------------------------|-------------|------|
| Injection energy          | 7           | MeV  |
| Extraction energy         | 60~230      | MeV  |
| Circumference             | 30.9        | m    |
| Maximum repetition rate   | 0.5         | Hz   |
| Maximum $\beta_x/\beta_y$ | 5.8/6.0     |      |
| Extraction $v_x/v_y$      | 1.678/1.794 |      |

## EXTRACTION SYSTEM SCHEME

The scheme of extraction system for XiPAF synchrotron is shown in Fig.1, the extraction elements consist of four sextupoles (SR1, SR2, SC1, SC2), one electrostatic wire septum (ES), two septum magnets (MS1, MS2) and

one RF-KO kicker. As showed in Fig. 1, one pair sextupole magnets SR1 and SR2 are used for resonance excitation. The phase advance between SR1 and SR2 is about  $5\pi/3$ , and they have same strength but opposite sign., which leads to the same function on resonance but cancellation of the chromaticity correction. Another pair sextupole magnets SC1 and SC2 are used for chromaticity correction. The phase advance between SC1 and SC2 is also about  $5\pi/3$ , and they have same strength and same sign, which leads to the same function on chromaticity without affecting the resonance.

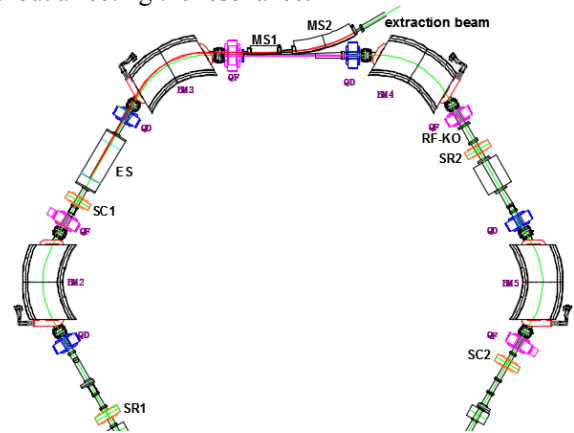


Figure 1: The extraction system scheme for XiPAF synchrotron.

The ES is used to give a kick to the particles entering the ES gap by the electrostatic field in order to separate from the circulating beam remaining inside the separatrix. In addition, two septum magnets MS1 and MS2 are used to deflect the beam toward the beam transport line for extraction. The main parameters of ES, MS1 and MS2 are listed in Table 2.

Table 2: Main Parameters of ES, MS1 and MS2

| Parameter                  | ES  | MS1  | MS2   |
|----------------------------|-----|------|-------|
| Kick angle (mrad)          | 11  | 87.3 | 453.8 |
| Max. magnetic field (T)    | /   | 0.34 | 0.81  |
| Max. electric field (MV/m) | 5.7 | /    | /     |
| Effective length (m)       | 0.8 | 0.6  | 1.3   |
| Septum thickness (mm)      | 0.1 | 15   | 30    |

The ES is closed to the focusing quadrupole where the beta function has large value, and the phase advance between ES and MS1 is 92 degrees. Based on the formula (1), a large horizontal deflection will be obtained at the septum magnet MS1, which makes the design of MS1 easier.

# DESIGN OF THE 230 MeV PROTON ACCELERATOR FOR XI'AN PROTON APPLICATION FACILITY

S.X. Zheng, Q.Z. Xing, X.L. Guan, H.J. Yao, C. Cheng, T.B. Du, H.Y. Zhang, G.R. Li, L. Du, R. Tang, M.W. Wang, L. Wu, Y. Yang, H.J. Zeng, Q. Zhang, Z. Yang, H.P. Jiang, C.T. Du, Q.Z. Zhang, W.H. Huang, C.X. Tang, H.B. Chen, D. Wang, X.W. Wang<sup>†</sup>, Key Laboratory of Particle & Radiation Imaging (Tsinghua University), Ministry of Education, Beijing 100084, China also at Laboratory for Advanced Radiation Sources and Application, Tsinghua University, Beijing 100084, China

also at Department of Engineering Physics, Tsinghua University, Beijing 100084, China

Z.M. Wang, C. Zhao, B.C. Wang, Y.H. Yan, Y.P. Wang, H. Zhang, M.T. Qiu, W. Chen, State Key Laboratory of Intense Pulsed Radiation Simulation and Effect (Northwest Institute of Nuclear Technology), Xi'an, 710024, China

W.Q. Guan, Y. He, J. Li, NUCTECH Co. Ltd., Beijing 100084, China

S. Y. Lee, Indiana University, Bloomington, IN 47405 USA

## Abstract

We report a design of the 230 MeV proton accelerator, the Xi'an Proton Application Facility (XiPAF), which will be located in Xi'an city, China. The facility will provide proton beam with the maximum energy of 230 MeV for the research of the single event effect. The facility, composed of a 230 MeV synchrotron, a 7 MeV H<sup>+</sup> linac injector and two experimental stations, will provide a flux of 10<sup>5</sup>~10<sup>8</sup> p/cm<sup>2</sup>/s with the uniformity of better than 90% on the 10 cm×10 cm sample.

## INTRODUCTION

To fulfil the need of the experimental simulation of the space radiation environment, especially the investigation of the single event effect, the project of Xi'an Proton Application Facility (XiPAF) is under construction in Xi'an City, China. The facility is mainly composed of a 230 MeV synchrotron and a 7 MeV H<sup>+</sup> linac injector and two experimental stations. A proton flux of 10<sup>5</sup>~10<sup>8</sup> p/cm<sup>2</sup>/s with the uniformity of better than 90% on the 10 cm×10 cm sample is designed. Table 1 shows the parameters of the synchrotron and linac injector.

Table 1: Main Parameters of the XiPAF

| Parameter   | Injector       | Synchrotron                      |
|---|----------------|----------------------------------|
| Ion type  | H <sup>+</sup> | Proton                           |
| Output energy (MeV)                                 | 7              | 60~230                           |
| Peak current (mA)                                   | 5              |                                  |
| Repetition rate (Hz)                                | 0.1~0.5        | 0.1~0.5                          |
| Beam pulse width                                    | 10~40 μs       | 1~10 s                           |
| Max. average current (nA)                           | 100            | 30                               |
| Flux (p/cm <sup>2</sup> /s) (10×10cm <sup>2</sup> ) |                | 10 <sup>5</sup> ~10 <sup>8</sup> |

The schematic layout of the XiPAF Accelerator system is presented in Fig. 1. The H<sup>+</sup> beam is produced at the ion source (IS), accelerated to 7 MeV in linac injector, and then transferred to synchrotron through Medium Energy Beam Transport (MEBT). This H<sup>+</sup> beam is stripped into

protons by carbon foil in synchrotron and it is accelerated up to 230 MeV. Then the beam is extracted to experimental station through High Energy Beam Transport (HEBT). The HEBT have two beamlines, where T2 is used for 60 to 230 MeV proton application extracted from synchrotron directly, and the T1 can degrade the proton energy from 60 MeV to 10 MeV for low energy application. The lowest extraction energy from the synchrotron is 60 MeV.

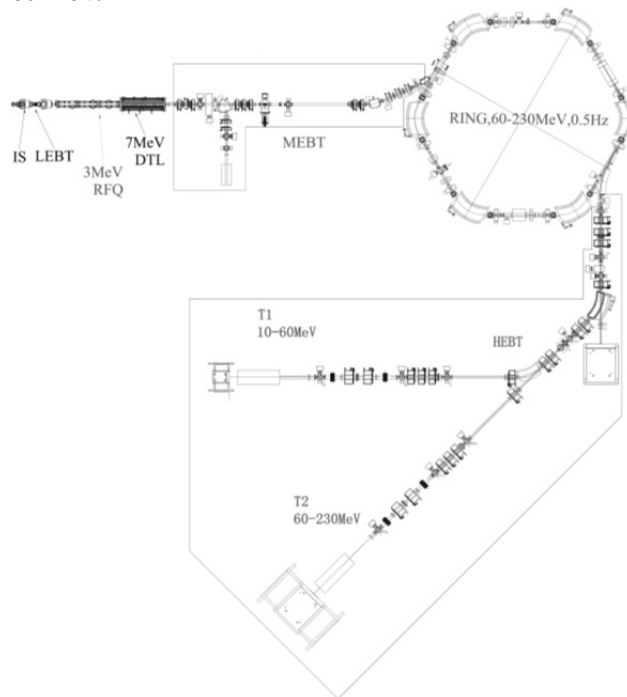


Figure 1: Layout of XiPAF accelerator system.

The main features of this accelerator are listed as follow:

- H<sup>+</sup> injection enables transverse space painting flexibility in order to alleviate space charge effects at low energy.
- The 6-fold “Missing-dipole” FODO structure simplifies the lattice design and work point tuning.

<sup>†</sup> wangxuewu@tsinghua.edu.cn

# COLD AND HIGH POWER TEST OF LARGE SIZE MAGNETIC ALLOY CORE FOR XiPAF'S SYNCHROTRON

G.R. Li, S.X. Zheng\*, H.J. Zeng, Z. Yang, H.J. Yao, X.L. Guan, X.W. Wang, W.H. Huang,  
 Key Laboratory of Particle & Radiation Imaging (Tsinghua University),  
 Ministry of Education, Beijing 100084, China,  
 also at Laboratory for Advanced Radiation Sources and Application,  
 Tsinghua University, Beijing 100084, China,  
 also at Department of Engineering Physics, Tsinghua University, Beijing 100084, China

## Abstract

A compact magnetic alloy (MA) loaded cavity is under development for XiPAF's synchrotron. The cavity contains 6 large size MA cores, each is independently coupled with solid state power amplifier. Two types of MA core are proposed for the project. We have developed a single core model cavity to verify the impedance model and to test the properties of MA cores under high power state. The high power test results are presented and discussed.

## INTRODUCTION

Xi'an Proton Application Facility (XiPAF), under construction in Xi'an, China, is dedicated to radiation applications like proton therapy, single event effects (SEE) study [1]. XiPAF's accelerator complex is composed of a 7 MeV Linac, a compact synchrotron (7~230 MeV) and two application beam lines. The synchrotron works in slow cycling mode and can accelerate proton beam from 7 MeV to 230 MeV in 0.5 s.

We propose to use a compact MA loaded cavity for beam acceleration because: 1. MA material has the property of wide band, thus we can use a single cavity to cover the large frequency range of our machine. This property can also simplified the control system compared to ferrite loaded cavity; 2. For slow cycling operation of our machine, a voltage of several hundred volts is enough, so the cooling of MA loaded cavity would not cause serious problem.

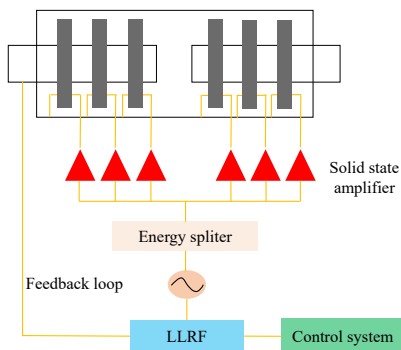


Figure 1: MA loaded RF system for XiPAF's synchrotron.

The schematic design of our MA loaded cavity is shown in Fig. 1. The cavity contains 6 large size MA cores. The impedance of each core will be designed close to  $50\ \Omega$ , so they can be independently coupled with solid state power amplifier without special impedance match. The main parameters of the cavity are listed in Table. 1.

Table 1: Parameters of the MA Loaded Cavity

| Parameter                       | Value | Unit     |
|---------------------------------|-------|----------|
| Frequency range                 | 1~7   | MHz      |
| Harmonic number                 | 1     |          |
| Max. Voltage                    | 800   | V        |
| Core number                     | 6     |          |
| Shunt impedance per core        | ~80   | $\Omega$ |
| Max. power dissipation per core | ~110  | W        |
| Q value                         | ~0.5  |          |
| Core outer diameter             | 450   | mm       |
| Core inner diameter             | 300   | mm       |
| Core thickness                  | 25    | mm       |

Two local company in China have provided two types of large size MA core (see Fig. 2):

- Type A: The material of ribbon is 1K107 produced by AT&M<sup>1</sup>. The thickness of ribbon is 18  $\mu\text{m}$ . The core is solidified with epoxy resin.
- Type B: The material of ribbon is FT-3M, which is the most widely used material in this area. The thickness of ribbon is 18  $\mu\text{m}$ . The core is solidified with silica gel.

We have carried out several experiments of both low power and high power to test the performance of large size MA cores.

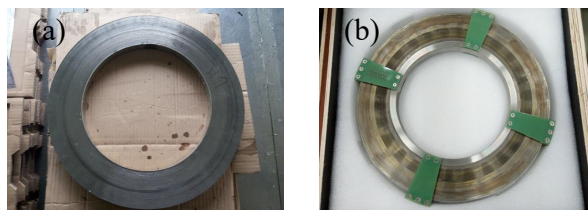


Figure 2: Large size MA cores, (a) Type A, (b) Type B.

\* zhengsx@tsinghua.edu.cn

<sup>1</sup> <http://www.atmcn.com/>

## PRESSURE PROFILES CALCULATION FOR THE CSRm AND BRing

P. Li<sup>†</sup>, J.C. Yang, Y.J. Yuan, J.C. Wang, J. Meng, C. Luo, Z. Chai, R.S. Mao, M. Li, W.L. Li, Z.Q. Dong, W.H. Zheng, X.C. Kang, S.P. Li, Institute of Modern Physics, Chinese Academy of Sciences, Lanzhou 730000, China

### Abstract

A new large scale accelerator facility is being designed by Institute of Modern Physics (IMP) Lanzhou, which is named as the High Intensity heavy-ion Accelerator Facility (HIAF). This project consists of ion sources, Linac accelerator, synchrotrons (BRing) and several experimental terminals. During the operation of Bring, the heavy ion beams will be easily lost at the vacuum chamber along the BRing when it is used to accumulate intermediate charge state particles. The vacuum pressure bump due to the ion-induced desorption in turn leads to an increase in beam loss rate. In order to accumulate the beams to higher intensity to fulfil the requirements of physics experiments and for better understanding of the dynamic vacuum pressure caused by the beam loss, a dynamic vacuum pressure simulation program has been developed. Vacuum pressure profiles are calculated and compared with the measured data based on the current synchrotron (CSRm). Then the static vacuum pressure profiles of the BRing and one type of pump which will be used in the BRing are introduced in this paper.

### INTRODUCTION

The HIAF project consists of ion sources, Linac accelerator, synchrotrons and several experimental terminals. The Superconducting Electron-Cyclotron-Resonance ion source (SECR) is used to provide highly charged ion beams, and the Lanzhou Intense Proton Source (LIPS) is used to provide  $H_2^+$  beam. The superconducting ion Linac accelerator (iLinac) is designed to accelerate ions with the charge-mass ratio  $Z/A=1/7$  (e.g.  $^{238}U^{34+}$ ) to the energy of 17 MeV/u. Ions provided by iLinac will be cooled, accumulated and accelerated to the required intensity and energy (up to  $1.4 \times 10^{11}$  and 800 MeV/u of  $^{238}U^{34+}$ ) in the Booster Ring (BRing), then fast extracted and transferred either to the external targets or the Spectrometer Ring (SRing). As a key part of the HIAF complex, SRing is designed as a multifunction experimental storage ring. A TOF detector system will be installed for nuclei mass measurements with isochronous mode. An electron target with ultra-low temperature electron beam will be built for Dielectronic Recombination (DR) experiments. Both stochastic cooling and electron cooling systems are considered to be equipped in order to provide high quality beams for experiments and compensate energy losses of internal target experiments. MRing is used for the ion-ion merging [1]. The layout of the HIAF project is shown in Fig. 1.

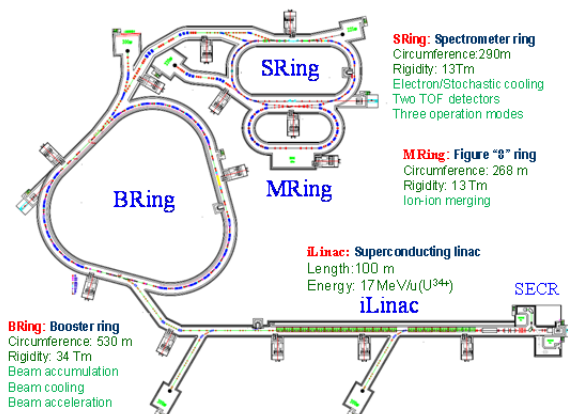


Figure 1: Layout of HIAF project.

## CSRm VACUUM PRESSURE PROFILE

### Static Pressure Profiles

The HIRFL-CSR complex consists of the main cooler storage ring (CSRm), Radioactive Ion Beam line (RIB) production and transfer line two (RIBLL2), experimental storage ring (CSRe), and experimental stations. The two existing cyclotrons, the Sector Focus Cyclotron and Separated Sector Cyclotron, at the Heavy Ion Research Facility in Lanzhou (HIRFL) are used as the injector system. The heavy ion beams from HIRFL are injected into the CSRm, then accumulated, electron cooled, and accelerated, before being extracted to the CSRe for internal target experiments and other physics experiments [2].

CSRm is a racetrack shape synchrotron that consists of four arc sections with the circumferences of 161.00 m. Each arc section is composed of four dipoles, five focusing quadrupoles, and three defocusing quadrupoles.

The total volume of the CSRm vacuum system is about 7200 L and the total inner surface is about 160 m<sup>2</sup> (not including the equipment inside the vacuum system). Sputter ion pumps (SIP) and titanium sublimation pumps (TSP) are selected as the main pumps, which are distributed in about 4 m along the rings according to the calculation. Sputter ion pumps with pumping speeds of 200–400 l/s remove non-getterable gases such as methane and argon. Titanium sublimation pumps have a high capacity for hydrogen at very low pressure, where the residual gas is mainly H<sub>2</sub> (90%). The pumps have an area of 5000 cm<sup>2</sup> of sublimated titanium and a pumping speed of approximately 2000 l/s for active gases [3].

The dynamic vacuum pressure calculation method which developed from the VAKDYN code [4] is implemented to calculate the equilibrium pressure profile for the CSRm. The newly developed simulation code is named as HIAF-DYSD. For the computation of the

<sup>†</sup> LIPENG@IMPCAS.AC.CN

# TRANSVERSE BEAM SPLITTING MADE OPERATIONAL: RECENT PROGRESS OF THE MULTI-TURN EXTRACTION AT THE CERN PROTON SYNCHROTRON

A. Huschauer\*, J. Borburgh, S. Damjanovic, S. S. Gilardoni, M. Giovannozzi, M. Hourican,  
K. Kahle, G. Le Godec, O. Michels, G. Sterbini, CERN, Geneva, Switzerland  
C. Hernalsteens, Ion Beam Applications, Louvain-la-Neuve, Belgium

## Abstract

Following a successful commissioning period, the Multi-Turn Extraction (MTE) at the CERN Proton Synchrotron (PS) has been applied for the fixed-target physics programme at the Super Proton Synchrotron (SPS) since September 2015. This exceptional extraction technique was proposed to replace the long-serving Continuous Transfer (CT) extraction, which has the drawback of inducing high activation in the ring. MTE exploits the principles of non-linear beam dynamics to perform loss-free beam splitting in the horizontal phase space. Over multiple turns, the resulting beamlets are then transferred to the downstream accelerator. The operational deployment of MTE was rendered possible by the full understanding and mitigation of different hardware limitations and by redesigning the extraction trajectories and non-linear optics, which was required due to the installation of a dummy septum to reduce the activation of the magnetic extraction septum. The results of the related experimental and simulation studies, a summary of the 2015 performance analysis, as well as more recent performance improvements are presented in this paper.

## INTRODUCTION

To provide high-intensity beams for fixed target physics at the SPS, the longitudinal structure delivered by the PS has to comply with certain requirements. In order to reduce beam loading and to provide an almost continuous spill towards the experimental facilities, uniform filling of the SPS is desired. Considering that the length of the SPS is about eleven times the circumference of the PS, and that a gap for the rise time of the SPS kickers is needed, the non-resonant CT process was proposed in 1973 [1]. This extraction technique, which occurs over five turns at 14 GeV/c, allows to optimize the duty cycle as only two subsequent extractions from the PS are necessary. On the downside, the CT extraction comes with the major drawback of significant beam loss occurring at multiple locations around the ring [2], leading to high dose to personnel during accelerator repair and maintenance as well as to long cool down times.

Therefore, the MTE technique was proposed to replace the CT process in 2001 [3]. MTE is a resonant extraction mechanism, which exploits advanced concepts of non-linear beam dynamics and applies a fourth order stable resonance to perform beam splitting in the horizontal phase space. The

resulting beamlets - one core and four islands - are then extracted over five turns.

Due to the complexity of the MTE scheme, its operational implementation has had to overcome many challenges. In 2010, about one month of operational experience could be gathered with this novel technique, and two major issues were identified [4]:

- (1) significant fluctuations in the efficiency of the transverse splitting, the losses at extraction and the trajectories in the transfer lines, and
- (2) unacceptably high radioactive activation of the magnetic extraction septum (SMH16).

In order to overcome the second problem, a so-called dummy septum (TPS15), i.e. a passive absorber to shield SMH16, was developed and installed in straight section (SS) 15 of the PS during the Long Shutdown 1 (LS1) between 2013 and 2014 [5]. A certain fraction of the losses during the extraction is intrinsic to the process itself and the debunched longitudinal structure of the beam: during the rise time of the fast kickers, the continuous beam is swept from the internal to the external side of SMH16, causing unavoidable beam loss. Using TPS15, the activation of SMH16 can be reduced by relocating these losses from SS16 to the well-shielded SS15. It was only after the installation of this device that the MTE commissioning could be resumed.

In this paper, several experimental and simulation studies are presented, which allowed to increase the understanding of the MTE process and eventually led to the implementation of appropriate measures to overcome the two aforementioned problems. As a result of these studies, the MTE process was operationally deployed and has been used to deliver high-intensity beams to the SPS as of September 2015. Since then, it has successfully replaced the CT extraction [6].

Furthermore, an analysis of the MTE performance in 2015 and recent operational improvements, which aim at increasing the robustness of this extraction technique, are discussed.

## PERIODIC OSCILLATIONS OF THE SPLITTING EFFICIENCY

The efficiency of the transverse splitting is the natural figure-of-merit of the MTE performance and is defined as

$$\eta_{\text{MTE}} = \frac{\langle I_{\text{Island}} \rangle}{I_{\text{Total}}}, \quad (1)$$

where  $\langle I_{\text{Island}} \rangle$  and  $I_{\text{Total}}$  stand for the average intensity in each island and the total beam intensity, respectively. The

\* alexander.huschauer@cern.ch

# MACHINE ELEMENT CONTRIBUTION TO THE LONGITUDINAL IMPEDANCE MODEL OF THE CERN SPS

T. Kaltenbacher\*, F. Caspers, C. Vollinger  
CERN, Geneva, Switzerland

## Abstract

This contribution describes the current longitudinal impedance model of the SPS and studies carried out in order to improve, extend and update it. Specifically, new sources of impedances have been identified, evaluated and included in the model. One finding are low Q and low-frequency (LF; here below 1 GHz) resonances which occur due to enamelled flanges in combination with external cabling e.g. ground loops. These resonances couple to the beam through the gap with enamel coating which creates an open resonator. Since this impedance is important for beam stability in the CERN Proton Synchrotron (PS), RF by-passes were installed on the enamelled flanges, and their significance for the SPS beam is currently under investigation. Simulations, bench and beam measurements were used to deduce model parameters for beam dynamic simulations.

## INTRODUCTION

A significant SPS upgrade is mandatory in order to meet the expectations for the planned LHC upgrade scenarios [1] since there are still intensity limitations apparent for future high-intensity LHC beams [2, 3]. Beam measurements and the current longitudinal beam coupling impedance model of the SPS [4] have unveiled the main contributors to the resistive impedance which are vacuum flanges, and the 200 MHz cavities to name but a few. The main contributor to the high R/Q impedances are the kicker magnets and again the 200 MHz cavities [3].

Vacuum flanges in the SPS were found to be responsible for single- and multi-bunch longitudinal instabilities. Therefore, an impedance reduction campaign of these vacuum flanges (VF) during the Long Shutdown 2 (LS2 in 2019) is LIU baseline. However, it is not yet clear if the flange insulation has to be maintained or not. In order to answer this question, a campaign is planned during a technical stop in 2016 [5] to shortcircuit all insulated VF of the 109 QF (quadrupole focusing magnet) short straight sections (SSS) by so-called soft clamps. Detailed beam parameter measurements before and after the deployment of these soft clamps will provide the basis for the decision whether the VF can maintain their enamel insulation or not. Based on this decision, the current flange shield design for impedance reduction will have to be reviewed or can be kept. This is very important, since many of the positions that have to be shielded are equipped with enamelled flanges. In the PS [6], insulated vacuum flanges are used to avoid eddy currents induced by fast ramping (ramp rates  $\approx 2.3$  T/s) of C-shaped magnet, and to avoid that ground loops are closed via the

beam pipe. From measurements, it could be shown that the flange capacitance and the connected CBN (ground loops) form a resonator with a resonant frequency of about 1.5 MHz which had to be dampened with by means of RF-bypasses. As before for the PS, also in the SPS, the enamelled flanges were introduced to avoid eddy current propagation along the beam pipe, and in addition to allow a sectorising of the vacuum system such that only *one* ground connection is installed at each half-cell (approx. every 32 m). In the SPS however, the ramping rates of H-window magnets are about 10 times slower than in the PS and induced net currents on the beam pipe are thus considerably smaller as well. From laboratory measurements, it could be shown that the induced current from focusing quadrupole magnets (QF) is below 1.5 A and from defocusing quadrupole magnets (QD) less than 200 mA. In addition, from measurements, it could be shown that in the SPS, a resonator which is formed by the flange capacitance and the ground loop, is resonating at about 2.5 MHz. The same measurements also indicated a number of resonances at higher frequencies, i.e. at about 20 MHz, about 60 MHz, and higher. It should be mentioned already here that these resonances show a spread around the indicated frequencies due to slight variations in the grounding loop lengths and topology, as is illustrated in Fig. 1. Consequently, the current impedance model has to be extended to include these low-frequency resonances occurring due to enamelled flanges.

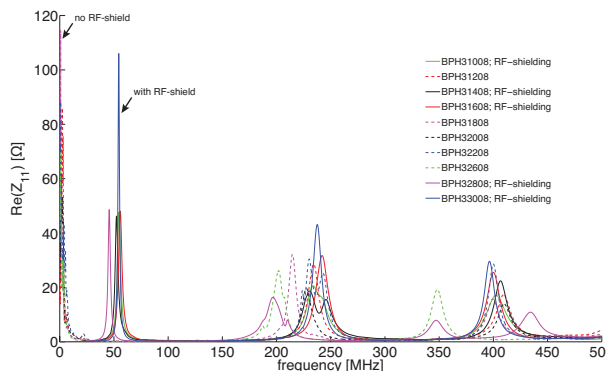


Figure 1: Differentially measured reflection coefficient  $S_{11}$  was used to calculate the real part of input impedance  $Z_i - Re(Z_i)$  - of 10 QF SSS with and without RF-shield.

## MEASUREMENTS

In order to evaluate these low frequency resonances, two different type of measurements were performed with a vector network analyser (VNA) in the SPS. Firstly, measurements of reflection S-parameters ( $S_{11}$ ) were carried out to obtain

\* Thomas.Kaltenbacher@cern.ch

# THE SPS 200 MHz TWC IMPEDANCE AFTER THE LIU UPGRADE

T. Roggen<sup>\*†</sup>, R. Calaga, F. Caspers, T. Kaltenbacher, C. Vollinger,  
CERN, Geneva, Switzerland

## Abstract

As a part of the LHC Injectors Upgrade project (LIU) the 200 MHz Travelling Wave Cavities (TWC) of the Super Proton Synchrotron (SPS) will be upgraded. The two existing five-section cavities will be rearranged into four three-section cavities (using two existing spare sections), thereby increasing the total voltage from 7 MV ( $I_{RF} = 1.5$  A, current LHC) to 10 MV ( $I_{RF} = 3.0$  A, HL-LHC) [1, 2]. Projections of the HL-LHC (High Luminosity Large Hadron Collider) era are conceived by the macro-particle simulation code BLoND [3], that makes use of an impedance model of the SPS, developed from a thorough survey of machine elements [4]. This paper analyses the impedance contribution of the 200 MHz cavities in the two configurations, using electromagnetic simulations. Measurements of the existing cavities in the SPS and a single-section prototype are also presented.

## INTRODUCTION

The 200 MHz TWC system of the SPS currently consist of two four-section cavities and two five-section cavities. To guarantee stability of the future HL-LHC beams in the SPS, the required controlled longitudinal emittance blow-up will have to be increased. This implies a larger bucket and voltage amplitude, but one must not forget that the increased intensity will also cause more beam loading in the cavities, which has to be compensated by the RF system as well. The existing two five-section cavities with the available 1 MW power plant will struggle with the future HL-LHC beams, and solutions were proposed in [1]. The two existing five-section cavities will be rearranged into four three-section cavities (using two existing spares), and two additional power plants of 1.4 MW/cavity are foreseen. The two four-section cavities will remain in their current configuration. This will not only be beneficial for the fundamental mode, but the total impedance will reduce by 20% in this new configuration [1].

For projections of the HL-LHC era requirements, the macro-particle simulation code BLoND [3] is used. It relies on an impedance model of the SPS, developed from a thorough survey of machine elements [4]. In this paper the impedance contribution of the 200 MHz cavities in the two configurations is assessed using measurements taken in situ in the tunnel, laboratory measurements of a single section on the surface and electromagnetic simulations (CST Studio Suite [5]). In particular, attention will go to the 628 MHz Higher Order Mode (HOM) couplers, since recent studies showed that the intensity threshold for beam stability can be

improved when, amongst others, the impedance contribution of the longitudinal 628 MHz HOM is reduced at least by a factor of 2 [6, 7].

## SINGLE SECTION CAVITY

### General Description

The currently installed SPS 200 MHz TWC system, described in [8], consists of two four-section cavities and two five-section cavities. A single section of 11 cells is available on the surface as well for additional measurements. This 11-cell section is a spare section, which is closed, as in the tunnel, by two lids to allow measurements. No power couplers are installed on this section and as for the HOM couplers only the four 628 MHz HOM couplers with detachable 50  $\Omega$  loads are put into place (Fig. 1). The couplers for the longitudinal 938 MHz HOMs and the couplers for the transverse 460 MHz HOMs were not installed. This choice is motivated by two aspects: In the first place their effect on the 628 MHz HOM damping is considered minimal to non-existing. In the second place, and more importantly, the single-section cavity study was done to reassure that a known setup could be modelled and simulated correctly. The requirement for the model is that it represents exactly the laboratory setup, and as such a laboratory setup with as little (unnecessary) complexity as possible is an obvious choice. It should be noted that spare 938 MHz HOM couplers are available, in the event this would be desired. On the other hand, no spare 460 MHz HOM couplers were available. Typical transmission and reflection measurements were performed between two probes, mounted on the beam pipe axis, between different 628 MHz HOM couplers, or combinations of both. In addition, the RF voltage feedback pick-up loops, used to measure the Fundamental Pass Band (FPB) field flatness, served as a measurement interface with the cavity as well.

Table 1: Resonant measurements of the SPS 200 MHz single-section cavity around 628 MHz, with no loads on the 628 MHz HOM couplers.

| Freq [MHz] | R/Q [ $\Omega$ ] | $Q_0$ |
|------------|------------------|-------|
| 624.3      | 0.5              | 18400 |
| 626.8      | 10               | 22300 |
| 628.8      | 56               | 18000 |
| 631.6      | 27               | 19500 |
| 634.3      | 4.6              | 17800 |

<sup>\*</sup> Fellowship co-funded by the European Union as a Marie Curie action (Grant agreement PCOFUND-GA-2010-267194) within the Seventh Framework Programme for Research and Technological Development.

<sup>†</sup> toon.roggen@cern.ch

# THE NEW HL-LHC INJECTION AND TRANSPORT PROTECTION SYSTEM

F. M. Velotti<sup>1</sup>, W. Bartmann, C. Bracco, M. A. Fraser, B. Goddard, V. Kain, A. Lechner, M. Meddahi, CERN, Geneva, Switzerland

<sup>1</sup> also at EPFL, Lausanne, Switzerland.

## Abstract

The High-Luminosity LHC (HL-LHC) upgrade represents a challenge for the full chain of its injectors. The aim is to provide beams with a brightness a factor of two higher than the present maximum achieved. The 450 GeV beams injected into the LHC are directly provided by the Super Proton Synchrotron (SPS) via two transfer lines (TL), TI2 and TI8. Such transfer lines are both equipped with a passive protection system to protect the LHC aperture against ultra-fast failures of the extraction and transport systems. In the LHC instead, the injection protection system protects the cold apertures against possible failures of the injection kicker, MKI. Due to the increase of the beam brightness, these passive systems need to be upgraded. In this paper, the foreseen and ongoing modifications of the LHC injection protection system and the TL collimators are presented. Simulations of the protection guaranteed by the new systems in case of failures are described, together with benchmark with measurements for the current systems.

## INTRODUCTION

The high brightness of the HL-LHC beams represent an unprecedented challenge for the full set of the passive protection devices of the LHC injection and transport system. An upgrade of the main injection absorber, TDI, is foreseen in order to maintain the necessary protection of the LHC cold aperture. Also, the SPS-to-LHC transfer line collimators will be replaced with more suitable devices for the aimed beam brightness.

The LHC injection system is composed by: injection septum MSI, injection kicker MKI, injection dump TDI and two auxiliary absorbers TCLIA and TCLIB; all acting on the vertical plane. The HL-LHC injection system will not be too different from the present one. The main modification is represented by the new TDI, i.e. the segmented TDI (TDI-S).

The TDI-S will be composed by three separated blocks: the first two blocks will be 1.425 m, made of Graphite (R4550 or similar), the last one instead will be made of higher Z material (60 cm of Aluminium and 70 cm of Copper). Every block will be separated from each other by 125 cm and the last block is also 2 mm further away from the circulating beam than the others to avoid direct impact of the beam. This is the design baseline at the moment of writing this paper.

Among the other modifications, it is worth to mention also

the slightly different crossing and separation schemes as well as the upgrade of the transfer line collimators (TCDI). The TCDIs upgrade represents a key upgrade because the aperture of the LHC (especially the horizontal one) during the transport from the SPS is directly protected only by these collimators. They are designed to protect the LHC and the MSI from any kind of failures of the SPS extraction and TL elements.

The protection against fast losses relies on prompt detection of the change in field of the magnet under observation. The MSI (its time constant is about 1 s) is constantly monitored from different systems (Fast Extraction Interlock and Fast Magnet Current Monitor), which guarantee an adequate protection and redundancy. For ultrafast failures of the SPS extraction kickers, the TCDIs represent the last resort to protect the MSI and the LHC arc aperture.

In case of ultrafast failure of the LHC injection kicker instead, the LHC (HL-LHC) injection protection devices are the one responsible to for the protection of the vertical LHC aperture. The TDI (TDI-S) is the main protection against MKI failures - it is installed about 90° vertical phase-advance from the MKI to maximise the protection guaranteed. The TCLIA and TCLIB protect against possible phase-advance errors between MKI and TDI; they are placed at  $\Delta\mu_y \approx 180^\circ + 20^\circ$  and  $\Delta\mu_y \approx 360^\circ - 20^\circ$  from the TDI respectively.

In this paper the following notation will be used:

$$\sigma_{LHC} \equiv \sqrt{\beta(s) \text{ 3.5 mm mrad}/(\beta\gamma)} \quad (1)$$

$$\sigma_{HLLHC} \equiv \sqrt{\beta(s) \text{ 2.5 mm mrad}/(\beta\gamma)}, \quad (2)$$

where  $\beta(s)$  is the beta-function at an  $s$  location and  $(\beta\gamma)$  is the product of the relativistic factors.

## TRANSFER LINE COLLIMATORS

The main aim of the TL collimators is to ensure adequate protection of the LHC cold apertures. From the LHC Design Report [1], the minimum available aperture in the arc is  $7\sigma_{LHC}$ , hence this represents the target protection for the TL collimation system.

In order to define the collimator jaws aperture needed to guarantee the above cited protection, all possible sources of error have to be taken into account. All the considered errors are listed in Table 1; summing these contributions linearly, considering a typical beam size of 0.5 mm, the total error is  $\approx 1.4\sigma_{LHC}$  [2]. The maximum escaping amplitude in a "three-phase" collimation system is given by pure geometrical considerations, i.e.  $A_{max} = A_{jaw}/\cos(\pi/6)$ ; where  $A_{jaw}$  is the required jaw position, including errors. For the

# CORRECTOR MAGNETS FOR THE CBETA AND eRHIC PROJECTS AND OTHER HADRON FACILITIES\*

N. Tsoupas<sup>†</sup>, S. Brooks, A. Jain, F. Meôt, V. Ptitsyn, and D. Trbojevic  
 Brookhaven National Laboratory, Upton, NY 11973, USA

## Abstract

The CBETA project [1] is a prototype electron accelerator for the proposed eRHIC project [2]. The electron accelerator is based on the Energy Recovery Linac (ERL) and the Fixed Field Alternating Gradient (FFAG) principles. The FFAG arcs of the accelerator are comprised of one focusing and one defocusing quadrupoles which are designed as either, iron dominated or Halbach-type permanent magnet quadrupoles [3]. We present results from 2D and 3D electromagnetic calculations on corrector electromagnets for both the iron dominated, and Halbach type quadrupoles.

## INTRODUCTION

The proposed eRHIC accelerator [2] will collide 20 GeV polarized electrons with 250 GeV polarized protons or 100 GeV/n polarized  $^3\text{He}^{+2}$  ions or other non-polarized heavy ions. The electron accelerator of the eRHIC will be based on a 1.665 GeV Energy Recovery Linac (ERL) placed in the RHIC tunnel with two recirculating rings placed also in the RHIC tunnel alongside the hadron RHIC accelerator. Fig. 1 is a schematic diagram of the eRHIC accelerator showing the hadron accelerator (blue ring), and the electron accelerator (red ring).

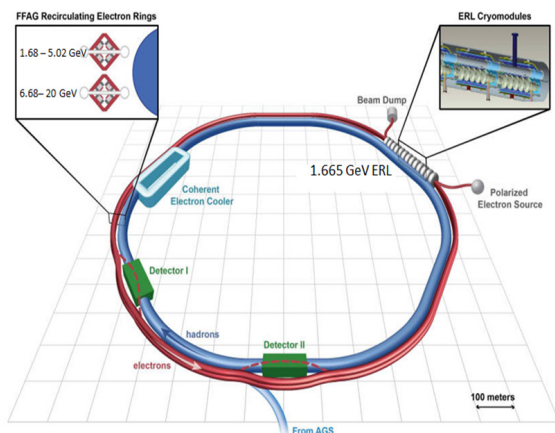


Figure 1: Schematic diagram of the eRHIC accelerator. The blue and red rings are the hadron and the electron accelerators respectively. The right insert is the ERL and the left insert is a cross section of the two FFAG rings of the electron accelerator. The green rectangles are the experimental areas for the electron-hadron collisions.

\* Work supported by the US DOE

<sup>†</sup> tsoupas@bnl.gov

The 1.655 GeV ERL is shown as insert in the top right corner and the cross section of the two recirculating electron rings shows in the insert on the top left corner. The experimental areas of the electron-hadron collisions are the green rectangles. Two important concepts are involved in the electron accelerator, namely, the ERL and the FFAG concepts. The ERL concept provides 1.665 GeV of energy to the electron bunches each time they pass through the ERL for the electrons to achieve the top energy of the 20 GeV before the collision with the hadrons. Following the collision the electrons deliver back to the ERL the 20 GeV of energy by recirculating 12 times through the ERL, each time delivering to the ERL 1.665 GeV of energy. Since it takes 12 passes for the electrons to achieve the 20 GeV of energy, and also 12 passes to give back the energy to the ERL, the electron bunches circulating in the accelerator have 12 different energies, ranging from 1.685 to 20 GeV. The three electron bunches with the energies 1.685, 3.350 and 5.015 GeV are circulating in one FFAG arc and the rest of the bunches with energy range from 6.68 GeV to 12.0 GeV in the second FFAG arc. Thus this FFAG places electron bunches with large energy range in a small transverse distance of ~22 mm in each of the FFAG arcs. The CBETA which is the prototype of the eRHIC accelerator will employ both, the ERL and FFAG concepts and is under construction in Cornell University. Fig.2 is a layout of the accelerator showing the ERL (LA) the FFAG sections (FA, ZA, ZB, and FB) and the splitter/merger sections (TX, SX).

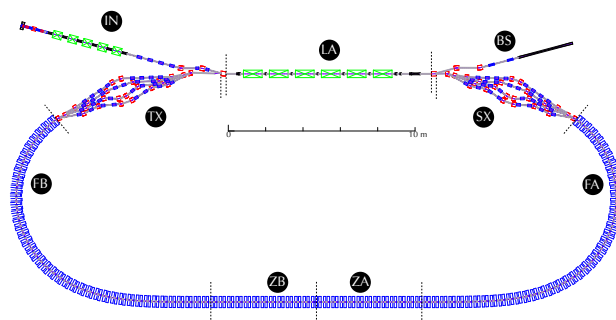


Figure 2: Layout of the CBETA accelerator. The section labeled (LA) is the ERL, The sections labeled (FA), (ZA), (ZB), and (FB) are the FFAG which will accommodate 4 energies of the recirculating electron bunches.

The FFAG arcs for either eRHIC or CBETA accelerators consists of FODO cells, each cell comprised of one focusing and one defocusing quadrupole. The top plot in Fig. 3 shows the orbits, the middle plot the  $\beta_{x,y}$  functions, and the bottom the  $\eta_{x,y}$  dispersion functions of the electron bunches with

# MITIGATION OF NUMERICAL NOISE FOR BEAM LOSS SIMULATIONS

F. Kesting<sup>\*1,2</sup>, G. Franchetti<sup>2,1</sup>

<sup>1</sup> Institute for Applied Physics (IAP), University of Frankfurt, Germany

<sup>2</sup> GSI, 64291 Darmstadt, Germany

## Abstract

Numerical noise emerges in self-consistent simulations of charged particles, and its mitigation is investigated since the first numerical studies in plasma physics [1–3]. In accelerator physics, recent studies find an artificial diffusion of the particle beam due to numerical noise in particle-in-cell tracking [4], which is of particular importance for high intensity machines with a long storage time, as the SIS100 at FAIR [5] or in context of the LIU upgrade [6] at CERN. In beam loss simulations for these projects artificial effects must be distinguished from physical beam loss. Therefore, it is important to relate artificial diffusion to artificial beam loss, and to choose simulation parameters such that physical beam loss is well resolved. As a practical tool, we therefore suggest a scaling law to find optimal simulation parameters for a given maximum percentage of acceptable artificial beam loss.

## HEAVY-ION BEAM LOSSES

The uncontrolled loss of charged particles is an important issue in high energy particle accelerators. For 1 GeV proton beams, it was found that 1 W/m is the maximum tolerable beam loss to allow hands-on-maintenance [7]. If more the energy is deposited, a worker would be exposed a too high dose during maintenance, and hence a health hazard.

However, this limit of energy deposition is only valid for 1 GeV proton operation. According estimates for heavy-ion machines were only found recently [8] by dedicated simulation studies in which a uniform beam loss along a beam pipe is considered. The pipe is irradiated for 100 days, while the effective dose rate was calculated four days after the radiation stopped. Then, the residual activity is compared to the residual activity caused by 1 GeV protons, in order to infer a scaling law for heavy ions. Using this scaling law, we estimate the maximum acceptable beam loss per run in the SIS100 for U<sup>+28</sup> particle beams at different energies, see the Table 1.

Table 1: Maximum Acceptable Beam Loss

| part. energy | energy dep. | # particles         |
|--------------|-------------|---------------------|
| 200 MeV/u    | 75 W/m      | $1.1 \cdot 10^{13}$ |
| 500 MeV/u    | 23 W/m      | $1.3 \cdot 10^{12}$ |
| 1000 MeV/u   | 12 W/m      | $3.4 \cdot 10^{11}$ |

The design goal of the SIS100 is a maximum of  $5 \cdot 10^{11}$  particles of U<sup>+28</sup> stored in the machine, such that only the loss of a full 1GeV/u Uranium beam depicts a hazard. For

\* f.kesting@gsi.de

particle beams with less energy a complete, but uniform, beam loss can be tolerated.

Further, beam loss may cause a heating of superconducting structures, such that the material changes to the normal conducting phase. This may lead to a serious machine damage, or at least will require maintenance, and thus an interruption of beam time. It was found at the Large Hadron Collider (LHC) at CERN, that a nominal beam loss of the order of  $10^{-6}$  corresponding to  $10^6$  protons can cause a magnet quench [9]. The limit on the nominal beam loss for the LHC is exceptionally small, because the beam energy and the and the intensity are very high compared to other machines. Simulation studies on the superconducting magnets of the SIS100 synchrotron at FAIR show that there is no risk of a magnet quench [10].

The lifetime of organic insulators and protection diodes in superconducting magnets is expected to give the most restrictive limit to beam loss for the SIS300 synchrotron. It was found in simulation studies that a maximum of 2 percent nominal beam loss can be tolerated for this machine [11].

In summary, the maximum acceptable beam loss varies greatly for various scenarios, such that different upper bounds are required for artificial beam loss in numerical simulations.

## ARTIFICIAL BEAM LOSS

In the following chapter, we present an analytic model to predict artificial beam loss induced by numerical noise in particle-in-cell tracking. Beam loss occurs whenever the emittances of a single particle  $i$  are larger than the acceptance of the machine. A collimator allows controlled particle loss, as particles with large amplitudes can be removed without activating the accelerator structures. By adjusting the geometry of a collimator, the acceptance of a machine can be set to the required size. The rms emittance of a particle beam is given by

$$\epsilon_x = \sqrt{\langle x^2 \rangle \langle x'^2 \rangle - \langle x x' \rangle^2}, \quad (1)$$

and accordingly for the  $y$ -plane. Here,  $\langle \cdot \rangle$  is the moment of the according coordinate, and

$$\langle x^2 \rangle = \sigma_x^2 \quad \langle x'^2 \rangle = \sigma_{x'}^2, \quad (2)$$

are the variances of the phase space coordinates, which quantify the beam size.

The rms emittance of a beam grows linearly in the presence of numerical noise, as long as numerical noise is weak and not correlated. The average emittance growth per integration step of length  $\Delta s$  was derived from a single particle

# STATUS OF THE BEAM INSTRUMENTATION SYSTEM OF CSNS

J.L. Sun<sup>#</sup>, W.L. Huang, P. Li, F. Li, M. Meng, R.Y. Qiu, J.M. Tian, Z.H. Xu, T Yang, L. Zeng, T.G. Xu<sup>#</sup>, Institute of High Energy Physics, Chinese Academy of Sciences, China

## Abstract

The beam instrumentation system has been developed to tune and investigate the high intensity proton beam in the China Spallation Neutron Source (CSNS) project. All the physical design of the monitors has been finished and start the system set up procedure. Many kinds of beam monitors are required to measure wide dynamic range of the beam parameters, e.g. intensity, energy. Construction and application of beam monitor system are described in this paper and the first test results during the RFQ and DTL1 commissioning will be introduced also.

## INTRODUCTION

The CSNS is designed to accelerate proton beam pulses to 1.6 GeV kinetic energy at 25 Hz repetition rate, striking a solid metal target to produce spallation neutrons. The accelerator provides a beam power of 100 kW on the target in the first phase. It will be upgraded to 500 kW beam power at the same repetition rate and same output energy in the second phase. A schematic layout of CSNS phase-1 complex is shown in Figure 1. In the phase one, an ion source produces a peak current of 25 mA H- beam. RFQ linac bunches and accelerates it to 3 MeV. DTL linac raises the beam energy to 80 MeV. After H- beam is converted to proton beam via a stripping foil, RCS accumulates and accelerates the proton beam to 1.6 GeV before extracting it to the target [1, 2].

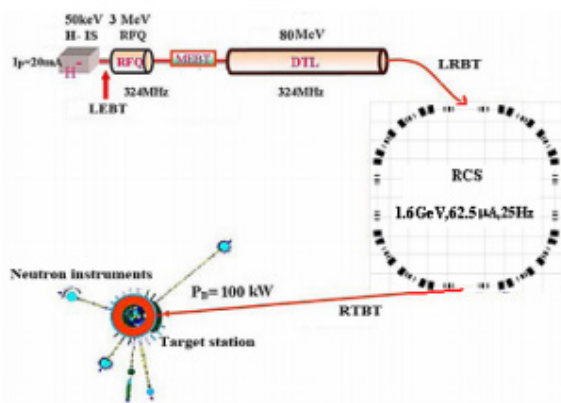


Figure 1: Schematics of the CSNS complex.

## BEAM MONITORS

For the entire beam instrumentation system of CSNS, amounts of beam monitors are installed along the beam line, including beam position monitor (BPM), beam current monitor, beam profile monitor, beam loss monitor (BLM) and so on. Layout of the beam instrumentation system as shown in Figure 2.

<sup>#</sup>sunjl@ihep.ac.cn, xutg@ihep.ac.cn

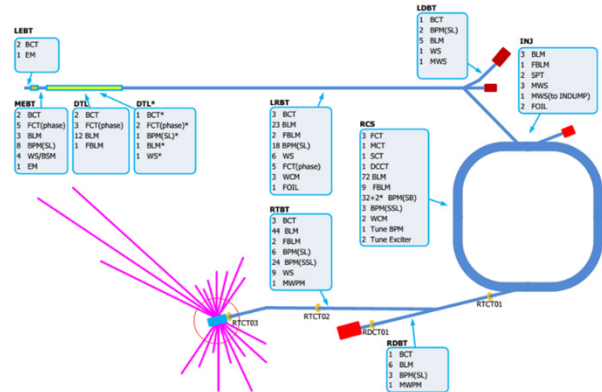


Figure 2: Layout of the beam instrumentation system of CSNS.

## Beam Current Monitor

Two types of current transformers have been developed, the fast current transformer (FCT) and normal CT. FCT has a response time less than 300 ps, and used to measure the beam energy by using the TOF method, there are 5 FCT installed in the MEBT after the RFQ, and four of them were used to measure the beam energy during the RFQ commissioning, as shown in Figure 3. The measurement result is 3.1 MeV while the design energy is 3.0 MeV.

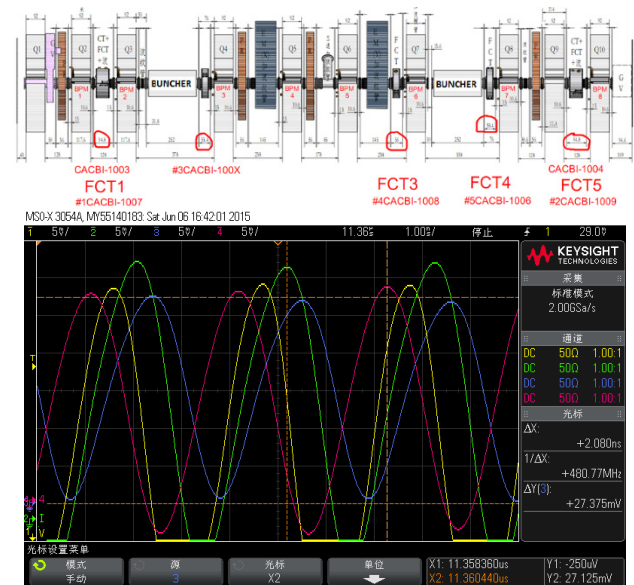


Figure 3: Layout of the MEBT, 5 FCT are labeled by red circle (up) and the beam phase measured by an oscilloscope (down).

Wall current monitor (WCM) is another way to measure the beam current. Two different design were finished based on different requirements. The WCM for LINAC as

# XAL APPLICATIONS DEVELOPMENT FOR CSNS TRANSPORT LINES

Yong Li, W.B Liu, Z.P Li, J. Peng

Dongguan Campus, Institute of High Energy Physics, Dongguan 523803, China

## Abstract

XAL is an application programming framework initially developed at the Spallation Neutron Source (SNS). It has been employed as a part of control system via connection to EPICS to provide application programs for beam commissioning at the China Spallation Neutron Source (CSNS). Several XAL-based applications have been developed for Beam Transport line at CSNS and successfully applied in the MEBT and DTL-1 beam commissioning. These applications will be discussed in this paper.

## INTRODUCTION

The CSNS, including of proton accelerator, target station and neutron spectrometers, is a large facility to produce neutron by 1.6 GeV protons colliding a target of heavy metal [1]. The accelerator is mainly composed of a linac with a modest but upgradable energy and a rapid cycling synchrotron (RCS) of the fixed energy at 1.6 GeV. The installation and beam commissioning of the front end of linac, medium energy beam transport line (MEBT) and first section of the drift tube linac (DTL-1) was finished. The beam commissioning of DTL2-4 and the linac to ring beam transport line (LRBT) is upcoming this September.

XAL [2] is a Java framework for developing accelerator physics applications for the commissioning and operation of the SNS. It was used and developed by many accelerator laboratories, e.g. SNS, SLAC, FRIB, LANL, etc. XAL was designed to be extensible and has evolved to support ongoing accelerator operations. CSNS and SNS have lots of similarities in both physics and hardware. Therefore, the XAL was selected as the tool for beam commissioning of CSNS accelerator.

Some of the applications in XAL can be directly used, such as general applications like SCNAD-1D, SCNAD-2D, some physical applications like orbit correction, MPX [3], etc. However, more XAL applications can only be transplanted after appropriate modifications for the reason of the differences of hardware devices or data formats. For example, The PASTA application [4], which is for the adjustment of the phase and amplitude of the cavity, has been changed a lot for CSNS. The reason is that the BPMs were used in SNS for the phase scanning while FCT were used in CSNS. Meanwhile, a number of new XAL-based applications have also been developed, some of which are described as below.

## APPLICATIONS WITH DATABASE

Due to the advantages of data management and data query, database is used by more and more accelerator laboratories for the management of the data with large

volume. According to their own consideration, different database management system was used in different laboratories. The Oracle is used in SNS, the J-PARC choose PostgreSQL, FRIB use MYSQL, and in our case we choose the MYSQL database.

Database related applications are widely used in the beam commissioning. Applications in XAL, like Score [5], PVlogger choose the database to logger signal and restore machine. Some examples of physical applications used database in CSNS will be presented.

## Model Management

Model management is one of the most important applications in the beam commissioning, which is responsible for the management of the lattice model, model storage, lattice calculation, etc.

Based on the lattice and model service architecture diagram [6], the client application was developed to manage models. Fig 1 is the operation interface, which provides three model sources: database, local file, and the XML file. The models will be displayed according to the serial number, model name, date, energy, and comments when connecting to the database. The model can be founded by filtering the letter in the model table or searching by time span. The device information including position, type, the magnet field and cavity field will be displayed in the table below when a model is chosen. We can put the stored values to control system for the selected magnets or certain types of magnets. The lattice calculation for the current model can be carried out and the results also can be displayed with graphics. This function has been embedded in the MPX application.

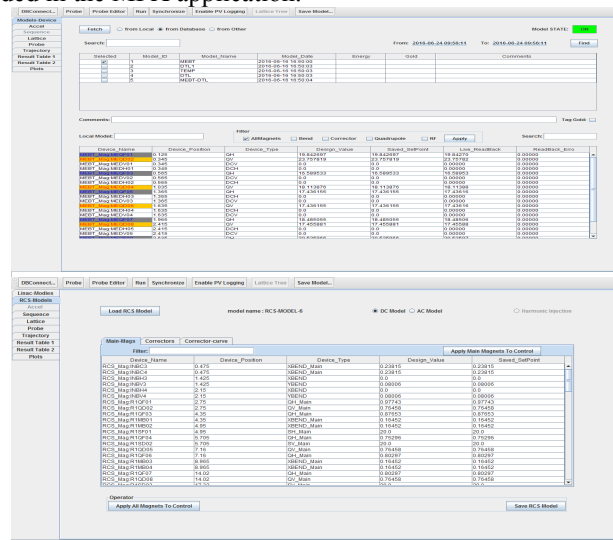


Figure 1: Model management application (The above is for Linac, the below is for RCS).

# SPACE CHARGE EFFECTS OF HIGH INTENSITY BEAMS AT BRING\*

J. Li<sup>#</sup>, J.C. Yang, IMP CAS, Lanzhou, 730000, China

## Abstract

Space charge effects perform one of the main intensity limitations for low energy synchrotron. Large tune spread and crossing resonance stop-bands can hardly be avoided for intensive heavy ion beam at high intensity. Several subjects like Betatron and structure resonance, and tune spread are discussed. Simulations are carried out for  $^{238}\text{U}^{34+}$  focusing on emittance and intensity change during RF capture at the injection energy at the booster ring of the High Intensity heavy ion Accelerator Facility (HIAF).

## INTRODUCTION

The HIAF [1] is a new heavy ion accelerator complex under feasibility study for construction by Institute of Modern Physics (IMP). It consists of two accelerators: a linear accelerator – iLinac (17 MeV/u for  $^{238}\text{U}^{34+}$ , 48 MeV for proton) and a booster ring – BRing (0.2~0.8 GeV/u for  $^{238}\text{U}^{34+}$ , 9.3 GeV for proton). Schematic layout of the HIAF complex is illustrated in Fig. 1. The figure also shows a superconducting ECR ion source and an intense proton source LIPS, a high precision spectrometer ring – SRing (0.2~0.8 GeV/u for  $^{238}\text{U}^{92+}$ ), a merging ring – MRing (0.2~0.8 GeV/u for  $^{238}\text{U}^{92+}$ ), a radioactive beam transfer line – HFRS and five experimental terminals – T1~T5. Considering heavy-ion feature of the HIAF, we focus our study on  $^{238}\text{U}^{34+}$  in this report.

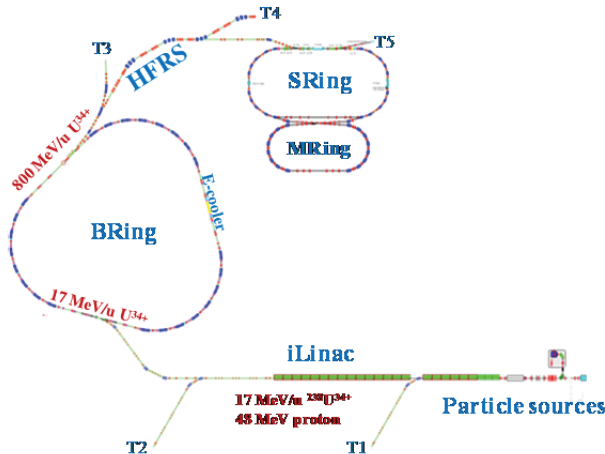


Figure 1: Layout of the HIAF complex.

## OVERVIEW OF THE BRING

The BRing performs the step to increase beam intensity up to space charge limit at the injection energy and to accelerate storage beam to extraction energy, i.e. to accelerate  $1 \cdot 10^{11}$  ions from 17 MeV/u to 0.2~0.8 GeV/u for  $^{238}\text{U}^{34+}$ . It operates under fast cycle mode with 1ms

injection plateau for two-plane painting and slow mode with almost additional 10s reserved for electron cooling. Main parameters of the BRing are summarized in Table 1.

Table 1: Main parameters of the BRing

|                                 |                                  |                           |
|---------------------------------|----------------------------------|---------------------------|
| Circumference                   | 492.53 m                         |                           |
| Super-periodicity               | 3                                |                           |
| Bunching factor                 | 0.35~0.4                         |                           |
| Acceptance (x/y, $\delta p/p$ ) | 200/100 $\pi$ mmrad, $\pm 0.5\%$ |                           |
| Particle type                   | proton                           | $^{238}\text{U}^{34+}$    |
| Injection energy                | 48 MeV                           | 17 MeV/u                  |
| Cycle mode                      | EX+PT (fast)                     | PT (fast)<br>PT+EC (slow) |
| Betatron tune                   | (11.45, 11.42)                   | (8.45, 8.42)              |

\*EX: Charge exchange, PT: painting, EC: electron cooling, fast: fast cycle mode, slow: slow cycle mode.

Lattice of the BRing is three-fold symmetrical with each super-period consists of an eight-FODO-like arc and an about 60 m long dispersion-free straight section featured with the length of 16 m drift reserved for either electron cooler, painting injection, or six RF acceleration cavities. Fig. 2 shows a layout of the BRing Twiss parameters and horizontal beam envelope for one super-period.

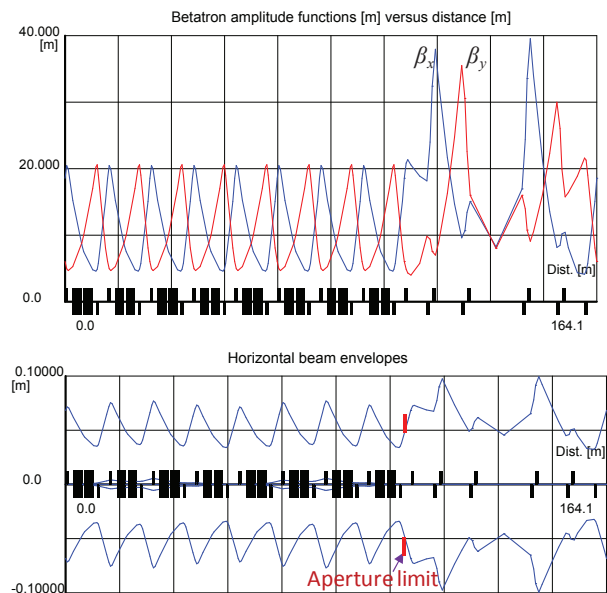


Figure 2: The BRing Twiss parameters and horizontal beam envelope for one super-period.

\*Work supported by NSFC (Grant No. 11475235)  
#lijie@impcas.ac.cn

# OVERVIEW OF THE ESSnuSB ACCUMULATOR RING

M. Olvegård, T. Ekelöf, Uppsala University, Sweden  
 E. Benedetto, M. Cieslak-Kowalska, M. Martini, H. Schönauer, E. Wildner  
 CERN, Geneva, Switzerland

## Abstract

The European Spallation Source (ESS) is a research center based on the world's most powerful proton driver, 2.0 GeV, 5 MW on target, currently under construction in Lund. With an increased pulse frequency, the ESS linac could deliver additional beam pulses to a neutrino target, thus giving an excellent opportunity to produce a high-performance ESS neutrino Super-Beam (ESSnuSB). The focusing system surrounding the neutrino target requires short pulses. An accumulator ring and acceleration of an  $H^-$  beam in the linac for charge-exchange injection into the accumulator could provide such short pulses. In this paper we present an overview of the work with optimizing the accumulator design and the challenges of injecting and storing  $1.1 \cdot 10^{15}$  protons per pulse from the linac. In particular, particle tracking simulations with space charge will be described.

## INTRODUCTION

Starting in a few years, the European Spallation Source (ESS) [1] in Lund, Sweden, will provide users with high-flux spallation neutrons for a large variety of experiments where neutrons are needed as a probe. The neutron production is based on a superconducting high-power proton linac which generates a 2 GeV proton beam with 5 MW average power on target. See Table 1 for a selection of the beam parameters at the end of the ESS linac. This impressively powerful proton driver has drawn the attention of particle physics. In particular, the ESS neutrino Super Beam (ESSnuSB) project plans to use a 5 MW beam from the ESS linac to produce an intense neutrino beam in a dedicated target station [2, 3]. The neutrino super beam will be sent in the direction of Garpenberg, Sweden, 540 km from Lund, where a 0.5 Megaton Water Cherenkov detector is located in an underground mine to detect them. Along the propagation to Garpenberg the neutrinos in the super beam, which consists purely of either muon neutrinos or muon antineutrinos, will oscillate to different flavor states and might thus be detected as muon or electron neutrinos in the Cherenkov detector. The flux of electron and muon neutrinos and antineutrinos will be detected with the aim of discovering and measuring leptonic charge-parity (CP) violation. Leptonic CP violation has been long foreseen and ESSnuSB has a high sensitivity to measure it due to the optimal positioning of the detector at the second oscillation maximum [3].

In order for the experiment to be completed within the planned 10 years of operation, ESSnuSB need the high beam intensity to be preserved all the way from the linac to the target. Firstly, the pulse repetition frequency of the linac must be increased such that the nominal duty factor

Table 1: Nominal Beam Parameters at the End of the ESS Linac

|                       |      |     |
|-----------------------|------|-----|
| Beam energy           | 2.0  | GeV |
| Pulse beam current    | 62.5 | mA  |
| Pulse duration        | 2.86 | ms  |
| Pulse repetition rate | 14   | Hz  |
| Beam power            | 5    | MW  |

of 4% is doubled. In this way 5 MW would be dedicated to the neutron production and another 5 MW to the neutrino generation. Furthermore, the neutrino target station is equipped with a magnetic focusing device, a van der Meer horn, which focuses the secondary pions that are generated as the protons from the ESS hits the target. The horn focuses pions of one sign and defocuses pions of the opposite sign. The sign of the pions to be focused is changed by reversing the direction of the current in the magnet coil. The pions decay predominantly into a muon and a muon neutrino. The former is absorbed before it has time to decay further whereas the latter continues to travel through the earth towards Garpenberg. The neutrino flux at the detector can be optimized by tuning the focusing of the secondary pions. The positively charge pions produce neutrinos and the negatively charged pions produce antineutrinos.

The horn consists of a toroidal magnet where the particle must cross the current conductor to reach the magnetic field region. Roughly 350 kA is needed to generate the necessary field, a current which leads to ohmic heating of the surface [4]. This means that the horn cannot be powered during the 2.86 ms of the duration of the ESS linac pulse. The pulse must be reduced to a few microseconds, while preserving the total beam power delivered to the target. An accumulator ring placed at the end of the linac has been designed for this pulse compression. There, the long pulses from the ESS linac will be transformed into shorter pulses of 1.32  $\mu$ s duration, with a correspondingly increased pulse current. A schematic of the implantation of the ESSnuSB accumulator ring and target station is shown in Fig. 1.

Each pulse from the ESS linac contains  $1.1 \cdot 10^{15}$  protons. The filling of the ring with this very high charge can only be done through injection painting with charge exchange. That means that  $H^-$  ions are accelerated in the linac and transferred to the ring. At the injection point the ions are stripped off their two electrons using a foil, or possibly in the future with laser stripping. This implies that the linac will have to operate alternately with protons and  $H^-$ . The modifications to the linac required for neutrino production have been investigated thoroughly, see [5] for details.

There are several beam pulse configurations available for simultaneous production of neutrons and neutrinos, all of

# LONGITUDINAL PARTICLE TRACKING CODE FOR A HIGH INTENSITY PROTON SYNCHROTRON

M. Yamamoto\*, Japan Atomic Energy Agency, Tokai, Ibaraki 319-1195, Japan

## Abstract

We have been developing a longitudinal particle tracking code to design and investigate the beam behavior of the J-PARC proton synchrotrons. The code simulates the longitudinal particle motion with a wake voltage and a space charge effect. The code also calculates a longitudinal emittance and a momentum filling factor at an rf bucket under the multi-harmonic wake voltage and the space charge effect. The most different point from the other codes is that a revolution frequency of a synchronous particle is exactly calculated from a bending magnetic field pattern, and it is independent of an acceleration frequency pattern. This feature is useful to check an adiabaticity of the synchrotron. We will describe the specification of the code.

## INTRODUCTION

The longitudinal particle tracking code is a powerful tool to investigate the beam behavior in the synchrotron. Although an analytic treatment can be applied for some simple conditions [1], it is very difficult to evaluate the accurate beam behavior under the complicated conditions such as a multi-turn injection, the beam loading effect, the space charge effect, and so on. Many codes has been developed so far and there are some publicly available codes such as ESME [2] and BLoND [3].

We have also been developing a longitudinal particle tracking code for the J-PARC since 1997 [4], and it is aimed at the high intensity proton synchrotron where an acceleration voltage is generated by a Magnetic Alloy (MA) loaded rf cavity [5]. Since the MA cavity has a broadband impedance, we have to pay attention of the beam loading not only for the fundamental acceleration harmonic but also the higher harmonics. The higher harmonics induce the rf bucket distortion, unwanted emittance growth, and they sometimes cause the beam loss.

The J-PARC synchrotrons utilize a multi-harmonic beam loading compensation system by a feedforward method [6, 7]. Our code has been originally developed to estimate how higher harmonics should be compensated. Thereafter, the calculation procedure of the beam emittance and the momentum filling factor under the multi-harmonic beam loading is adapted to check the tolerance of the rf bucket.

We will describe the some basic equations and approaches for simulating the high intensity proton beam. Although the descriptions are only mentioned for the J-PARC, they are also adapted for the other high intensity proton synchrotrons.

\* masanobu.yamamoto@j-parc.jp

## BASIC FEATURES

Our code uses a macro particles of around six thousands per bunch. This number comes from the multi-turn injection at the Rapid Cycling Synchrotron (RCS). The Linac beam is injected into the RCS during 306 turns, and 20 macro particles are injected on each turn. The total number of the macro particles per bunch becomes the multiplication of them.

### Difference Equation of Motion

Our code is based on a difference equation of the longitudinal motion [8] as same as the other codes. Our code choose a time from the beginning of the acceleration as the longitudinal coordinate system although a phase of the sinusoidal wave for the fundamental acceleration voltage is sometimes chosen in the other codes. The basic simultaneous equations are:

$$(\Delta E)_{\text{turn}} = eV_t(t) - \Delta E_s \quad (1)$$

$$(\Delta T_{\text{rev}})_{\text{turn}} = T_{\text{revs}} \left( \frac{1 + \alpha \frac{\Delta p}{p_s}}{1 + \frac{\Delta \beta}{\beta_s}} - 1 \right) \quad (2)$$

The variables in eqs. (1) and (2) are:

|   |   |
|---|---|
| $(\Delta E)_{\text{turn}}$              | Difference of the energy gain per turn between the arbitrary particle and the synchronous one       |
| $(\Delta T_{\text{rev}})_{\text{turn}}$ | Difference of the revolution period per turn between the arbitrary particle and the synchronous one |
| $V_t(t)$                                | Total voltage per turn for the arbitrary particle at a time $t$                                     |
| $\Delta E_s$                            | Energy gain per turn for the synchronous particle   |
| $T_{\text{revs}}$                       | Revolution period for the synchronous particle  |
| $p_s$                                   | Momentum of the synchronous particle  |
| $\Delta p$                              | Difference of the momentum between the arbitrary particle and the synchronous one                   |
| $\beta_s$                               | $\beta$ of the synchronous particle   |
| $\Delta \beta$                          | Difference of $\beta$ between the arbitrary particle and the synchronous one                        |
| $e$                                     | Elementary electric charge  |
| $\alpha$                                | Momentum compaction factor  |

The reason why we choose the time coordinate system is that it is useful to simulate the case that the frequency of the

# INTERPRETATION OF WIRE-SCANNER ASYMMETRIC PROFILES IN A LOW-ENERGY RING

M. Cieslak-Kowalska, CERN, Geneva, Switzerland and EPFL, Lausanne, Switzerland

E. Benedetto, CERN, Geneva, Switzerland

## Abstract

In the CERN PS Booster, wire-scanner profile measurements performed at injection energy are affected by a strong asymmetry. The shape was reproduced with the code PyORBIT, assuming that the effect is due to the beam evolution during the scans, under the influence of space-charge forces and Multiple Coulomb Scattering at the wire itself. Reproducing the transverse profiles during beam evolution allows to use them reliably as input for simulation benchmarking.

## INTRODUCTION

The PSB, the first circular accelerator in the CERN injector chain, is made of 4 rings stacked on top of each other. It operates on energy range from 50 MeV to 1.4 GeV. The acceleration cycle of the beam lasts 500 ms. PS Booster provides full beam range to various CERN users with beam intensities varying from  $40 \times 10^{10}$  p+ to  $800 \times 10^{10}$  p+ per ring and transverse normalized emittances between 1 mm.mrad and 15 mm.mrad.

One of the PSB goals is to provide to the LHC high quality beam in terms of high brightness, defined as the intensity divided by the transverse emittance.

Usually, emittance measurements are taken at the extraction energy flat top, however in order to perform some dedicated measurements explained later in the paper and benchmark them with simulations, we collected data at the beginning of the acceleration ramp. The beam profiles measured at the injection energy are asymmetric (Figure 1) and in this paper we try to explain this effect.

We assume that the asymmetry is due to two effects and their superposition.

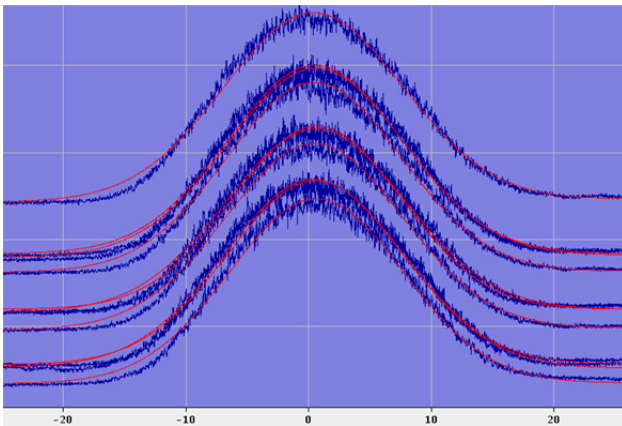


Figure 1: Example of an asymmetric measured vertical profile in PS Booster, at 60 MeV at C406.

The first effect is the Multiple Coulomb Scattering of the beam at the wire itself. Protons of the beam interact with the atoms of the material of the wire scanner and due to electromagnetic interactions change their transverse momenta, which results in emittance growth. We measured this effect and we present the experimental results compared with the data from numerical simulations and analytical estimates. Thanks to this experiment, we defined an equivalent of the wire thickness used for further simulations.

The second effect is the space charge, which is very strong in the range of the PSB operation energies, and might induce emittance blow-up during the measurement time. Due to space-charge, the beam suffers from emittance blow up or losses, depending on the actual tune and the tune necktie which overlaps machine resonances. Moreover, for several beams like EAST-type beams and some special LHC beams, for which the final emittance is reached via transverse scraping [1], we observe tails repopulation due to the space charge itself.

An example of the reconstructed profile after transverse shaving is presented in this paper.

## PS Booster Wire Scanners

The PSB is equipped with 8 independently operated, 25  $\mu\text{m}$ -thick carbon wire scanners - one per plane for each of the 4 PSB rings. The user is able to measure the beam profile twice during one cycle: with the “IN” and the “OUT” scan indicating the direction of the wire move. The “IN” scan goes from negative values (-50 mm) to positive (+50 mm), according to the PSB convention, and the opposite for the “OUT” scan. Three speed of the wire are available: 10 m/s, 15 m/s and 20 m/s. Assuming 10 m/s wire speed, the measurement of a beam with an emittance of 2 mm mrad takes about 3 ms.

## EMITTANCE BLOW UP DUE TO THE SCATTERING AT THE WIRE

The emittance blow up due to the scattering at the wire depends on the energy of the impacting beam which translates into a different scattering angle. We performed an experiment in which we swapped the wire scanner at low energy with a vertical “IN” scan in order to induce emittance blow up and then we measured the increase of emittance at extraction energy with a vertical “OUT” scan. As a reference, we considered measurements with the “OUT” scan, with the “IN” scan launched before injection, i.e. with no beam in the machine. The measured beam had a normalized emittance of  $\sim 2.2$  mm mrad in both planes and an intensity of  $I = 160 \times 10^{10}$  p+. Data was

# GENERAL FORMULA TO DEDUCE THE SPACE CHARGE TUNE SPREAD FROM A QUADROPOLAR PICK-UP MEASUREMENT

E. Métral<sup>†</sup>, CERN, Geneva, Switzerland

## Abstract

In 1966, W. Hardt derived the oscillation frequencies obtained in the presence of space charge forces and gradients errors for elliptical beams. Since then, a simple formula is usually used to relate the shift of the quadrupolar mode (obtained from the quadrupolar pick-up) and the space charge tune spread, depending only on the ratio between the two transverse equilibrium beam sizes. However, this formula is not always valid, in particular for machines running close to the coupling resonance  $Q_x = Q_y$  with almost round beams. A new general formula is presented, giving the space charge tune spread as a function of i) the measured shift of the quadrupolar mode, ii) the ratio between the two transverse equilibrium beam sizes and iii) the distance between the two transverse tunes.

## INTRODUCTION

The incoherent direct space charge tune spread is a fundamental parameter in the beam dynamics of high-intensity high-brightness beams but most of the time it is only computed analytically or simulated. It would be good to be able to measure it in running machines, which is possible with quadrupolar pick-ups by looking at the shift of the quadrupolar mode with intensity (note that there is no shift of the dipole mode with intensity due to the direct space charge as the latter follows the evolution of the beam centre and does not modify its motion). Since the derivation from W. Hardt of the oscillation frequencies obtained in the presence of space charge forces and gradients errors for elliptical beams [1], a simple formula is usually used to relate the (horizontal) space charge tune spread to the (horizontal) shift of the quadrupolar mode due to intensity, which depends only on the ratio between the equilibrium rms vertical beam size  $\sigma_{y0}$  and the equilibrium rms horizontal beam size  $\sigma_{x0}$  [2,3,4]

$$\Delta Q_{x,\text{spread}}^{sc} = \frac{2Q_{x0} - Q_{2x}}{\frac{1}{2} \left( 3 - \frac{1}{1 + \frac{\sigma_{y0}}{\sigma_{x0}}} \right)}, \quad (1)$$

where  $2Q_{x0}$  is the low-intensity quadrupolar tune and  $Q_{2x}$  is the intensity-dependent quadrupolar tune.

However, Eq. (1) is not always valid and it corresponds to the case when the coupling between the two transverse planes, introduced by space charge, is neglected. This formula is in particular not valid for machines running close to the coupling resonance  $Q_x = Q_y$  with almost

round beams, which is the case of many machines (and in particular of the CERN LHC injectors where we plan to measure the space charge tune spread using quadrupolar pick-ups) and the purpose of this paper is to provide the more general formula which depends also on the distance between the two transverse tunes [5]. Note that the extreme cases of a small or large tune split were already discussed in Ref. [6] for the case of a round beam.

The (2D) transverse envelope equations are first reviewed in Section 1, as well as the coupled equations to be solved in the presence of small perturbations on top of equilibrium beam sizes. The usual Eq. (1) is then recovered in Section 2 in the uncoupled case. The new formula providing the space charge tune spread in the general case (i.e. also close to the coupling resonance) is finally derived and discussed in Section 4.

## TRANSVERSE ENVELOPE EQUATIONS

The (2D) transverse envelope equations are now well-known and used [7,8] in particular since the work of Sacherer [9] who showed that the envelope equations derived by Kapchinsky and Vladimirsky (known as the KV equations) [10] for a continuous beam with uniform charge density and elliptical cross-section are also valid for general beam distributions if one considers the second moments only. Considering a particle in an ensemble of particles which obeys the single-particle equations, adding the space charge force to the external (linearized) force and averaging over the particle distribution, the equations of motion for the centre of mass can be obtained (note that due to Newton's third law the average of the space charge force is zero). Looking at the second moments and in particular at the position and momentum offsets of the particles from their respective averages, the 2D transverse envelope equations can finally be obtained [7,8]

$$a'' + K_x a - \frac{2K_{sc}}{a+b} - \frac{\epsilon_x^2}{a^3} = 0, \quad (2)$$

$$b'' + K_y b - \frac{2K_{sc}}{a+b} - \frac{\epsilon_y^2}{b^3} = 0,$$

with

$$a = 2\sigma_x, \quad b = 2\sigma_y, \quad (3)$$

$$\epsilon_x = 4\epsilon_{x,rms}, \quad \epsilon_y = 4\epsilon_{y,rms}, \quad (4)$$

where ' stands for the derivative with respect to the azimuthal coordinate  $s$ ,  $\sigma_{x,y}$  are the transverse rms beam sizes,  $K_{x,y}$  describe the transverse external forces,  $\epsilon_{x,y,rms}$  are the transverse rms beam emittances and  $K_{sc}$  is a coef-

<sup>†</sup> Elias.Metral@cern.ch

# SPACE CHARGE MODULES FOR PyHEADTAIL

A. Oeftiger\*, CERN, Meyrin, Switzerland; S. Hegglin, ETH Zürich, Zürich, Switzerland

## Abstract

PyHEADTAIL is a 6D tracking tool developed at CERN to simulate collective effects. We present recent developments of the direct space charge suite, which is available for both the CPU and GPU. A new 3D particle-in-cell solver with open boundary conditions has been implemented. For the transverse plane, there is a semi-analytical Bassetti-Erskine model as well as 2D self-consistent particle-in-cell solvers with both open and closed boundary conditions. For the longitudinal plane, PyHEADTAIL offers line density derivative models. Simulations with these models are benchmarked with experiments at the injection plateau of CERN's Super Proton Synchrotron.

## INTRODUCTION

The self-fields of particle beams superpose the electromagnetic fields applied by magnets and radio frequency (RF) cavities in synchrotrons. The corresponding space charge effects lead to defocusing in the transverse plane and focusing (defocusing) in the longitudinal plane for operation above (below) transition energy. For non-linear beam distributions, space charge results in a tune spread which is an important factor e.g. when investigating betatron resonances or the influence of Landau damping during instabilities. We present the implemented space charge models of the collective effects simulation software PyHEADTAIL [1] which is developed in Python. PyHEADTAIL models beam dynamics by transversely tracking macro-particles linearly between interaction points around the circular accelerator. Longitudinal particle motion is modelled either by linear tracking or non-linear (sinusoidal) drift-kick integration. The forces from collective effect sources such as electron clouds, wake fields from impedances or space charge are integrated over the respective distance and applied as a momentum kick at the following interaction point [2]. Recently, large parts of PyHEADTAIL have been parallelised for NVIDIA graphics processing units (GPU) architectures [3]. Our particle-in-cell library PyPIC used for the self-consistent space charge models in PyHEADTAIL especially benefited from these efforts – the corresponding speed-ups are reported here.

This paper is structured as follows: we first address the implemented space charge models, which is followed by our GPU parallelisation strategies and achieved improvements, and, finally, we compare simulation results with measurements at CERN's Super Proton Synchrotron (SPS). Our developed software and libraries are available online [4].

## SPACE CHARGE MODELS

A PyHEADTAIL macro-particle beam of intensity  $N$ , particle charge  $q$  and particle mass  $m_p$  is described by the

\* adrian.oeftiger@cern.ch, also at EPFL, Lausanne, Switzerland

6D set of coordinates  $(x, x', y, y', z, \delta)$ , where  $x$  denotes the horizontal offset from the reference orbit,  $y$  the vertical offset,  $x' = p_x/p_0$  and  $y' = p_y/p_0$  the corresponding transverse normalised momenta for  $p_0 = \gamma m_p \beta c$  the total beam momentum,  $z$  denotes the longitudinal offset from the synchronous particle in the laboratory frame and  $\delta = (p_z - p_0)/p_0$  the relative momentum deviation. Most of the space charge models are based on “beam slices” which represent longitudinally binned subsets of the beam distribution. The density per slice is determined by nearest grid point (NGP) interpolation (i.e. lowest order).

## Longitudinal Space Charge

For an emittance-dominated bunched beam, which is usually the case in a circular accelerator, the longitudinal electric field depends on the local line density  $\lambda(z)$ . Beams in CERN's circular accelerators typically have a very long bunch length in comparison to the vacuum tube diameter. Therefore, the non-linear image fields suppressing the longitudinal electric field have to be taken into account for the longitudinal space charge model. In PyHEADTAIL we provide such a so-called  $\lambda'(z)$  model following the extensive analysis in [5, chapter 5]. The space charge forces are computed assuming a linear equivalent field

$$E_z^{\text{equiv}}(z) = -\frac{g}{4\pi\epsilon_0\gamma^2} \frac{d\lambda(z)}{dz}, \quad (1)$$

where  $g$  denotes the geometry factor and  $\epsilon_0$  the vacuum permittivity. Conceptually, the real longitudinal profile is treated like a parabolic line density

$$\lambda(z) = \frac{3Nq}{4z_m} \left(1 - \frac{z^2}{z_m^2}\right) \quad (2)$$

with parabolic bunch half length  $z_m$ . In particular, this model identifies the mean value of the real electric field  $\langle z E_z^{\text{real}}(z) \rangle_z$  (which includes the non-linear image effects) with the corresponding analytical expression for the parabolic distribution with the generalised geometry factor  $g$ , which then absorbs the image field contributions. Our implemented model is valid for bunches satisfying  $z_m > 3r_p$  where  $2r_p$  denotes the diameter of a perfectly conducting cylindrical vacuum tube. In this case, the geometry factor  $g$  becomes independent of the bunch length and can be averaged over the whole distribution yielding [5, Eq. (5.365b)]

$$g = 0.67 + 2 \ln \left( \frac{r_p}{r_b} \right) \quad (3)$$

where  $r_b$  denotes the radial half width of a transversely round ellipsoidal beam with uniform charge distribution. As a further remark, [5, chapter 6] also discusses the case of two parallel conducting plates with distance  $2r_p$ , for which the

# SPACE CHARGE MITIGATION WITH LONGITUDINALLY HOLLOW BUNCHES

A. Oeftiger\*, S. Hancock, G. Rumolo, CERN, Meyrin, Switzerland

## Abstract

Hollow longitudinal phase space distributions have a flat profile and hence reduce the impact of transverse space charge. Dipolar parametric excitation with the phase loop feedback systems provides such hollow distributions under reproducible conditions. We present a procedure to create hollow bunches during the acceleration ramp of CERN's PS Booster machine with minimal changes to the operational cycle. The improvements during the injection plateau of the downstream Proton Synchrotron are assessed in comparison to standard parabolic bunches.

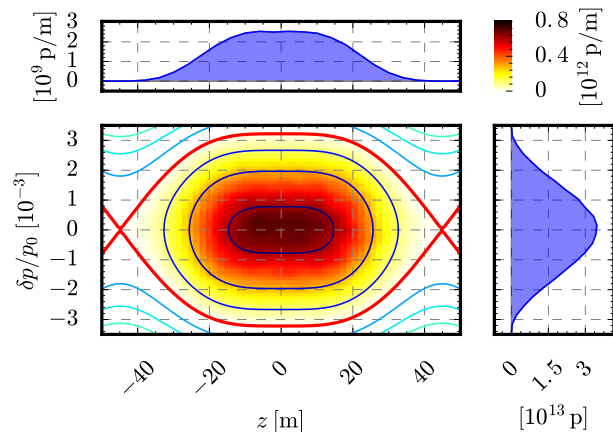
## INTRODUCTION

In the framework of the LHC Injectors Upgrade (LIU) project, the Large Hadron Collider (LHC) will have to be provided with beams of double intensity  $N$  but approximately the same transverse normalised emittances  $\epsilon_{x,y}$  compared to present operation [1]. Each synchrotron of the LHC injector chain has been assigned an emittance blow-up and beam loss budget [2, Table 1]. In particular, the Proton Synchrotron (PS) is allowed a budget of  $\Delta\epsilon/\epsilon_{ini} \leq 5\%$  and  $\Delta N/N_{ini} \leq 5\%$ . For the LIU beam parameters, the present pre-LIU machine conditions are found to exceed these values [3] which is why a series of machine upgrades are foreseen [4].

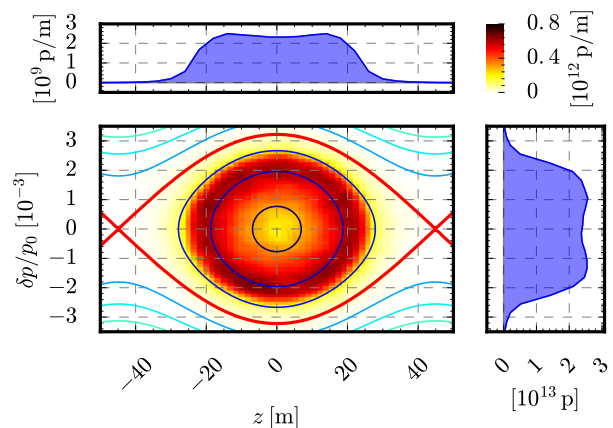
The most important limiting factor in the PS is direct space charge. Since the incoherent transverse space charge tune spread scales with the inverse energy, the 1.2 s long PS injection plateau during the standard double-batch (72-bunches) 25 ns LHC beam production is the most critical time. Therefore, the injection energy will be increased from the present  $E_{kin} = 1.4$  GeV to 2 GeV.

Given the constraints on the normalised transverse emittances, intensity and bunch length, a further common strategy to mitigate space charge impact is to reshape the longitudinal beam profile of the usually Gaussian or even rather quasi-parabolic bunches. The canonical approach is to use a double RF harmonic in bunch lengthening mode (BLM) during the critical cycle times to diminish (or cancel) phase focusing around the RF bucket centre. This RF potential deformation results in both a larger RF bucket area (longitudinal acceptance) and flatter iso-Hamiltonian contours around the centre (and therefore bunch distributions with depressed line densities). An alternative to reshaping the longitudinal profile indirectly via a modified Hamiltonian is to alter the phase space distribution directly. This consideration leads us to the concept of "hollow" bunches. Figure 1 illustrates these two cases by plotting the longitudinal phase space  $(z, \delta)$  with  $z$  the longitudinal bucket centre offset,  $\delta = (p - p_0)/p_0$  the relative momentum deviation and  $p_0$  the total momentum.

\* adrian.oeftiger@cern.ch, also at EPFL, Lausanne, Switzerland



(a) Double-harmonic bucket in BLM (i.e.  $180^\circ$  relative phase and  $V_{h=2} = V_{h=1}/2$ ) populated with a matched distribution (note the quasi-Gaussian distribution in the momentum projection).



(b) Single-harmonic bucket at the same fundamental RF voltage populated with a hollow distribution. The spatial projection is flat equivalent to the second harmonic case, but additionally also the momentum projection becomes flat.

Figure 1: Longitudinal phase space plots  $(z, \delta)$  from PyHEADTAIL simulations comparing between double-harmonic shaped and hollow bunches.

The lower left shows the momentum  $\delta$  versus the coordinate  $z$ , the separatrix in red encloses the RF bucket. The density of the particle distribution is given by the heat map in the upper right corner. In addition, the iso-Hamiltonian contours indicate the momentary flow of particle trajectories. The upper plot shows the spatial projection and the plot to the right the momentum projection.

In this paper, we present hollow bunches as a viable additional tool to mitigate space charge and hence to reach the required LIU goals. This study has been tailored to the characteristics of LHC beams and involves minimal changes

# DYNAMIC BETA AND BETA-BEATING EFFECTS IN THE PRESENCE OF THE BEAM-BEAM INTERACTIONS

X. Buffat, L. Medina, T. Pieloni \*, C. Tambasco, R. Tomás, CERN, Geneva, Switzerland,  
J. Barranco and P. Gonçalves Jorge, EPFL, Lausanne, Switzerland.

## Abstract

The Large Hadron Collider (LHC) has achieved correction of beta beat down to better than 5%. The beam-beam interactions at the four experiments result as extra quadrupole error in the lattice. This will produce a change of the beta\* at the experiments and a beating along the arcs which for the High Luminosity LHC (HL-LHC) will be very large. Estimations of these effects will be given with the characterisation of the amplitude dependency. A first attempt to correct his beating is also discussed.

## INTRODUCTION

Head-On (HO) Beam-Beam (BB) collisions as well as Long-Range (LR) interactions induce a force on the particles that depends on their amplitude. For small amplitude particles (i.e. below  $\approx 1\sigma$ ), the force is approximately linear which means that the particles traveling see the beam coming from the opposite direction as a defocusing quadrupole when they are close enough to the beam center. Beam-beam interactions will induce a change in the  $\beta$ -function all along the accelerator [1]. In the simplest case for small amplitudes, one can derive analytically the change of the  $\beta$ -function coming from N small quadrupole errors (i.e. head-on collisions at small amplitudes) at positions  $s_i$  ( $i = 1, \dots, N$ ) [2]:

$$\frac{\Delta\beta(s)}{\beta_0(s)} = \frac{2\pi\xi}{\sin(2\pi Q_0)} \sum_{i=0}^N \cos(2|\mu_0(s) - \mu_0(s_i)| - 2\pi Q_0). \quad (1)$$

During the 2015 LHC Physics Run a study of possible impacts of the dynamic beta effects of beam-beam on the collider performances, modifying the  $\beta^*$  at the two high luminosity experiments. While the effect on the LHC performances has been shown to be of maximum 1% level the study has highlighted a much more relevant contribution to the beating along the circumference with possible implications to machine protections. The LHC  $\beta$ -beating from the lattice imperfections is measured and corrected in commissioning phase to a level between the 5-7% [5, 6]. The measurements and corrections are performed with single beams and beam-beam effects are not accounted for. Studies of the implications in  $\beta$ -beating for the LHC configuration of 2015 have shown that in collisions a beating of up to 8% is expected mainly due to the head-on collisions with a beam-beam parameter  $\xi$  of approximately 0.0037 per Interaction Point (IP). The computed  $\beta$ -beating for the LHC set-up of 2015 are shown in Figure 1. The beating comes mainly from

the head-on collisions at the IPs, two in the cases shown in this paper. The maximum beating expected is obtained when full head-on collision is established.

A similar effect is expected for the High Luminosity LHC (HL-LHC) case, where due to the much stronger head-on ( $\xi_{bb} \approx 0.01$  per IP), a maximum  $\beta$ -beating of approximately 15% and 24% is expected for the case of two and three head-on collisions, respectively. In Figure 2 the  $\beta$ -beating for the HL-LHC is shown for the baseline scenario defined in [3] with two head-on collisions in the ATLAS and CMS experiments. For the HL-LHC the effect is independent on the  $\beta^*$  as the beam-beam parameter is when no crossing angle is present at the IP as for the crab-crossing scenario.

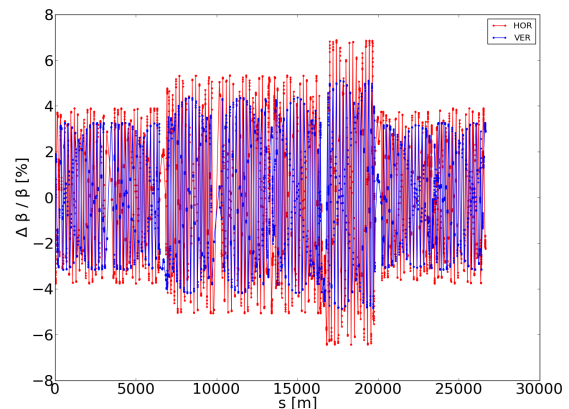


Figure 1: Beta-beating as a function of the longitudinal coordinate in the LHC for two head-on collisions at IP1 and IP5.

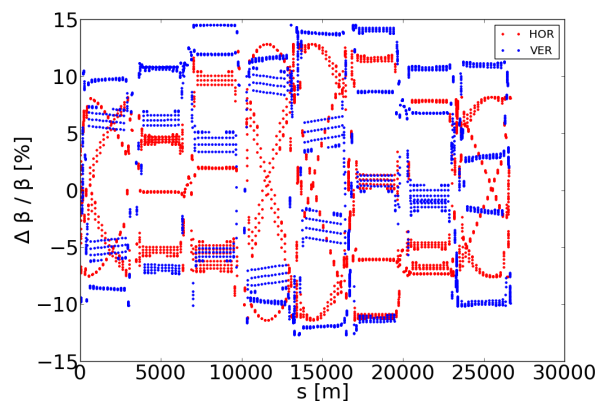


Figure 2: Beta-beating computed for the HL-LHC baseline scenario as a function of the longitudinal coordinate.

\* tatiana.pieloni@cern.ch

# CERN PS BOOSTER LONGITUDINAL DYNAMICS SIMULATIONS FOR THE POST-LS2 SCENARIO

D. Quartullo\*, CERN, Geneva, Switzerland - Università di Roma La Sapienza  
S. Albright, E. Shapochnikova, H. Timko, CERN, Geneva, Switzerland

## Abstract

The CERN PS Booster is the first synchrotron in the LHC proton injection chain, it currently accelerates particles from 50 MeV to 1.4 GeV kinetic energy. Several upgrades foreseen by the LHC Injectors Upgrade Program will allow the beam to be accelerated from 160 MeV to 2 GeV after Long Shutdown 2 in 2021. The present RF systems will be replaced by a new one, based on Finemet technology. These and other improvements will help to increase the LHC luminosity by a factor of ten. In order to study beam stability in the longitudinal plane simulations have been performed with the CERN BLoND code, using an accurate longitudinal impedance model and a reliable estimation of the longitudinal space charge. Particular attention has been dedicated to the three main features that currently let the beam go stably through the ramp: Double RF operation in bunch-lengthening mode to reduce the transverse space charge tune spread, exploitation of feedback loops to damp dipole oscillations, and controlled longitudinal emittance blow-up. RF phase noise injection has been considered to study if it could complement or substitute the currently used method based on sinusoidal phase modulation.

## INTRODUCTION

In 2021, after Long Shutdown 2 (LS2), all the injectors of the LHC will be upgraded according to the LHC Injectors Upgrade (LIU) program [1]. These improvements will contribute to an increase of the LHC luminosity by a factor of ten, meeting the expectations of the HL-LHC project.

CERN's PS Booster (PSB) is the first synchrotron in the LHC proton injection chain, it currently receives particles from the linear accelerator Linac2 at 50 MeV kinetic energy and accelerates them up to 1.4 GeV before extraction to the Proton Synchrotron (PS). In the post LS2 scenario, following the specifics of the LIU PSB program, Linac2 will be replaced by the new Linac4 and the injection energy will be increased to 160 MeV, in addition nominal LHC-type beams will be extracted at 2 GeV.

The PSB currently has three RF systems. Acceleration is done at  $h=1$ , while the  $h=2$  system is used at injection and during the ramp in bunch lengthening mode to reduce the peak line density and minimize the transverse space charge tune spread. A high harmonic cavity ( $h \leq 16$ ) is used to blow up the longitudinal emittance of the beam in a controlled way, since high emittance bunches are needed in the PSB for stability and in the PS for space charge reduction before bunch splitting at flat bottom. In the post-LS2 scenario these three RF systems will be replaced by wide-band Finemet

loaded cavities [2], which will be modular and will allow multi-harmonic operation. All the functionalities given by the current systems will be supplied by the new system as well.

In a future scenario where a lot of beam parameters will change, and where the momentum program and some impedance contributions (of RF systems and other ring components) will be different, it is vital to predict possible instabilities, which may lead to particle losses and deterioration of beam quality during the ramp and at extraction.

The most reasonable tool for this is reliable multi-particle longitudinal tracking, and the CERN BLoND code [3] has been adapted for this purpose. BLoND was conceived in 2014 and has been used extensively to simulate longitudinal dynamics of the various CERN rings (LEIR, PSB, PS, SPS and LHC) for both ions and protons. Several features are included: Acceleration, multiple RF systems, collective effects, multibunch operation, low level RF feedbacks, phase modulation or phase noise injection for controlled longitudinal emittance blow-up.

This paper describes features of the BLoND code together with obtained results. We start with an explanation of how the induced voltage is derived turn by turn, show how to numerically calculate an accurate phase shift program in double RF bunch-lengthening mode with a voltage ratio of 3/4 (currently used for LHC beams) with intensity effects and then we will briefly present the low level RF feedbacks used in the PSB and a result from their implementation in BLoND. Finally the theory behind controlled longitudinal emittance blow-up with RF phase noise injection will be introduced and the corresponding algorithm in the code will be explained. RF phase noise has never been tested in the PSB but simulations can reveal its usability in this particular case.

## INDUCED VOLTAGE CALCULATION

### *Longitudinal Space Charge and Impedance Model*

The longitudinal space charge effect is significant in non-relativistic machines so an accurate calculation of its contribution is very important. Let's call  $Z_{sc}$  the purely imaginary space charge impedance and  $\lambda(t)$  the longitudinal bunch profile such that  $\int_T dt \lambda(t) = N$ , where  $N$  stands for the beam intensity; here  $t$  is the time longitudinal coordinate and  $T = [0, T_{rev}]$  is the one-turn time interval. The space charge induced voltage can be calculated with good approximation using

$$V_{sc}(t) = \frac{e}{\omega_{rev}} \frac{|Z_{sc}|}{n} \frac{d}{dt} \lambda(t), \quad (1)$$

\* danilo.quartullo@cern.ch

# ON THE IMPACT OF NON-SYMPLECTICITY OF SPACE CHARGE SOLVERS\*

M. Titze<sup>†</sup>, CERN, Geneva, Switzerland  
and Humboldt-University of Berlin, Germany

## Abstract

To guarantee long-term reliability in the predictions of a numerical integrator, it is a well-known requirement that the underlying map has to be symplectic. It is therefore important to examine in detail the impact on emittance growth and noise generation in case this condition is violated. We present a strategy of how to tackle this question and some results obtained for particular PIC and frozen space charge models.

## INTRODUCTION

A typical application of a space charge solver is to simulate the behaviour of a beam of charged particles over a reasonably long period of time inside a storage ring. In particular this is the case when studying emittance growth near resonance lines in a tune diagram [1].

On the one hand, it is a well-known fact that the simulation of a system admitting a Hamiltonian has to be symplectic in order to remain on the energy shell [2]. On the other hand, this basic condition is usually violated if one integrates the underlying equations of motion in a straightforward manner. Probably the most simplest example when this happens is the Explicit-Euler method. But also in the sophisticated case of a space charge solver, now acting on the set of bunches in a large dimensional phase space, symplecticity is not necessarily be fulfilled as we shall see.

In this article we present results in which we tested an analytic (Basetti-Erskine) solver, and a so-called (2 + 5)-D Particle-In-Cell (PIC) solver, which are both implemented inside the widely-used space charge tracking program PyORBIT, against the usual symplecticity condition. Both methods involve the addition of so-called space charge nodes at particular steps around the ring, which simulate the result of interaction between the charged particles. Our reference case will be the (uncoupled) plain tracking case obtained with PyORBIT and MAD-X.

The symplecticity checks were performed by using two different, but closely related, methods of numeric differentiation. These methods are straightforward and can basically be applied to any tracking code. We are mainly considering a test ring of 1km circumference with 416 space charge nodes, but also use a FODO map with just 4 nodes.

We will see that, as the reader probably might have expected, up to the precision of our methods the previously mentioned PIC solver violates the symplecticity condition, while the analytic solver is symplectic. We expect that the

outcome of this violation might have an influence on long-term studies involving PIC solvers. One such effect which clearly distinguish both methods is the generation of noise in the transversal emittances in the PIC case [3]. The natural question thus arises whether the symplecticity violation is the main driving term behind this behaviour.

In order to give an indication to the answer, we performed several tracking studies, using a low number of macroparticles, on a FODO cell and a small test ring. There are several reasons for choosing a low number: Firstly, due to the fact that we need at least to check the Jacobi-Matrix, we can not go much higher. Secondly, it turned out that a small ring with reasonable parameters can mimik a similar situation with a large phase-space. However, the outcome is also varying more, which has to be taken care off by simulating the same situation several times.

## SYMPLECTICITY CHECKS

Before we are able to apply the numeric differentiation methods, let us remark that PyORBIT is not dumping the beam in canonical coordinates, a fact which must be taken into account.

### Numeric Differentiation Method

A straightforward way of how to check the symplecticity of a numerical integrator at a given point  $x$  is to approximate its Jacobi-Matrix by 1D fits for every pair of directions. Namely, if  $M: P \rightarrow P$  denotes the given map from  $2k$ -dimensional phase space  $P \subset \mathbb{K}^{2k}$  to itself, we specify a step size<sup>1</sup>  $\epsilon$  and approximate  $\partial_j M_i(x)$  for a given point  $x$  by the slope of a linear fit of the values  $M_i(x + k\epsilon b_j)$ ,  $k \in \mathbb{Z}$ , where the  $b_j$  denotes a basis and  $M_i$  the  $i$ th component with respect to that basis.

Then the symplecticity condition is checked by computing  $R := (M')^{tr} J M' - J$ , where  $M' = (\partial_j M_i(x))_{ij}$  is the now determined Jacobi-Matrix of  $M$  at  $x$  and  $J$  the matrix representation of the given symplectic structure in the above basis. In the following we will understand by the (Frobenius) norm of  $R$  the distance of  $M$  at a given point  $x \in P$  towards symplecticity.

If we assume that in every direction  $b_j$  the amount of bunch configurations  $x + k\epsilon b_j$  for varying  $k$  is the same number  $K$ , and if we denote the number of particles by  $N$ , we effectively have to track  $36N^2K$  times through the ring to compute the entire Jacobi-Matrix. It is therefore not feasible to perform this computation for a large number of particles.

<sup>1</sup> In general this step size has to be chosen separately for every direction and component.

\* Work supported by German Federal Ministry of Education and Research (BMBF)

<sup>†</sup> malte.titze@cern.ch

# SIMPLE MODELS FOR BEAM LOSS NEAR THE HALF INTEGER RESONANCE WITH SPACE CHARGE

C. M. Warsop, D. J. Adams, B. Jones, B. G. Pine, ISIS, Rutherford Appleton Laboratory, U.K.

## Abstract

The half integer resonance is often used to define the high intensity limit of medium or low energy hadron rings where transverse space charge is significant. However, the mechanism leading to particle loss as beam approaches this resonance, which thus defines the limit, is not clearly understood. In this paper we explore simple models, based on single particle resonance ideas, to see if they describe useful aspects of motion as observed in simulations and experiments of 2D coasting beams on the ISIS synchrotron. Single particle behaviour is compared to 2D self-consistent models to assess when coherent motion begins to affect the single particle motion, and understand the relevance of coherent and incoherent resonance. Whilst the general problem of 2D resonant loss, with non-stationary distributions and non-linear fields is potentially extremely complicated, here we suggest that for a well-designed machine (where higher order pathological loss effects are avoided) a relatively simple model may give valuable insights into beam behaviour and control.

## INTRODUCTION

### Background

The half integer resonance is often taken as defining the high intensity limit of hadron rings, where there is the expectation that lower order, quadrupole errors will drive the dominant loss. However, the details of mechanisms driving particle emittance growth and loss as beam approaches resonance are not well understood.

Whilst the well known intensity limit based on the incoherent tune shift gives a useful rule of thumb, it over estimates losses as it neglects coherent motion of the beam [1]. The coherent model, on the other hand, gives a fuller, self-consistent picture by taking into account the envelope modulation, and predicts resonance at the higher, coherent limit. However, coherent theory is based on Kapchinskij-Vladimirskij (KV) distributions and RMS equivalent models that are only valid as long as RMS emittances are conserved, i.e. when there is no emittance growth. Therefore, they cannot be used to understand particle motion and loss as beam approaches resonance. To derive models to explain such losses, a modified single particle model is required that includes the effect of the coherent response of the beam.

As a first step, this paper analyses single particle motion in the frozen space charge case for a representative waterbag beam. An initial comparison with coherent theory is also given. Future work will build on these results, exploring their limitations with detailed self-consistent simulations.

### Building on Experimental Results from ISIS

The idea that single particle models should be useful for describing half integer resonance comes from experimental observations on the ISIS proton synchrotron [2]. Extensive experimental and simulation work studying the approach of half integer resonance in 2D coasting beams have characterized the evolution of transverse beam profiles in detail [2, 3]. Comparison of these results with comprehensive ORBIT models indicated that "lobe" features on profiles corresponded to half integer resonant islands. This suggests that a useful starting point for models is single particle theory, with the expectation that corrections for coherent effects will be required.

Below we calculate particle trajectories for resonant particle motion in a frozen space charge model, next we analyse the main dependencies this predicts for driving term strength, tune and intensity. Finally, we discuss and compare predictions with those from coherent theory, and outline future work.

## FROZEN WATERBAG MODEL

This analysis considers the motion of a test particle, in a smooth focusing system, in the space charge field of a *frozen* waterbag beam distribution. This distribution is chosen as a representative case that includes key features a KV distribution does not: it has tune variation with amplitude and is non-stationary. It is the initial motion of this non-stationary distribution that we are interested in for studying the onset of resonance. This non-stationary waterbag beam would redistribute in any realistic *non-frozen* beam model, and this means the Hamiltonian derived below is certainly not an invariant over long time scales. Usually the type of analysis used here assumes resonance with long term invariance with KV beams, e.g. [4]. However, what is of interest here is the short term motion of a beam; its initial redistribution as it approaches resonance. Therefore, we use this "*short term invariant*" to predict the initial trajectories of particles, before the beam redistributes significantly. This should indicate how the beam behaves on approaching resonance.

The analysis of particle motion is made difficult by the piecewise definition required for the space charge potential inside and outside the waterbag beam. This complication is removed using the method of phase averaging, following work in [4]. This gives a smoothed action-angle approximation, from which we can extract particle motion.

### Phase Averaged Hamiltonian

We analyse the motion of a test particle in the field of a 4D, axisymmetric waterbag beam with radius  $a$  of the form  $n(r) = n_0(1 - \frac{r^2}{a^2})$ , (for  $r \leq a$ , zero otherwise) with  $r^2 =$

# DEVELOPMENT OF PHYSICS MODELS OF THE ISIS HEAD-TAIL INSTABILITY

R.E. Williamson, B. Jones, C.M. Warsop, ISIS, Rutherford Appleton Laboratory, STFC, UK

## Abstract

ISIS is the pulsed spallation neutron and muon source at the Rutherford Appleton Laboratory in the UK. Operation centres on a rapid cycling proton synchrotron which accelerates  $3 \times 10^{13}$  protons per pulse from 70 MeV to 800 MeV at 50 Hz, delivering a mean beam power of 0.2 MW.

As a high intensity, loss-limited machine, research and development at ISIS is focused on understanding loss mechanisms with a view to improving operational performance and guiding possible upgrade routes. The head-tail instability observed on ISIS is of particular interest as it is currently a main limitation on beam intensity.

Good models of impedance are essential for understanding instabilities and to this end, recent beam-based measurements of the effective transverse impedance of the ISIS synchrotron are presented. This paper also presents developments of a new, in-house code to simulate the head-tail instability and includes benchmarks against theory and comparisons with experimental results.

## INTRODUCTION

The transverse head-tail instability is a main concern for high intensity operation in many hadron synchrotrons including ISIS and its proposed upgrades. The instability imposes a limit on beam intensity through associated beam loss and the subsequent undesired machine activation. However classical theories, such as the model of Sacherer [1], do not include space charge and associated tune spreads which are required for accurately modelling high intensity beams.

Recent work [2 – 4] has put forward limited theoretical models to treat head-tail motion in the presence of space charge. However, currently there is no comprehensive model of head-tail with space charge. Testing of these models against observations is required to ascertain fully their usefulness and limits. As such, numerical simulations have been employed [5] to analyse collective effects and link experimental results to theory. Ultimately, understanding head-tail in high intensity beams may allow improved operations avoiding the instability, with lower beam losses and the possibility of higher beam intensities.

### *The ISIS Synchrotron*

ISIS operation centres on a rapid cycling synchrotron (RCS) with a 163 m circumference composed of 10 superperiods. It accelerates  $3 \times 10^{13}$  protons per pulse (ppp) from 70 – 800 MeV on the 10 ms rising edge of a sinusoidal main magnet field. The repetition rate of 50 Hz results in an average beam power on target of 0.2 MW.

Injection is via charge exchange of a 70 MeV, 25 mA  $H^-$  beam over  $\sim 130$  turns with painting over both transverse acceptances, collimated at  $300 \pi$  mm mrad. The unchopped, injected beam is non-adiabatically bunched and accelerated by the ring dual harmonic RF system ( $h = 2$  and 4). Nominal betatron tunes are  $(Q_x, Q_y) = (4.31, 3.83)$  with peak incoherent tune shifts exceeding  $\sim -0.5$ . The beam intensity is loss limited with the main driving mechanisms being foil losses, longitudinal trapping, transverse space charge and the head-tail instability [6].

Measurements on ISIS have consistently shown that the two proton bunches exhibit vertical head-tail motion over 1 – 2.5 ms into the 10 ms acceleration cycle [7, 8]. The instability is suppressed by ramping the vertical tune down, away from the integer ( $Q_y = 4$ ) during the time of the instability. However, with rising operating intensities, beam losses associated with head-tail increase and lowering the tune further tends to induce beam loss associated with the half integer resonance [9, 10].

Recent studies have shown that the instability is present with dual harmonic RF acceleration as well as with single harmonic RF [10, 11], and possibly worse with the second harmonic. Work is ongoing to develop a feedback system to damp the instability [12] alongside studies modelling and understanding the instability mechanism.

This study presents initial developments in building impedance and instability simulation models of the ISIS synchrotron. Beam-based measurements of the effective transverse impedance are presented. These allow for a better understanding of the driving force behind the head-tail instability.

A new in-house macro-particle simulation code, currently in development to simulate the head-tail instability as observed on ISIS, is also introduced. Convergence tests of the code are presented together with benchmarks against theory. Simulations are compared to experimental data from ISIS with single harmonic RF acceleration. Plans for future experimental studies, simulation and theory work are outlined.

### *Head-Tail Observations*

ISIS operates at the natural machine chromaticities ( $\xi_x = \xi_y = -1.4$  [13]), without sextupole correction. As mentioned above, the impedance acting on the beam leads to a coherent vertical instability early in the acceleration cycle. Measurements have been made using a vertical beam position monitor (BPM) over 0 – 5 ms during acceleration in the case of lower intensity beams ( $5 \times 10^{12}$  ppp) and single harmonic RF. Measurements at this intensity minimise the effect of space charge and allow direct comparison with Sacherer theory. Further measurements at high intensity and with dual harmonic

# BEAM ACCELERATION AND TRANSITION CROSSING IN THE FERMILAB BOOSTER\*

V. A. Lebedev<sup>†</sup>, J.-F. Ostiguy, C.M. Bhat  
Fermilab, Batavia, IL, USA

## Abstract

To suppress eddy currents, the Fermilab rapid cycling Booster synchrotron has no beam pipe; rather, its combined function dipoles are evacuated, exposing the beam directly to the magnet laminations. This arrangement significantly increases the resistive wall impedance of the dipoles and, in combination with the space charge impedance, substantially complicates longitudinal dynamics at transition. Voltage and accelerating phase profiles in the vicinity of transition are typically empirically optimized to minimize beam loss and emittance growth. In this contribution, we present results of experimental studies of beam acceleration near transition. Using comparisons between observed beam parameters and simulations, we obtain accurate calibrations for the rf program and extract quantitative information about parameters of relevance to the Booster laminated magnets longitudinal impedance model. The results are used to analyse transition crossing in the context of a future 50% increase in beam intensity planned for PIP-II, an upgrade of the Fermilab accelerating complex.

## INTRODUCTION

Over the 40 years existence of Fermilab Booster the beam intensity has increased steadily to respond to the demands of the experimental program. In recent years this pace has increased to accommodate a succession of neutrino experiments. To meet the needs of the LBNF/DUNE experimental program, the next planned upgrade of the Fermilab accelerating complex referred to as PIP-II, calls for an additional 50% increase in beam intensity.

Early on, transition crossing has been identified as a machine performance bottleneck. Although transition crossing has evolved into a sophisticated and well-tuned operational procedure, an increase in intensity beyond the current level requires quantitative understanding of all effects driving the process. In this paper we present results of studies aimed at understanding the dynamics of beam acceleration and transition crossing in sufficient details to construct a model with predictive ability. The model aims not only at investigating the impact of an intensity increase on performance, but also at investigating ways to minimize beam loss and emittance growth due to transition crossing.

It is well-known that a jump in accelerating phase from  $\phi_{acc}$  to  $\pi - \phi_{acc}$  is required to preserve longitudinal motion stability. In the absence of beam induced forces and motion non-linearity the dynamics below and above transition is symmetric resulting in no emittance growth at transition.

In practice the beam induced forces, break this symmetry as well as motion linearity. The result is an intensity dependent focussing mismatch and non-linear distortions of the bunch phase space. The subsequent synchrotron oscillations lead to filamentation and emittance growth.

In contrast to other fast cycling proton synchrotrons, the Fermilab Booster has no dedicated vacuum chamber inside its dipoles; rather, the entire volume between the magnet poles is evacuated. While this arrangement eliminates the issues associated with eddy currents induced by the time-varying bend field in a conventional chamber, having the beam directly exposed to the pole laminations substantially increases the wall impedance. The bunch length achieves its minimum at transition. The corresponding increase in peak current causes an increase in beam induced voltage. The very low synchrotron frequency enhances the non-linearity contribution to emittance growth.

Table 1 presents Booster parameters relevant to beam acceleration and transition crossing.

Table 1: Major Booster Parameters

|                        |                     |
|------------------------|---------------------|
| Injection energy       | 0.4 GeV             |
| Extraction energy      | 8 GeV               |
| Ramp rate              | 15 Hz               |
| Harmonic number        | 84                  |
| Circumference          | 474.2 m             |
| Momentum compaction    | 0.03346             |
| Maximum rf voltage     | 1.2 MeV             |
| RF frequency swing     | 37.9-52.8 MHz       |
| Number of bunches      | 82                  |
| Nominal beam intensity | $4.2 \cdot 10^{12}$ |

## MEASUREMENTS

To minimize problems with possible signal distortion in electronics and data acquisition as well as possible miscalibrations, raw signals were acquired from a resistive wall monitor (RWM) and from the circuit presenting the analog sum of rf voltages for all cavities (RFSUM). In addition, the signal from a beam position monitor used by the radial position feedback system (RPOS) was recorded. The data were acquired with a multi-channel digital oscilloscope. A sampling rate of 1.2 GHz was selected so as to measure both voltage waveform and the longitudinal density distribution with sufficient resolution. The RWM and RFSUM signals completely characterize the beam behaviour in the longitudinal plane including the amplitude and phase of the accelerating voltage. As will be seen below, the RPOS signal provides accurate calibrations of the rf voltage and phase. Because of the oscilloscope memory limit of  $4.5 \cdot 10^6$  samples, the duration of each measurement was set to 3.6 ms. Since this interval is much shorter than the complete 33.3 ms accelerating cycle, data were acquired only during

\* Work performed for Fermi Research Alliance, LLC under Contract No.

DE-AC02-07CH11359 with the United States Department of Energy

<sup>†</sup> val@fnal.gov

# SUPPRESSION OF HALF-INTEGERS RESONANCE IN FERMILAB BOOSTER\*

A. Valishev<sup>†</sup>, V. Lebedev, Fermilab, Batavia, IL, USA

## Abstract

The particle losses at injection in the FNAL Booster are one of the major factors limiting the machine performance. The losses are caused by motion nonlinearity due to direct space charge and due to nonlinearity introduced by large values of chromaticity sextupoles required to suppress transverse instabilities. The report aims to address the former - the suppression of incoherent space charge effects by reducing deviations from the perfect periodicity of linear optics functions. It should be achieved by high accuracy optics measurements with subsequent optics correction and by removing known sources of optics perturbations. The study shows significant impact of optics correction on the half-integer stop band with subsequent reduction of particle loss. We use realistic Booster lattice model to understand the present limitations, and investigate the possible improvements which would allow high intensity operation with PIP-II parameters.

## INTRODUCTION

The Booster has been the workhorse of the Fermilab accelerator complex for several decades and continues to deliver high-intensity high-repetition rate proton beams for the physics program. Recent improvements allowed to obtain beam acceleration at each Booster cycle. It increased the effective ramp rate from 7 to 15 Hz and played a significant role in attaining the 700 kW operation for NOvA experiment [1]. The Booster intensity is limited by particle losses throughout the injection, acceleration, and extraction cycle, which lead to the radio-activation of the accelerator components and enclosure. Consequently, the examination of the loss sources and development of ways to mitigate them are the continued focus of efforts. It becomes especially important in view of the upgrade plans for the PIP-II project [2]. The area of interest for the present report is the particle losses induced by direct space charge interaction at injection energy.

The studies of space charge effect in FNAL Booster have a long history. A massive campaign to simulate and mitigate the losses at injection was undertaken during the Tevatron collider Run II [3-7]. In particular, it was determined that the extraction dogleg that disturbs the 24-fold lattice symmetry of the Booster and thus enhances the half-integer stop band can have a significant impact on the single-particle dynamics [4]. The importance of half-integer resonance has been realized by Sacherer [8] and later research confirmed and enhanced the aspects of interplay between space-charge and lattice resonances [9-13]. Also, significant progress has been made in the accurate measurement

and reconstruction of the Booster optics model owing to the implementation of the LOCO algorithm [13]. This makes it possible to model the beam dynamics with the actual machine configuration in operations and then perform predictable adjustments.

The present work aims at i) revisiting the space-charge dynamics in the FNAL Booster making use of the recent improvements in the lattice model and understanding the main limiting factors; ii) proposing operational improvements to reduce particle losses; iii) making projections towards operation with PIP-II parameters or even higher intensity.

## APPROACH AND TOOLS

In the present study we concentrate solely on the incoherent single-particle effects arising through the time-modulation of nonlinear transverse self-field within the bunch and the betatron and synchro-betatron resonances leading to the beam emittance growth and particle losses. We also limit the time period of interest to a few hundred turns right after the beam injection and bunching and before the energy ramp. Such approach allows to use relatively simple tools for the modelling of space-charge effects – the so-called frozen space-charge model that implies Gaussian beam density profile. We also approximate the smooth azimuthal distribution of space-charge action by a number of thin kicks along the orbit. The advantage of such approach is the fast calculation time and the availability of reasonable well developed and tested tracking codes. In the future the simulations will be augmented by the true self-consistent PIC tools.

We use the simplified and realistic Booster lattice models [13] to quantify the requirements on optics control that would help mitigating particle losses at injection. The simplified representation is a 24-cell symmetric lattice with some artificially introduced gradient errors, which emulate the beta-beating of the realistic lattice.

The code used in this study was Lifetrac [14], a particle tracking code developed for modelling beam-beam interactions. The machine lattice was modelled using the element-by-element drift-kick approximation. The lattice data are imported from MAD-X [15] model files where the element slicing is performed using the methods available internally in MAD-X. For the purpose of this work the slicing was done with the so-called Teapot algorithm [16]. The thin lens tracking is implemented following [17], and makes use of the paraxial approximation for the multipole elements and properly treats non-paraxial effects in the drifts. This method proved to be accurate for the LHC and DAΦNE tracking studies [18].

We used 120 thin beam-beam elements (17 per betatron period) to model the action of space-charge. The simplifications limiting the physics model in the study were: i)

\* Fermilab is operated by Fermi Research Alliance, LLC under Contract No. DE-AC02-07CH11359 with the United States Department of Energy.

<sup>†</sup> valishev@fnal.gov

# ELECTRON LENS FOR THE FERMILAB INTEGRABLE OPTICS TEST ACCELERATOR\*

G. Stancari<sup>†</sup>, A. Burov, K. Carlson, D. Crawford, V. Lebedev, J. Leibfritz, M. McGee, S. Nagaitsev, L. Nobrega, C. S. Park, E. Prebys, A. Romanov, J. Ruan, V. Shiltsev, Y.-M. Shin<sup>1</sup>, C. Thangaraj, A. Valishev, Fermilab, Batavia IL, USA, and D. Noll, IAP Frankfurt, Germany  
<sup>1</sup>also at Northern Illinois University, DeKalb IL, USA

## Abstract

The Integrable Optics Test Accelerator (IOTA) is a research machine currently being designed and built at Fermilab. The research program includes the study of nonlinear integrable lattices, beam dynamics with self fields, and optical stochastic cooling. One section of the ring will contain an electron lens, a low-energy magnetized electron beam overlapping with the circulating beam. The electron lens can work as a nonlinear element, as an electron cooler, or as a space-charge compensator. We describe the physical principles, experiment design, and hardware implementation plans for the IOTA electron lens.

## INTRODUCTION

High-power accelerators and high-brightness beams are needed in many areas of particle physics, such as the study of neutrinos and of rare processes. The performance of these accelerators is limited by tolerable losses, beam halo, space-charge effects, instabilities, and other factors. Nonlinear integrable optics, self-consistent or compensated dynamics with self fields, and beam cooling beyond the present state of the art are being studied to address these issues. Moreover, nonlinearity, chaos, and the quest for integrability under controlled experimental conditions sheds light on the behavior of dynamical systems in general.

The Integrable Optics Test Accelerator (IOTA) is a research storage ring with a circumference of 40 m being built at Fermilab [1, 2]. Its main purposes are the practical implementation of nonlinear integrable lattices in a real machine, the study of space-charge compensation in rings, and a demonstration of optical stochastic cooling. IOTA is designed to study single-particle linear and nonlinear dynamics with pencil beams of 150-MeV electrons. For experiments on space-charge dynamics, 2.5-MeV protons will be injected.

In accelerator physics, nonlinear integrable optics involves a small number of special nonlinear focusing elements added to the lattice of a conventional machine in order to generate large tune spreads while preserving dynamic aperture [3]. This provides improved stability to perturbations and mitigation of collective instabilities through decoherence and Landau damping.

One way to generate a nonlinear integrable lattice is with specially segmented multipole magnets [3]. There are also

two concepts based on electron lenses [4]: (a) axially symmetric thin kicks with a specific amplitude dependence [5–7]; and (b) axially symmetric kicks in a thick lens at constant amplitude function [8, 9]. These concepts use the electromagnetic field generated by the electron beam distribution to provide the desired nonlinear transverse kicks to the circulating beam. In IOTA operations with protons, the electron lens can also be used as an electron cooler [10] and as a space-charge compensator [11–13].

In this paper, we summarize the functions of the electron lens in IOTA and discuss current plans to build and test the experimental apparatus.

## ELECTRON LENS IN IOTA

In an electron lens, the electromagnetic field generated by a pulsed, magnetically confined, low-energy electron beam is used to actively manipulate the dynamics of the circulating beam [14–16]. Electron lenses have a wide range of applications [17–26]. In particular, they can be used as nonlinear elements with tunable shape as a function of betatron amplitude.

### *Nonlinear Integrable Optics*

The goal of the nonlinear integrable optics experiments, including the ones with electron lenses, is to achieve a large tune spread, of the order of 0.25 or more, while preserving the dynamic aperture and lifetime of the circulating beam. Experimentally, this will be observed by recording the lifetime and turn-by-turn position of a low-intensity, low-emittance 150-MeV circulating electron bunch, injected and kicked to different betatron amplitudes, for different settings of the nonlinear elements (magnets or electron lenses).

There are two concepts of electron lenses for nonlinear integrable optics: thin radial kick of McMillan type and thick axially-symmetric nonlinear lens in constant amplitude function.

**Thin Radial Kick of McMillan Type** The integrability of axially symmetric thin-lens kicks was studied in 1 dimension by McMillan [5, 6]. It was then extended to 2 dimensions [7] and used to improve the performance of colliders [27]. To implement this concept, the electron lens has to have a specific current-density distribution:  $j(r) = j_0 a^4 / (r^2 + a^2)^2$ , where  $j_0$  is the current density on axis and  $a$  is a constant parameter (effective radius). Moreover, the betatron phase advance in the rest of the ring must be near an odd multiple of  $\pi/2$ . In this scenario, the electron

\* Fermilab is operated by Fermi Research Alliance, LLC under Contract No. DE-AC02-07CH11359 with the United States Department of Energy. Report number: FERMILAB-CONF-16-244-AD-APC.

<sup>†</sup> Email: (stancari@fnal.gov).

# SPIN TRACKING OF POLARIZED PROTONS IN THE MAIN INJECTOR AT FERMILAB\*

M. Xiao<sup>†</sup>, Fermilab, Batavia, IL 60565, USA

W. Lorenzon and C. Aldred, University of Michigan, Ann Arbor, MI 48109-1040, USA

## Abstract

The Main Injector (MI) at Fermilab currently produces high-intensity beams of protons at energies of 120 GeV for a variety of physics experiments. Acceleration of polarized protons in the MI would provide opportunities for a rich spin physics program at Fermilab. To achieve polarized proton beams in the Fermilab accelerator complex, shown in Fig.1, detailed spin tracking simulations with realistic parameters based on the existing facility are required. This report presents studies at the MI using a single 4-twist Siberian snake to determine the depolarizing spin resonances for the relevant synchrotrons. Results will be presented first for a perfect MI lattice, followed by a lattice that includes the real MI imperfections, such as the measured magnet field errors and quadrupole misalignments. The tolerances of each of these factors in maintaining polarization in the Main Injector will be discussed.

## INTRODUCTION

The Main Injector is a multi-purpose synchrotron [1] which ramps up the proton beam from a kinetic energy of 8 GeV to 120 GeV. It provides neutrino beams for the MINOS, MINERvA and NOvA experiments, as well as the future Long-Baseline Neutrino Facility and Deep Underground Neutrino Experiment. It will also provide muon beams for Fermilab's Muon g-2 and Mu2e experiments. It delivers beam to the SeaQuest fixed-target experiment and to a dedicated facility for testing of detector technologies.

The acceleration of polarized protons in the MI was initially studied with the use of two superconducting helical dipole Siberian snakes. However, in 2012 it was discovered that there was no longer sufficient space in the MI to place two Siberian snakes at opposite sides of the ring [2]. A solution using one 4-twist Helical Snake in the MI [3] was found that seemed promising to provide polarized proton beams to the experiments. Spin tracking studies in the MI became necessary to reveal if it was possible or not in practice to produce and maintain a polarized proton beam in the Fermilab accelerators using single Siberian snakes in the larger synchrotrons. This report presents studies to determine the intrinsic spin resonance strengths for the relevant synchrotrons using a perfect lattice. This is followed by the implementation of various realistic imperfections, such as magnet field errors and quadrupole misalignments, into the MI lattice to study the tolerances of closed orbit corrections in maintaining polarization. All

\* Work supported by U.S. Department of Energy under the contract No. DE-AC02-76CH03000 and the National Science Foundation under Grant 1505458

<sup>†</sup>meiqin@fnal.gov

results presented here assume that the Siberian snake is a point-like spin flipper. The simulation using a single 4-twist helical dipole and its imperfection will be discussed at a later stage.

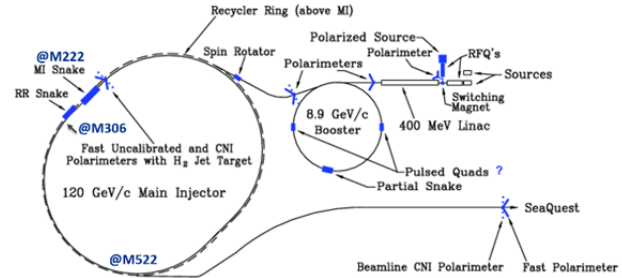


Figure 1: Main Injector accelerator complex conceptual layout showing equipment needed for polarized proton beam (in blue).

## SPIN DYNAMICS OF THE POLARIZED PROTON

For a beam of particles, the polarization vector is defined as the ensemble average of spin vectors. The evolution of the spin vector of a beam of polarized protons in external magnetic fields is governed by the Thomas-BMT equation [4]

$$\frac{d\vec{S}}{dt} = \frac{e}{\gamma m} \vec{S} \times \left[ (1+G)\vec{B}_\perp + (1+G)\vec{B}_\parallel + \left( G\gamma + \frac{\gamma}{\gamma+1} \right) \frac{\vec{E} \times \vec{\beta}}{c} \right] \quad (2.1)$$

where the polarization vector  $\vec{S}$  is expressed in the frame that moves with the particle.  $\vec{B}_\perp$  and  $\vec{B}_\parallel$  are the transverse and longitudinal components of the magnetic fields in the laboratory frame with respect to the velocity  $\vec{\beta}c$  of the particle. The vector  $\vec{E}$  stands for the electric field,  $G$  is the anomalous gyromagnetic g-factor, and  $\gamma mc^2$  is the energy of the moving particle. In a pure magnetic field,  $\vec{E} = 0$ .

In the SU(2) representation, the spin vector can be expressed with two-component spinor  $\psi = (\psi_1, \psi_2)^T$  where  $\psi_1, \psi_2$  are complex numbers. The conversion between SU(2) and SO(3) is

$$\vec{S} = \psi^\dagger \vec{\sigma} \psi \quad (2.2)$$

where  $\vec{\sigma} = (\sigma_1, \sigma_2, \sigma_3)$  are Pauli matrices. Due to the unitarity of the spin vector,  $P = |\psi_1|^2 + |\psi_2|^2$ ,  $P$  is the polarization.  $P=1$  for a single particle. In spinor notation, the T-BMT equation can be written as

$$\frac{d}{dt} \psi = -\frac{i}{2} (\vec{\sigma} \cdot \vec{\omega}) \psi \quad (2.3)$$

# THE DESIR FACILITY AT GANIL-SPIRAL2: THE TRANSFER BEAM LINES

L. Perrot<sup>†</sup>, P. Blache, S. Rousselot, Université Paris-Saclay, Université Paris Sud, CNRS-IN2P3-IPN, Orsay, France

## Abstract

The new ISOL facility SPIRAL2 is currently being built at GANIL, Caen France. The commissioning of the accelerator is in progress since 2015. SPIRAL2 will produce a large number of new radioactive ion beams (RIB) at high intensities. In 2019, the DESIR facility will receive beams from the upgraded SPIRAL1 facility of GANIL (stable beam and target fragmentation), from the S3 Low Energy Branch (fusion-evaporation and deep-inelastic reactions). In order to deliver the RIB to the experimental set-ups installed in the DESIR hall; 110 meters of beam line are studied since 2014. This paper will focus on the recent studies which have been done on these transfer lines: beam optics and errors calculations, quadrupoles, diagnostics and mechanical designs.

## THE DESIR FACILITY WITHIN THE SPIRAL2 PROJECT

SPIRAL2 is a major extension project of the GANIL facility in Caen, France dedicated to the production of heavy ion beams at high intensities and of very exotic nuclides. With SPIRAL2, the French and International communities will make decisive steps in the understanding of the atomic nucleus and of the nucleosynthesis processes occurring in astrophysics. The collection of nuclear data will help preparing the next generation of nuclear reactors and the production of new isotopes suitable to nuclear medicine will be investigated. In addition, a high intensity fast neutron source will open new research domains in material science [1]. The SPIRAL2 facility will produce a large number of new radioactive ion beams (RIB) at high intensity. These beams will be produced using a new linear accelerator that will deliver deuterons up to 40MeV at 5mA intensity, protons up to 33MeV at 5mA and ions with  $A/Q=3$  up to 14.5MeV/u at 1mA (see Fig. 1) [2].

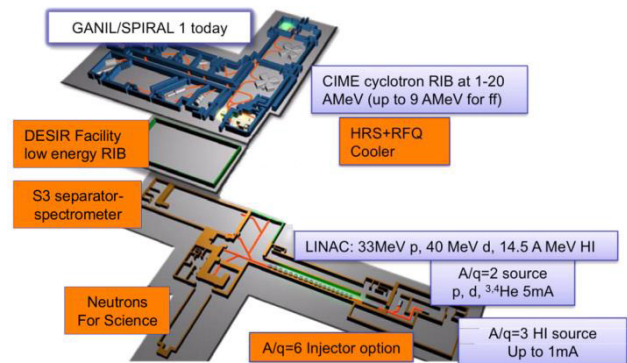


Figure 1: Scheme of the SPIRAL2 facility.

The DESIR (Decay, Excitation and Storage of Radioactive Ions) facility will receive beams delivered by the S3-LEB (Low Energy Branch of the new Super Separator Spectrometer) of SPIRAL2 [3]. Nuclides will be produced in fusion-evaporation, transfer and deep-inelastic reactions, and will notably consist in refractory elements. Finally, RIB produced in the fragmentation of high-intensity heavy ions and/or thick targets at the upgraded SPIRAL1 facility will also be available at DESIR [4]. The Steering comity of the SPIRAL2 project promote the phase 1+ witch include the DESIR facility with its transfer beam line coming from S3 and SPIRAL1.

Nuclear physics as well as fundamental weak-interaction physics and astrophysics questions will be addressed by means of laser spectroscopy, decay studies, mass spectrometry and complementary trap-assisted measurements. Experience at other ISOL facilities evidences that ion beams with a high degree of purity are required to push experiments towards the limits of nuclear stability [5, 6, 7].

## GENERAL PRINCIPLES FOR DESIGN

The DESIR facility consists to a 1500 m<sup>2</sup> experimental hall and 97m of upstream and interconnected beam lines. Along these lines, a RFQ-Cooler [8] and a High Resolution Separator (HRS) [9] will be in charge to provide a reduction of the emittance and high purification of the beams coming from S3-LEB and SPIRAL1 (see Fig. 2). The RFQ-Cooler will be located just before the HRS. Beam coming from S3-LEB or SPIRAL1 will can be injected in this branch or by-passed for direct injection up to the DESIR hall according physics experimental requirements. Experimental set-ups will be located in the large hall (see Fig. 2).

\* Work supported by the French research agency (ANR), through the program "Investissements d'Avenir", EQUIPEX Contract number ANR-11-EQPX-0012

<sup>†</sup> perrot@ipno.in2p3.fr

# STATUS OF THE BEAM DYNAMICS DESIGN OF THE NEW POST-STRIPPER DTL FOR GSI - FAIR

A. Rubin<sup>†</sup>, D. Daehn, X. Du, L. Groening, M.S. Kaiser, S. Mickat, GSI, Darmstadt, Germany

## Abstract

The GSI UNILAC has served as injector for all ion species since 40 years. Its 108 MHz Alvarez DTL providing acceleration from 1.4 MeV/u to 11.4 MeV/u has suffered from material fatigue and has to be replaced by a new section [1]. The design of the new post-stripper DTL is now under development in GSI. An optimized drift tube shape increases the shunt impedance and varying stem orientations mitigate parasitic rf-modes [2]. This contribution is on the beam dynamics layout.

## INTRODUCTION

The existing UNiversal Linear ACcelerator UNILAC at GSI (Fig. 1) serves as injector for the Facility for Anti-proton and Ion Research (FAIR), which is under constructing now at GSI [3]. The UNILAC will provide all primary ions but protons.

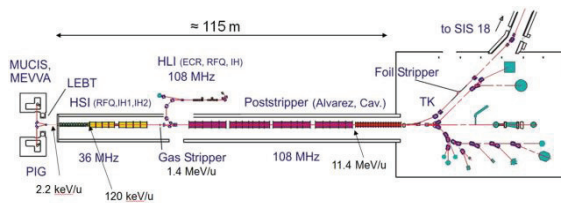


Figure 1: The UNiversal Linear ACcelerator (UNILAC) at GSI.

Due to the FAIR [4] requirements the UNILAC needs a considerable upgrade in nearest future. The existing post-stripper DTL suffered considerably from material fatigue during the last four decades and the amount of resources required for its maintenance increases continuously [5]. Replacement by a completely new DTL is due. The beam design parameters of the upgraded UNILAC are listed in Tab. 1.

Table 1: Parameters of the Upgraded UNILAC

|                      |              |
|----------------------|--------------|
| Ion A/q              | $\leq 8.5$   |
| Beam Current         | 1.76 A/q mA  |
| Input Beam Energy    | 1.4 MeV/u    |
| Output Beam Energy   | 3-11.7 MeV/u |
| Beam Pulse Length    | 200 $\mu$ s  |
| Beam Repetition Rate | 10 Hz        |
| Rf Frequency         | 108.408 MHz  |

## BEAM DYNAMICS SIMULATIONS FOR THE 1<sup>ST</sup> ALVAREZ TANK

Beam dynamics simulations for the new post-stripper DTL were done for  $^{238}\text{U}^{28+}$  using the TraceWin code [6]. The behaviour of the beam in the proposed structure was investigated for different zero current phase advances, as without current, as for the current of 15 mA. Input rms emittances were chosen as  $E_x=E_y=0.175\text{mm}\cdot\text{mrad}$  (norm.),  $E_z=16.57\text{deg}\cdot\text{MeV}$ . Periodic solutions were found for each case. The smallest transverse emittance growth along the 1<sup>st</sup> tank A1 (15mA) was obtained for a zero current phase advance  $k_0$  of  $55^\circ$ - $90^\circ$ . It confirms results of the measurements in frame of the HIPPI experiments [7,8]. The initial zero current phase advances  $k_0$  of  $65^\circ$ - $90^\circ$  also correspond to the stability areas of the Hofmann stability chart (Fig. 2).

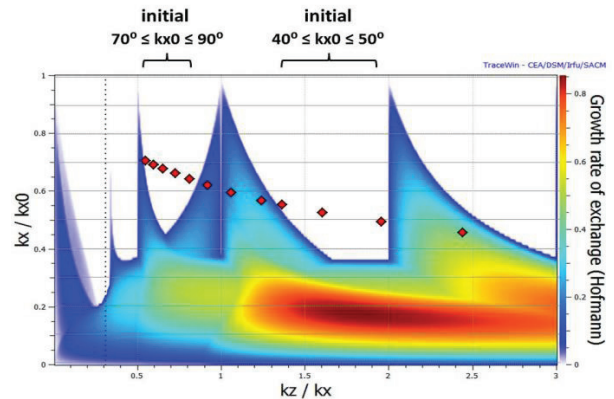


Figure 2: Initial zero current phase advances at Hofmann stability chart for the 1<sup>st</sup> tank of the new Alvarez-DTL.

Concerning the electric and magnetic field models the following cases for tank A1 were studied:

- "hard edge" model for E-field and B-field with identical quadrupoles in each drift tube (effective length of 96mm);
- 3D field maps for E-field, analytical field model for B-field with identical quadrupoles;
- 3D field maps for E-field and B-field with identical quadrupoles;
- "hard edge" model for E-field and B-field with three groups of quadrupoles (effective lengths 96 mm, 122 mm and 140 mm);
- 3D field maps for E-field, analytical field model for B-field with three groups of quadrupoles as above.

<sup>†</sup> a.rubin@gsi.de

# BEAM DYNAMICS SIMULATIONS AND CODE COMPARISON FOR A NEW CW RFQ DESIGN

Sergey Polozov<sup>1,2</sup>, Winfried Barth<sup>1,3,4</sup>, Timur Kulevoy<sup>1,2</sup>, Stepan Yaramyshev<sup>\* 1,3</sup>

<sup>1</sup> National Research Nuclear University - Moscow Engineering Physics Institute, Moscow, Russia

<sup>2</sup> Institute for Theoretical and Experimental Physics of NRC Kurchatov Institute, Moscow, Russia

<sup>3</sup> GSI Helmholtzzentrum fuer Schwerionenforschung, Darmstadt, Germany

<sup>4</sup> Helmholtz-Institut Mainz, Germany

## Abstract

Research and development of CW applications is an important step in RFQ design. The RF potential should be limited by 1.3-1.5 of Kilpatrick criterion for the CW mode. A 2 MeV RFQ is under development for the compact CW research proton accelerator, as well as for planned driver linac in Russia. The maximum beam current is fixed to 10 mA; the operating frequency has been set to 162 MHz. The new RFQ linac design will be presented and beam dynamics simulation results will be discussed. Calculations of the beam dynamics are provided using the codes BEAMDULAC (developed at MEPHI for linac design) and DYNAMION. A comparison of the software performance is presented.

## INTRODUCTION

The development of CW high-power proton linacs with 1.0-2.0 GeV beam energy is a very actual aim of crucial accelerator technology. Such linac is useful for large scale research complexes as spallation neutron sources or accelerator driven systems. Low or medium-energy linacs can be used for several applications as boron-neutron capture therapy (BNCT), high productivity isotopes generation and material science [1-4]. Also compact research facilities, for example SARAF at Soreq Centre [5], are the modern trend for high intensity CW proton and deuteron linac development.

In 2013 the Russian accelerator-driver concept has been developed by the collaboration of researchers from MEPHI, ITEP and Kurchatov Institute [6-9]. The proposed linac layout is close to the conventional scheme: an RFQ and an RF focusing section up to 30 MeV as normal conducting part [10] and independently phased SC cavities for medium and high beam energies. Three different RF focusing methods were discussed: RF crossed lenses [11], radio-frequency quadrupoles with modified profile of electrodes [12] and axi-symmetrical RF focusing (ARF) [13]. Three branches of experimental beam lines, delivering beam energy of 3, 30 and 100 MeV for dedicated experiments, are foreseen as the main feature of the proposed concept.

A preliminary design of a CW RFQ linac has been already started at MEPHI and ITEP [14, 15]. The recent detailed layout of the presented 2 MeV CW RFQ is based on a preliminary concept, exploiting long-term experience for proton and heavy ion linac development at MEPHI [16], ITEP [17,18], as well as decades of GSI expertise in

construction, optimization and routine operation of linac facilities [19-24]. Most recently, the prototype for a heavy ion CW linac with a SC main part is under construction at GSI and HIM in frame of a collaboration with IAP (University Frankfurt) [25].

The beam dynamics simulations for the new RFQ accelerating-focusing channel, as well as an analysis of the RFQ characteristics, have been performed by means of different software to provide for a cross-check of the design features and the calculated results. The main RFQ parameters are summarized in Tab.1.

Table 1: Main Parameters of the CW RFQ

| Ions                      | protons       |
|---------------------------|---------------|
| Input energy              | 46 keV        |
| Output energy             | 2.0 MeV       |
| Frequency                 | 162 MHz       |
| Voltage                   | 90 kV         |
| Length                    | 345 cm        |
| Average radius            | 0.530 cm      |
| Vanes half-width          | 0.412 cm      |
| Modulation                | 1.000 - 2.250 |
| Synchr. phase             | -90° - -33°   |
| Max. input beam current   | 10 mA         |
| Max. input beam emittance | 6 cm·mrad     |
| Particle transmission     | > 99%         |

## DESCRIPTION OF THE CODES

The presented RFQ accelerating-focusing channel has been designed at MEPHI by means of the BEAMDULAC code [26]. A cross-check, including calculations of RFQ characteristics and beam dynamics simulation, was performed by use of the DYNAMION software [27].

The BEAMDULAC code has been developed at MEPHI for self-consistent beam dynamics investigations in RF linacs and transport channels. The motion equation for each particle is solved under implementation of the external electromagnetic fields and the inter-particle Coulomb field simultaneously. The BEAMDULAC code utilizes the cloud-in-cell (CIC) method for accurate treatment of the space charge effects. It allows consideration of the shielding effect, which is sufficiently important for transverse focusing in the narrow channel. The fast Fourier transform (FFT) algorithm is used to solve the Poisson equation on a 3D grid. The obtained Fourier series for the space charge potential can be analytically differentiated, and thus each component of the Coulomb electrical field can be found as a series with known coefficients. The dedicated version of the

\* s.yaramyshev@gsi.de

# THE SIMULATION STUDY OF BEAM DYNAMICS FOR CSNS LINAC DURING BEAM COMMISSIONING

Y. Yuan<sup>†,1,2</sup>, H. Ji<sup>1,2</sup>, S. Wang<sup>1,2</sup>, J. Peng<sup>1,2</sup>

<sup>1</sup>China Spallation Neutron Source, Institute of High Energy Physics, Chinese Academy of Sciences, Dongguan, China

<sup>2</sup>Dongguan Institute of Neutron Science, Dongguan, China

## Abstract

China Spallation Neutron Source (CSNS) is a high intensity accelerator based facility. Its accelerator consists of an H<sup>-</sup> injector and a proton Rapid Cycling Synchrotron. The injector includes the front end and linac. The RFQ accelerates the beam to 3MeV, and then the Drift Tube Linac (DTL) accelerates it to 80MeV[1]. An Medium Energy Beam Transport (MEBT) matches RFQ and DTL, and the DTL consists of four tanks. Commissioning of the MEBT and the first DTL tank (DTL1) have been accomplished in the last run. Due to the difference of actual effective length and theoretical effective length of magnets in MEBT and DTL1, in order to compare its impact of beam transport, this paper takes a beam dynamics simulation on beam transport in MEBT and DTL1 with IMPACT-Z code[2]. Meanwhile, the transport of beam with different emittance in MEBT and DTL1 is studied because of the large emittance at RFQ exit. All the simulation includes magnet error and RF error.

## INTRODUCTION

Before the magnet measurement, the magnet effective length of lattice is theoretical value, so the commissioning software and the beam dynamics simulation both take this value. After the magnet measurement, the magnet effective length closer to the actual situation is given. In order to compare its effects on beam transport in MEBT and DTL1, under circumstance of match, the three-dimensional code IMPACT-Z is taken to study. Due to the large emittance at the exit of RFQ in the beginning, some steps had been taken to decrease emittance in order to avoid more beam loss. Before these steps, the transport of beam with different emittance at the exit of RFQ needs to be considered. All the simulation includes magnet error and RF error.

## SIMULATION STUDY OF BEAM DYNAMICS ON MEBT AND DTL1

CSNS/DTL consists of four accelerating cavities, the length among the cavities is designed to maintain longitudinal continuity. Figure 1 shows the layout of the front end and linac, inside the red box is MEBT and DTL. The last beam commissioning includes MEBT and DTL1. Correspondingly, in this paper, the simulation study have

been taken on MEBT and DTL1. Beam is matched from RFQ exit to DTL1 entry by MEBT. Corresponding to the theoretical effective length and actual effective length of magnets, there are two lattices for MEBT and DTL1 which are both matched. Through comparing beam emittance growth of two lattices, the difference between them can be gotten.

Through giving different beam emittance from small to large at RFQ exit, the simulation can get the influence of initial emittance on the beam transportation in DTL1, and get the results how much emittance does RFQ exit achieved when beam loss occurs.

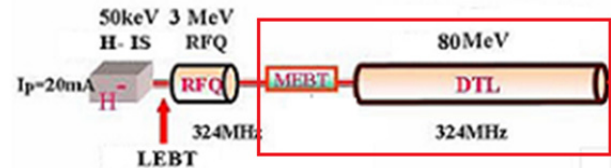


Figure 1: Layout of the front end and linac.

## Emittance Growth with Different Magnet Effective Length

In the simulation, the initial distribution of particles is 6D water bag, the number of macro particles is 100,000, the currents of beams is 15mA, the normalized RMS emittance of beam at RFQ exit is  $0.2 \pi$  mm.mrad. Table 1 shows all the theoretical static errors about magnet and RF. In this simulation, assumed errors just include quadrupole magnet alignment error and RF amplitude error. Figure 2 is a comparison of the horizontal emittance evolution of beam along linac. Figure 3 is a comparison of the vertical emittance evolution of beam along linac.

Table 1: Theoretical Static Errors

| Errors  | Range          |
|---|----------------|
| <i>Quad alignment error (transverse displacement)</i> | $\pm 0.1$ mm   |
| <i>Quad alignment error (roll error)</i>              | $\pm 3$ mrad   |
| <i>Quad gradient error</i>                            | $\pm 1\%$      |
| <i>RF amplitude error</i>                             | $\pm 1\%$      |
| <i>RF phase error</i>                                 | $\pm 1$ degree |

<sup>†</sup>yuanyue@ihep.ac.cn

# BEAM DYNAMICS STUDY OF C-ADS INJECTOR-I WITH DEVELOPING P-TOPO CODE\*

Zhicong Liu<sup>1,2</sup>, Chao Li<sup>†</sup>, Qing Qin<sup>†</sup>, Yaliang Zhao<sup>1</sup>, Fang Yan<sup>1</sup>,

<sup>1</sup>Key Laboratory of Particle Acceleration Physics and Technology, Institute of High Energy Physics, Chinese Academy of Sciences, Beijing, China

<sup>2</sup>University of Chinese Academy of Sciences, 100049, Beijing, China

## Abstract

A parallelized, time-dependent 3D particle simulation code is under developing to study the high-intensity beam dynamics in linear accelerators. The self-consistent space charge effect is taken into account with the Particle-In-Cell (PIC) method. In this paper, the structure of program and the parallel strategy are demonstrated. Then, we show the results of code verification and benchmarking. It is proved that the solvers in P-TOPO code and parallel strategy are reliable and efficient. Finally, the beam dynamics simulation of C-ADS Injector-I at IHEP are launched with P-TOPO and other codes. The possible reasons for the differences between results given by separated codes are also proposed.

## INTRODUCTION

A new particle simulation code Parallelized-Trace of Particle Orbits (P-TOPO) is now under development to study space charge effect at high intensity linacs [1-5]. The motivation is to improve the efficiency and calculation capability, based on the OpenMP techniques, of the TOPO code [6]. In the P-TOPO code, the basic elements, which supply external field to particles in linear accelerator, such as multi-pole, solenoid, RFQ, superconducting cavities, are modelled analytically or represented by field map obtained from CST. The internal interactive space charge field between particles is solved with the classic PIC method [7].

The Injector-I of Chinese Accelerator Driven Sub-Critical System (C-ADS) project is composed of ECRIS, LEPT, RFQ, MEBT1, SC section and MEBT2, which is under beam commissioning in IHEP. In recent experiment, a 10.1 MeV, 10.03 mA pulse beam is successfully achieved [8]. In this paper we will give a brief introduction of Injector-I and show the beam simulation results in detail with P-TOPO code. In section 2, the brief structure and parallelization strategy of P-TOPO are introduced. In section 3, code verification and benchmarking are given. In section 4, simulation results of C-ADS Injector-I are given by P-TOPO code and other widely used codes. Several reasons are proposed to interpret the difference among results given by P-TOPO and other codes. Conclusion and summary are given in section 5.

\* Supported by the Ministry of Science and Technology of China under Grant no.2014CB845501.

† Email address: lichao@ihep.ac.cn; qinq@ihep.ac.cn;

## P-TOPO

P-TOPO is developed with C++ language and parallelized based on the OpenMP techniques to achieve a high beam processing. Now, it can be run at PC with any number of cores. The structure of this program is as Fig. 1.

1) The MAIN class is in charge of getting the electric-magnetic field from external elements or inner space charge field, and particle updating under the effect of these obtained fields.

2) The Lattice class composed of elements class could be used to establish accelerator lattice with great flexibility. The external field supplied by certain element could be represented by a field map from CST or by analytical approximation.

3) The Beam class saves the beam information and calculates the beam parameters, like twiss parameters, emittance, beam size, et.

4) The Distribution class serves as initial particle distribution generator for specific type.

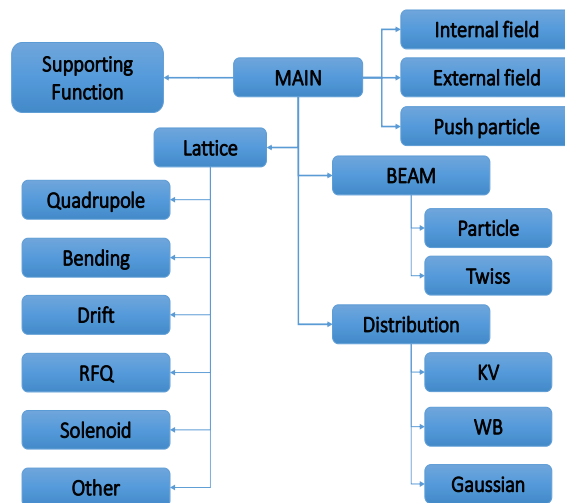


Figure 1: Layout of P-TOPO.

The parallelization occurs mainly in getting internal field, external field and particle pusher, where no interaction exists between different processing. Take the PIC module for example, it requires 4 separated steps to get the internal space charge field.

Step1, Weighting particles to grids;

Step2, Solving potential on the grids by FFT;

Step3, Obtaining the electric field on grid by the difference of the electric potential field;

# BEAM STEERING STUDIES FOR THE SUPERCONDUCTING LINAC OF THE RAON ACCELERATOR

Hyunchang Jin\*, Ji-Ho Jang, Dong-O Jeon

Institute for Basic Science, Yuseong-daero 1689-gil, Yuseong-gu, Daejeon, Korea

## Abstract

The RAON accelerator of Rare Isotope Science Project (RISP) has been developed to accelerate various kinds of stable ion beams and rare isotope beams for a wide range of science experiments. In the RAON accelerator, the superconducting linac (SCL) will be installed for the acceleration of the beams and it is composed of tens of cryomodules which include superconducting radio frequency cavities. Between two cryomodules, there is a warm section and two quadrupoles are located in the warm section with a beam diagnostics box in between. Also, in this warm section, one horizontal corrector and one beam position monitor (BPM) are mounted inside of first quadrupole, and one vertical corrector is located inside of second quadrupole for the beam steering. With these correctors and BPMs, the beam steering studies are carried out as varying the number of correctors and BPMs in the SCL of the RAON accelerator and the results are presented.

## INTRODUCTION

The RAON accelerator [1] has been developed by the Rare Isotope Science Project (RISP) to accelerate and transport the rare isotope and stable ion beams from proton to uranium for a various kind of science experiments. The beams created by an electron cyclotron resonance ion source (ECR-IS) or an isotope separation on line (ISOL) system are transported to the radio frequency quadrupole (RFQ) after the low energy beam transport (LEBT) [2] and re-accelerated by the low energy superconducting linac (SCL1 or SCL3). These beams can be used for the low energy experiments or accelerated again by the high energy superconducting linac (SCL2) after passing through the charge stripping section [3] for the high energy experiments. Figure 1 shows the layout of the RAON accelerator.

The superconducting linacs of the RAON accelerator are divided into three sections, which are named SCL1, SCL2, and SCL3, depending on the type and number of superconducting cavities and the purpose of the beam acceleration. The SCL1 and SCL3 include two types of cavities, quarter-wave resonator (QWR) and half-wave resonator (HWR) and accelerate mainly the stable ion beams and the rare isotope beams, respectively. On the other hand, the SCL2 consists of two types of single spoke cavities (SSR1 and SSR2) and accelerates again the beams accelerated by the SCL1 or SCL3. The reference frequency of each section is also different depending on the type of cavity and it is 81.25 MHz for QWR cavities, 162.5 MHz for HWR cavities, and 325 MHz for

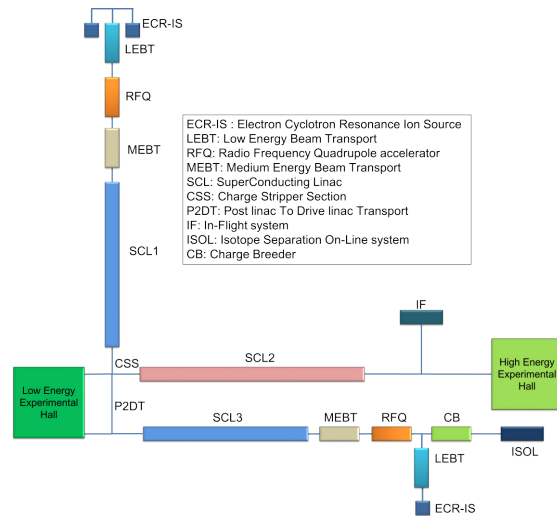


Figure 1: Layout of the RAON accelerator.

SSR cavities, respectively. For the beam focusing and diagnostics at the superconducting linac, there is a warm section, which includes two quadrupoles, between cryomodules. At each warm section, a horizontal and a vertical correctors are mounted inside of first and second quadrupoles, respectively, and a beam-position monitor (BPM) is installed at first quadrupole for the beam steering. The schematic view of the SCL1 is shown in Fig. 2. In order to steer the distorted beam orbit to the reference orbit at the RAON accelerator, the beam steering studies has been carried out from the low energy section to the high energy section by using the singular value decomposition (SVD) [4] method and a graphical user interface (GUI) has also been developed with a beam optics code, DYNAC [5] and a computing program, MATLAB [6]. In this paper, the results of the beam steering simulations at the SCL1 will be presented and we will describe the simulation results for the cases with different number and location of correctors and BPMs.

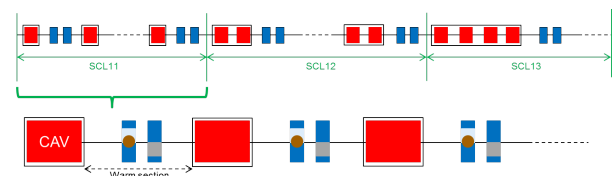


Figure 2: Schematic view of the SCL1. At each warm section, one horizontal corrector and one BPM are mounted at first quadrupole, and one vertical corrector is located at second quadrupole for the beam steering.

\* hcjin@ibs.re.kr

# ANALYTICAL APPROACH FOR ACHROMATIC STRUCTURE STUDY AND DESIGN

H. Y. Barminova, NRNU MEPhI, Moscow, Russia  
A. S. Chikhachev, SSC VEI, Moscow, Russia

## Abstract

The analytical approach is proposed to study the achromatic structures. The fully kinetic self-consistent time-dependent models are implemented in the approach. The method allows to predict the beam phase portrait behavior in magnetic fields of the structure with easy scaling and wide physical generality. The preliminary results of the method application for the bending magnets and the quadrupoles are presented.

## INTRODUCTION

Achromatic structures are the important elements of the modern accelerator facilities [1-3]. The choice of suitable achromatic structures for the specific accelerator facility is a significant part of the facility research and development. The beam dynamic simulation with the help of numerous program codes (as example, [4-6]) is usually applied for this aims. In the case of multi-parameter task of charged particle beam formation with high intensity and high brightness the analytical approach is an attractive tool to describe the beam dynamics because it allows the task scalability and predicts the beam behavior with the most physical generality. Such an approach becomes possible, for instance, while using the self-consistent time-dependent models [7-9]. These models are the modifications of well-known Kapchinsky-Vladimirsky model (K-V model), which describes quasistationary continuous beam. In the paper presented the 2D and 3D models are used for the analysis of the beam phase portrait behavior in the dipole and quadrupole magnets, involved into the achromatic structure. These models are fully kinetic and time-dependent and correspond to uniformly charged intense beam both continuous and bunched. The models consider the continuous beam with elliptical cross-section and the bunched beam shaped as an ellipsoid with various relations between the semiaxes.

## MOTION IN BENDING MAGNET

To describe analytically the motion of the beam with elliptical cross-section in the bending magnet the model is developed, corresponding to the uniformly charged beam. Some idealization of the task geometry is applied, namely, the bunch should have the most size in the coordinate direction corresponding to the direction of the magnetic force lines (2D approximation), and the magnetic field has a sharp edge, i.e. at this step the fringe fields of the dipole magnet are not taken into account. In addition, we assume the simple beam structure when it

consists of one kind of the particle with the same values of both the charge and the mass.

Let us begin from the case of non-relativistic and non-intense or emittance-dominant beam. The approximation of uniformly charged beam moving in the uniform external field allow to write the invariant  $I$  for the linear equations of the beam particle motion:

$$I = \frac{(u \dot{x} - ux \dot{)}^2}{\epsilon_x^2} + \frac{(v \dot{y} - vy \dot{)}^2}{\epsilon_y^2} + \frac{x^2}{u^2} + \frac{y^2}{v^2} + C_0(x \dot{y} - y \dot{x}) \quad (1)$$

where  $x, y$  – the coordinate axes, connected with the beam mass center and rotating with the mass center in the laboratory coordinate system,  $u, v$  – the auxiliary time-dependent functions,  $C_0$  – the mean angular momentum of the particle, the dot means the differentiation with respect to the time.

The kinetic distribution function  $f$  corresponding to the particle oscillations in the plane of the turn may be written as

$$f = \kappa \delta(I - 1), \quad (2)$$

where  $\kappa$  – the normalization constant,  $\delta$  – the delta function. Such function automatically satisfies to Vlasov equation and really describes the beam with elliptical cross-section in the plane of the turn:

$$n = \int f(I) dx dy = \frac{\pi \kappa}{uv} \epsilon_1 \epsilon_2 \sigma(1 - Ax^2 - By^2 - Cxy) \quad (3)$$

where

$$A = \frac{1}{u^2} - \frac{C_0^2 \epsilon_2^2}{4v^2}, B = \frac{1}{v^2} - \frac{C_0^2 \epsilon_1^2}{4u^2}, C = C_0 \left( \frac{u}{v} - \frac{v}{u} \right).$$

Here  $\sigma$  is Heaviside function,  $\epsilon_1, \epsilon_2$  – the values, which characterize the partial emittances of the beam in the cross-section, corresponding to the plane of the turn.

Using the equations (1) and (2), one can obtain for the beam rms values:

$$\frac{1}{R_x^2} = \left( A + B + ((A - B)^2 + C^2)^{1/2} \right) / 2$$

$$\frac{1}{R_y^2} = \left( A + B - ((A - B)^2 + C^2)^{1/2} \right) / 2 \quad (4)$$

# ESSnuSB PROJECT TO PRODUCE INTENSE BEAMS OF NEUTRINOS AND MUONS

E. Bouquerel\* on the behalf of the ESSnuSB project,  
*IPHC, UNISTRA, CNRS, 23 rue du Loess, 67200, Strasbourg, France*

## Abstract

A new project for the production of a very intense neutrino beam has arisen to enable the discovery of a leptonic CP violation. This facility will use the world's most intense pulsed spallation neutron source, the European Spallation Source (ESS) under construction in Lund. Its linac is expected to be fully operational at 5 MW power by 2023, using 2 GeV protons. In addition to the neutrinos, the ESSnuSB proposed facility will produce a copious number of muons at the same time. These muons also could be used by a future Neutrino Factory to study a possible CP violation in the leptonic sector and neutrino cross-sections. They could be used as well by a muon collider or a low energy nuSTORM. The layout of such a facility, consisting in the upgrade of the linac, the use of an accumulator ring, a target/horn system and a megaton Water Cherenkov neutrino detector, is presented. The physics potential is also described.

## ESSvSB PROJECT

The ESSvSB (standing for European Spallation Source Neutrino Super Beam) project proposes to study a Super Beam which uses the high power linac of the ESS facility [1] based at Lund in Sweden as a proton driver and a MEMPHYS type detector [2, 3] located in a deep mine at a distance of about 500 km, near the second neutrino oscillation maximum (Fig. 1).

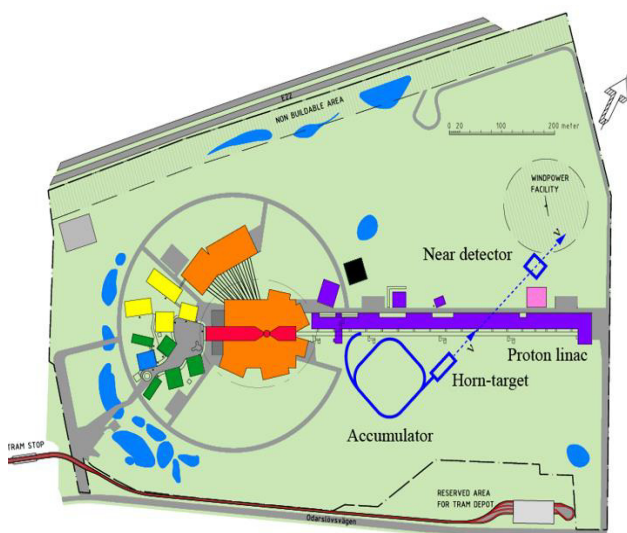


Figure 1: ESSvSB layout on top of the ESS facility.

\* Elia.Bouquerel@iphc.cnrs.fr

## The ESS Linac

ESS will deliver a first proton beam for neutron production at reduced energy and power by 2019. A proton beam of the full design power 5 MW and energy 2.0 GeV will be delivered by 2023. There will be 14 pulses of 62.5 mA current and 2.86 ms length per second (Table 1). In order for the ESS to be used to generate a neutrino beam in parallel with the spallation neutrons, some modifications of the proton linac are necessary. A preliminary study of these modifications that are required to allow simultaneous acceleration of  $H^+$  (for neutron production) and  $H^-$  (for neutrinos) ions at an average power of 5 + 5 MW has been made [4].

Table 1:  $\mu$  Main ESS Facility Parameters [1]

| Parameter                      | Value   |
|--------------------------------|---------|
| Average beam power             | 5 MW    |
| Proton kinetic energy          | 2.0 GeV |
| Average macro-pulse current    | 62.5 mA |
| Macro-pulse length             | 2.86 ms |
| Pulse repetition rate          | 14 Hz   |
| Max. acc. cavity surface field | 45 MV/m |
| Max. linac length              | 352.5 m |
| Annual operating period        | 5000 h  |
| Reliability                    | 95%     |

## The Accumulator Ring and Beam Switchyard

An accumulator ring to compress the pulses to few  $\mu s$  is mandatory to avoid overheating issues of the neutrino targets. A first estimation gives a ring having a circumference of 376 m [5] (Table 2). Each pulse from the ESS linac will contain  $1.1 \times 10^{15}$  protons, which for a normalized beam emittance of  $200 \pi$  mm mrad in the ring by multi-turn injection (the emittance from the linac should be in the order of a few mm-mrad) will lead to the space-charge tune shift of about 0.75.

Table 2: Accumulator Parameters [5]

| Parameter             | Value        |
|-----------------------|--------------|
| Circumference         | 376 m        |
| Number of dipoles     | 64           |
| Number of quadrupoles | 84           |
| Bending radius        | 14.6 m       |
| Injection region      | 12.5 m       |
| Revolution time       | 1.32 $\mu s$ |

The  $H^-$  ions will be fully stripped during the injection into the accumulator using either stripping foils or a laser-stripping device [5, 6]. The extraction of the beam from the ring needs a group of kickers that should have a rise time of not more than 100 ns.

# LASER STRIPPING H<sup>+</sup> CHARGE EXCHANGE INJECTION BY FEMTOSECOND LASERS

T. Gorlov, SNS Project, Oak Ridge National Laboratory, Oak Ridge, Tennessee 37831

## Abstract

A new method of H<sup>+</sup> laser assistant charge exchange injection using femtosecond laser pulses is considered. The existing method uses a divergent laser beam that allows compensation for the angular and momentum spread of the stripped beam. The femtosecond laser pulse has a similar property that can cover the spread and yield efficient laser stripping. Results of simulations with realistic femtosecond laser and H<sup>+</sup> beam parameters are discussed. The proposed method may have some benefits for particular technical conditions over other methods.

## INTRODUCTION

Femtosecond lasers may be applied for H<sup>+</sup> charge exchange injection method or laser stripping. Laser stripping has been actively developed at the SNS project over the past decade. Theoretical investigation began in [1]. Practical application has been proven for stripping of short (6 ps) pulses [2] and for long (10 us) pulses of H<sup>+</sup> [3]. The second step of the three-step laser stripping scheme [1] considers resonant excitation of the H<sup>0</sup> beam by laser at the incidence angle  $\alpha$ :

$$\omega_0 = \gamma_p(1 + \beta_p \cos(\alpha))\omega \quad (1)$$

where  $\beta_p$  and  $\gamma_p$  are relativistic factors of the H<sup>0</sup> beam with longitudinal momentum  $p$ . Equation (1) represents a precise resonant condition for monochromatic laser frequency  $\omega$  and discrete atomic excitation frequency  $\omega_0$ . Longitudinal momentum spread  $\delta p$  of a realistic beam spreads out particles from resonance particle with design momentum  $p$ . As a result, most particles are not excited and stripped. In this way, longitudinal momentum spread complicates laser stripping and presents a challenging practical problem. This section presents a qualitative review of the methods of compensating  $\delta p$  in terms of (1), skipping the complicated mathematical mechanism of laser-bunch interaction.

Paper [1] proposed the use of a divergent laser beam with at an angle of  $\delta\alpha$  to cover the spread  $\delta\gamma(\delta p)$ ,  $\delta\beta(\delta p)$ . A laser beam with angle of about 0.5 mrad provides good resonance conditions for all the particles of the bunch. This method has been tested experimentally [2, 3].

Another method of  $\delta p$  compensation has been proposed in [4] and developed in [5]. It involves broadening the discrete atomic resonance frequency  $\omega_0$  by applying an electric field in the particle's rest frame or a magnetic field in the laboratory frame. All off-resonance particles can be excited by using wide continuum atomic resonance

$\delta\omega_0$  when a high energy atom is emerged into a strong magnetic field in the laboratory frame.

This paper discusses another method of momentum beam compensation which involves broadening the laser frequency  $\omega$  in terms of (1). The picosecond laser pulse that has been considered in [2] or [3] has a narrow band frequency  $\omega$  which may be broadened by using femtosecond laser pulses. The spectrum  $f(\omega')$  of finite laser pulse

$$E(t) = E_0 e^{-\frac{t^2}{4\sigma^2}} \cos(\omega t) = \int_{-\infty}^{\infty} f(\omega') \cos(\omega' t) d\omega' \quad (2)$$

with pulse length  $\sigma$  (in terms of energy) can be calculated by Fourier transform

$$f(\omega') = \frac{E_0 \sigma e^{-\sigma^2(\omega' + \omega)^2} (1 + e^{4\sigma^2 \omega \omega'})}{2\sqrt{\pi}} \quad (3)$$

The RMS width  $\sigma_\omega$  of the function is estimated to be

$$\sigma_\omega \approx \frac{1}{\sigma} \sqrt{\frac{1}{2} - \frac{1}{\pi}} = \frac{0.42}{\sigma} \quad (4)$$

A shorter pulse has a wider spectrum. The required laser pulse width  $\sigma_t$  may be estimated by differentiating  $\omega$  over momentum  $p$  and equating  $d\omega$  to  $\sigma_\omega$ . The SNS accelerator has a relative longitudinal momentum spread ( $\Delta p/p \approx 10^{-4}$ ) and the laser pulse width  $\sigma_t$  is estimated to be about 1 ps. This rough estimate indicates that a sub-picosecond or femtosecond laser pulse is required to compensate the longitudinal momentum spread for high efficiency excitation.

All three methods have their relative advantages and disadvantages and each method can become more convenient for accelerator with particular parameters. The divergent laser beam method allows for adjustment of the incidence angle  $\alpha$  for beam energy in a wide range; however, it requires precise laser optics tuning. The atomic broad shape resonance method does not require tuning the laser beam optics but may require a more complicated (or simplified) magnet system for stripping the H<sup>+</sup> beam. It also requires more beam energy [5]. The third method differs from the others by using femtosecond lasers. The H<sup>+</sup> bunch usually has a multi-picosecond width that requires about the same longitudinal width as the laser to achieve adequate interaction overlap. For this reason, a femtosecond laser pulse is difficult to use for stripping the H<sup>+</sup> bunch at a nonzero incidence angle of  $\alpha$ . Adequate overlap with femtosecond pulse is only achieved by using head-on interaction or setting the angle at 0. As existing

This work has been supported by Oak Ridge National Laboratory, managed by UT-Battelle, LLC, under contract DE-AC05-00OR22725 for the U.S. Department of Energy.

ISBN 978-3-95450-178-6

# EFFECT OF BEAM LOSSES ON WIRE SCANNER SCINTILLATOR READOUT, HYPOTHESIS AND PRELIMINARY RESULTS

B. Cheymol\*, European Spallation Source, Lund, Sweden

## Abstract

In an hadron accelerator, the characterization of the beam transverse halo can lead to a better understanding of the beam dynamics and a reduction of the beam losses. Unfortunately the effect of losses on beam instrumentation implies a reduction of the instrument sensitivity due to the background noise.

In this paper, we will discuss the effect of losses on the wire scanner scintillator foreseen for the ESS linac, in particular the different hypothesis for the input will be describes and preliminary results will be present.

## INTRODUCTION

In the elliptical sections of the ESS linac [1] the Wire Scanner (WS) station will be equipped with scintillators to measure the hadronic shower created by a thin tungsten wire [2]. One of the main reasons is that above 200 MeV the secondary emission signal is not strong enough to measure directly the current produced in the wire, the signal from a scintillator will be stronger and also cleaner, but this detector will be also sensitive to radiation induced by beam losses. Preliminary simulations have been performed to check this effect and define beam loss limits for the WS operation.

Several beam losses scenario have been simulated with the Monte Carlo (MC) code FLUKA [3] in order to estimate the influence of losses on the beam profile measurement. Note that all the particles distributions presented in this paper are not the results of beam dynamic simulations.

## HYPOTHESIS AND INPUT PARAMETERS

### Hypothesis

To simplify the problem, we propose to study the effect of various beam losses scenario in a single elliptical period (one elliptical cryomodule followed by one quadrupole doublet). It was assumed, in a first approximation, that the contribution from upstream or downstream losses will be either too low to be detected or easily removed in the data analysis.

A simplified geometry of an elliptical cryomodule has been implemented in the MC code, only the main components have been simulated, all the cryogenic pipe, cable, RF guide have not been implemented in the simulated geometry. Despite the fact that the Medium and High  $\beta$  cavities are slightly different, the geometry is independent of the beam energy, a 5 cells cavity has been chosen for this study, which the one foreseen to be installed in the High  $\beta$  section for beam energy above 570 MeV, the length of the cryomodule is about 6.5 meters. The quadruples consists in a single volume of copper. The author would like to emphasis that

no electromagnetic field has been implemented in the simulations.

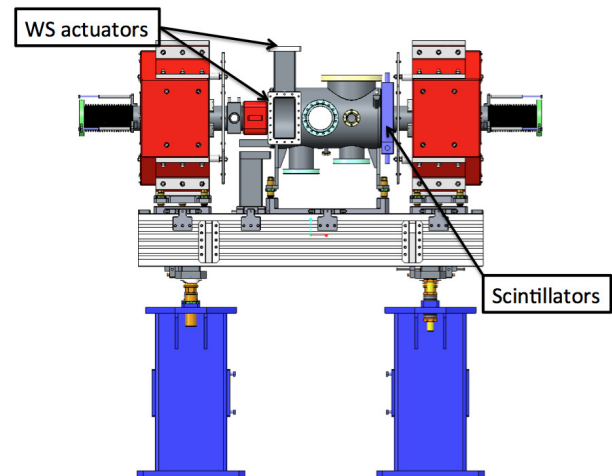


Figure 1: Preliminary design of the elliptical LWU, the length flange to flange is 1920 mm (courtesy of STFC Daresbury Laboratory).

The Linac Warm Unit (LWU) chamber has been simulated (see Fig. 1), the scintillator are attached to this chamber, the detector assembly is shown in Fig. 2. The minimum aperture in the LWU is 100 mm.

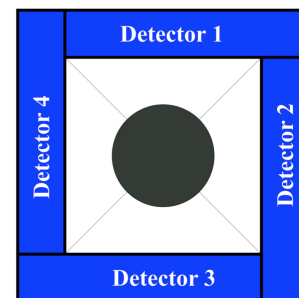


Figure 2: Detector assembly for the ESS WS system.

The scintillator material in these simulations are not the one foreseen to be used for the ESS WS system, in preliminary design phase of the WS detector BGO crystal was the primary candidate for the scintillator and all the simulations presented in this paper have been performed with this type of scintillator. nevertheless, since the geometry is identical, the signal to noise ratio shall be comparable for both versions of the detector.

For this simulations and in a first approximation, the beam sizes of the core were assumed to be constant in the cold linac with  $\sigma_x = \sigma_y = 2$  mm. The beam has no energy spread.

\* benjamin.cheymol@ess.se

# EFFECTS OF ENERGY DEPOSITION MODELS AND CONDUCTIVE COOLING ON WIRE SCANNER THERMAL LOAD, ANALYTICAL AND FINITE ELEMENT ANALYSIS APPROACH

B. Cheymol\*, European Spallation Source, Lund, Sweden

## INTRODUCTION

A number of wire scanners will be installed in the ESS linac [1] to measure beam profile and perform emittance measurement with a 3-gradients type method. The ESS wire scanner will be equipped with 33 μm for carbon wire in the warm linac and a 40 μm for tungsten wire in the cold linac.

Due to the high power on the beam, the duty cycle has to be reduced to allow the insertion of interceptive devices, preliminary estimations of the wire thermal load [2] show that the wire can withstand the 2 dedicated modes:

- A slow tuning mode (i.e. 50 μs, up to 62.5 mA, 1 Hz).
- A fast tuning mode (i.e. 10 μs, up to 62.5 mA, 14 Hz).

The temperatures have been estimated with a simple analytical model assuming no conductivity effect, the energy deposited in the wire has been estimated with the stopping power extracted from table and assuming a constant thickness of the wire equal to its diameter, this paper proposes to update the estimation of the wire temperature with different model for the energy deposition and to compare the results of the analytical model to the results of a Finite Element (FE) analysis. In all the document, the beam intensity is equal to 65 mA.

## ANALYTICAL MODEL PARAMETERS

The thermal load on wire induced by the beam could in the worst case damage the wire. Given a linac pulse, populated by  $N_{part}$  particles with RMS transverse beam sizes  $\sigma_x$  and  $\sigma_y$ , traversing a wire, the induced temperature can be calculated as:

$$\Delta T = \frac{N_{part}}{\rho C p(T) V} \frac{\Delta E}{2\pi\sigma_x\sigma_y} e^{-\left(\frac{x^2}{2\sigma_x^2} + \frac{y^2}{2\sigma_y^2}\right)} \quad (1)$$

Where  $Cp(T)$  is the specific heat capacity of the material of the wire,  $\rho$  is the wire material density and  $V$  volume of the wire and  $\Delta E$  the energy deposited in the wire per particle.

### Wire Material Properties

An analytical model of the specific heat capacity of the carbon and of the tungsten has been used for the estimation of the temperature, data can be found in [3] and [4]. The density of the materials (respectively 1.8 g·cm<sup>-3</sup> for carbon and 19.25 g·cm<sup>-3</sup> for tungsten) as well as the emissivity (0.8 for carbon and 0.1 for tungsten) were assumed to be independent of the temperature in a first approximation.

\* benjamin.cheymol@esss.se

### Cooling Process

In first approximation, the conductive cooling is negligible, thus it is assumed that the wire cooling is dominated by black body radiation, described by Stefan-Boltzmann law. The heat radiated from the wire surface is proportional to the fourth power of the temperature. The difference from the ideal black-body radiation is described by a factor called emissivity and the radiated power is given by :

$$P = \sigma \varepsilon A (T^4 - T_0^4) \quad (2)$$

Where  $\sigma$  is the Stefan-Boltzmann constant,  $\varepsilon$  the emissivity,  $A$  the area of the body,  $T$  its temperature and  $T_0$  the ambient temperature (set in all the studies presented in the document at 298 K). After a linac pulse the temperature variation can be calculated as:

$$\frac{dT}{dt} = \frac{\sigma \varepsilon A (T^4 - T_0^4)}{\rho C p(T) V} \quad (3)$$

Other processes like thermoionic emission or wire sublimation are more efficient at high temperature, nevertheless for the ESS wire scanners and in general for wire scanners (or SEM grid) use at low energy beam, the thermoionic emission will perturb the signal from secondary emission. The wire temperature shall be kept below 2000 K to avoid this effect, thus these processes are neglected in this note.

### Energy Deposition Models

The energy deposited per particle has been estimated with the stopping power extracted from tables and the length of interaction assuming a constant stopping power across the wire diameter. For low beam energy, the stopping power increases when the particles move into the wire material. Assuming a constant stopping power, calculated for the incident beam energy leads to underestimation of the deposited energy.

For simplification, in the analytical model, the energy deposited by each particle crossing the wire is identical. This assumption leads to error due to the cylindrical geometry of the wire if the wire diameter is taken as interaction length. To reduce this error, an equivalent thickness of the wire can be calculated as:

$$e_{equ.} = \frac{\pi d}{4} \quad , \quad (4)$$

where  $d$  is the wire diameter.

The equivalent thickness of the wire is reduced by  $\approx 25\%$  compared to the wire diameter, the energy deposition is

# HIGH POWER AND HIGH DUTY CYCLE SLIT AND GRID SYSTEM FOR HADRON ACCELERATOR COMMISSIONING

B.Cheymol\*, A. Ponton, European Spallation Source, Lund, Sweden

## INTRODUCTION

Transverse emittance is one of the key measurements to be performed during the commissioning of the low energy sections of an hadron linac. The good knowledge of the beam transverse phase space allows a safe and efficient operation of the machines by using the results of the measurement for beam dynamic simulations.

In this paper we will discuss the accuracy and the limits of the transverse emittance measurement performed with the slit-grid method based on the ESS beam parameters at the RFQ (beam energy equal to 3.62 MeV) and DTL tank 1 (beam energy equal to 21 MeV) output [1]. The goal of this paper is to set the limits of the operating domain of the slit and grid system in machine similar to ESS, in particular to achieve emittance measurement with a beam pulse length up to 1 ms. The authors assume that the emittance will be measured on a diagnostic test bench with a matching sections.

In the following the emittance is referred to the RMS normalized emittance, the slit geometrical parameters are summarized in Fig. 1 for reference, the angle of the slit is the angle between one slit blade and the z-axis of the beam.

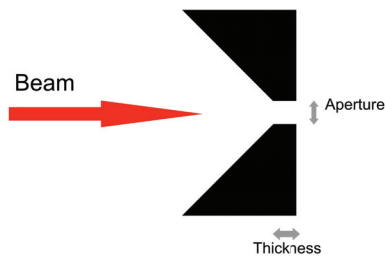


Figure 1: Schematic diagram of the slit used in the simulations (dimensions are not on scale).

## BEAM DISTRIBUTIONS

At the exit of the RFQ and the DTL, beam sizes are too small to use interceptive devices with pulses longer than 20-50  $\mu$ s. In order to reach relatively high duty cycle, the beam sizes at the slit location must be increased to reduce the thermal load, in addition the beam divergence has to be kept small enough to avoid angular cut in the transverse phase space during the emittance measurement, in a ideal case, the beam shall be parallel in both transverse planes, thus to expand the beam with small emittance increase and keep the divergence small enough a triplet of quadrupoles is mandatory.

Based on these specifications and similar quadrupoles characteristics from other facilities, preliminary simulations

\* benjamin.cheymol@esss.se

were performed with the TraceWin code [2] in order to generate beam sources which can be used as input for all the studies presented in this paper. Without a full optimization of the beam dynamics, these inputs have been considered as test cases for the design of an emittance meter. The Fig. 2 and Fig. 3 show the transverse phase spaces for the RFQ and DTL at the output to the triplet, the Twiss parameters are summarized in Table 1.

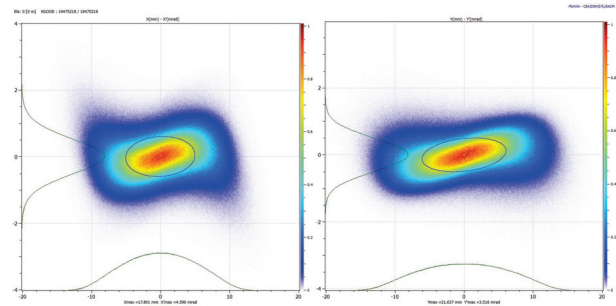


Figure 2: Transverse phase space distributions at the end RFQ matching section.

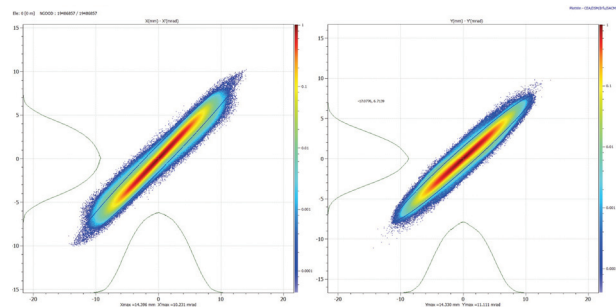


Figure 3: Transverse phase space distributions at the end DTL matching section.

Table 1: Beam Parameter Expected at 150 mm Upstream The Theoretical Slit Position For The RFQ and DTL Cases

| Location                | RFQ    |        | DTL    |        |
|-------------------------|--------|--------|--------|--------|
|                         | H      | V      | H      | V      |
| $\alpha$                | -0.076 | -0.216 | -6.19  | -5.25  |
| $\beta$ [mm/ $\pi$ rad] | 8.41   | 12.52  | 8.58   | 7.64   |
| $\epsilon_{norm.}$      | 0.2633 | 0.2601 | 0.3303 | 0.3103 |

In both cases, the beams have been transported from the RFQ entrance to the end of the matching section, The particles distributions are taken at 150 mm upstream the theoretical slit position in order to reserve space for mechanical integration.

# SCINTILLATOR DETECTORS FOR THE ESS HIGH ENERGY WIRE SCANNER

B. Cheymol\*, European Spallation Source, Lund, Sweden

## Abstract

In the ESS linac [1], during commissioning and restart phase, wire scanner (WS) will be used intensively to characterize the transverse beam profiles. At low energy, the mode of detection is based on Secondary Emission (SE), while at energies above 200 MeV, the primary mode of detection will be the measurement of the hadronic shower created in the thin wire.

In this paper we will present the design and the output signal estimation of the shower detector, based of inorganic crystal and silicon photodetector

## INTRODUCTION

In the ESS superconducting linac and downstream, 8 WS stations will be installed along the beam line. Each station will be equipped with two linear actuator to sample the separately the transverse planes and the last 5 stations, in the elliptical sections and in the transfer line to the target, will be used in shower detection mode in addition of the SE signal from the wire. The actuator fork will be equipped with a 40  $\mu\text{m}$  tungsten wire, for the ones to be used in the shower mode, the detectors will be positioned 400 mm downstream the wire [2].

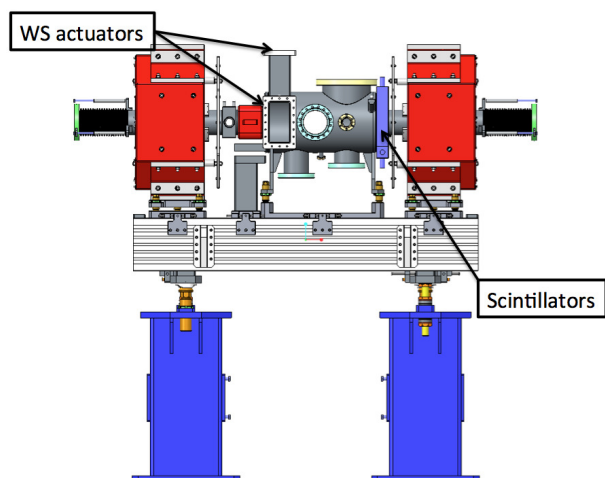


Figure 1: Preliminary design of the elliptical LWU, the total length flange to flange is  $\approx 1932$  mm, WS actuators are not shown (courtesy of STFC Daresbury Laboratory).

As shown in Fig. 1, due to the low energy of beam compared to proton synchrotron, the full system will be installed in a Linac Warm Unit (LWU), between two quadrupoles. This geometry has been chosen in order to avoid perturbation of the hadronic shower if the detectors would have been installed downstream the quadruple.

\* benjamin.cheymol@ess.se

## DETECTOR CONCEPT

In high energy physics experiment, wavelength shifting (WLS) fibers are often used to collect the light from scintillator in order to reduce calorimeter geometry complexity [3]. The same approach can be use for the ESS wire scanner, not to simplify the geometry but to protect the photodetector from radiation.

The light generated in the scintillator can be collected through a fiber. which can transport the light to the photodetector installed in an area with less radiation compare to the accelerator tunnel. In an ideal case, the photodetector can be installed in the klystron gallery in the same electronic cabinet as its front end electronic and its digitizer card.

### Detector Architecture

The acquisition electronic of the ESS WS is currently under development at Sincrotrone Elettra Trieste. For the SEM mode, it is foreseen to use two separated channels per wire, one with high gain and low bandwidth the other with a low gain and high bandwidth. With this setup it will possible to get a high dynamic range for the profile in a single scan. The same concept will be used for the scintillator readout.

Previous simulations show that 4 separated detector are needed to insure good homogeneity of the signal across the beam pipe [2], each detector will be connected to 2 Front-End (FE) electronic as for the SEM mode. The assembly geometry of the detector is shown in Fig. 2.

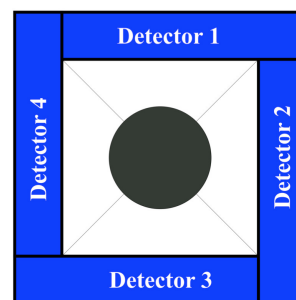


Figure 2: Detector assembly for the ESS WS system.

A combination of WLS fiber and clear fiber will be used to transport the light from the detector to a radiation free area, the detector architecture is shown in Fig. 3.

The scintillation light will be collected by two WLS fiber on each detector assembly, since the attenuation length of this fiber is high (few meters), their lengths have to be kept as short as possible. Silica fiber have a low attenuations, and are better candidates to transport the light over a long distance, for the ESS application the length from the WS station in the tunnel to the electronic rack in the klystron gallery is about 60 meters.

# ONLINE MEASUREMENT OF THE ENERGY SPREAD OF MULTI-TURN BEAM IN THE FERMILAB BOOSTER AT INJECTION\*

J. Nelson, Brown University, Providence, RI, U.S. A.  
 C.M. Bhat<sup>†</sup> and B. S. Hendricks, Fermilab, Batavia IL, U.S.A.,

## Abstract

We have developed a computer program interfaced with the ACNET environment of Fermilab accelerators to measure energy spread of the proton beam from the LINAC at an injection into the Booster. It uses a digitizing oscilloscope and provides users an ability to configure the scope settings for optimal data acquisition from a resistive wall current monitor. When the program is launched, a) a *one shot timeline* is generated to initiate beam injection into the Booster, b) a gap of about 40 ns is produced in the injected beam using a set of fast kickers, c) collects line charge distribution data from the wall current monitor for the first 200 μs from the injection and d) performs complete data analysis to extract full beam energy spread of the beam. The program also gives the option to store the data for off-line analyses. We illustrate a case with an example. We also present results on beam energy spread as a function of beam intensity from recent measurements.

## OVERVIEW

In recent years Fermilab has undertaken significant improvements to the existing accelerators to meet its high intensity proton demands for accelerator based HEP experiments onsite as well as long baseline neutrino experiments. One of the important aspects of this program is “Proton Improvement Plan” [1] with a baseline goal to extract the beam at 15 Hz rate from the Booster all the time with about 4.6E12 p/Booster cycle. With PIP -II [2], it is foreseen to increase the Booster beam delivery cycle rate from 15 Hz to 20 Hz, replace the existing normal conducting LINAC by superconducting RF LINAC and increase beam intensity by 50%. Hence, the current Booster plays a very significant role at least the next one and half decades in the Fermilab HEP program.

In support of the proposed upgrades to the Booster, a thorough understanding of the properties of the beam at injection is crucial; in particular, monitoring energy spread of the beam from the LINAC after the completion of injection. In the past, many attempts have been made to measure beam energy spread (e.g., ref. [3]) in bits and pieces using up dedicated beam time; often such measurements are carried out only soon after a major maintenance period. Furthermore, all the past measurements were on partial turn beam in the Booster. During 2013-2014, we developed a very robust method [4] to measure the beam energy spread on the multi-turn beam after creating a notch of width ≈ 40 nsec in the injected beam. These attempts lead us to develop an application software to automatize beam energy spread measurement at injection on request. In this

paper we explain the general principle, various functionalities of the software and illustrate with recent measurements.

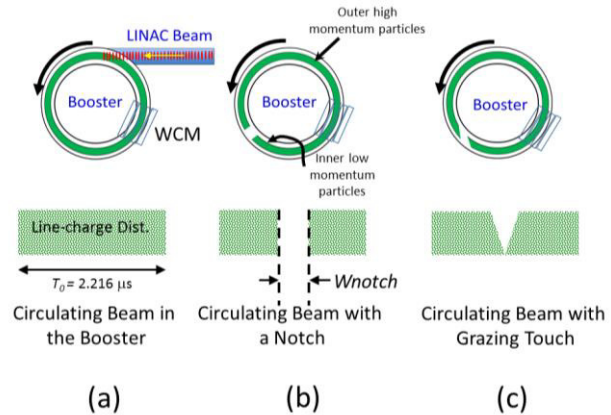


Figure 1: Schematic of newly injected multi-turn beam from the LINAC with a notch and notch filling due to slippage of the particles.

## APPLICATION SOFTWARE

### Physics Behind the Program

Particle beam that exits a pre-accelerator will always be having an energy spread  $\Delta E$  (full) about its mean (synchronous) energy  $E_s$ . When such a beam is injected into a synchrotron and accumulates, the higher and lower momentum particles slip differently relative to the synchronous particle while they circulate in the synchrotron. A schematic view of particle distribution of such a beam injected from the LINAC into the Booster is shown in Fig. 1(a). However, to differentiate between fast moving particles from the slow moving particles, one can create a notch (Fig. 1(b)) of width “*Wnotch*” in a fully debunched beam using a fast beam kicker and monitor the slippage of particles relative to particles with synchronous energy (see Fig. 1(c)). Evolution of line-charge distribution measured using a wall current monitor (WCM) for each case is shown in Fig 1 for clarity. By measuring the notch width and the time required for the highest momentum particles to cross (or touch in WCM data) the lowest momentum particles, “*Tgraze*”, we can extract the beam energy spread using,

$$\Delta E = \frac{\beta^2 E_s}{|\eta|} \frac{Wnotch}{Tgraze}$$

Where,  $\beta$  is the relativistic speed and  $\eta$  is the slip factor of the Booster lattice ( $\approx -0.4582$ ).

\* Work supported by Fermi Research Alliance, LLC under Contract No. De-AC02-07CH11359 with the United States Department of Energy  
<sup>†</sup> cbhat@fnal.gov

# FERMILAB BOOSTER TRANSITION CROSSING SIMULATIONS AND BEAM STUDIES \*

C.M. Bhat<sup>†</sup> and C.Y. Tan, Fermilab, Batavia, IL 60510, USA

## Abstract

The Fermilab Booster accelerates beam from 400 MeV to 8 GeV at 15 Hz. In the PIP (Proton Improvement Plan) era, it is required that Booster deliver  $4.2 \times 10^{12}$  protons per pulse to extraction. One of the obstacles for providing quality beam to the users is the longitudinal quadrupole oscillation that the beam suffers from right after transition. Although this oscillation is well taken care of with quadrupole dampers, it is important to understand the source of these oscillations in light of the PIP II requirements that require  $6.5 \times 10^{12}$  protons per pulse at extraction. This paper explores the results from machine studies, computer simulations and solutions to prevent the quadrupole oscillations after transition.

## INTRODUCTION

The Fermilab Booster was built in the 1970s [1] and will remain the workhorse for the PIP (Proton Improvement Plan) II era for many years until it is replaced. From the start of its operational life to the present (2016), the beam flux per hour through it has increased by an order of magnitude. See Fig. 1. The goal of PIP is to provide  $4.2 \times 10^{12}$  protons per pulse at extraction. And in the PIP II era, Booster is required to provide  $6.5 \times 10^{12}$  protons per pulse at extraction. There can be many show stoppers that prevent us from achieving the PIP II goals. [2] One obstacle that we have identified is transition crossing.

The traditional belief at Fermilab is that transition crossing in Booster is dominated by space charge effects or other beam intensity effects. [3–5] Many simulations have been done to reproduce measurements and to suggest methods to help the beam cross transition properly. However, from what we can see, these simulations only use a select few Booster beam pulses for comparison which we have found to be very naïve. In our experience, there is sufficient pulse to pulse variation in any measurement that we need to have a large enough sample set to actually be able to have any insight into the problem.

Therefore, in order to avoid the pitfall of using too few data sets, we have collected sufficient Booster transition crossing data for our analysis. We will use this data to generate a hypothesis as to what causes the beam to suffer from quadrupole oscillations after it crosses transition. We will then test our hypothesis with computer simulations. And finally, we will suggest methods for mitigating this problem.

\* Operated by Fermi Research Alliance, LLC under Contract No. DE-AC02-07CH11359 with the United States Department of Energy.

<sup>†</sup> cbhat@fnal.gov

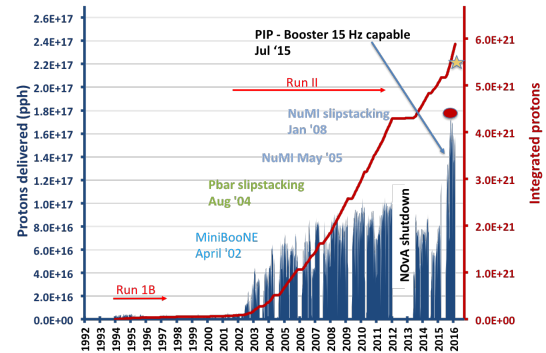


Figure 1: The proton flux per hour in Booster increased from  $< 10^{16}$  to  $> 10^{17}$  over a decade.

## MOTIVATION

One of the recent striking observations that led to suspect the traditional lore mentioned earlier was that the amplitude of the longitudinal quadrupole oscillations measured with a wall current monitor (Fig. 2) did not scale at least as a quadratic w.r.t. beam current,  $I_b$ . (Note: it is quadratic because we are using a wall current monitor to measure the quadrupole oscillations and thus the measured amplitude contains a factor of  $I_b$ . For example, the emittance growth from space charge effects has another factor of  $I_b$ . [6]). In fact, it looked like the amplitude of the quadrupole oscillations was independent of  $I_b$  after normalizing the measured amplitude w.r.t.  $I_b$ . An example of what we saw is shown in Fig. 3 for  $4.5 \times 10^{12}$  and  $2.5 \times 10^{12}$  protons per Booster batch where the quadrupole dampers have been set to a very low gain value (0.1 units). These plots trace the evolution of the  $I_b$  normalized  $2 \times$  synchrotron peak during the ramp. We noticed that the maximum amplitude of the quadrupole peak is  $\sim 0.5$  units in both cases and is independent of  $I_b$ .

These observations motivated us to investigate whether the source of quadrupole oscillations is, in fact, a bucket mismatch rather than from space charge or other beam intensity effects.

## DATA COLLECTION AND ANALYSIS

The wall current data clearly exhibits quadrupole oscillations after transition. In order to clearly see these oscillations, the data has to be processed to reveal the amplitude modulation. This is easily done by peak detecting the data. Two examples of the wall current data after peak detection and filtering is shown in Fig. 4.

The plots shown in Fig. 4 were taken with the quadrupole dampers on and with  $\sim 4.5 \times 10^{12}$  protons. Under these

# STUDY OF MAGNETS SORTING OF THE CSNS/RCS DIPOLES AND QUADRUPOLES\*

Y. An<sup>1,2,#</sup>, S. Xu<sup>1,2</sup>, S. Wang<sup>1,2</sup>, Y. Li<sup>1,2</sup>, J. Peng<sup>1,2</sup>, H. Ji<sup>1,2</sup>

<sup>1</sup>Institute of High Energy Physics, Chinese Academy of Sciences(CAS), Beijing 100049, China

<sup>2</sup>Dongguan Neutron Science Center, Dongguan 523803, China.

## Abstract

The Rapid Cycling Synchrotron plays an important role in the China Spallation Neutron Source. RCS accumulates and accelerates the proton beams from 80MeV to 1.6GeV for striking the target with the repetition rate of 25Hz. RCS demands low uncontrolled loss for hands on maintenance, and one needs a tight tolerance on magnet field accuracy. Magnet sorting can be done to minimize linear effects of beam dynamics. Using closed-orbit distortion (COD) and beta-beating independently as the merit function, and considering maintaining the symmetry of the lattice, a code based on traversal algorithm is developed to get the dipoles and quadrupoles sorting for CSNS/RCS. The comparison of beam distribution, collimation efficiency and beam loss are also investigated according to beam injection and beam accelerating.

## INTRODUCTION

The CSNS accelerator consists of a low energy H<sup>-</sup> Linac and high energy RCS. H<sup>-</sup> beam with energy of 80MeV is scraped and transformed into proton beam by the carbon foil located in the injection region. After around two hundred turn accumulation, the proton beam is accelerated to 1.6GeV and then extracted to strike the target with the design power of 100KW. For the convenience of maintenance and high power requirements, the uncontrolled beam loss should be less than 1 Watt/m. In order to achieve this goal, the expected magnet errors are designed to be in the order of 10<sup>-3</sup> for main dipoles and quadrupoles. Table 1 shows the main parameters of RCS [1].

Table 1: Main Parameters of RCS

| Parameters      | Units | Values |
|-----------------|-------|--------|
| Circumference   | m     | 227.92 |
| Repetition Rate | Hz    | 25     |
| Average current | μA    | 62.5   |
| Inj. Energy     | MeV   | 80     |
| Ext. Energy     | GeV   | 1.6    |
| Beam Power      | kW    | 100    |
| Quad            |       | 48     |
| Dipole          |       | 24     |

\*Work supported by National Natural Science Foundation of China (11405189)

#anyw@ihep.ac.cn

|                    |             |
|--------------------|-------------|
| Corrector          | 16/16       |
| BPM                | 32/32       |
| Nominal Tunes(H/V) | 1 4.86/4.78 |

As a key component of CSNS, RCS consists of 4-fold symmetric structure, and each of which is constructed by a triplet cell. Figure 1 shows the twiss parameters of RCS [2]. The long drift is reversed for the installation of cavities, collimator, injection elements and extraction elements, and the dispersion function in this area is designed to be zero. The short drift in the arc of the accelerator is reserved for installation of BPMs, correctors, sextupoles, and so on.

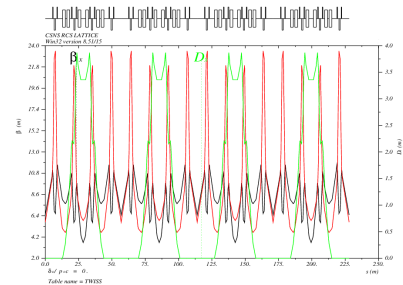


Figure 1: Twiss parameters of CSNS/RCS.

In section 2 we present in detail the sorting strategies. In section 3 we apply them to the CSNS/RCS model. In section 4 we investigate the sorting effects according to beam injection and beam accumulation. Conclusion is drawn in section 5.

## SORTING STRATEGIES

### Algorithm Description

Supposing there is  $M$  magnets should be arranged in  $M$  locations, the problems seems to be settled to find the solution of permutation of the  $M$  magnets. Now the steps of solving the problem are described as follows:

i) If there are two magnets, and the magnets indexes are  $A$  and  $B$ , the solution can be described as the order  $\{A, B\}$  or  $\{B, A\}$ ;

ii) If there are three magnets, and the magnets indexes are  $A, B$  and  $C$ . Firstly, the  $C$  magnet is fixed in the third location, and then the other two magnets can be sorted

# TRANSIENT BEAM LOADING BASED CALIBRATION FOR CAVITY PHASE AND AMPLITUDE SETTING

Rihua Zeng\*, European Spallation Source ERIC, Lund, Sweden  
Olof Troeng†, Lund University, Sweden

## Abstract

Traditional phase scan method for cavity phase and amplitude setting is offline and hard to track the variations of environment and operation points. An alternative beam loading based calibration method is investigated in this paper, which might become useful online/real time calibration method.

## INTRODUCTION

Setting correctly phase and amplitude for accelerating cavity is crucial in beam commissioning and beam operation. The phase refers here the synchronous phase which is defined as, for a given particle traversing the cavity, the phase shift from RF phase at which it obtain the maximum energy gain. It is equivalent to the phase angle between beam and accelerating voltage in vector diagram. The amplitude refers here the cavity voltage, which is defined as the absolute value of the line integral of the electric field seen by the beam along the accelerating axis, which reflects the maximum achievable energy gain for beam acceleration.

This paper introduce some general methods used for phase and amplitude setting in different accelerators, analyse the advantage and disadvantage of theses methods, and then discuss an online beam based calibration method which seems promising and very suitable to be employed at ESS.

## PHASE SCAN

Phase scan methods are referring here to the way of calibrating setting point for RF cavities by scanning RF phase and amplitude, measuring beam arrival times at down-stream locations, comparing measured phase to model predicted data, and identifying the best-matched data for calibration.

### *ΔT-method*

The ΔT-method is a classical phase scan method and used widely in normal conducting linac such as in LAMPF, Fermilab, JPARC and SNS. Linear system response is assumed in ΔT-method and it is only valid in the vicinity of design phase and amplitude. ΔT-method is a cavity-by cavity operation, assuming that the cavities upstream to the one being adjusted are “on”, and the cavities downstream are “off”. Beam phases (or beam arrival time) are provided by two downstream BPMs. The two BPMs can be neighbouring each other, or separated by several cryo-modules, which depends on the specific location of cavity (the sensitivity of beam velocity to energy gain becomes low as beam energy

goes high) being adjusted. The cavities between two BPMs are usually detuned more than 10 cavity bandwidth.

The general procedures of the ΔT-method are listed below [1, 2]:

- Find approximate phase and amplitude set point, by observing BPM signals and beam loading effect, and doing RF based calibration.
- Cavity being adjusted is off. Record two downstream BPMs phases  $\phi_{\text{bpm1-0}}$  and  $\phi_{\text{bpm2-0}}$ .
- Ramp the cavity being adjusted to nominal field calibrated by RF power based measurement (amplitude accuracy in RF based calibration is around 10%).
- Turn on beam with low repetition rate, low beam intensity and low beam pulse length.
- Record two downstream BPMs phases  $\phi_{\text{bpm1}}$  and  $\phi_{\text{bpm2}}$ .
- Calculate relative changes of BPMs phases between cavity “on” and “off”  $\Delta\phi_{\text{bpm1}} = \phi_{\text{bpm1-0}} - \phi_{\text{bpm1}}$  and  $\Delta\phi_{\text{bpm2}} = \phi_{\text{bpm2-0}} - \phi_{\text{bpm2}}$ . Plot  $\Delta\phi_{\text{bpm1}}$  and  $\Delta\phi_{\text{bpm2}}$ .
- Scan the cavity RF phase with certain phase step (for example  $0.5^\circ$ ) over the certain range (for example,  $\pm 5^\circ$ ) of design phase, and repeat above procedures at each phase step, to generate a constant-amplitude, variable-phase curve in  $(\Delta\phi_{\text{bpm1}}, \Delta\phi_{\text{bpm2}})$  plane.
- Calculate the slope of the curve, which depends on cavity amplitude, and compare it with the slope values of model predict curves at different amplitude. These predicted curves have a common point of intersection.
- Use some fitting algorithm to determine best-fit amplitude.
- Having determined proper amplitude, it is now possible in model to calculate the transfer function relating  $\Delta\phi_{\text{bpm1}}$  and  $\Delta\phi_{\text{bpm2}}$  to phase deviation  $\Delta\phi$  and energy deviation  $\Delta W$  at the entrance of cavity with respect to nominal value.  $\Delta\phi$  and  $\Delta W$  can then be determined.
- Correct the phase set point, and if necessary, correct as well the input energy at cavity entrance according to the result in last step.

### *Signature Matching*

Unlike the ΔT-method having a linear system response and small input energy displacement restriction, signature matching method can work at large displacement of initial conditions. In high energy part, signature matching methods can easily scan the phase over  $360^\circ$  at different amplitude, and make good match with model predict curve. However, at low energy linac, cavity phase scan can only be several ten degrees where beam stay sufficiently bunched to produce good signals at downstream BPMs, and the accuracy indicated at SNS for low energy part is not good enough. ΔT-method is probably necessary to get a good setting ac-

\* rihua.zeng@ess.se

† oloft@control.lth.se

# MEASUREMENT AND INTERPRETATION OF TRANSVERSE BEAM INSTABILITIES IN THE CERN LARGE HADRON COLLIDER (LHC) AND EXTRAPOLATIONS TO HL-LHC

E. Métral<sup>†</sup>, G. Arduini, J. Barranco, N. Biancacci, X. Buffat, L.R. Carver, G. Iadarola, K. Li, T. Pieloni, A. Romano, G. Rumolo, B. Salvant, M. Schenk, C. Tambasco, CERN, Geneva, Switzerland

## Abstract

Since the first transverse instability observed in 2010, many studies have been performed on both measurement and simulation sides and several lessons have been learned. In a machine like the LHC, not only all the mechanisms have to be understood separately, but the possible interplays between the different phenomena need to be analyzed in detail, including the beam-coupling impedance (with in particular all the necessary collimators to protect the machine but also new equipment such as crab cavities for HL-LHC), linear and nonlinear chromaticity, Landau octupoles (and other intrinsic nonlinearities), transverse damper, space charge, beam-beam (long-range and head-on), electron cloud, linear coupling strength, tune separation between the transverse planes, tune split between the two beams, transverse beam separation between the two beams, etc. This paper reviews all the transverse beam instabilities observed and simulated so far, the mitigation measures which have been put in place, the remaining questions and challenges and some recommendations for the future.

## INTRODUCTION

The first transverse instability in the LHC was observed during the first ramp tried with a single bunch of  $\sim 10^{11}$  p/b (on both beams B1 and B2) on 15/05/2010, with neither Landau octupoles (dedicated magnets used to provide transverse Landau damping and whose maximum absolute current is 550 A) nor transverse damper [1]. A dedicated study was then performed on 17/05/10 at 3.5 TeV starting with a Landau octupole current of  $-200$  A (the minus sign refers to the focusing octupole family, which corresponds to a negative amplitude detuning) and reducing it in steps until the bunch became unstable between  $\sim -20$  A and  $-10$  A. Figure 1(left) shows the measurement of the instability rise-time ( $\sim 10$  s) in the time domain while Fig. 1(right) reveals the behaviour in the frequency domain, where the similar rise-time, from the (azimuthal) mode  $-1$ , could also be deduced [1]). This instability has been found to be in good agreement with prediction from the impedance model (within a factor  $\sim 2$  or less), requiring a modest amount of Landau octupole current. Further measurements were performed in 2010 and 2011 in multi-bunch (with trains of bunches), revealing also a relatively good agreement with the impedance model (within a factor  $\sim 2$ ) [2].

<sup>†</sup> Elias.Metral@cern.ch

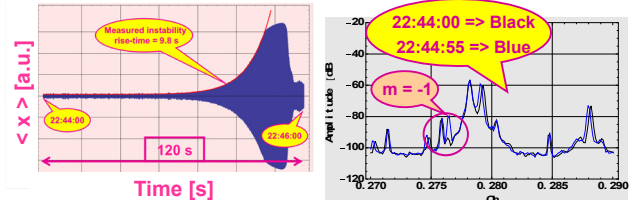


Figure 1: Dedicated single-bunch instability measurement at 3.5 TeV, two days after the first LHC transverse instability observed in 2010: (left) in the time domain and (right) in the frequency domain.

Things started to become more involved when we tried to push the performance of the LHC in 2011, and in particular in 2012. Several instabilities were observed at different stages of the LHC cycle, which perturbed the intensity ramp-up. All these instabilities could be cured by increasing the current of the Landau octupoles, the chromaticities and/or the gain of the transverse damper, except one transverse instability which remained at the end of the betatron squeeze [3,4]. Since then, transverse instabilities have been a worry for the future operation of the LHC and for HL-LHC [5].

The instability observations, the actions taken and the lessons learned are reviewed in Section 1 for the Run 1 (2010 to 2012), in Sections 2 and 3 for 2015 and 2016 respectively, while the future is discussed in Section 4.

## RUN 1 (2010-2012)

The operation during Run 1 was performed with the 50 ns bunch spacing beam and with a lower energy (3.5 TeV first and then 4 TeV in 2012), and three types (in fact two after careful analysis) of instabilities perturbed the intensity ramp-up, which are discussed below.

### *In Collision: “snowflakes”*

These instabilities happened always in the horizontal plane only and for both beams (see an example in Fig. 2). It concerned initially only the IP8 private bunches, i.e. the bunches colliding only at the Interaction Point 8. This was rapidly identified and these instabilities disappeared once the filling scheme was modified. The interpretation of this mechanism is that it happens on selected bunches with insufficient tune spread (and thus Landau damping) due to no head-on collisions, or transverse offsets [3,4].

# IDENTIFICATION AND REDUCTION OF THE CERN SPS IMPEDANCE

E. Shaposhnikova, T. Argyropoulos, T. Bohl, A. Lasheen, J. Repond, H. Timko  
CERN, Geneva, Switzerland

## Abstract

The first SPS impedance reduction programme has been completed in 2001, preparing the ring for its role as an injector of the LHC. This action has eliminated microwave instability on the SPS flat bottom and later nominal beam could be delivered to the LHC. The High Luminosity (HL-) LHC project is based on beam with twice higher intensity than the nominal one. One of the important SPS intensity limitations are longitudinal instabilities with minimum threshold reached on the 450 GeV flat top. In this paper the work which was carried on to identify the impedance sources driving these instabilities is described together with the results expected from the next campaign of the SPS impedance reduction planned by the LHC Injector Upgrade (LIU) project.

## INTRODUCTION

The LHC beam with 4 batches of 72 bunches with nominal intensity of  $1.2 \times 10^{11}$  p/b and spaced at 25 ns is operational in the SPS and was used by the LHC. During special machine development (MD) sessions the SPS has been able to deliver at top energy (450 GeV) up to four batches with bunch intensity of  $1.4 \times 10^{11}$ . This beam had nominal longitudinal and smaller than nominal transverse emittances.

The baseline LHC upgrade (HL-LHC) scenario is based on the SPS beam with 288 bunches of  $2.3 \times 10^{11}$  p/b spaced at 25 ns or 144 bunches of  $3.6 \times 10^{11}$  p/b at 50 ns [1].

Presently the intensity of the LHC beam is limited by beam loading in the 200 MHz Travelling Wave cavities. In the frame of the LIU (LHC Injectors Upgrade) project [2] the 200 MHz RF system will be significantly upgraded. The plan includes the shortening of the existing long cavities from 5 to 4 sections together with doubling of the total RF power [3]. These modifications should allow the beam intensity of  $2.4 \times 10^{11}$  p/b to be accelerated to the top energy, but without any margin due to longitudinal instabilities which lead to emittance blow-up. This beam should be injected into the 400 MHz RF system of the LHC. To avoid increase of relative particle losses in the LHC, the average bunch length at the SPS extraction should not exceed the present value of 1.65 ns achieved with available voltage of 7 MV.

Longitudinal beam instabilities observed during acceleration ramp have extremely low threshold (6 times below the nominal intensity). Even recently the impedance sources driving this instability were not exactly known [4]. In the present operation the LHC beam is stabilised by the 4th harmonic (Landau) RF system operating in bunch-shortening (BS) mode and controlled longitudinal emittance blow-up, however for the HL-LHC beam the longitudinal emittance

needed for beam stability could be too large for acceleration and extraction to the LHC. So during the last few years significant efforts went in identification of the impedance sources driving longitudinal instabilities and building the reliable impedance model of the SPS. The results of these studies are presented below.

## LONGITUDINAL INSTABILITIES

### Single-bunch Instability

A strong dependence of bunch length on intensity is observed on the SPS 450 GeV/c flat top for single bunches with intensities similar to that required for the LHC upgrade scenarios. This bunch lengthening exists in both single and double RF operation and could not be explained by the potential well distortion from the defocusing voltage due to the SPS reactive impedance with  $\text{Im}Z/n=3.5$  Ohm [5]. The results of measurements imply that the threshold of microwave instability is hit during the acceleration cycle. The threshold depends on voltage program used for acceleration [6] and on the flat top is higher for the larger RF voltage. For bunches with longitudinal emittance ( $2\sigma$ ) of 0.27 eVs the threshold of fast instability is around  $1.8 \times 10^{11}$ , see Fig.1.

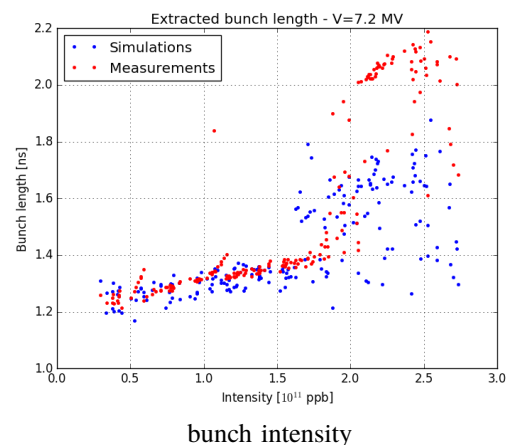


Figure 1: Measured (red) and simulated (including ramp, blue symbols) bunch length at 450 GeV/c as a function of intensity for a single bunch in a single 200 MHz RF system with 7.2 MV. Voltage program with 7 MV during the 2nd part of the ramp.

Taking into account slow-developing instability during the ramp, for bunches with injected emittance around 0.25 eVs the threshold on the flat top is close to  $1.0 \times 10^{11}$  in a single 200 MHz RF system and to  $1.2 \times 10^{11}$  in a double RF operation with voltage ratio around 0.1 [6].

# ELECTRON CLOUD IN THE CERN ACCELERATOR COMPLEX

G. Rumolo, H. Bartosik, E. Belli, G. Iadarola, K. Li, L. Mether, A. Romano, M. Schenk  
CERN, Geneva, Switzerland

## Abstract

Operation with closely spaced bunched beams causes the build-up of an Electron Cloud (EC) in both the LHC and the two last synchrotrons of its injector chain (PS and SPS). Pressure rise and beam instabilities are observed at the PS during the last stage of preparation of the LHC beams. The SPS was affected by coherent and incoherent emittance growth along the LHC bunch train over many years, before scrubbing has finally suppressed the EC in a large fraction of the machine. When the LHC started regular operation with 50 ns beams in 2011, EC phenomena appeared in the arcs during the early phases, and in the interaction regions with two beams all along the run. Operation with 25 ns beams (late 2012 and 2015), which is nominal for LHC, has been hampered by EC induced high heat load in the cold arcs, bunch dependent emittance growth and degraded beam lifetime. Dedicated and parasitic machine scrubbing is presently the weapon used at the LHC to combat EC in this mode of operation. This talk summarises the EC experience in the CERN machines (PS, SPS, LHC) and highlights the dangers for future operation with more intense beams as well as the strategies to mitigate or suppress the effect.

## AN OVERVIEW OF ELECTRON CLOUD IN THE CERN ACCELERATORS

### The Proton Synchrotron (PS)

In the PS, the electron cloud (EC) was first observed in 2001 during the last part of the cycle for the production of the so-called LHC-type beams, i.e. the beams of the type needed for the LHC filling. The production scheme of these beams in the PS is based on two or three steps of bunch splitting in order to obtain at the exit of the PS bunch trains with 50 ns or 25 ns spacing, respectively. In either case, the final stage of bunch splitting takes place at the top energy (26 GeV/c) and is followed by adiabatic bunch shortening and fast bunch rotation shortly before extraction [1]. These two processes are meant to shorten the bunches from their 15 ns length after the last splitting to 12 and then 4 ns, respectively, and make them suitable to be injected into the SPS. Therefore, these beams only circulate in the PS for few tens of msec with a structure prone to EC formation (beam parameters are summarized in Table 1).

During this short time before extraction, an EC was initially revealed in 2001 by the presence of a baseline drift in the signal from the pick up as well as beam transverse instabilities [2]. In March 2007, an experiment for dedicated EC measurements was set up at the PS to be able to directly measure the electron signal by using a shielded biased pick up [3] and confirm its presence in the machine in the last phase of the LHC beams production. These studies confirmed that

the EC develops during the last 40 to 50 ms before ejection, i.e. when the bunches are shortened by the RF gymnastics.

Table 1: Relevant beam parameters in the PS during the flat top RF gymnastics for the two bunch spacings of 50 and 25 ns

|  | 50 ns                               | 25 ns   |
|--|-------------------------------------|---------|
| Beam energy (GeV)                          | 26                                  |         |
| Bunch intensity ( $\times 10^{11}$ ppb)    | 1.3-2.0                             | 1.3-1.6 |
| Bunch length (ns)                          | 15 $\rightarrow$ 12 $\rightarrow$ 4 |         |
| Number of bunches                          | 36                                  | 72      |
| Transv. norm. emittances ( $\mu\text{m}$ ) | 1-2                                 | 2-3     |

In the years 2011-2014, new systematic measurements of EC and effects on the beam have been performed at the CERN-PS with the goals of:

- Studying the dependence of the EC build-up evolution on some controllable beam parameters (bunch spacing, bunch intensity, bunch length);
- Collecting time resolved experimental data of EC build-up in some desired sets of beam conditions;
- Characterising the EC instability at 26 GeV.

These sets of data can serve two purposes. First, comparing them with build-up and instability simulations will allow us to validate (or improve) the simulation model on which our tools are based. Second, by matching the simulations to the experimental data in all the different beam conditions, we can pin down the secondary electron yield, SEY or  $\delta_{max}$ , of the beam chamber and extrapolate then how much EC we can expect in the PS with the higher intensity beams foreseen in the frame of the LHC Injector Upgrade (LIU) project [4], and whether that can be detrimental to the beam.

### The Super Proton Synchrotron (SPS)

The SPS has been suffering from EC formation since it first began to take and accelerate 25 ns beams produced in the PS with the scheme explained above. Observations of pressure rise, beam instability, emittance growth were first made in the early 2000 and all these effects strongly limited the capability of this accelerator of handling LHC-type beams [5]. While the coherent instabilities could be suppressed by the use of the transverse damper (against the horizontal coupled bunch oscillations) and running with sufficiently high chromaticity (against the strong single bunch effect in the vertical plane), emittance growth and positive tune shift along the bunch train could still be measured, pointing to the continuing presence of a strong EC inside the beam chamber. All

# SPACE CHARGE DRIVEN BEAM LOSS FOR COOLED BEAMS AND MITIGATION MEASURES IN THE CERN LOW ENERGY ION RING

H. Bartosik, S. Hancock, A. Huschauer, V. Kain, CERN, Geneva, Switzerland

## Abstract

The performance of the CERN Low Energy Ion Ring (LEIR) with electron cooled lead ion beams is presently limited by losses, which occur during RF capture and the first part of acceleration. Extensive experimental studies performed in 2015 indicate that the losses are caused by the interplay of betatron resonances and the direct space charge detuning, which is significantly enhanced during bunching. Mitigation measures have already been identified and successfully tested, such as reducing the peak line charge density after RF capture, i.e. increasing the rms longitudinal emittance, and compensating third order resonances using existing harmonic sextupole correctors. New record intensities at extraction have been achieved. This talk describes the main experimental results from the 2015 measurement campaign including already implemented mitigation measures and the proposed strategy for even further increasing the LEIR intensity reach in the future.

## INTRODUCTION

The Low Energy Ion Ring (LEIR) is the first synchrotron of the Large Hadron Collider (LHC) heavy ion injector chain at CERN. LEIR has accumulated, cooled and stacked ion beams of oxygen ( $O^{4+}$ ), lead ( $Pb^{54+}$ ) and argon ( $Ar^{11+}$ ). During several machine development studies (MDs) with lead ions in late 2012 and early 2013, total intensities of up to  $9.5 \times 10^{10}$  charges could be achieved during the coasting beam phase. However, significant beam loss during and after RF-capture limited the available intensity at extraction to about  $6.3 \times 10^{10}$  charges [1,2]. In the framework of the LHC Injectors Upgrade (LIU) project, this intensity limitation for lead ion beams in LEIR has been identified as one of the main performance bottle-necks of the LHC ion injector chain [3]. In view of achieving the beam parameters required for the future LHC operation with lead ions in the High Luminosity LHC (HL-LHC) era [4], an intense machine development program was started at the end of 2015, with the aim of understanding and mitigating the particle loss in LEIR. The main outcomes of these studies will be presented in this paper.

The LEIR cycle presently used for filling the LHC with lead ion beams has a length of 3.6 s. In this scheme, seven injection pulses from Linac3, which are spaced by 200 ms (5 Hz injection rate), are accommodated on the injection plateau at a kinetic energy of 4.2 MeV/u. LEIR features a multi-turn injection with simultaneous stacking in momentum and in both transverse phase spaces. The nominal machine optics with the working point  $(Q_x, Q_y) = (1.82, 2.72)$  was tuned to optimize the injection efficiency [5]. Injection efficiencies of 50-70% are achieved in routine oper-

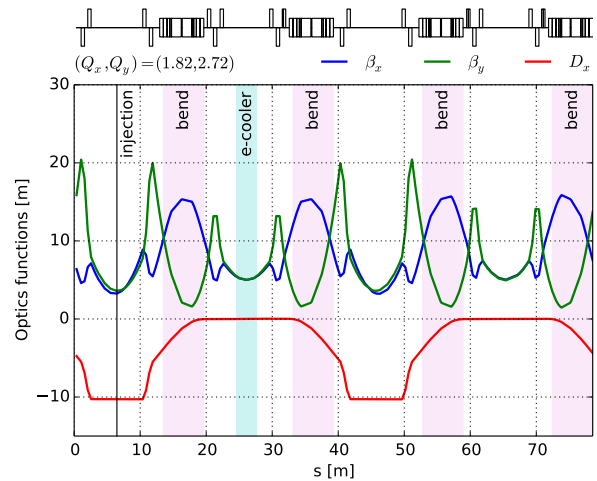


Figure 1: Optics functions along the LEIR circumference. The solenoid of the electron cooler slightly perturbs the lattice symmetry.

ation, which is close to the maximum efficiency predicted by simulations [6]. Figure 1 shows the optics functions with their quasi-twofold periodicity around the 78 m machine circumference of LEIR.

The phase space volume of the injected and accumulated beam is reduced by electron cooling. Subsequently, the coasting beam is captured into two bunches using a double harmonic RF system ( $h=2+4$ ) in bunch lengthening mode, accelerated to a kinetic energy of 72.2 MeV/u and extracted towards the Proton Synchrotron (PS). The basic machine and beam parameters for  $Pb^{54+}$  ions are summarized in Table 1.

Table 1: LEIR Parameters for  $Pb^{54+}$  Ions

|                         | Injection  | Extraction |
|-------------------------|------------|------------|
| kinetic energy          | 4.2 MeV/u  | 72.2 MeV/u |
| relativistic $\beta$    | 0.095      | 0.392      |
| relativistic $\gamma$   | 1.0045     | 1.087      |
| circumference           | 25 $\pi$ m |            |
| transition $\gamma_t$   | 2.84       |            |
| working point $Q_x/Q_y$ | 1.82/2.72  |            |

Figure 2 shows the intensity evolution along the LEIR magnetic cycle for different Linac3 beam current levels with typical loss patterns. Injection efficiencies of 50-70% and low beam loss rates during the electron cooling on the injection plateau are achieved even with the presently maximum available Linac3 pulse current of about 30  $\mu$ A. At the moment, the accumulation of seven Linac3 pulses does not

# FIRST ANALYSIS OF THE SPACE CHARGE EFFECTS ON A THIRD ORDER COUPLED RESONANCE

G. Franchetti, GSI, Darmstadt, Germany

S. Gilardoni, A. Huschauer, F. Schmidt, R. Wasef, CERN, Geneva, Switzerland

## Abstract

The effect of space charge on bunches stored for long term in a nonlinear lattice can be severe for beam survival. This may be the case in projects as SIS100 at GSI or LIU at CERN. In 2012, for the first time, the effect of space charge on a normal third order coupled resonance was investigated at the CERN-PS. The experimental results have highlighted an unprecedented asymmetric beam response: in the vertical plane the beam exhibits a thick halo, while the horizontal profile has only core growth. The quest for explaining these results requires a journey through the 4 dimensional dynamics of the coupled resonance investigating the fixed-lines, and requires a detailed code-experiment benchmarking also including beam profile benchmarking. This proceeding gives a short summary of the experimental results of the 2012 PS measurements, and address an interpretation based on the dynamics the fixed-lines.

## INTRODUCTION

Space charge induced emittance growth and beam loss can be divided into two big classes. The beam loss deriving from the incoherent effects of space charge on lattice nonlinearities (this proceeding), and the beam loss that may arise from the growth of the coherent modes self-consistently excited by the space charge [1].

The incoherent effects of space charge in coasting beams create an emittance growth when the space charge detuning overlaps a machine resonance. However, the incoherent space charge tune-shift also stabilizes the emittance growth by bringing particles out of the resonance as they grow in transverse amplitude. The space charge induced beam loss in a nonlinear machine becomes dramatic for bunched beams when the synchrotron motion and space charge induce a periodic crossing of a machine resonance. A single resonance crossing in a conventional RF bucket with synchrotron tune of  $Q_s \sim 10^{-2}$  produces a small emittance growth because of the relatively fast resonance crossing, but the cumulative effect arising from repeated resonance crossing, more than 300-400 crossing, makes large impact creating a beam diffusion to large transverse amplitudes, hence may lead to a steady beam loss over all the storage time.

For one dimensional resonances the mechanism leading to emittance growth and beam loss is explained in terms of instantaneous stable islands in the two-dimensional phase space and their crossing the particle orbits because of the combined effect of space charge and synchrotron motion Ref. [2]. This mechanism requires a long term storage, which typically corresponds to a number of turns equivalent to 100 or more synchrotron oscillations. Experimental and

numerical studies on beam survival and emittance growth in this regime have investigated the one dimensional resonance  $4Q_x = 25$  in Ref. [3], and  $3Q_x = 13$  in Ref. [4]. The relevance of these studies is significant for SIS100 [5], and for LIU [6] at CERN, as well as for all accelerators operating with high intensity beams in regimes of long term storage.

## RESULTS AND DISCUSSION

Coupled nonlinear resonances, of which the simpler class is the  $Q_x + 2Q_y = N$ , leads to significant difficulties in presence of space charge, and experimental studies are mandatory to unravel the complex dynamics. The effect of space charge on these type of resonances was studied in the CERN-PS in 2012 for the resonance  $Q_x + 2Q_y = 19$ . In this proceeding we present a short summary of the full experiment analysis. A more comprehensive presentation of the experimental results and discussion is part of a future publication.

In the experiment, in a resonance-free region of the tune diagram the third order resonance  $Q_x + 2Q_y = 19$  was excited with sextupoles with strength of  $K_3 \approx 0.015 \text{ m}^{-2}$ . The experimental campaign used a beam with  $55 \times 10^{10}$  proton per bunch, which produced an incoherent space charge tune-shift of  $\Delta Q_x \approx -0.05$ ,  $\Delta Q_y \approx -0.07$ . The beam was stored for  $\sim 0.5 \times 10^6$  turns, i.e. 1.1 seconds at an energy of 2 GeV, and beam profile measurements were taken at the beginning and at the end of the storage time. For several machine tunes, initial and final beam profiles were compared with the finding of an unexpected beam response to the distance from the resonance. When the space charge tune-spread overlaps the third order resonance and the machine tune is close to the resonance without beam loss, the beam profiles evolve differently in the transverse planes: in horizontal plane the beam exhibits core growth, whereas in the other plane a large halo is formed. This is shown in Fig. 1a,b for the tunes  $Q_{x0} = 6.104$ ,  $Q_{y0} = 6.476$ . The asymmetry of the beam profile is quite evident and shows that a new and more complex dynamics is driving the beam halo formation. In the picture are also shown the profiles from computer simulation as obtained from MADX, and MICROMAP (see Ref. [7] for a general code benchmarking discussion). Figure 1c shows the overall beam response in the experiment. The profiles in Fig. 1a,b correspond to the largest emittance growth.

The explanation of the halo-core finding can be approached starting with a detuning analysis. The theory of the resonances (see Ref. [8,9]) shows that the more convenient quantity to measure the distance from the third order resonance is

$$\Delta_{r0} = Q_{x0} + 2Q_{y0} - 19.$$

# INTENSITY EFFECTS IN THE FORMATION OF STABLE ISLANDS IN PHASE SPACE DURING THE MULTI-TURN EXTRACTION PROCESS AT THE CERN PS

S. Machida\*, C.R. Prior, STFC Rutherford Appleton Laboratory, Didcot, UK  
 S. Gilardoni, M. Giovannozzi, S. Hirlander<sup>1</sup>, A. Huschauer<sup>1</sup>, CERN, Geneva, Switzerland  
<sup>1</sup>also at Vienna University of Technology, Vienna, Austria

## Abstract

The CERN PS utilises a Multi-Turn Extraction (MTE) scheme to stretch the beam pulse length to optimise the filling process of the SPS. MTE is a novel technique to split a beam in transverse phase space into nonlinear stable islands. The recent experimental results indicate that the positions of the islands depend on the total beam intensity. Particle simulations have been performed to understand the detailed mechanism of the intensity dependence. The analysis carried out so far suggests space charge effects through image charges and image currents on the vacuum chamber and the magnets iron cores dominate the observed behaviour. In this talk, the latest analysis with realistic modelling of the beam environment is discussed and it is shown how this further improves the understanding of intensity effects in MTE.

## INTRODUCTION

The Multi-Turn Extraction (MTE) scheme at CERN was conceived as method of beam transfer from the PS to the SPS to minimise beam loss [1]. It has been demonstrated experimentally several times [2] and is now in daily operation. It has also been suggested that an inverse process could be utilised for Multi-Turn Injection (MTI).

The mechanism of beam splitting and preservation of the separated beamlets can be identified as a nonlinear resonant driving term (octupole in this study) and amplitude dependent tune shift. In other words, the essential ingredients are the non-zero harmonic component of the multipole potential and zero-th component of the multipole potential (this can be the same multipole as the other). It is, however, not clear how the beam intensity affects the dynamics.

Experimental observation shows that the beamlets move outward as the beam intensity increases [3]. We have included a simple model of space charge effects in the MTE simulation that starts after the process of beam splitting to see how the beam intensity changes the beamlets' position in the phase space.

## MODEL

Generally speaking, when space charge effects are included in particle tracking simulation, the charge distribution of each beamlet as well as its position in the transverse phase space should be updated self-consistently. The distributions are no longer determined only by the lattice elements. On the other hand, the beamlets are reasonably separated in the

configuration space. Therefore we assume that only the position of each beamlet is modified by the interaction between the charge centres of the beamlets and is insensitive to the details of the charge distribution. This justifies the introduction of a frozen space charge model. The charge distribution is fixed at the start of the simulation and not updated after each integration step. However, one significant difference from the ordinary frozen model for a single beam is that the beamlet positions are calculated iteratively. When there is only a single beam, it always sits at the centre of phase space, which may be slightly shifted by closed orbit distortion. When there are multiple beamlets, contributions to the space charge potential from other beamlets produce dipole kicks which we take into account to solve for the beamlet positions self-consistently.

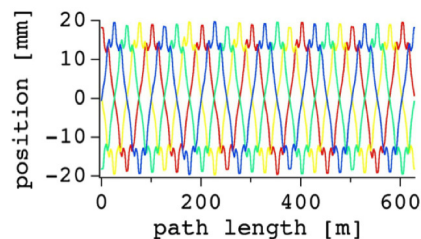


Figure 1: Position of the stable fixed points around the ring. They are all connected to make a closed orbit returning to the initial point after 4 turns.

In practice, to include space charge effects among the beamlets, the position of stable fixed points without space charge is first calculated everywhere in the ring, along an orbit that returns to the initial phase space point after 4 turns. This closed orbit is in addition to the normal orbit around the centre which comes back to the initial point on every turn. The position around the ring is shown in Fig. 1. Different colours indicate the evolution of each fixed point, but they are all connected making one single closed orbit. Once the fixed point positions are identified, space charge effects can be included by centring the space charge potential at that position. With a small time step, typically 10 ns, a particle is tracked taking into account the external magnetic lattice as well as the space charge potential.

Obviously, the closed orbit coming back after 4 turns under space charge is different from the orbit without space charge. That means that the position of the beamlets has to be adjusted to the new position and then the closed orbit has to be calculated again. This iteration repeats until the closed orbit found by the particle tracking agrees with the position

\* email address: shinji.machida@stfc.ac.uk

# BROADBAND FEEDBACK SYSTEM FOR INSTABILITY DAMPING IN THE SNS RING\*

N. J. Evans<sup>†</sup>, Oak Ridge National Laboratory, Oak Ridge, TN, USA

## Abstract

The transverse feedback system in the Accumulator Ring of the Spallation Neutron Source (SNS) is intended to damp broadband ( $\approx 40$ -120 MHz), coherent betatron motion due to e-p interaction. The SNS feedback system is based on an analog delay-line model with some signal conditioning and tuning parameters implemented digitally. This system provides a simple setup with two primary knobs, phase and gain, as well as an equalizer. This simplicity comes at the cost of some flexibility normally found in a standard mode-by-mode design, namely mode-by-mode phase, and gain control. In this paper we discuss the design, tuning, evaluation, and operation of the SNS feedback damper, and discuss the tradeoffs implicit in the design of the system.

## INTRODUCTION

Table 1 lists parameters of the SNS ring running in 1.4 MW neutron production operation. The purpose of the ring is to accumulate  $\approx 10^{14}$  protons over 1 ms, about 1000 turns, to deliver a short intense pulse of protons to the neutron production target. This millisecond long cycle is repeated at 60 Hz. Since the early days of the design of the SNS ring, e-p instability due to the interaction of electrons in the vacuum vessel with the proton beam has been a serious concern necessitating the inclusion of many mitigation measures [1].

Table 1: SNS Ring Parameters for 1.4 MW Operation

| Parameter             | Value                   |
|-----------------------|-------------------------|
| Energy                | 939.5 MeV               |
| Revolution Period     | 955 ns                  |
| RF 1st (2nd) harm     | 6.5(3.5) kV             |
| Circumference         | 248 m                   |
| Bunch Length(FW)      | 650 ns                  |
| Charge                | 25 $\mu\text{C}$        |
| $\delta$ p/p Inj(Ext) | $10^{-4}$ ( $10^{-3}$ ) |
| Pipe Radius           | $\geq 10\text{cm}$      |
| $\eta$                | -0.2173                 |
| $\nu_{H,V}$           | 6.205, 6.165            |

The nature of e-p interaction leads to a broadband spectrum of coherent transverse betatron oscillation, in the case of SNS this spectrum has been observed in the range  $\approx 40$ -120 MHz [2, 3]. The frequency spectrum evolves throughout a cycle, typically broadening toward higher frequencies

as accumulation progresses. During dedicated study cycles in 2008, the e-p instability was induced in 8.5, 10 and 20  $\mu\text{C}/\text{pulse}$  beam at low repetition rate by changing various parameters such as storage time and 2<sup>nd</sup> harmonic RF cavity voltage. During these studies experimenters observed beam loss, and high frequency beam oscillation of several cm [3], but only in configurations specially tuned to produce the instability.

Broadband motion attributed to e-p has been seen in the SNS ring during normal operation, high frequency oscillation has only produced peak amplitudes  $< 1.5$  mm during normal operation. This motion has not limited high intensity operation, up to the design power of 1.4 MW (24  $\mu\text{C}/\text{pulse}$ ), achieved in the Fall of 2015. The broadband transverse damper system in the SNS Accumulator ring was designed to address broadband betatron oscillation due to e-p interaction spanning the range from  $\approx 40$ -120 MHz. Despite the fact e-p has not lead to operation limiting losses, the damper system has been used to suppress motion due to e-p interaction.

The state-of-the-art in broadband transverse damping typically makes use of a separate processing channel for each mode, or equivalently each time-slice of the bunch within the resolution of the system, e.g. JPARC, CERN SPS, among others [4, 5]. Each channel consists of a separate FIR filter used to tune the phase and gain of the feedback signal based on the history of that mode, or slice, over several turns.

The SNS system forgoes the complexity associated with such a design, instead using a delay-line model with certain digital signal processing elements to ease system setup. The feedback system is tuned for all modes simultaneously using a single gain, and phase knob. This simplicity comes at the cost of decreased flexibility with respect to tuning the phase and gain of each mode independently.

## DAMPER SYSTEM

Figure 1 shows a schematic of the SNS damper system including: the stripline pickup and kicker, Low-level RF(LLRF), ADC, FPGA with processing blocks, DAC and power amplifiers.

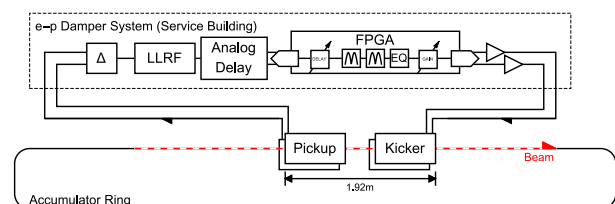


Figure 1: Schematic layout of the damper system.

\* ORNL is managed by UT-Battelle, LLC, under contract DE-AC05-00OR22725 for the U.S. Department of Energy.

<sup>†</sup> evansnj@ornl.gov

# R&D ON BEAM INJECTION AND BUNCHING SCHEMES IN THE FERMILAB BOOSTER \*

C. M. Bhat<sup>#</sup>

Fermilab, Batavia, IL 60510, USA

## Abstract

Fermilab is committed to upgrade its accelerator complex to support HEP experiments at the intensity frontier. The ongoing Proton Improvement Plan (PIP) enables us to reach 700 kW beam power on the NuMI neutrino targets. By the end of the next decade, the current 400 MeV normal conducting LINAC will be replaced by an 800 MeV superconducting LINAC (PIP-II) with an increased beam power >50% of the PIP design goal. Both in PIP and PIP-II era, the existing Booster is going to play a very significant role, at least for next two decades. In the meanwhile, we have recently developed an innovative beam injection and bunching scheme for the Booster called "early injection scheme" that continues to use the existing 400 MeV LINAC and implemented into operation. This scheme has the potential to increase the Booster beam intensity by >40% from the PIP design goal. Some benefits from the scheme have already been seen. In this paper, I will describe the basic principle of the scheme, results from recent beam experiments, our experience with the new scheme in operation, current status, issues and future plans. This scheme fits well with the current and future intensity upgrade programs at Fermilab.

## INTRODUCTION

Nearly one and a half decades ago, Fermilab started focusing on upgrades to its accelerator complex towards the intensity frontier that would substantially increase the average beam power delivered to the fixed target HEP experiments (as well as support then ongoing ppbar collider program) thereby transforming the facility into a world class accelerator based neutrino facility.

Currently, the chain of accelerators in the complex consists of an RFQ, 400 MeV normal conducting RF LINAC, 0.4-8 GeV rapid cycling Booster, 8 GeV permanent magnet Recycler Ring and 8-120 GeV (or 150 GeV) Main Injector. The last three machines in this chain are synchrotrons. The primary goal of the upgrades was delivering 700 kW of beam power at 120 GeV on the NuMI/NOvA target (a high energy neutrino experiment), and simultaneously provide proton beams to the low energy neutrino and fixed target experiments.

In 2010, after two and a half decades of successful operation of the Tevatron ppbar collider, the energy frontier HEP programs moved to the LHC at CERN. Since then many new developments have taken place at Fermilab. The Recycler, originally used as the primary

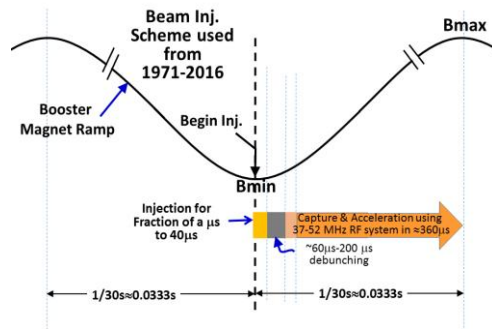


Figure 1: Schematic of the beam injection scheme in operation for the past forty five years of the Booster.

anti-proton storage ring during the Tevatron collider era, has been upgraded to a high intensity proton storage ring that can be used as an injector to the Main Injector. This increased the Main Injector duty factor by nearly 30%. Though the Fermilab Booster is one of the oldest rapid cycling proton synchrotron in the world [1, 2] that cycles at 15 Hz and is in operation since 1971, until 2002 it delivered the beam on average at a rate of  $\approx 1$  Hz or less with a maximum beam intensity of  $\sim 3.5E12$  p per Booster cycle (ppBc). During 2002-15 the beam delivery rate from the Booster has been increased to about seven cycles per sec as MiniBooNE and MINOS came online. The PIP was established around 2010 [3] to support the newly proposed NOvA, g-2, Mu2e, and short-baseline neutrino experiments which demanded doubling the Booster beam repetition rate from 7.5 Hz to 15 Hz with about  $4.6E12$  ppBc. The foreseen Proton Improvement Plan-II [4, 5] supports the long-term physics research programs by providing MW type beam power to LBNE while sending beam to the on-going HEP experiments and forms a platform for the future of the Fermilab. The main components of the PIP-II are a new 800 MeV superconducting LINAC as an injector to the Booster and increase the Booster beam delivery repetition rate to 20 Hz with about  $6.7E12$  ppBc. In any case, the Booster is going to play a very important role at least for the next two decades and will remain the workhorse in the Fermilab accelerator complex.

Booster uses sinusoidal magnetic ramp for beam acceleration. Its cycle rate is locked to 60 Hz ComEd power distribution system. The Booster has a circumference of 473.8 m with 96 combined function magnets distributed on a FOODOOD (DOODFOF) 24 symmetric lattice period with independently controllable power supplies to its correctors to control its transverse dynamics. The fundamental accelerating RF system operates with a harmonic number  $h=84$  and sweeps its

\* Work supported by Fermi Research Alliance, LLC under Contract No. De-AC02-07CH11359 with the United States Department of Energy  
# cbhat@fnal.gov

# INJECTION PAINTING IMPROVEMENTS IN THE J-PARC RCS

S. Kato<sup>†</sup>, H. Harada, K. Horino, H. Hotchi, M. Kinsho, K. Okabe, P. K. Saha, Y. Shobuda, T. Takayanagi, N. Tobita, and T. Ueno  
 J-PARC center, Japan Atomic Energy Agency, Ibaraki, Japan

## Abstract

In the J-PARC 3GeV RCS, the injection painting is essential method for the reduction of the space charge force. In the transverse painting, the H<sup>-</sup> beam from Linac is distributed on the large phase-space area of the ring orbit during multiple turns. To implement this method, painting magnets form the time variable beam orbit. Therefore, the precise output current control of the magnet power supply was required. Because the power supply was controlled by mainly feedforward signal, we developed the iterative tuning method for the optimum feedforward parameter determination. As a result, we could reduce the tracking error of the current compared to before. In addition, we improved the measurement method of the footprint of the painting process. In the adjustment of the painting, we adopted the additional correction of the current tracking based on the measured footprint. As a result, the intended painting process and area were achieved accurately. Thus we established the precise control technique of the injection painting.

## INTRODUCTION

The 3 GeV rapid cycling synchrotron (RCS) of the Japan Proton Accelerator Research Complex (J-PARC) serves as a high intensity proton driver aiming to achieve a 1 MW beam power. The 400 MeV H<sup>-</sup> beam from Linac is converted to proton at the injection point by the charge-exchange foil and stored during injection period of 0.5 ms repeatedly using the multi-turn charge-exchange injection method. The RCS accelerates protons up to 3 GeV with a repetition rate of 25 Hz. The beam is provided as the neutron source for the Materials & Life Science Experimental Facility (MLF) and as the injection beam for the 50 GeV main ring (MR). The current progress of the hardware and commissioning is described in the reference [1] in detail.

The RCS is adopted the transverse injection painting in order to distribute the injection beam on the large phase-space area intentionally and mitigate the space-charge force which can become the beam loss source. The scheme of that is as follows [2]. The schematic view of the injection area and the variation of the horizontal orbit during the painting are shown in Fig. 1. In the horizontal plane, during the 0.5 ms injection period, four shift-bump magnets (SB1-4) shape the fixed bump orbit. In addition, four paint-bump magnets (PB1-4) shape the time dependent bump orbit. Fig. 1a(A) shows the bump orbit at the injection start timing (t = 0). The injection track is matched to this bump orbit at the injection point. During multi-turn injection, the track of H<sup>-</sup> beam is fixed and the

ring orbit is shifted slightly from the charge-exchange foil by decreasing the time dependent bump orbit height as shown in Fig. 1b(A) and Fig. 1c(A). Therefore, the injection beam changes its position and angle with respect to time along major axis in the phase-space ellipse of the ring orbit as shown in Fig. 1(B). As a result, the circulating beam becomes so broader compared with the Linac beam and the space-charge force is mitigated. In addition, the number of the charge-exchange foil hits by the circulating beams is decreased because the circulating beam is shifted from the foil.

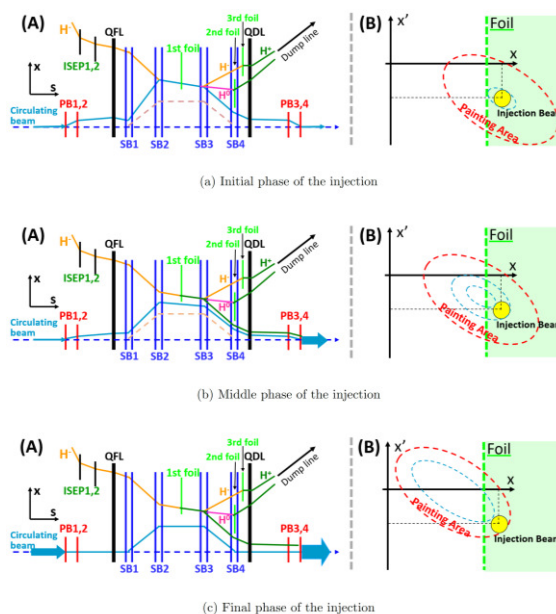


Figure 1: The horizontal orbit variation around the injection point during the injection period. Figure (A) indicates the orbits of the injection and the circulating beam. Figure (B) indicates the phase-space of the position and angle at the injection point.

In the vertical plane, two vertical paint magnets installed at the injection line change the injection beam angle at the injection point. The injection beam is brought closer to the central orbit from the edge of the painting area or vice versa in the phase-space ellipse of the ring orbit along angular axis. In the RCS, painting from the center to the outside in both horizontal and vertical phase-space is called Correlated Painting. On the other hand, painting from the outside to the center in vertical phase-space different from the horizontal painting is called Anti-Correlated Painting. When the injection beam position and angle are changed along the radial direction in proportion to the square root of the time, the beam is uniformly distributed on the phase-space area. Therefore, for

<sup>†</sup> skato@post.j-parc.jp

# H<sup>-</sup> CHARGE EXCHANGE INJECTION ISSUES AT HIGH POWER\*

M.A. Plum, Oak Ridge Spallation Neutron Source,  
Oak Ridge National Laboratory, Oak Ridge, TN, USA

## Abstract

At low beam powers H<sup>-</sup> charge exchange injection into a storage ring or synchrotron is relatively simple. A thin stripper foil removes the two “convoy” electrons from the H<sup>-</sup> particle and the newly-created proton begins to circulate around the ring. At high beam powers there are complications due to the heat created in the stripper foil, the power in the H<sup>0</sup> excited states, and the power in the convoy electrons. The H<sup>-</sup> injected beam power at the Oak Ridge Spallation Neutron Source is the highest in the world. Although the SNS ring was carefully designed to operate at this level there have been surprises, primarily involving the convoy electrons. Examples include damage to the foil brackets due to reflected convoy electrons and damage to the electron collector due to the primary convoy electrons. The SNS Second Target Station project calls for doubling the beam power and thus placing even more stress on the charge-exchange-injection beam-line components. In this presentation we will compare charge-exchange-injection designs at high-power facilities around the world, discuss lessons learned, and describe the future plans at SNS.

## INTRODUCTION

Charge exchange injection (CEI) is important because it is the only way to achieve low-beam-loss multi-turn injection into a storage ring or synchrotron. Accelerators that do not use CEI for multi-turn injection lose about 10% of the beam due to injection inefficiency. This may not be a problem for low injected beam powers, but for today’s high-power storage rings and synchrotrons it makes anything other than CEI infeasible. Additionally CEI allows the newly injected beam to be deposited inside the phase space of the circulating beam, thus reducing the final emittance. Without CEI,  $\epsilon_{TOTAL} > N * \epsilon_{INJECTED}$ , where N is the number of turns injected. With CEI,  $\epsilon_{TOTAL} \ll N * \epsilon_{INJECTED}$ .

The only practical way today to achieve CEI is by using stripper foils. Alternative technologies such as a flowing sheet of mercury, or gas jets, are only applicable in special cases. Laser stripping is a promising technology but it is not ready yet.

At the Oak Ridge Spallation Neutron Source the injected H<sup>-</sup> beam power is 1.5 MW – more than a factor of 10 higher than any other H<sup>-</sup> injection system. The SNS has a unique arrangement of stripper foils and bending magnets to mitigate the inevitable complications of high power injection. Overall the SNS CEI system works well, but we have encountered some surprises as we have been work-

\*ORNL is managed by UT-Battelle, LLC, under contract DE-AC05-00OR22725 for the U.S. Department of Energy. This research was supported by the DOE Office of Science, Basic Energy Science, Scientific User Facilities.

ing to increase the beam power to the design value of 1.4 MW on target.

## BRIEF HISTORY OF CEI

Multi-turn CEI was invented and first demonstrated at BINP in Novosibirsk in 1966 [1]. A 1 MeV H<sup>-</sup> ion beam was first stripped to H<sup>0</sup> by a CO<sub>2</sub> gas jet, then drifted through one of the ring dipole magnets, then stripped to H<sup>+</sup> by a hydrogen gas jet. The first experiments with this technique were amazingly productive and innovative, and produced results that impacted both proton beam injection and high intensity proton beam dynamics for many years.

The first use of a stripper foil for CEI was at the ZGS Booster project at ANL in Argonne in 1972. The stripper foils were 36 x 100 mm<sup>2</sup> pieces of 35 μm-thick poly-paraxylene mounted to a disk rotating at 1800 rpm, with the rotation synched to the booster injection cycle such that the foil was only in the path of the beam during injection. It is ironic that the world’s first stripper foil mechanism was also the most complicated – but it worked very well. The expected lifetime of these foils was just two hours – so even from the very first use of stripper foils lifetime was an issue. A graphical history of CEI beam powers around the world is shown in Fig. 1. The three highest H<sup>-</sup> injected beam powers are for the Los Alamos PSR (80 – 100 kW), J-PARC RCS (133 MW design), and SNS (1.5 MW design).

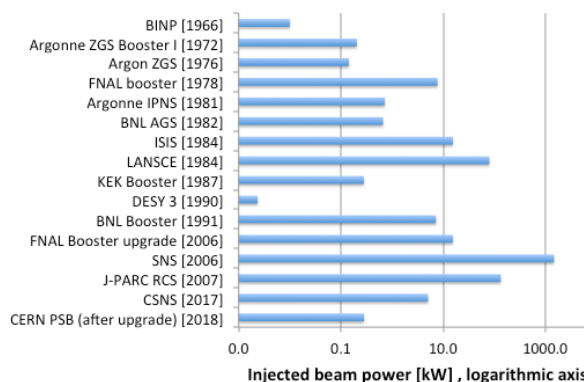


Figure 1: Summary of H<sup>-</sup> beam powers used for CEI, from the first use of CEI to future facilities.

## COMPLICATIONS OF CEI

Complications of CEI include 1) beam loss caused by foil scattering, 2) stripper foil lifetime, 3) control and disposal of un-stripped and partially stripped beam, 4) beam loss caused by H<sup>0</sup> excited states, 5) control of the stripped (convoy) electrons. The first three complications have been well addressed by other authors and so they will be only briefly mentioned here.

# AN EXPERIMENTAL PLAN FOR 400 MeV $H^-$ STRIPPING TO PROTON BY USING ONLY LASERS IN THE J-PARC RCS

P.K. Saha\*, H. Harada, S. Kato, M. Kinsho, J-PARC Center, KEK & JAEA, Japan  
Y. Irie, I. Yamane, High Energy Accelerator Research Organization, KEK, Japan

## Abstract

In the 3-GeV Rapid Cycling Synchrotron of Japan Proton Accelerator Research Complex, we are planning for a proof-of-principle experiment to demonstrate 400 MeV  $H^-$  stripping to proton by using only laser system. In order to avoid high magnetic field required in the process of laser-assisted  $H^-$  stripping, especially for lower  $H^-$  energies, we are studying the possibilities of using only laser system. The method is a three step process, same as the laser-assisted  $H^-$  stripping at the Spallation Neutron Source in Oak Ridge but lasers are used instead of high field magnets in the 1st step for an  $H^-$  conversion to  $H^0$  and in the 3rd step for an excited  $H^0$  ( $H^{0*}$ ) conversion to a proton. A Nd:YAG laser, wavelength of 1064 nm can be properly used for both 1st and 3rd steps, where commercially available the most powerful excimer laser will be used for  $H^0$  excitation ( $n=3$ ) in the 2nd step. Although detail R&D studies are necessary to reach to the ultimate goal and needs to proceed step by step. A tentative schedule to carry out the experiment is set to be at the end of 2017. A detail of the present method and the expected outcome are presented in this paper.

## INTRODUCTION

A stripper foil plays an important role for multi-turn  $H^-$  stripping injection in order to increase the beam current in the circular accelerators. Recently, beam power of 1 MW and above have successfully been achieved by such a conventional injection method [1, 2]. Although continuous efforts on durable foil production made remarkable progress on the foil lifetime [3], it is still unclear how to deal with multi-MW beam power. It may be hard to maintain a reliable and longer lifetime due to overheating of the foil and may be it is the most serious concern and a practical limitation to realize a multi-MW beam power. Other than foil lifetime, the residual activation near the stripper foil due to the foil scattering beam loss during multi-turn injection is also another uncontrollable factor and a serious issue for facility maintenance.

Figure 1 shows pictures of stripper foil before and after only 0.3 MW operation at 3-GeV RCS (Rapid Cycling Synchrotron) of J-PARC (Japan Proton Accelerator Research Organization). Although the foil was continuously used for nearly 5 months operation but the beam power was less than one third of the designed 1 MW. The total injected charge on the foil was nearly 1300 C and by taking into account the calculated average foil hits (10) of each injected proton, the total charge via foil was estimated to be 13000 C. Figure 2 shows a trend of the unstripped (missing)  $H^-$  due to the

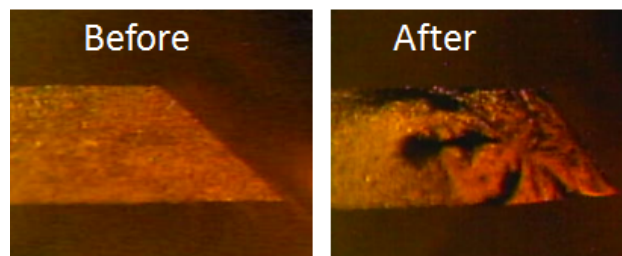


Figure 1: Stripper foil before and after operation with 0.3 MW beam power for about 5 months in the 3-GeV RCS of J-PARC. Deformation of the foil due to beam irradiation can easily be seen.

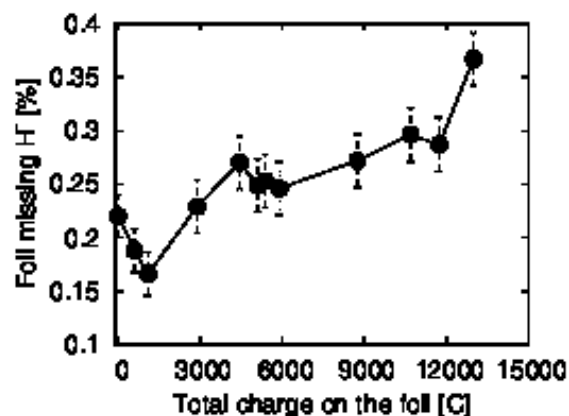


Figure 2: A trend of the stripper foil missing  $H^-$  measured at the waste beam dump. The missing  $H^-$  was increased nearly 3 times higher as compared to that in the beginning of the operation. At the designed operation even if a foil does not brake, the practical limitation of the foil lifetime may comes from the foil degradation.

stripper foil deformation as shown in Fig. 1. Those missing  $H^-$  was further stripped to protons by one of the secondary foil but directed to the waste beam dump. The missing  $H^-$  was measured to be increased nearly 3 times higher than those in the beginning of the operation. Ideally the waste beam should be only 0.3%, which are all the single electron stripped  $H^0$  but almost no missing  $H^-$ . However, due the uncontrolled beam halos in the  $H^-$  beam, small vertical size of foil as well as beam positioning as close as to the horizontal edge of the foil in order to minimize circulating beam hitting the foil during multi-turn injection, there was about 0.2% missing  $H^-$  in the beginning. The missing  $H^-$  were reduced to about 0.1% by further tuning the  $H^-$  beam and adjusting the foil position as well. The operation of the machine even with such a foil deformation and missing  $H^-$

\* E-mail address: saha.pranab@j-parc.jp

# BEAM DYNAMICS CHALLENGES IN THE ESS LINAC

Yngve Inntjore Levinsen, M. Eshraqi, R. Miyamoto, M. Munoz, A. Ponton, R. De Prisco  
European Spallation Source (ESS), Lund, Sweden

## Abstract

The European Spallation Source (ESS) will be the world's brightest neutron source. It will be driven by a 5 MW proton linac that delivers a 2.86 ms pulse at 14 Hz, which means the peak beam power is 125 MW. This requires a careful design of the lattice structures, in order to allow for safe and reliable operation of the accelerator. We will discuss some of the design choices and some of the particular challenges that were faced during the design of the ESS lattice.

## INTRODUCTION

The European Spallation Source ERIC project is already well into the construction phase [1], with an expected first beam on target in mid 2019. The long pulse spallation source is the first of its kind. The linear accelerator (linac) will provide an unprecedented proton beam power of 5 MW, with a proton beam current of 62.5 mA and a 2 GeV beam energy on target with a duty factor of 4 %. The linac is superconducting which allows for the long pulse length of 2.86 ms, and a 14 Hz pulse repetition rate.

The different sections of the ESS linac are listed in Table 1, and shown in Fig. 1. The normal conducting front-end consists of a  $\sim 2.5$  m long LEBT after the ion source, followed by a  $\sim 4.55$  m long 4-vane RFQ, a  $\sim 3.8$  m long MEBT and 5 DTL tanks totalling  $\sim 39$  m in length. There are three superconducting sections, first 13 spoke modules at the same radiofrequency as the normal conducting front-end of 352.21 MHz, then elliptical cavities at double the frequency. The two elliptical sections are called medium- $\beta$  and high- $\beta$ . A contingency space of 15 periods is left in for future upgrades. The total length of the accelerator including the transfer line is about 600 m.

Table 1: The Overview of the Different Sections of the ESS Linac

|               | Energy [MeV] | # modules | cav./mod. (Cells) | Length [m] |
|---------------|--------------|-----------|-------------------|------------|
| Source        | 0.075        | -         | 0                 | -          |
| LEBT          | 0.075        | -         | 0                 | 2.4        |
| RFQ           | 3.65         | 1         | 1                 | 4.6        |
| MEBT          | 3.65         | -         | 3                 | 3.8        |
| DTL           | 90.0         | 5         | -                 | 39         |
| Spokes        | 216          | 13        | 2                 | 56         |
| Med.- $\beta$ | 571          | 9         | 4(6C)             | 77         |
| High- $\beta$ | 2000         | 21        | 4(5C)             | 179        |
| HEBT          | 2000         | -         | -                 | 241        |

From a beam dynamics perspective, the main challenges associated with building such a high power linac are resulting from the high beam current. The result is strong space-

charge forces which is challenging to accurately model and design for, and the low loss requirement of only 1 W/m means that an excellent control of the beam halo is required. Further, there is a high number of RF components that needs phase and amplitude corrections with beam. Due to the tight loss tolerances and need for high availability and reliability, there are tight requirements for dynamic errors of the RF phase and amplitude (with respect to the beam).

The design of the ESS lattice has been discussed in several earlier papers [1–6], including studies of the beam dynamics in individual sections as well as integrated studies [7, 8]. The design has undergone several changes since the TDR was released in 2012 [9]. The most significant change is that the beam energy has been reduced from 2.5 GeV to 2.0 GeV, while the beam current has been increased from 50 mA to 62.5 mA to keep the same 5 MW proton beam power at the target. The reduced space for accelerating structures has been converted to contingency space, so that the full upgrade to 3.5 GeV is still possible.

## NORMAL CONDUCTING LINAC FRONT-END

The ion source is a microwave discharge ion source [10]. The source is designed to be able to provide a maximum of about 80 mA of proton beam current, with a pulse length flattop of up to 3 ms. The source voltage is 75 kV. The design choice is based on having a reliable high-current source with a long mean time between failures (MTBF). This is essential given the high reliability demands of a facility like ESS. The reliability of the ion source is expected to be very close to 100 %.

The low energy beam transport (LEBT) following the ion source consists of two solenoids of 330 mm length to focus the DC beam pulse, as well as a chopper and diagnostics to characterise the beam. The chopped beam is dumped on a cone aperture just before the RFQ entrance. A space-charge compensation of around 95 % is needed in order to meet the nominal performance.

The radio-frequency quadrupole (RFQ) is a 4-vane type with a length of 4.55 m. The RFQ is shown in simulations to have a very good beam capture, providing above 95 % of beam transmission through the structure under the assumption of a good space-charge compensation in the LEBT. The requirement is that at least 90 % of the beam should be transmitted through the RFQ. At the RFQ exit the beam energy has reached 3.62 MeV.

Between the RFQ and the drift tube linac (DTL), a matching is needed. This is done by the medium energy beam transport (MEBT), consisting of 11 quadrupoles and 3 RF buncher cavities. Additionally the head of the pulse coming from the LEBT will be degraded because there is a time

# HIGH CURRENT URANIUM BEAM MEASUREMENTS AT GSI-UNILAC FOR FAIR

W. Barth<sup>1,2</sup>, A. Adonin<sup>1</sup>, Ch. E. Düllmann<sup>1,2,3</sup>, M. Heilmann<sup>1</sup>, R. Hollinger<sup>1</sup>, E. Jäger<sup>1</sup>, O. Kester<sup>1</sup>,  
J. Khuyagbaatar<sup>1,2</sup>, J. Krier<sup>1</sup>, E. Plechov<sup>1</sup>, P. Scharrer<sup>1,2,3</sup>, W. Vinzenz<sup>1</sup>, H. Vormann<sup>1</sup>,  
A. Yakushev<sup>1,2</sup>, S. Yaramyshev<sup>1</sup>

<sup>1</sup> GSI Helmholtzzentrum für Schwerionenforschung, Darmstadt, Germany

<sup>2</sup> Helmholtz Institut Mainz, Germany

<sup>3</sup> Johannes Gutenberg-Universität Mainz, Germany

## Abstract

In the context of an advanced machine investigation program supporting the ongoing UNILAC (Universal Linear Accelerator) upgrade program, a new uranium beam intensity record ( $\approx 10$  emA,  $U^{29+}$ ) at very high beam brilliance was achieved last year in a machine experiment campaign at GSI. The UNILAC as well as the heavy ion synchrotron SIS18 will serve as a high current heavy ion injector for the new FAIR (Facility for Antiproton and Ion Research) synchrotron SIS100. Results of the accomplished high current uranium beam measurements applying a newly developed pulsed hydrogen gas stripper (at 1.4 MeV/u) will be presented. The paper will focus on the evaluation and analysis of the measured beam brilliance and further implications to fulfil the FAIR heavy ion high intensity beam requirements.

## INTRODUCTION

Meeting the FAIR science requirements [1] higher beam intensities have to be achieved in the present GSI-accelerator complex, through faster cycling and, for heavy ions, lower charge state which enters quadratically into the space charge limit (SCL). The desired beam energy of up to 1.5 GeV/u for radioactive beam production will be delivered by the synchrotron SIS100. Recently GSI put effort into increasing the uranium beam intensity delivered to the SIS18. An advanced machine investigation program for the UNILAC is aimed at meeting the FAIR requirements. For uranium (FAIR reference ion) the UNILAC has to deliver at least  $3.3 \times 10^{11}$   $U^{28+}$ -particles during 100  $\mu$ s.

In the High Current Injector (HSI) comprising an IH-RFQ and an IH-DTL, the beam is accelerated up to 1.4 MeV/u. In the gas stripper section the initial charge

state ( $4+$ ) is increased; an uranium beam ( $28+$  or higher charge state) is matched to the Alvarez DTL. After acceleration up to the final UNILAC-beam energy of 11.4 MeV/u the transfer line (TK) to the SIS18 provides optionally foil stripping and a charge state separator (Fig. 1).

High current uranium beam machine experiments at HSI and the gas stripper section were conducted in November 2015. A multi-aperture extraction system for extracting a high brilliant ion beam from the VARIS ion source [2] was used. The RFQ-cavity underwent a dedicated conditioning and development program, providing for reliable rf-operation. These measures facilitated an extensive beam optimizing program and thus the success of this measurement campaign. The pulsed hydrogen stripping target [3,4] was further optimized aiming for operation at the maximum achievable average charge state. The high current measurements were therefore carried out for charge state  $29+$ . The measured beam brilliance before the Alvarez-DTL was evaluated in detail. Due to an upgrade program, which renews the rf-amplifier system of the UNILAC post stripper (Alvarez) only three of the five Alvarez tanks were in operation. Thus, the achievable high current beam brilliance at injection into the SIS18 is currently estimated by using front-to-end high-current measurements [5] with a proton beam (with the same space charge capability as for the uranium beam) performed in 2014. Supplemented by extensive beam simulations [6] that were carried out recently for injection of a high-intensity uranium beam into the SIS18, the beam intensity, achievable from the FAIR injector chain, could be estimated.

## HIGH CURRENT PROTON BEAM EMITTANCE MEASUREMENTS

The horizontal beam emittance is one of the crucial quantities at a fixed beam intensity to characterize the high-current capability of a synchrotron injector. The high current proton beam emittance growth inside the Alvarez was measured to be 17% (rms) [5] (Fig. 2). Considering the overall beam transmission of 90%, the loss of beam brilliance inside the Alvarez is 23%; the subsequent transport into the transfer line was accomplished without particle loss. However, due to a vertical bottle neck in the transfer line an additional loss of 15% was measured. The

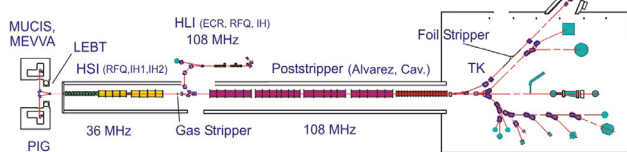


Figure 1: Schematic overview of the GSI UNILAC and experimental area. [1]

# ADVANCES IN THE DEVELOPMENT OF THE ESS-BILBAO PROTON INJECTOR

Z. Izaola\*, I. Bustinduy, J. Corres, D. de Cos, C. de la Cruz, G. Harper, R. Miracoli, J. L. Muñoz, I. Rueda, A. Vizcaino, and A. Zugazaga, ESS-Bilbao, Spain

## Abstract

We present the last advances in the operation and construction of the ESS-Bilbao 3 MeV proton beam injector. The proton ECR source allows to change the distance between the plasma chamber and the first extraction electrode, acceleration gap. The beam has been characterised at different acceleration gaps by current transformers, wire scanners and photographs of 2d profiles. In addition, we present the status of the construction of the RFQ; which is at its beginning.

## INTRODUCTION

ESS-Bilbao aims to develop an accelerator components for ESS. One of the main contribution is the Medium Energy Beam Transport (MEBT). If project schedule allows we plan to test the MEBT with a proton beam. To achieve this goal, we are building an injector composed of a proton Ion Source (ISHP) [1], Low Energy Beam Transport (LEBT) [2] and a Radio-Frequency Quadrupole (RFQ) [3].

The injector is expected to produce a proton beam with an energy of 45 keV and high intensity with a rms emittance around  $0.25 \pi$  mm mrad in order to fulfil the requirements of the RFQ. One innovative feature of ISHP is the possibility to vary the gap between the plasma chamber and the extraction electrodes; the so called acceleration gap.

This paper, firstly, discuss the general layout of the LEBT. Secondly, it shows the result of various measurement campaign aiming to optimise and understand the beam. Finally, it discuss briefly the design of the RFQ and the current status of its construction.

\* zunbeltz.izaola@essbilbao.org

## THE LOW ENERGY BEAM TRANSPORT

The Bilbao Accelerator LEBT (Figure 1) is composed of two solenoids placed at fixed positions, producing tunable magnetic fields. The solenoids have a smaller internal radius (involving more turns) at their ends than in their centres [4]. This way, the magnetic field profile along the axis is flatter than the one achieved with an uniformly shaped solenoid; which would present a typical bell-shaped magnetic field profile. Besides, the variable radius approach creates a magnetic field that remains confined within the solenoid limits, avoiding perturbations on any nearby elements (e.g. other solenoids and the vacuum pump).

In order to save beam-line space, each solenoid includes a set of two crossed ( $x/y$ ) dipoles of the  $\cos \theta$  type. The dipoles are capable of steering the beam to correct for misalignment of the beam line components, reaching a deflection up to  $\pm 4^\circ$  of the protons. The presence of the dipoles limits the aperture to 100 mm [2].

Although the complete LEBT is equipped with three diagnostic boxes; one before the first solenoid, one between solenoids and one after the second solenoid; at this first stage we use only one solenoid and two boxes (Figure 2). The first box is equipped with an AC Current Transformer (ACCT1), a double-wire Wire Scanner (WS1) and a retractile beam collimator (BC) with a 5 mm radius hole to create a pencil beam. The second box contains a second ACCT2, a second WS (WS2), a quartz window for fluorescence measurements and a retractile beam shutter that protects the quartz. The two wires of the WS are at  $45^\circ$  from the horizontal and vertical directions. A Princeton Instrument CCD camera

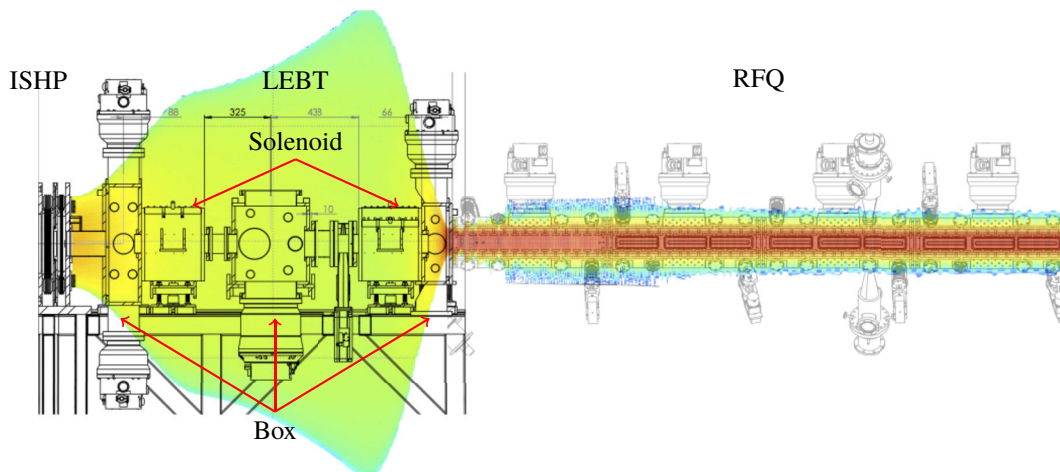


Figure 1: Schematic layout of the ESS-Bilbao injector from the  $H^+$  Ion Source (left), through the LEBT (middle), to the RFQ (right). The coloured shadow represents the beam beam density along the injector.

# BEAM COMMISSIONING RESULTS FOR THE CSNS MEBT AND DTL-1

J. Peng<sup>†</sup>, Y.W An, M.Y Huang, L.S Huang, Y. Li, M.T Li, Z.P Li, Y.D Liu, X.H Lu, S.Y Xu  
Y. Yuan, S. Wang, S.N Fu

Dongguan Campus, Institute of High Energy Physics, Dongguan 523803 China

## Abstract

The China Spallation Neutron Source (CSNS) is designed to deliver a 1.6GeV proton beam to a solid metal target for neutron scattering research. It will be constructed in two phases. In the 1<sup>st</sup> phase, the beam power is designed to be 100kW. In the 2<sup>nd</sup> phase, the beam power will be upgraded to 500kW by doubling the linac output energy and beam current. The accelerator complex consists of a 50keV H<sup>-</sup> ion source, a 3MeV radio frequency quadrupole (RFQ), an 80MeV drift tube linac (DTL), and a 1.6GeV rapid-cycling synchrotron (RCS). Until March 2016, the front end and the first tank of DTL have been fully commissioned. The primary design goals of peak current, transverse emittance and beam energy have been achieved. This paper reports on the methods and the results of the commissioning.

## INTRODUCTION

The China Spallation Neutron Source (CSNS) is located in southeast China. The accelerator complex consists of a 50keV H<sup>-</sup> ion source, a 3MeV radio frequency quadrupole (RFQ), an 80MeV drift tube linac (DTL), a 1.6GeV rapid-cycling synchrotron (RCS) and several beam lines [1]. The RF frequency for both RFQ and DTL is 324MHz. Until March 2016, two runs of beam commissioning have been completed. In the 1<sup>st</sup> run, the front-end has been commissioned and the primary goal is realized [2]. Beam with 15mA peak current, 500μs pulse length and 50% beam-on duty factor has successfully transported through the MEBT into a temporary dump. In the 2<sup>nd</sup> run, the DTL tank1 has been commissioned with a temporary beam line. Due to the limited capacity of the temporary dump, the pulse length was shortened to 400μs (chopped) and the repetition rate was reduced to 5Hz. The other parameters like beam peak current and energy have reached the design values. A summary of baseline design parameters and beam commissioning results is shown in Table 1.

## MEBT COMMISSIONING RESULTS

The MEBT is used for matching beam output from the RFQ into the following DTL transversely and longitudinally. It consists of 10 quadrupoles, 6 steering magnets and two 324MHz bunchers. The schematic layout of the MEBT is shown in Fig. 1. Besides optic elements, there is a suit of diagnostics to monitor beam.

<sup>†</sup> pengjun@ihep.ac.cn

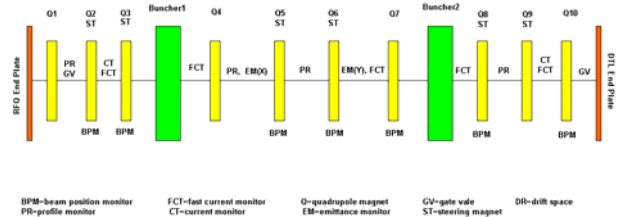


Figure 1: Layout of the CSNS MEBT.

Table 1: CSNS design vs. achieved beam parameters

|   | Baseline Design or Goal | Achieved   |
|---|-------------------------|------------|
| MEBT beam pulse length [μs]                     | 420                     | 500        |
| MEBT pulse repetition rate [Hz]                 | 25                      | 25         |
| Chopping rate [%]                               | 50                      | 50         |
| LEBT peak current [mA]                          | 20                      | 31         |
| MEBT peak current [mA]                          | 15                      | 18         |
| DTL1 peak current [mA]                          | 15                      | 18         |
| MEBT horiz emittance [π mm mrad (rms, norm)]    | 0.22                    | 0.21       |
| MEBT vertical emittance [π mm mrad (rms, norm)] | 0.22                    | 0.20       |
| MEBT Beam Energy [MeV]                          | 3.026                   | 3.02±0.015 |
| DTL1 output energy [MeV]                        | 21.67                   | 21.7±0.022 |

## Transverse Twiss Parameters

For estimation of Twiss parameters at the beginning of the MEBT, beam profiles were measured with four wire scanners in the MEBT. If the wire scanner data is Gaussian and of high quality the easiest way to compute the beam sizes is fitting the profile with a Gaussian distribution. However, Gaussian fit may not accurately represent the beam profile with halo. To calculate the RMS radius of this kind of profile, direct statistical calculation may be more suitable. Fig. 2 shows an example of the beam profile. The horizontal profile looks like Gaussian distribution while the vertical profile has significant halo “shoulders” [3].

After processing wire scanner data, estimation of the Twiss parameters was performed using beam sizes in conjunction with a beam propagation model. Table 2 lists the obtained Twiss parameters at the beginning of the MEBT.

## OPERATIONAL EXPERIENCE AND FUTURE PLANS AT ISIS

D.J. Adams, C.M. Warsop, B. Jones, B. Pine, H. Smith, R. Williamson, A. Seville, R. Mathieson, I.S.K. Gardner, D. Wright, A.H. Kershaw, A. Pertica, A. Letchford, STFC, Oxford, UK

### Abstract

The ISIS spallation neutron and muon source has been in operation since 1984. The accelerator complex consists of an H<sup>-</sup> ion source, 665 keV RFQ, 70 MeV linac, 800 MeV proton synchrotron and associated beam transfer lines. The facility currently delivers  $\sim 2.8 \times 10^{13}$  protons per pulse (ppp) at 50 Hz, which is shared between two target stations. High intensity performance and operation are dominated by the need to minimise and control beam loss, which is key to sustainable machine operation, allowing essential hands-on maintenance. The facility has had several upgrades including an RFQ, Second Harmonic RF system, beam diagnostic DAQ improving beam control and a Second Target station. Future upgrades include a ring damping system and MEBT injection chopper. Operational experience of ISIS and its upgrades are discussed as well as current and future R&D projects.

### INTRODUCTION

The ISIS neutron facility has been in operation since 1984 providing neutron and muon beams to the user community for a wide spectrum of materials research [1]. The facility originally consisted of an H<sup>-</sup> ion source, 665 kV pre-injector, 70 MeV four tank drift tube linac injecting into a 163 m circumference, proton synchrotron. Un-chopped beam injected into the ring using H<sup>-</sup> charge exchange accumulates  $2.75 \times 10^{13}$  protons over 130 turns, non-adiabatically trapped, and fast extracted at 50 Hz delivering a 160 kW beam to a depleted uranium target.

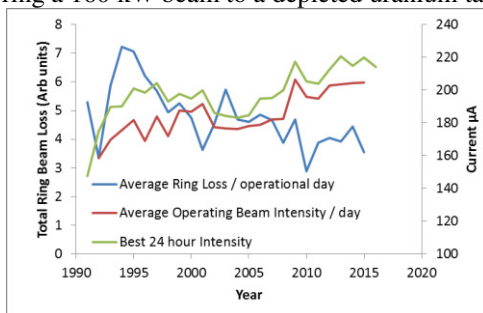


Figure 1: Operating ring beam loss and intensity since 1992.

As with any accelerator facility, post commissioning, there have been many incremental developments to increase operating intensity and improve beam loss control. The main upgrades have been Straight 1 (2002), Pre-Injector (2004), Ring Dual Harmonic RF (DHRF) cavities (2006-2012), Second Target Station (2007), Downstream Extracted Proton Beam line (EPB) refurbishments (2007-2015), with continued machine physics R&D improvements throughout the whole period.

The main challenge for high intensity operation of the facility is minimising and controlling beam losses,

especially in the ring, which activate machine components restricting hands on maintenance. Fig. 1 shows yearly average total ring beam loss, operating intensity and best 24 hour operating intensity since 1992. The trend is for decreasing beam loss and increasing operating intensity to the point where we now routinely operate in excess of 220  $\mu\text{A}$ , 176 kW. Whilst upgraded hardware has improved machine reliability this paper concentrates on upgrades and operational experience which have aided beam control.

### MAIN ACCELERATOR UPGRADES

#### Pre-Injector Upgrade

The original pre-injector section of the accelerator consisted of a 665 kV Cockcroft Walton accelerator, Fig. 2 left, followed by a quadrupole and RF buncher matching section delivering a 19 mA, H<sup>-</sup> beam to linac tank 1. As part of an intensity upgrade, to meet the demands of increased beams for the second target station, this section was replaced by 3 solenoids and an RFQ in 2004 [2], Fig. 2 right. After 18 months commissioning and soak testing in a dedicated test facility the new components were installed in the accelerator and have been very successful and reliable. The main commissioning issues were surface cleaning inside the RFQ, required to meet high RF field levels.



Figure 2: Cockcroft Walton set (left) and new RFQ (right).

Typical operation now delivers 35 mA beams to tank 1 with 95 % transmission efficiency. Transverse mis-match into tank 1 reduces the beam current to 26 mA which is then maintained through the remaining linac tanks for injection into the ring [3].

#### Dual Harmonic RF Upgrade

The ring RF system was originally composed of six,  $h=2$ , ferrite loaded cavities delivering up to 160 kV/turn. Ring injection accumulated a DC beam which was then trapped into two bunches non-adiabatically and accelerated up to 800 MeV in 10 ms. Beam losses of 10 % limited operation to  $\sim 200 \mu\text{A}$ . The dual harmonic upgrade [4,5], saw the addition of four,  $h=4$ , cavities with 80 kV/turn total peak. Increased bucket acceptance and

# IFMIF-EVEDA RFQ, MEASUREMENT OF BEAM INPUT CONDITIONS AND PREPARATION TO BEAM COMMISSIONING

M. Comunian<sup>†</sup>, L. Bellan<sup>1</sup>, E. Fagotti, A. Pisent, Istituto Nazionale di Fisica Nucleare Laboratori Nazionali di Legnaro, Legnaro, Italy

<sup>1</sup>also at Univ. degli Studi di Padova, Padova, Italy

## Abstract

The commissioning phase of the IFMIF-EVEDA RFQ requires a complete beam characterization with simulations and measurements of the beam input from the IFMIF-EVEDA ion source and LEBT, in order to reach the RFQ input beam parameters. In this article, the simulations of source LEBT RFQ will be reported with the corresponding set of measurements done on the Ion source and LEBT.

## THE IFMIF-EVEDA PROJECT

The Linear IFMIF Prototype Accelerator (LIPAc) is an high intensity deuteron linear accelerator [1]; it is the demonstrator of the International Fusion Material Irradiation Facility (IFMIF) machine within the Engineering Validation Engineering Design Activities (EVEDA) scope. It is presently in an advanced installation phase at Rokkasho under the Fusion Energy Research and Development Directorate National Institutes for Quantum and Radiological Science and Technology (QST), in the prefecture of Aomori, Japan. LIPAc has been designed and constructed mainly in European labs with participation of JAEA in the RFQ couplers. It is composed of an injector delivered by CEA-Saclay [2], a RFQ [3] designed made and delivered by INFN on April 2016, a superconducting Linac designed by CEA-Saclay [4], RF power, Medium and High Energy Beam Transfer lines and a beam dump designed by CIEMAT [5].

## THE IFMIF-EVEDA RFQ

The Radio Frequency Quadrupole (RFQ) 0.1 - 5 MeV, 130 mA, is an Italian in-kind contribution to the IFMIF-EVEDA project, under the INFN responsibility.

The RFQ design method has been aimed to the optimization of the voltage and R0 law along the RFQ, the accurate tuning of the maximum surface field and the enlargement of the acceptance in the final part of the structure. As a result, a length shorter than in all previous design characterizes this RFQ; very low losses (especially at higher energy) and small RF power dissipation [6].

In Table 1 and Fig. 1 are reported the main RFQ parameters along its length.

## LAYOUT OF INSTALLED SOURCE AND LEBT

The injector is composed of a 2.45 GHz ECR ion source based on the CEA-Saclay SILHI source design and a LEBT line that will transport and match the beam into the RFQ thanks to a dual solenoid focusing system with integrated H/V steerers.

<sup>†</sup> Michele.comunian@lnl.infn.it

Table 1: RFQ Main Parameters

|                             |             |                    |
|-----------------------------|-------------|--------------------|
| Length                      | 9.814       | m (5.7 $\lambda$ ) |
| Total Cell number           | 489         |                    |
| Voltage Min/Max             | 79.29/132   | kV                 |
| Max modulation m            | 1.8         |                    |
| Min aperture "a"            | 3.476       | mm                 |
| R0 min/Max                  | 5.476/7.102 | mm                 |
| Ratio $\rho$ /R0 (constant) | 0.75        |                    |
| Final Synch. phase          | -35.5       | Deg                |
| Max Surf. Field (1.76 Kp)   | 24.7        | MV/m               |

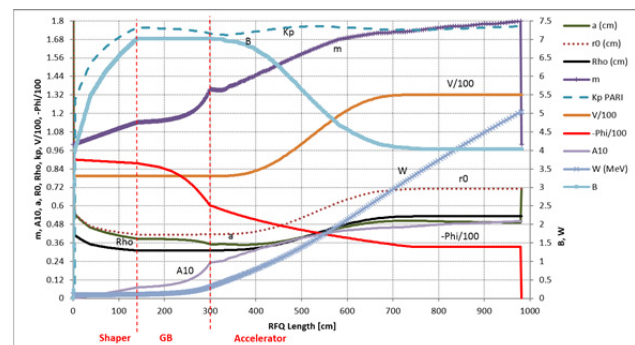


Figure 1: Parameters evolution along the RFQ.

The components of the LEBT are:

- Two solenoids with integrated steerers.
- Injection cone with repeller electrode after the two solenoids.
- Middle solenoids diagnostic box equipped with Doppler Shift Spectrometer instrumentation, Farady cup, Four Grid Analyser and Residual Gas Analyser.
- End diagnostic box after the solenoids, with an Allison scanner and self-polarised beam stop.

The commissioning is started in 2015 and will continue in 2016 interleaved with the RFQ installation in order to optimize the project schedule.

Design simulations show that to have less than 10% losses in the RFQ, the injected D<sup>+</sup> beam must be 140 mA/100 keV CW with a normalized RMS emittance of 0.25 mm·mrad.

Commissioning activities use an equal generalised perveance H<sup>+</sup> beam at RFQ injection, which consists of half current and half energy compare to deuterons at nominal conditions. This is done to allow hands-on maintenance activities since the activation power of 50 keV protons is negligible. Moreover, an electrostatic chopper has been implemented in between the two solenoids to provide sharp beam pulses of short length (~ 50-100  $\mu$ s) for machine protection system in view of the RFQ com-

# ESS LINAC PLANS FOR COMMISSIONING AND INITIAL OPERATIONS

R. Miyamoto\*, M. Eshraqi, M. Muños, ESS, Lund, Sweden

## Abstract

Beam commissioning of the proton linac of the European Spallation Source (ESS) is planned to be conducted in 2018 and 2019. At this stage, the last 21 cryomodules are not yet installed and the maximum beam energy and power are 570 MeV and 1.4 MW, with respect to the nominal 2 GeV and 5 MW. The linac will be operated in this condition until the remaining cryomodules are installed in two stages in 2021 and 2022. On top of the common challenges of beam dynamics and machine protection, commissioning of a large scale machine, such as the ESS linac within a relatively short integrated time of less than 40 weeks imposes an additional challenge to the scheduling and planning. This paper lays out the current plans of the ESS linac for its beam commissioning as well as the initial operation.

## INTRODUCTION

European Spallation Source (ESS), currently under construction in Lund, Sweden, is a neutron source driven by a proton linac. When the linac reaches its unprecedented design average power of 5 MW, the ESS will be the brightest neutron source in the world [1, 2]. It is planned that installation and commissioning of the ESS linac starts in 2017 and the first proton beam is delivered to the target by the end of 2019. The plan as the ESS facility is to start the user program in 2023 and gradually increase the neutron production and operation time towards the design specifications. Commissioning of a large-scale machine, such as the ESS linac, within a relatively short time imposes challenges on many areas including planning and preparations for the beam commissioning (BC). Many efforts have already been made for planning of the commissioning from the point of view of the installation [3, 4], radiation permit [5], beam diagnostics devices [6, 7], and control software [8]. In this paper, we review the procedures of the beam commissioning from the point of view of beam physics so that necessary types of lattice tuning and their methods are clarified and prepared prior to the beam commissioning.

## ESS LINAC OVERVIEW

### High Level Parameters

Table 1 lists the high level parameters of the ESS linac during the nominal operation. The 2 GeV energy, 62.5 mA current, and 4% duty cycle make average power of 5 MW. The long pulse length of 2.86 ms is a requirement from the users and thus fixed during any phase of operation. If the power is needed to be reduced during initial phases of operation, the peak current or repetition rate is reduced. A high availability of 95% is also a requirement from the users due to the nature of the user program [9].

\* ryoichi.miyamoto@esss.se

Table 1: High Level Parameters of the ESS Linac

| Parameter                  | Unit | Value         |
|----------------------------|------|---------------|
| Average beam power         | MW   | 5             |
| Maximum beam energy        | GeV  | 2             |
| Peak beam current          | mA   | 62.5          |
| Beam pulse length          | ms   | 2.86          |
| Beam pulse repetition rate | Hz   | 14            |
| Duty cycle                 | %    | 4             |
| RF frequency               | MHz  | 352.21/704.42 |
| Availability               | %    | 95            |

### Linac Structure

Figure 1 shows a schematic layout of the ESS linac. The initial part of the linac consists of an ion source (IS); two normal conducting accelerating structures, a radio frequency quadrupole (RFQ) and drift tube linac (DTL); and two beam transports, a low energy beam transport (LEBT) and medium energy beam transport (MEBT). These are referred to as the normal conducting linac (NCL) as a whole. In addition to provide acceleration, functionalities of the NCL include bunching in the RFQ and manipulations of the beam parameters. Once the beam exits the MEBT, there is no controlled change in the current and pulse length in the downstream section.

Following the NCL, there are three sections with different types of superconducting cavities, spoke cavities, medium- $\beta$  elliptical cavities, and high- $\beta$  elliptical cavities. These sections are referred to as SPK, MBL, and HBL for each and Superconducting Linac (SCL) as a whole. As seen in the figure, most of the energy gain is provided by the superconducting cavities in the SCL.

Another beam transport, a high energy beam transport (HEBT), follows the SCL. The HEBT has the same lattice structure as the HBL except the empty slots for the cryomodules, which allow to install additional cryomodules later in cases of contingencies or for an energy upgrade. At the end of the HEBT, there is a dipole for the upward bend and the linac is split into two from this point. When the dipole is off, the beam enters the dump line (DMPL) and is stopped by a tuning dump at the end. When the dipole is on the beam enters the dogleg and is bent back towards the target by another dipole after a 4.5 m elevation. After the second dipole is the final section of the linac and another beam transport, the accelerator-to-target (A2T) section. In the A2T, each pulse is sprayed over a rectangular region on the target surface by fast oscillating ( $\sim 29$  kHz in horizontal plane and  $\sim 40$  kHz in vertical plane) dipole magnets to reduce the intensity (*rastering* process).

Further details of each section are provided later during the discussion of the commissioning plan for each section.

## COMMISSIONING OF C-ADS INJECTOR I\*

Jianshe Cao<sup>†</sup>, FangYan, Cai Meng, Huiping Geng, Rong Liu, Yanfeng Sui, Qiang Ye  
Institute of High Energy Physics, Beijing, China

### Abstract

As a test facility, the design goal of C-ADS Injector I is a 10mA, 10MeV CW proton linac, which uses a 3.2MeV normal conducting RFQ and superconducting single-spoke cavities for accelerating. The RF frequency of C-ADS Injector I accelerator is 325 MHz. In accordance to the progress of construction and considering the technical difficulties, the beam commissioning of C-ADS Injector I is carried out in several phases. This paper will summarize the beam commissioning in every phases and focusing on the final phase.

### INTRODUCTION

“The China Accelerator Driven Sub-critical System (C-ADS)” is one of the “Strategic Priority Research Program” of CAS. Its main task is to cope with nuclear waste material and produce clean nuclear power. It have two injectors, C-ADS injector I is a 10MeV proton linac with 10mA continuous current made by IHEP. It consists of an ECR (Electron Cyclotron Resonance) ion source, a LEBT (Low Energy Beam Transport), a 3MeV RFQ (Radio-frequency Quadrupole) with 325MHz frequency and a superconductivity linac accelerator with 3~10MeV [1]. The schematic diagram of C-ADS injector I is shown in Fig.1, and the specifications of the injector I are also listed in table 1.

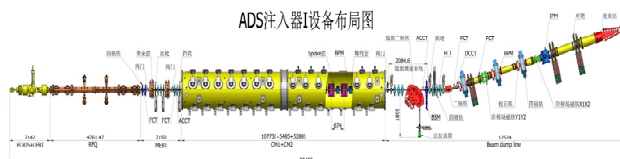


Figure 1: The Schematic diagram of C-ADS injector I.

Table 1: ADS Injector-I Test Facility Specifications

| ADS Injector-I test facility specifications |        |
|---|--------|
| Particle                                    | Proton |
| Output Energy (MeV)                         | 10     |
| Average Current (mA)                        | 10     |
| Beam power (kW)                             | 100    |
| Duty factor (%)                             | 100    |
| RF frequency (MHz)                          | 325    |

### COMMISSIONING PHASE AND RESULTS

As shown in Figure 1, the Injector-I testing facility is composed of an ECR ion source, a LEBT, a RFQ, a MEFT, a superconducting (SC) section, an energy Analy-

sis Magnet (AM) and a beam dump line. The designed output energy of the RFQ is 3.2MeV. The SC section includes two cryomodules (CM1&CM2) with 14  $\beta=0.12$  SC spoke cavities, 14 solenoids and 14 cold BPMs, which is used to boost the proton beam energy up to 10 MeV [2]. At present, the commissioning of CM1 & CM2 with narrow pulse beam (duty cycle: 0.04 %, 2Hz/20us) is completed.

### LEBT, RFQ, MEFT Commissioning

The LEBT connect the ECR source to the RFQ and provides the matching between the ECR and RFQ. The ion source provides 35keV CW or pulsed proton beam with average current over 10mA [2]. The Figure 2 shows the LEBT layout. The total length of the LEBT is 1.67m. It includes 2 solenoid, 1 DCCT, 1 ACCT and a chopping system. The chopper can provide short or long pulsed beam. Beam width can be adjusted start from 40 ns with repetition frequency of 1Hz up to 50Hz. The rise and down time is smaller than 20ns.

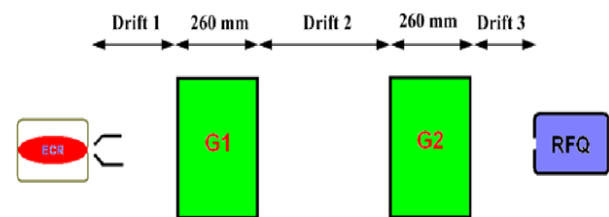


Figure 2: The layout of LEBT.

The emittance at the exit of the LEBT are measured by using Alison detector. The measurement result and the simulation result are shown in the Figure 3. The left on the Figure 3 is the simulated phase space 8.8cm downstream of the LEBT, and the right figure is the measured results. The both shape of the beam phase space looks very similar. Table 2 shows the designed twiss parameters and the measured results at the RFQ entrance. The twiss parameters are sensitive to the LEBT solenoid settings and we chose the one closet to the simulated parameters of the RFQ entrance in order to get matched beam [3].

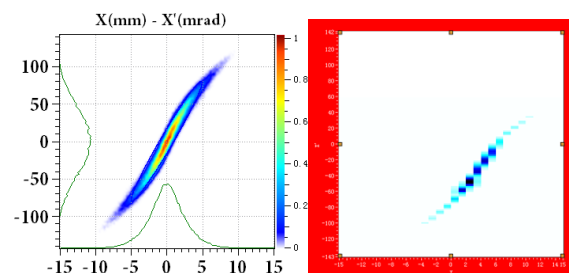


Figure 3: The simulation result (left) and the measurement result (right) of emittance at LEBT exit.

\*Work supported by CAS Strategic Priority Research Program-Future Advanced Nuclear Fission Energy (Accelerator-Driven Sub-critical System).

<sup>†</sup> caojs@ihep.ac.cn

# OBSERVATIONS OF COUPLING DURING ACCUMULATION USING A NON-DESTRUCTIVE ELECTRON SCANNER IN THE SPALLATION NEUTRON SOURCE ACCUMULATOR RING\*

R. Potts<sup>†1</sup>, W. Blokland, S. Cousineau, J.A. Holmes, ORNL, Oak Ridge, TN, 37831, USA  
<sup>1</sup>also at The University of Tennessee, Knoxville, 37996, USA

## Abstract

An electron scanner has been installed in the accumulator ring of the Spallation Neutron Source (SNS). The non-destructive device permits turn-by-turn measurements of the horizontal and vertical profiles of the proton beam during accumulation with fine longitudinal resolution. In this study the device is used to investigate the source of transverse coupling in the SNS ring and to understand the impact of space charge on the evolution of the coupled beam. We present experimental observations of coupling dependent on tune, injected intensity, and accumulated intensity for a simplified accumulation scenario with no RF and no injection painting. We also investigate the effects of varying the skew quadrupoles and tune for beams with the SNS production-style ring injection and ring RF patterns.

## INTRODUCTION

The SNS Accumulator Ring compresses up to 1050 turns of injected beam into a short 1  $\mu$ s pulse containing up to  $1.5 \times 10^{14}$  protons. Once accumulated, this pulse is delivered to a liquid mercury target for neutron spallation by way of the Ring-to-Target Beam Transport (RTBT). The target has specific requirements for beam size and profile uniformity in both transverse planes. One primary requirement is that the peak on-target density remain less than  $2.6 \times 10^{16}$  protons/m<sup>2</sup> for a 1.5 MW beam. In order to achieve the on-target requirements, independent control of the transverse beam distributions is necessary. Previous studies have shown a loss of independent control between the planes. Initially this effect was only intermittently observed by accelerator operators during production shifts. In 2011 and 2012, it was shown that at high beam intensities the final accumulated beam distribution in each plane depended on the initial distribution in the alternate plane [1, 2]. Initially, the primary hypothesis was that the loss of control was due to space charge and could be related to the Montague Resonance [3] due to the small tune split of the coupled beam configurations. In 2015, it was shown that at low beam intensities the beam emittances could be caused to couple and fully exchange between the transverse planes by configuring a small tune split [4]. In this paper we present results of additional experiments from continuing efforts to under-

stand the transverse coupling in the SNS Accumulator Ring. In previous studies, we have used traditional wire scanners to collect transverse beam profiles. This has proven to be a time prohibitive method to study beam oscillations. In this experiment we will use the Electron Scanner (ES), a novel diagnostic device recently developed in the SNS Accumulator Ring.

## ELECTRON SCANNER

The Electron Scanner obtains profiles by first passing an electron beam diagonally across the path of the accumulating proton beam. The electron beam is deflected in the presence of the electromagnetic field of the proton beam. The deflected path is then projected onto a fluorescent screen and an image is captured. The transverse profile is derived from the amount of the deflection along the projection [5]. The analysis, which can be run offline, slices through the center of the image and fits a gaussian peak to the pixel intensities along each slice to find the full set of (x, y) points. A spline curve is then fitted through the set of (x, y) points to calculate a smoother set of curve points so that a derivative can be taken to obtain a less noisy profile. The spline fit technique also allows the projection of the beam to be traced through the cut-outs made by the electron scanner beam markers, which are used to provide a scale for the profile width. A derivative with respect to position is calculated from the difference of the spline curve with respect to the path of an undeflected electron beam.

The electron scanner has several advantages over traditional wire scanners. The first advantage is the non-destructive nature of the electron scanner, which allows us to collect data parasitically to regular production operations. This means that the electron scanner could become a useful diagnostics tool for regular use during operations in the future. Second, the electron scanner has the ability to capture 20 ns slices of the accumulating proton beam. When examining many slices together, this can provide a detailed longitudinal profile. This differs from the wire scanners which sum along the longitudinal profile of the beam. Additionally, a short scan time means that the transverse profiles can be studied across the length of the beam bunch. Finally, Fig. 1 shows the locations of the electron scanner compared to the wire scanners. Its position in the accumulator ring and a 1 Hz scan rate allow the electron scanner to collect large data sets quickly and without requiring operator interruption. It should be noted that each electron scanner profile represents the profile from within a certain point of a single proton beam, while a wire scanner profile represents

\*ORNL is managed by UT-Battelle, LLC, under contract DE-AC05-00OR22725 for the U.S. Department of Energy. This research was supported by the DOE Office of Science, Basic Energy Science, Scientific User Facilities.

<sup>†</sup>pottsre@ornl.gov

# CODE BENCH-MARKING FOR LONG-TERM TRACKING AND ADAPTIVE ALGORITHMS

H. Bartosik, A. Huschauer, A. Oeftiger, F. Schmidt, M. Titze, CERN, Geneva, Switzerland  
 G. Franchetti, GSI, Darmstadt, Germany  
 J. Holmes, SNS, Oak Ridge, USA  
 Y. Alexahin, J. Amundson, V. Kapin, E. Stern, FERMILAB, Batavia, USA

## Abstract

At CERN we have ramped up a program to investigate space charge effects in the LHC pre-injectors with high brightness beams and long storage times. This is in view of the LIU upgrade project [1] for these accelerators.

These studies require massive simulation over large number of turns. To this end we have been looking at all available codes and started collaborations on code development with several laboratories: MAD-X frozen & adaptive mode [2] and integration into the main branch of the MAD-X in-house development [3] code, PyORBIT [4] from SNS, SYNERGIA [5] from Fermilab, MICROMAP [6] from GSI .

We have agreed with our collaborators to bench-mark all these codes in the framework of the GSI bench-marking suite [7], in particular the main types of frozen space charge and PIC codes are being tested.

We also include a study on the subclass of purely frozen and the adaptive frozen modes both part of MAD-X in comparison with the purely frozen MICROMAP code.

Last, we will report on CERN's code development effort to understand and eventually overcome the noise issue in PIC codes.

## INTRODUCTION

The aim of this study is threefold. On the one hand we would like to present the completion or near-completion of the GSI Bench-Marking Suite [7] of 2 PIC codes and the comparison with the results from 3 participating frozen SC codes. The second task is to report about the on-going study to understand how SC experiments compare with the various SC codes. To this end we are studying both the PS [8] and the SPS [9] at the integer resonance. This study of SC at the integer resonance in view of evaluating which tools are most suited to understand the dynamics is part of the mandate of a PhD [10] at CERN. Here we can just present a snapshot of what could be achieved up to this conference. Lastly, we would like to remind the community about the effect of grid noise on individual particles in the distribution. Techniques to overcoming this issue or at least minimizing its fake impact on the emittance evolution and particle loss will be crucial to see if PIC codes can be taken to use for long-term SC simulations or not. In fact, at this conference new concepts will be discussed that might do the trick. At CERN Malte Titze's [10] second part of his thesis is dedicated to such techniques.

## GSI BENCH-MARKING SUITE

With the upcoming Fair [11] and LIU [1] projects at GSI and CERN respectively, a new sequence of SC workshop has been started to review how our codes can be used to predict long-term SC effects on the dynamics of storage rings in the regime of high intensity. During this first joint GSI-CERN Space Charge Workshop [12] held at CERN in 2013, with a follow-up collaboration meeting in 2014 [13] it had been decided to start a collective effort to bench-mark several PIC codes with the GSI bench-marking suite that has been used for code bench-marking of a number of frozen SC codes in previous years. In particular, the teams of PyORBIT [4] from SNS, the latest incarnation of ORBIT, and the SYNERGIA [5] team of FERMILAB have made the effort to go through all the nine steps of this GSI bench-marking suite.

Figure 1 shows the 9<sup>th</sup> step of a long-term simulation over 100'000 turns of the SIS18 GSI ring. It is quite interesting to note that for some 10<sup>6</sup> macro-particles the SYNERGIA (2.5D solver) reproduces the results of the frozen SC codes. What is remarkable about this finding is the fact that also SYNERGIA as a PIC code is suffering from grid noise as shown below.

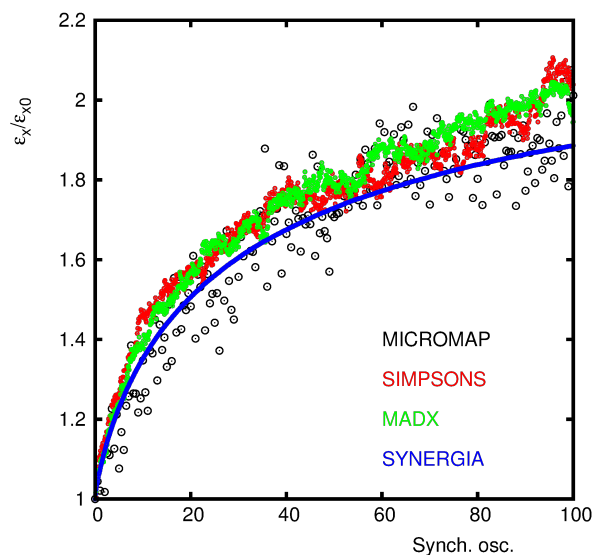


Figure 1: Emittance Evolution of the GSI SIS18 ring simulated with the 3 frozen SC Codes: MICROMAP, SIMPSONS, MAD-X and the PIC code SYNERGIA (1M macro-particles).

The complete results for both codes will now be introduced into the GSI bench-marking web site [7].

## CODE DEVELOPMENT FOR COLLECTIVE EFFECTS

K. Li\*, H. Bartosik, G. Iadarola, A. Oeftiger, A. Passarelli, A. Romano, G. Rumolo, M. Schenk,  
CERN, Switzerland,  
S. Hegglin, ETH Zürich, Switzerland

### Abstract

The presentation will cover approaches and strategies of modeling and implementing collective effects in modern simulation codes. We will review some of the general approaches to numerically model collective beam dynamics in circular accelerators. We will then look into modern ways of implementing collective effects with a focus on plainness, modularity and flexibility, using the example of the PyHEADTAIL framework, and highlight some of the advantages and drawbacks emerging from this method. To ameliorate one of the main drawbacks, namely a potential loss of performance compared to the classical fully compiled codes, several options for speed improvements will be mentioned and discussed. Finally some examples and applications will be shown together with future plans and perspectives.

### INTRODUCTION

Collective effects can lead to beam instabilities and brightness limitations and, thus, have a considerable detrimental impact on the performance of high brightness machines. Numerical modeling and simulations are a fundamental tool in understanding the physics of collective effects in circular particle accelerators. Moreover, they are a valuable means to evaluate and propose mitigation techniques to improve these limitations.

With the push towards higher brightness and higher energy these limitations play an increasingly important role. They involve several effects, among them impedance driven instabilities, electron cloud effects, the impact of long-range and head-on beam-beam collisions and single and multi-bunch effects.

In the past, simulation tools were often geared to modeling certain types or subsets of these effects. Meanwhile, the understanding of the individual effects has improved by a large amount and the combination of the different effects is now becoming increasingly important. To systematically study these combined effects on the beam stability, it is mandatory to bring together all the specific features of collective effects simulation codes.

In this paper we will investigate modern approaches to code development for collective effects. We will briefly illustrate the numerical modeling of collective effects in circular accelerators and then mention some general concepts and strategies for modern code style. We will then embark into a more specific discussion on the utilization of modern programming languages where we will use the example of the PyHEADTAIL framework. We will try to give an objective

view on the advantages this type of approach can provide and show how to cope with potential limitations. Finally, we will present some specific applications illustrating the particular usefulness of this type of approach.

### BASIC MODEL OF THE ACCELERATOR-BEAM SYSTEM

The numerical model that we will adopt to illustrate some of the concepts is the macroparticle model. Macroparticle models provide a direct and intuitive mapping of physics onto computer systems. Nearly any physical effect linked to particle beam dynamics can be easily implemented which makes these models extremely flexible and powerful. Macroparticles are essentially a numerical representation of a cluster of spatially neighbouring physical particles. As such, they follow the same dynamics following the same equations of motion that hold for physical particles.

A macroparticle system's dynamics is fully described by the evolution of its six phase space variables, the generalized coordinates and canonically conjugate momenta. Hence, a physical particle system, or a particle beam, can be easily represented via a macroparticle system on a computer system as an allocated chunk of memory where for each macroparticle all values of the six phase space variables are stored.

The accelerator is represented as a concatenation of elements each individually performing a distinct particle tracking. On a computer system, this can be represented by dedicated functions or methods that act on a macroparticle system in a defined and specific manner. Typically, a ring is split into a set of segments. A particle beam is transported from one segment to another by means of linear transfer matrices based on the machine optics in the transverse planes. In the longitudinal plane, tracking is performed assuming linear synchrotron motion, but also multi-harmonic RF systems can be easily taken into account as long a symplectic integration scheme is employed to assure numerical stability. Nonlinearities are treated via effective machine parameters such as chromaticity or detuning with amplitude by adjusting the phase advance of each individual macroparticle correspondingly after tracking along one segment. At each segment node, collective interactions can take place such as the application of different forms of wake field kicks, beam – electron cloud interaction, space charge kicks etc.

Typically, these effects are correlated with the longitudinal position of particles within the beam. To make the computations numerically efficient, a beam is longitudinally binned into a set of slices via a 1D particle-in-cell (PIC) algorithm. A single slice is then thought to be representative for all the macroparticles contained within. Collective

\* kevin.shing.bruce.li@cern.ch

# NUMERICAL MODELING OF FAST BEAM ION INSTABILITIES

L. Mether\*, G. Iadarola, G. Rumolo, CERN, Geneva, Switzerland

## Abstract

The fast beam ion instability may pose a risk to the operation of future electron accelerators with beams of high intensity and small emittances, including several structures of the proposed CLIC accelerator complex. Numerical models can be used to identify necessary vacuum specifications to suppress the instability, as well as requirements for a possible feedback system. Vacuum requirements imposed by the instability have previously been estimated for linear CLIC structures, using the strong-strong macroparticle simulation tool FASTION. Currently, efforts are being made to improve the simulation tools, and allow for equivalent studies of circular structures, such as the CLIC damping rings, on a multi-turn scale. In this contribution, we review the recent code developments, and present first simulation results.

## INTRODUCTION

Beam-induced ionization of residual gas present in the vacuum chamber of an accelerator, leads to the formation of ions and electrons along the beam path. Depending on several beam and machine parameters, such particles can accumulate into ion or electron clouds, which may cause serious beam degradation and the excitation of a two-stream instability. In electron machines with bunched beams, ion clouds build up if ions accelerated by a passing bunch do not have the time to reach the opposing chamber wall before the appearance of the subsequent bunch. In linacs, as well as in circular machines operating with a large clearing gap, the ion clouds can build up only over the passage of a bunch train, but may nevertheless lead to the development of an instability, the fast beam ion instability [1].

The Compact Linear Collider (CLIC) is a proposed TeV-scale high-luminosity linear electron-positron collider currently under study [2]. The collider could, in stages, reach a centre-of-mass energy up to 3 TeV, with roughly 20 km long main linacs. The linacs are designed to operate with trains of 312 or more short bunches with a minimum intensity of  $N = 3.7 \times 10^9$ , and a bunch separation of 0.5 ns. To maximize the luminosity, the transverse beam emittances, in particular in the vertical plane, need to be very small. These small emittance beams are produced in the CLIC injector complex, which consists of injector linacs, followed by two damping rings for each beam. The damping rings are designed to lower the normalized transverse emittances by several orders of magnitude from the injected values, down to the target extracted values of roughly 500 nm and 5 nm in the horizontal and vertical planes respectively. The beams are then further accelerated in a common linac before being transported through the main transfer lines to the beginning of the main linacs.

\* lotta.mether@cern.ch

Due to the high brightness and the short bunch separation of the CLIC beams, the electron beam is at serious risk of suffering from the fast beam ion instability in several structures along the accelerator complex. Whether an instability can develop depends on if the ion species present in the chamber are trapped by the beam, and the residual gas pressure is sufficiently high to excite an instability. Studies of ion trapping, as well as assessments of pressure thresholds for the onset of instability can successfully be made using numerical models. In the past, such studies have been performed for the major linear CLIC structures: the main linac and the main transfer line, using a dedicated simulation tool, FASTION, which was developed specifically for the purpose [3]. To be able to perform similar studies for the damping rings, a number of outstanding challenges need to be addressed.

In the following section, we describe our tools and procedures for modeling fast beam ion instabilities. We outline the main issues with extending the studies to synchrotrons, and describe the modifications made to accommodate them. Subsequently, we present first results from simulation studies of the instability in the CLIC main damping ring. We also discuss in more detail some of the general challenges related to numerical studies of fast beam ion instabilities, and the strategies and solutions we have adopted in our simulation tools in order to address these. In the final section, we draw some concluding remarks.

## SIMULATION TOOLS AND DEVELOPMENT

Macroparticle tracking simulations using the particle-in-cell (PIC) method, are a common tool for numerical studies of collective effects, and the one we employ in our model. Within this framework, the machine lattice is divided into a number of segments, each of which is represented by an interaction point where the electromagnetic beam-ion interaction along the segment is modeled in 2D. Ions are generated bunch by bunch, and the beam-ion interaction is simulated separately for each bunch along the train. In our studies, we use strong-strong simulation tools, *i.e.* both the beam and the ion cloud are represented by sets of macroparticles, which can be time-consuming, but offer a comprehensive model of the phenomenon. The ion macroparticles are regenerated in every interaction point, whereas the beam macroparticles, defined by their phase space variables, are transported between the interaction points using the linear transverse transfer matrices.

## FASTION

The FASTION code, written in the C language, was developed at CERN specifically to study the fast beam ion instability in linear CLIC machines. It allows to study a user defined gas composition with different species, defined through their

## BEAM DYNAMICS ISSUES IN THE FCC\*

W. Bartmann, M. Benedikt, M.I. Besana, R. Bruce, O. Brüning, X. Buffat, F. Burkart, H. Burkhardt, S. Calatroni, F. Cerutti, S. Fartoukh, M. Fiascaris, C. Garion, B. Goddard, W. Höfle, B. Holzer, J.M. Jowett, R. Kersevan, R. Martin, L. Mether, A. Milanese, T. Pieloni, S. Redaelli, G. Rumolo, B. Salvant, M. Schaumann, D. Schulte, E. Shaposhnikova, L.S. Stoel, C. Tambasco, R. Tomas, D. Tommasini, F. Zimmermann<sup>†</sup>, CERN, Switzerland; G. Guillermo, CINVESTAV Merida, Mexico; V. Kornilov, GSI Darmstadt, Germany; O. Boine-Frankenheim, U. Niedermayer, TU Darmstadt, Germany; T. Mitsuhashi, K. Ohmi, KEK, Japan; A. Chancé, B. Dalena, J. Payet, CEA, Saclay, France; P. Bambade, A. Faus-Golfe, J. Molson, LAL Orsay, France; J.-L. Biarrotte, A. Lachaize, IPNO, France; J. Fox, G. Stupakov, SLAC, U.S.A.; J. Abelleira, E. Cruz, A. Seryi, JAI Oxford, U.K.; R. Appleby, U. Manchester, U.K.; M. Boscolo, F. Collamati, A. Drago, INFN-LNF, Italy; J. Barranco, EPFL, Switzerland; S. Khan, B. Riemann, TU Dortmund, Germany

### Abstract

The international Future Circular Collider (FCC) study [1] is designing hadron, lepton and lepton-hadron colliders based on a new 100 km tunnel in the Geneva region. The main focus and ultimate goal of the study are high-luminosity proton-proton collisions at a centre-of-mass energy of 100 TeV, using 16 T Nb<sub>3</sub>Sn dipole magnets.

Specific FCC beam dynamics issues are related to the large circumference, the high brightness — made available by radiation damping —, the small geometric emittance, unprecedented collision energy and luminosity, the huge amount of energy stored in the beam, large synchrotron radiation power, plus the injection scenarios.

In addition to the FCC-hh proper, also a High-Energy LHC (HE-LHC) is being explored, using the FCC-hh magnet technology in the existing LHC tunnel, which can yield a centre-of-mass energy around 25 TeV.

### MOTIVATION AND SCOPE

The Large Hadron Collider (LHC) [2] and its high-luminosity upgrade, the HL-LHC [3], have an exciting physics programme, which, covering the next 20 years, extends through the mid 2030s. Counting from the start of its design study in 1983, more than 30 years were needed to design, build and commission the LHC. Therefore, the community must now urgently start preparing the next accelerator for the post-LHC period, as it has clearly been recognized by the 2013 Update of the European Strategy for Particle Physics [4].

A large circular hadron collider seems to be the only approach to reach energy levels far beyond the range of the LHC, during the coming decades, so as to provide access to new particles with masses up to tens of TeV, through direct production, as well as to obtain tremendously increased production rates for phenomena in the sub-TeV mass range, with

the corresponding greatly improved precision and enhanced sensitivity to new physics.

The energy reach of a high-energy hadron collider is simply proportional to the dipole magnetic field and to the bending radius:  $E \propto B \times \rho$ . Assuming a dipole field of 16 T, achievable with Nb<sub>3</sub>Sn technology, the ring circumference must be about 100 km in order to reach the target value 100 TeV for the centre-of-mass energy.

Figure 1 presents a schematic of the FCC tunnel along with a sketch of the hadron collider layout. Prior to FCC-hh installation, the new 100 km tunnel could host a high-luminosity circular  $e^+e^-$  collider (FCC-ee). Concurrent operation of hadron and lepton colliders is not foreseen however. In addition, the FCC study considers aspects of  $pe$  collisions (FCC-he), as could be realized, e.g., by colliding the electron beam from an energy recovery linac (ERL) with one of the two FCC-hh hadron beams.

In the frame of the FCC study another future hadron collider is being studied, the so-called High Energy LHC (HE-LHC). The HE-LHC would be based on FCC-hh magnet technology, but be installed in the existing 26.7 km tunnel, which is presently housing the LHC.

Historically, investigations of an earlier version of the HE-LHC [5] gave birth to the FCC concept.

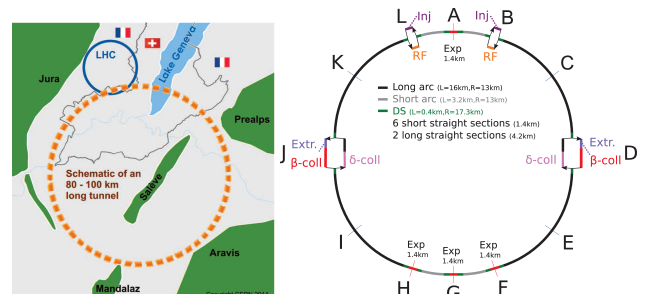


Figure 1: Left: Schematic of a 100 km tunnel for a Future Circular Collider (FCC) in the Lake Geneva basin. Right: Layout of the FCC-hh ring.

\* This work was supported in parts by the European Commission under the Capacities 7th Framework Programme project EuCARD-2, grant agreement 312453, and the HORIZON 2020 project EuroCirCol, grant agreement 654305, as well as by the German BMBF.

<sup>†</sup> frank.zimmermann@cern.ch

# STUDIES OF HIGH INTENSITY PROTON FFAGS AT RAL

C.R. Prior\*, STFC Rutherford Appleton Laboratory, Didcot, U.K.

## Abstract

The paper describes studies of high intensity proton accelerators for a next-generation source of short-pulse spallation neutrons. Along with conventional designs using rapid cycling synchrotrons, the long-term nature of the project provides scope for novel accelerator designs and developing technological ideas. A range of FFAG options is under consideration for the main spallation driver. Theory and simulation in the UK are combined with experimental studies of FFAGs in Japan, and a small prototype FFAG ring is planned to go on the FETS injector at the Rutherford Appleton Laboratory (RAL) for essential R&D. The paper covers the broad scope of the programme and details the success of the study to date.

## INTRODUCTION

After several years considering options to upgrade the aging ISIS spallation neutron source, there is renewed activity at RAL to explore options for a high intensity proton accelerator for next-generation neutron physics. Such a facility is being seen loosely as a successor to ISIS, which, despite its high productivity, is likely to have a limited life-span even with modest upgrades. Conventional designs using rapid cycling synchrotrons have been considered but, being long-term, the project provides opportunities for new proposals and an R&D programme based on developing technological ideas.

Existing spallation neutron sources generate a proton beam on target of up to  $\sim 1.5$  MW at an energy up to about 3 GeV. The facility with the highest mean beam power is SINQ at PSI [1], with a cyclotron operating in continuous wave mode. SNS at Oak Ridge [2] is based on a pulsed  $H^-$  linac filling an accumulator ring via charge exchange injection and routinely produces 1 MW. The neutron facility at J-PARC [3] also operates at the 1 MW level though, in contrast, the accelerating structures rely on a 400 MeV  $H^-$  linac and a 3 GeV rapid cycling synchrotron (RCS). The facility with the longest history of producing world-leading science is ISIS [4] at RAL with a total beam power of 160-180 kW. Users benefit from a wide range of instruments around two different neutron production targets. In a few years, ESS will come online as a major neutron source in Europe. As ESS is a long-pulse facility (with a linac driving a proton beam straight into a spallation target), ISIS's aim is to continue to be the main provider of experimental opportunities for short-pulse neutron studies. It can either be progressively upgraded - and this has been the object of studies in the past - or a completely new facility can be designed with a view to the long-term future.

\* chris.prior@trinity.ox.ac.uk

## ISIS PHASED UPGRADES

Several ideas for upgrading ISIS to the 1-5 MW level of beam power have been proposed in recent years. One is to replace the 70 MeV linac, which is the oldest part of the facility and already suffers from cavity breakdown and beam-loss, with a new linac operating at 180 MeV. Since tune shift depends on  $N/\beta^2\gamma^3$ , the higher energy would allow an increased number  $N$  of protons, provided practical issues such as a revised injection system can be accommodated in the ring. Another idea is to add a second RCS in series with the existing 800 MeV ring and increase the energy of the existing beam to around 3 GeV. The ring, shown in Fig. 1, would initially take the beam from ISIS by bucket-to-bucket transfer; however its design also allows for a completely new 800 MeV  $H^-$  linac to be installed at a later date, which would replace the present synchrotron. Such a system would use charge-exchange injection at 800 MeV, with phase-space painting to give a distribution that should be robust against intensity effects. Mean beam power at the target would be of the order of 2.5 MW with later upgrades to 5 MW. ISIS could continue to operate during the

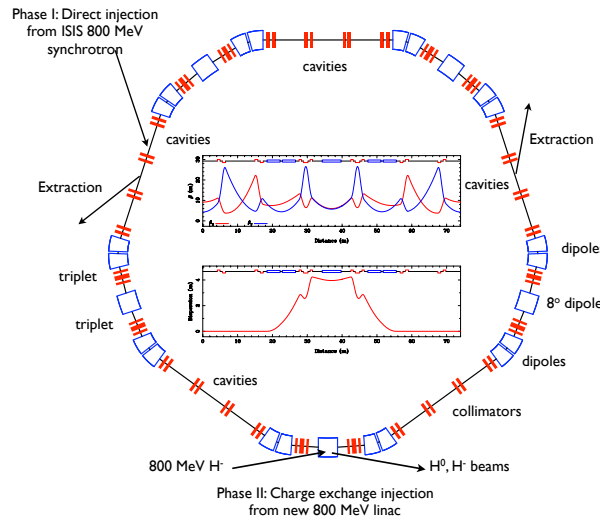


Figure 1: ISIS upgrade RCS showing lattice and optical parameters. Injection in the first phase would be directly from the present 800 MeV RCS, with a new system of  $H^-$  painting from a new linac in Phase II.

phased construction. Other options have also been considered, most notably an idea to build a second ring in the existing tunnel, but this would mean the neutron facility closing down for an extended period, so at this stage is not preferred.

A further aspect of the proton R&D programme at RAL is the development of a flexible high current  $H^-$  injector, known as FETS (Front-End Test Stand) [5]. This project has been important in covering novel ion source design, implementation of a 3-solenoid LEBT, design and construc-

# PERFORMANCE OF LINAC-4 INSTRUMENTATION DURING COMMISSIONING

U. Raich, CERN, Geneva, Switzerland

## Abstract

Linac-4 is CERN's new H<sup>-</sup> Linac, which will replace the aging Linac-2 proton machine. Linac-4 is being built and commissioned in stages. While the machine is permanently equipped with the standard beam instrumentation necessary to ensure smooth operation, three dedicated measurement benches have also been designed to commission the source and LEBT at 45 keV, the MEBT and its chopper at 3 MeV as well as the first DTL tank at 12 MeV and finally the full DTL at 50 MeV and CCDTL at 100 MeV. The beam after the PIMS structures at the Linac's full energy of 160 MeV will be sent to a beam dump and commissioned with permanently installed instruments. Installation and commissioning of the machine up to the CCDTL is now complete. This contribution will present the results from the various commissioning stages, showing the performance of the various diagnostic devices used and comparing the data obtained to simulations.

## ION SOURCE AND LEBT

Beam diagnostic devices measure the total beam current coming from the source with a Faraday Cup and a Beam Current Transformer (BCT) and the transverse beam distribution with a sandwich of horizontal and vertical wire grids.

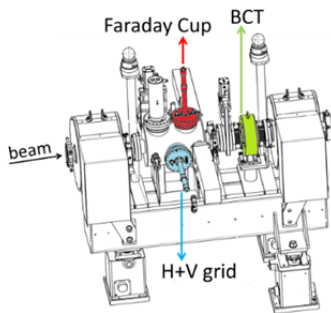


Figure 1: LEBT instrumentation.

As discussed below, the grid signal is dominated by the H<sup>-</sup> ion net charge deposition (negative) on the wires. Both the metallic wire frame and the wires themselves can be polarized in order to suppress secondary emission and repel low energy electrons emerging from the source.

The wire readout system allows signal sampling at 250 kHz such that the signals on the wires can be compared to the Faraday Cup signal.

As the 45 keV proton is stopped in the wire with a secondary emission yield estimated as ~ 3.5 charges per ion, a positive signal with the same overall shape as the negative Faraday Cup signal is expected. However, what was observed was the black trace in Figure 2.

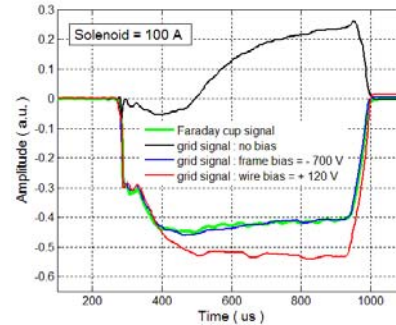


Figure 2: Comparison wire signal to Faraday Cup.

This can be understood as suppression of the secondary emission by strong space charge effects coming from the primary H<sup>-</sup> beam. When negatively polarizing the wire frame the secondary emission can be further suppressed such that the wire grid works only in charge collection mode and its wire signals (blue) are now negative, following the Faraday Cup signal (green). Polarizing the wires positively has the same effect but attracts additional background electron such that the signal is distorted (red).

In addition to the permanent instrumentation, the LEBT was temporarily equipped with a slit/grid emittance meter moved to various positions along the LEBT to verify the matching to the RFQ acceptance.

## THE MEBT OR CHOPPER LINE

The MEBT adapts the 3 MeV H<sup>-</sup> beam coming from the RFQ to the first cavity of the DTL Linac and implements a fast chopper to adapt the beam longitudinally for injection into the PS Booster. It contains two BCTs, which, in combination with the LEBT BCT, allows the transmission through the RFQ and chopper to be determined. It also contains two L-shaped wire scanners for transverse profile measurement [1].

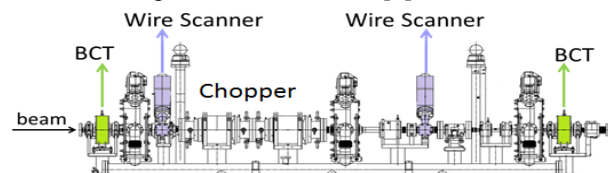


Figure 3: MEBT layout.

The correct functioning of the chopper was first verified with the vertical wire scanner observing the vertical beam deflection when the chopper is switched on, as shown in Figure. 4.

# HIGH POWER TARGET INSTRUMENTATION AT J-PARC FOR NEUTRON AND MUON SOURCES

Shin-ichiro Meigo\*, Motoki Ooi, Kiyomi Ikezaki, Tomoyuki Kawasaki, Hidetaka Kinoshita, Atsushi Akutsu, Masaaki Nisikawa and Shinpei Fukuta, J-PARC center, JAEA, 319-1195, Japan  
Hiroshi Fujimori, J-PARC center, KEK, 305-0801, Japan

## Abstract

Since 2008, the Japanese Spallation Neutron Source (JSNS) of J-PARC has produced a high-power proton beam of 300 kW. In order to operate with high intensity beam such as 1 MW, a reliable beam instruments are crucial. We developed profile monitor system by using SiC as sensor wires. Since pitting erosion was found at the vessel of the spallation neutron target at other facility of SNS, the beam current density at the target should be kept as low as possible. To decrease the beam current density at the target, a beam flattering system based on a non-linear optics with octupole magnets was developed. Beam profile at the target obtained with the Multi Wire Profile Monitor (MWPM) showed flat distribution and showed good agreement with the design calculation. Furthermore, the present status of the development of the beam instruments are also described.

## INTRODUCTION

In the Japan Proton Accelerator Research Complex (J-PARC) [1], a MW-class pulsed neutron source, the Japan Spallation Neutron Source (JSNS) [2], and the Muon Science facility (MUSE) [3] will be installed in the Materials and Life Science Experimental Facility (MLF) shown in Fig. 1. In 2015, we successfully ramped up beam power to 500 kW continuously<sup>1</sup> and delivered several shots of the 1-MW beam to the targets. To produce a neutron source, a 3 GeV proton beam collides with a mercury target, and to produce a muon source, the 3 GeV proton beam collides with a 2-cm-thick carbon graphite target. To efficiently use the proton beam for particle production, both targets are aligned in a cascade scheme, with the graphite target placed 33 m upstream of the neutron target. For both sources, the 3 GeV proton beam is delivered from a rapid cycling synchrotron (RCS) to the targets by the 3NBT (3 GeV RCS to Neutron facility Beam Transport) [4–6]. Before injection into the RCS, the proton beam is accelerated up to 0.4 GeV by a LINAC. The beam is accumulated in two short bunches and accelerated up to 3 GeV in the RCS. The extracted 3 GeV proton beam, with a 150 ns bunch width and a spacing of 600 ns, is transferred to the muon production target and the spallation neutron source.

Recently, pitting damage became evident in the mercury target container [7], and the extent of the damage is proportional to the fourth power of the peak current density of the proton beam. After operating the beam at high power, sig-

nificant pitting damage was observed at the spent mercury target vessel at JSNS and at the Spallation Neutron Source (SNS) in Oak Ridge National Laboratory [8, 9]. Using linear optics (i.e., quadrupole magnets) for beam transport, the peak current density can be reduced by expanding the beam at the target. However, beam expansion increases heat in the vicinity of the target, where shielding and the neutron reflector are located. Therefore, the peak current density is limited by the heat induced in the vicinity of the target. At the JSNS, the minimum peak current density is expected to be  $9 \mu\text{A}/\text{cm}^2$ , which gives a thermal energy density at the target of  $14 \text{ J}/\text{cm}^3/\text{pulse}$  [10]. Because the pitting damage goes as the fourth power of the peak density, scanning the beam with a deflecting magnetic field will not mitigate the pitting damage.

Beam profile monitoring plays an important role in comprehending the damage to the target. Therefore it is very important to watch continuously the status of the beam at the target at the JSNS especially for the peak current density. We have developed a reliable beam profile monitor for the target by using Multi Wire Profile Monitor (MWPM). In order to watch the two dimensional profile on the target, we have also developed the profile monitor based on the imaging of radiation of the target vessel after beam irradiation. In this paper, the present status of the beam monitor at the spallation neutron source is described.

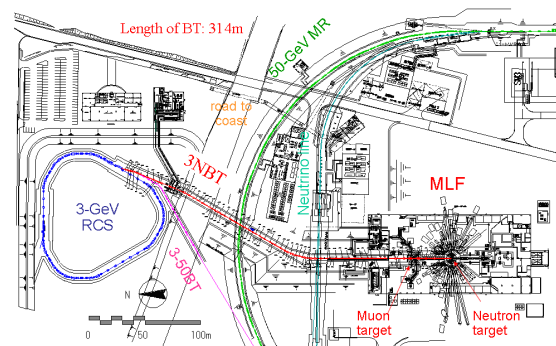


Figure 1: Plan of rapid cycling synchrotron (RCS) at the Materials and Life Science Experimental Facility (MLF) at J-PARC.

## BEAM MONITOR SYSTEM AT THE BEAM TRANSPORT TO THE TARGET

### Silicon Carbide Sensor Wire

In order to obtain the characteristics of the proton beam, diagnostic system based on a Multi Wire Profile Monitor

\* meigo.shinichiro@jaea.go.jp

<sup>1</sup> Recently the power is restricted to 200 kW due to no spare mercury target remaining since February 2016.

# THE APPLICATION OF THE OPTIMIZATION ALGORITHM IN THE COLLIMATION SYSTEM FOR CSNS/RCS

Hongfei Ji<sup>#</sup>, Sheng Wang, Mingyang Huang, Shouyan Xu  
 CSNS/IHEP, CAS, Dongguan, 523803, P.R. China  
 Yi Jiao, Na Wang, IHEP, CAS, Beijing 100049, P.R. China

## Abstract

The robust conjugate direction search (RCDS) method, which is developed by X. Huang from the SLAC National Accelerator Laboratory, has high tolerance against noise in beam experiments and thus can find an optimal solution effectively and efficiently. In this paper, the RCDS method is used to optimize the beam collimation system for Rapid Cycling Synchrotron (RCS) of the China Spallation Neutron Source (CSNS). A two-stage beam collimation system was designed to localize the beam loss in the collimation section in the RCS. The parameters of secondary collimators are optimized with RCDS algorithm based on detailed tracking with the ORBIT program for a better performance of the collimation system. The study presents a way to quickly find an optimal parameter combination of the secondary collimators for a machine model for preparation for CSNS/RCS commissioning.

## INTRODUCTION

The China Spallation Neutron Source (CSNS) is designed to provide a proton beam with beam power of 100 kW [1, 2]. The accelerator complex consists of an 80 MeV Linac and a 1.6 GeV Rapid Cycling Synchrotron (RCS) [3, 4]. In the RCS, the proton beam is accumulated through an anti-correlated painting scheme within 200 turns, and accelerated to 1.6 GeV in about 20000 turns [5, 6].

For the RCS, the space charge forces are strong and have a large impact on beam dynamics. The emittance growth and halo generation induced by space charge could lead to unacceptably high beam loss [7, 8]. Considering the requirements for hands-on and safe maintenance of the machine, the average particle loss should be controlled to a low level of 1 W/m [9]. To meet this requirement, a two-stage collimation system was designed to localize the beam loss in the collimation section in the RCS [10, 11].

The transverse collimation system consists of one primary collimator and four secondary collimators. The layout of the transverse collimation system and the optical parameters are shown in Fig. 1.

In the RCS, the aperture of each secondary collimator can be varied by adjusting the positions of four movable blocks. Now the RCS is under construction, and the collimation efficiency with different sets of collimator

parameters is evaluated with numerical simulation in this study. The collimation process in the presence of space charge is simulated with the Objective Ring Beam Injection and Tracking (ORBIT) code [12, 13]. Moreover, we introduce an algorithm, the Robust Conjugated Direction Search (RCDS) method, in the optimization. This method is effective in optimizing a multi-variable objective online and it has both high tolerance to noise and high convergence speed [14]. It has been used for online optimization of machine performance when the objective function can be measured [14-16].

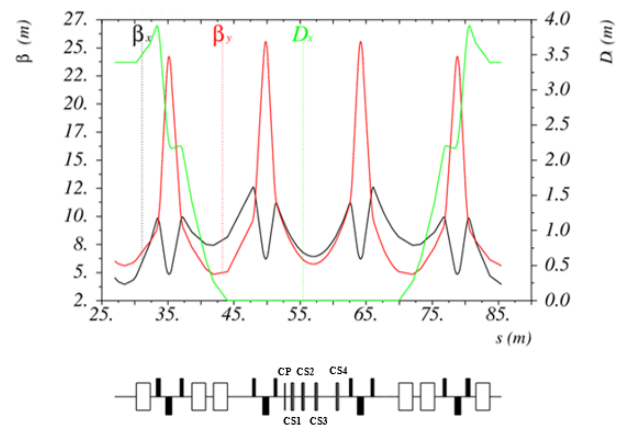


Figure 1: Optical functions along a ring super period of the RCS, and the layout of the transverse collimation system. CP represents the primary collimator. CS1, CS2, CS3 and CS4 represent four secondary collimators in sequence, respectively).

## PHYSICS ANALYSIS AND MODELING

To implement the application of the RCDS method in the optimization of the RCS collimation system, the model of an ORBIT instance to simulate the collimation process were determined.

### Physical Variables

In this study, the acceptance of the primary collimator is fixed to  $350 \pi \text{mm}\cdot\text{mrad}$  all the time, and the secondary collimators are tuned to optimize the performance of the collimation system.

The structure of a secondary collimator is shown in Fig. 2. Each of the secondary collimators is composed of four movable copper blocks with thickness of 200 mm. Two of the blocks are in the vertical direction and the other two, downstream of the vertical blocks, are in the

<sup>#</sup> jihf@ihep.ac.cn

# COLLIMATION DESIGN AND BEAM LOSS DETECTION AT FRIB\*

Z. Liu<sup>†</sup>, F. Marti, S. Lidia, S. Cogan, M. Ikegami, FRIB, East Lansing, Michigan, USA  
 T. Maruta, J-PARC/JAEA, Ibaraki, Japan  
 V. Chetvertkova, GSI, Darmstadt, Germany

## Abstract

As a multi-charge-state, heavy-ion, superconducting accelerator with a folded geometry, FRIB faces unique beam loss detection and collimation challenges to protect superconducting cavities from beam-induced damage. Collimation is especially important in the Folding Segment 1 where the multiple charge states are created by a charge stripper and selected by a charge selector. The transported ECR contaminants, interaction with the residual gas, and beam halo due to stripping could induced significant beam losses in this region. We have simulated the potential beam losses and planned collimation accordingly. A layered loss detection network is also specifically designed to visualize potential blind zones and to meet the stringent requirements on loss detection. The related sub-systems are designed and procured and are introduced in this paper.

## INTRODUCTION

As a superconducting heavy-ion accelerator, FRIB's folded structure adds additional difficulties to the machine protection and loss monitoring [1]. Among these difficulties, Folding Segment 1 (FS1) and low energy linac segment are two special regions:

Due to the charge stripper and charge selector in FS1, there are several additional beam loss sources, such as the ECR contaminants that are separated from primary beam after charge stripper, beam halo created by stripping, and

charge exchange with residual gas due to the higher pressure around charge selector. These losses require additional collimation planning in FS1.

Radiation cross talk from high energy linac segments and cavity X-ray background make small loss detection especially challenging in the low energy linac segments [1]. We have designed a bunch of loss detectors to compose a multiple layer beam loss monitoring network. Feasibility study has been carried out for each loss detector and DAQ scheme is designed according to detector sensitivity and MPS requirement respectively.

This paper introduces the collimation system design in FRIB FS1 and detectors in the beam loss monitoring network. The DAQ cards and data acquisition scheme is also introduced.

## COLLIMATION AT FRIB FS1

In FS1, the charge stripper and charge selector create five charge states from two, e.g. from  $U^{33+ \sim 34+}$  to  $U^{76+ \sim 80+}$ . The five charge states is then transported to Linac Segment 2 (LS2). Figure 1 shows the mechanical drawing of FS1 lattice, on which charge stripper and charge selector are pointed out.

Besides the large intentional beam losses of those charge states that are collimated by charge selector, there are several other potentially significant losses that may need to be collimated.

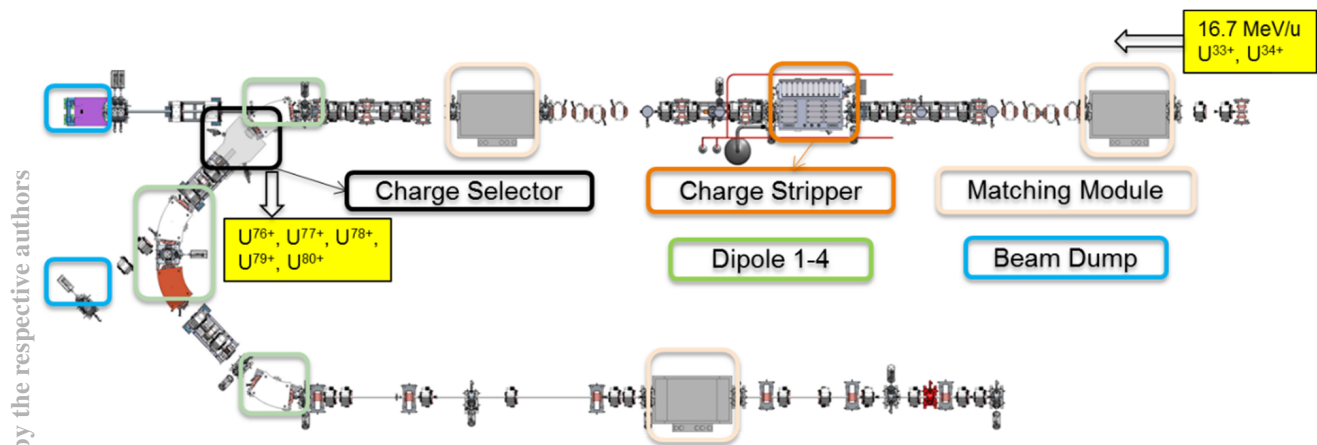


Figure 1: Mechanical drawing of FRIB FS1 lattice.  $U^{33+ \sim 34+}$  becomes  $U^{76+ \sim 80+}$  after charge selector.

## Collimation for ECR Contaminants

The most common contaminants are carbon, nitrogen and oxygen that are coming from outgassing of the ECR plasma chamber wall or hardware introduced by a specific run such as an oven. FRIB's high intensity requirement

\* This material is based upon work supported by the U.S. Department of Energy Office of Science under Cooperative Agreement DE-SC0000661.

<sup>†</sup> liuz@frib.msu.edu

# A COUPLED RFQ-IH-DTL CAVITY FOR FRANZ: A CHALLENGE FOR RF TECHNOLOGY AND BEAM DYNAMICS

R. Tiede, M. Heilmann\*, D. Mäder†, O. Meusel, H. Podlech, U. Ratzinger, A. Schempp,  
M. Schwarz, IAP, Goethe-University Frankfurt, Germany

## Abstract

For the ‘Frankfurt Neutron Source at the Stern-Gerlach-Zentrum’ (FRANZ) facility an inductively coupled combination of a 4-Rod-type Radio-Frequency-Quadrupole (4-Rod-RFQ) and an 8 gap interdigital H-type (IH-DTL) structure will provide the main acceleration of an intense proton beam from 120 keV to 2.0 MeV. The RFQ-IH combination with a total length of about 2.3 m will be operated at 175 MHz in cw mode. The expected total power need is around 200 kW. Due to the internal inductive coupling only one RF amplifier is needed, which significantly reduces the investment costs. At present the RFQ is installed separately in the beam line for conditioning up to the design rf power and for measuring the beam quality behind the RFQ. In parallel, the IH-DTL is rf tuned together with a dummy RFQ outside the FRANZ cave. This paper will present the status of the project with emphasis on key questions like beam dynamics constraints, rf tuning issues and technological challenges resulting from the high thermal load in cw operation.

## INTRODUCTION

At the FRANZ facility on the campus of the Frankfurt University physics faculty, a 2 MeV proton primary beam will produce 1 – 200 keV neutrons by the  ${}^7\text{Li}(p,n){}^7\text{Be}$  reaction with a maximum neutron yield at 30 keV. For such lower neutron energies, the FRANZ facility will provide intensities by two to three orders of magnitude larger than from existing accel. driven intense neutron sources [1].

The facility will mainly serve to nuclear astrophysics experiments [2], namely:

- Measurement of the differential neutron capture cross sections  $d\sigma/dE$ , with relevance to the stellar nucleosynthesis (slow neutron capture process). For this purpose, time-of-flight (TOF) measurements are needed and the FRANZ facility has to deliver 1 ns short proton bunches with a repetition rate of 250 kHz. In the so called “compressor mode” it is aimed to produce a neutron flux of  $1 \cdot 10^7$  /cm<sup>2</sup>/s at the sample.
- Measurement of integrated neutron capture cross sections. In the so called “activation mode” the facility is designed to produce  $10^{11}$  n/cm<sup>2</sup>/s in cw operation.

In order to fulfil these ambitious specifications, an intense primary proton beam of several mA (for the activation mode) and up to 140 mA (for the compressor mode) must be accelerated to 2.1 MeV with an energy variation of  $\pm 0.2$  MeV. In the first operation phase of FRANZ, the maximum proton beam current will be limited to 50 mA.

However, the in house developed filament driven source already delivered a 200 mA d. c. proton beam. The time structure needed for the TOF measurements will be applied by a chopper array integrated to the LEBT section, which will form macro pulses with a flat top of 50 ns and 250 kHz repetition rate. Behind the main linac, a Mobley type “bunch compressor” will merge 9 consecutive micro bunches as delivered by the linac and bunch the proton beam to the final length at target of around 1.1 ns.

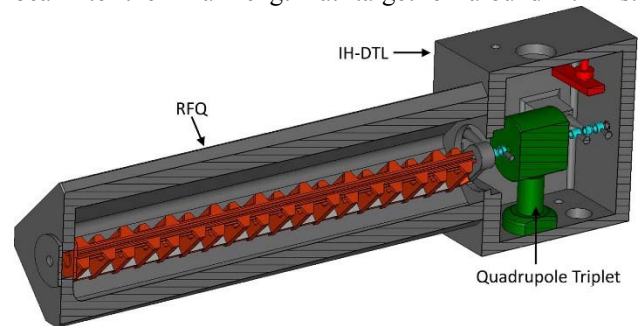


Figure 1: Coupled RFQ-IH-DTL cavity.

Table 1: Parameters of the Coupled Cavity

| Parameter                       | Value               |           |
|---------------------------------|---------------------|-----------|
| f [MHz]                         | 175                 |           |
| I [mA]                          | 50 (140)            |           |
| coupling factor k               | 0.004               |           |
|                                 | 4-Rod-RFQ           | IH-DTL    |
| energy range [MeV]              | 0.12 – 0.7          | 0.7 – 2.0 |
| total length [m]                | 1.7                 | 0.6       |
| rf losses [kW]                  | 95 (140)            | 60 (60)   |
| <b>4-Rod-RFQ</b>                |                     |           |
| electrode volt. [kV]            | 62 (75)             |           |
| R <sub>p</sub> [kΩm]            | 70                  |           |
| no. of stems                    | 18                  |           |
| <b>IH-DTL</b>                   |                     |           |
| eff. gap volt. [kV]             | 80 – 350 (80 - 350) |           |
| R <sub>shunt,eff</sub> [MΩ / m] | 62                  |           |
| no. of gaps                     | 8                   |           |

This paper focuses on the discussion of all points of interest related to the main accelerator component, an inductively coupled 4-Rod-RFQ & IH-DTL combination (see Figure 1): from beam dynamics to rf tuning aspects and right up to mechanical design challenges due to the high thermal load on the cavities at cw operation.

\* GSI Helmholtzzentrum, Darmstadt, Germany

† BEVATECH, Frankfurt, Germany

# OVERVIEW OF THE CSNS LINAC LLRF AND OPERATIONAL EXPERIENCES DURING BEAM COMMISSIONING

Zhencheng Mu<sup>†</sup>, Jian Li, Xin An Xu, Zonghua Zhang, Lin Yan Rong, Zhe Xin Xie, Wenzhong Zhou, Mei Fei Liu, Ma Liang Wan, Bo Wang, Yuan Yao, Chinese Spallation Neutron Source (CSNS), Dongguan, China

## Abstract

The CSNS proton linear accelerator (Linac) will deliver 81MeV proton beam to RCS ring. The Linac is comprised of H<sup>-</sup> ion source, RFQ, two Buncher cavities (MEBT), four DTL accelerators and one Debuncher cavity (LRBT). The RFQ accelerator is powered by two 4616 tetrodes, the maximum output power of each tube is 350kW. Three 25kW solid state amplifiers supply RF power to two Buncher cavities and one Debuncher cavity, respectively. The RF power sources of four DTL accelerators are four 3MW klystrons. Each RF power source owns a set of digital LLRF control system in order to realize an accelerating field stability of  $\pm 1\%$  in amplitude and  $\pm 1^\circ$  in phase. The front four LLRF control systems have been used in the beam commissioning of CSNS Linac in the end of 2015. This paper will introduce the design and the performance of the digital LLRF control system.

## INTRODUCTION

In the CSNS 81MeV proton linear accelerator (Linac), the RF power sources consist of two 350kW 4616 tetrodes, three 25kW solid state amplifiers, five 3MW klystrons (including spare one). Now, the 4616 tetrodes, two solid state amplifiers and the first Klystron power source have already supplied RF power to the corresponding accelerating cavities for the ageing process and beam commissioning. The installation and test of the rest three klystron power sources are still in process. The block diagram of the Linac RF system is shown in Figure 1 [1].

The RF field are controlled by eight almost the same digital LLRF controllers which are installed in cabinets. The prototype of the digital LLRF control system was developed in the 352MHz RFQ of IHEP, the design team have gathered much experiences from the operating process of the prototype. Based on the good design experiences of the prototype, the improvement and commissioning of the eight on-line LLRF hardwares are completed quickly, software algorithms are also completed with some elaborate improvements on time.

As shown in Figure 2, each LLRF control system consists of the 324MHz RF reference line, analog module (AM) and clock distribution module (CDM), digital control module (DCM) and the high power protection module (HPM). Because the AM and CDM are absolutely analog components, most analog components are susceptible to ambient temperature, so we put these two modules into a temperature stabilizing chamber. The DCM is mainly responsible for the stability of the RF field amplitude and phase, HPM can quickly cut off the RF drive in case of arc in the RF distribution system, VSWR over threshold or cavity vacuum fault, and so on. The field control algorithms and high power protection logics are designed through digital signal processing in FPGA and DSP. Various control parameters can be set from IPC human-computer interface through embedded Ethernet communication. The block diagram of the digital LLRF control system is showed in Figure 2.

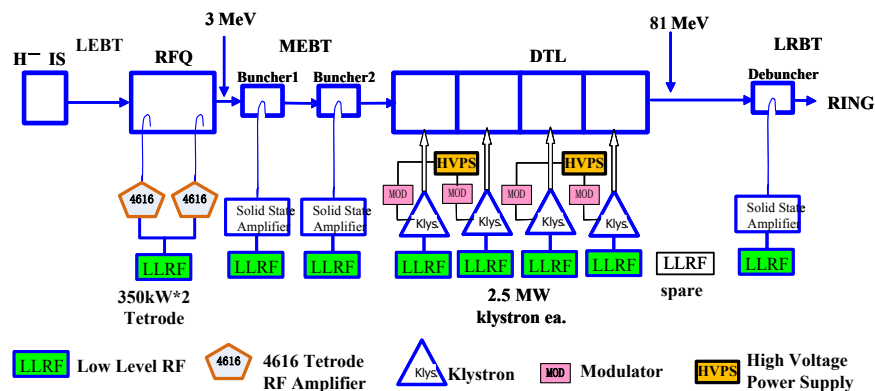


Figure. 1: Block diagram of the CSNS Linac RF system.

<sup>†</sup> muzc@ihep.ac.cn

# PRESENT STATUS OF THE HIGH CURRENT LINAC AT TSINGHUA UNIVERSITY AND ITS APPLICATION\*

Q.Z. Xing, S.X. Zheng, X.L. Guan, C. Cheng, T.B. Du, H.Y. Zhang, L. Du, R. Tang, L. Wu, H.P. Jiang, Q.Z. Zhang, C.T. Du, Q.K. Guo, D. Wang, C.X. Tang, X.W. Wang<sup>†</sup>, Key Laboratory of Particle & Radiation Imaging (Tsinghua University), Ministry of Education, Beijing 100084, China also at Laboratory for Advanced Radiation Sources and Application, Tsinghua University, Beijing 100084, China

also at Department of Engineering Physics, Tsinghua University, Beijing 100084, China  
W.Q. Guan, Y. He, J. Li, NUCTECH Co. Ltd., Beijing 100084, China

## Abstract

The CPHS (Compact Pulsed Hadron Source) linac at Tsinghua University, is now in operation as an achievement of its mid-term objective. Presently the RFQ accelerator is operated stably with the beam energy of 3 MeV, peak current of 26 mA, pulse length of 100  $\mu$ s and repetition rate of 20 Hz. After the maintenance the transmission rate of the RFQ accelerator had been recovered from 65% to 91%. The applications of the proton and neutron beams are introduced in this paper.

## INTRODUCTION

Since the first 3 MeV/44 mA proton beam of the CPHS (Compact Pulsed Hadron Source) linac at Tsinghua University was achieved in March 2013, the proton beam has been delivered to bombard the Beryllium target to produce neutrons for various applications [1][2]. The whole linac contains the ECR Ion Source (IS), the 4-vane Radio Frequency Quadrupole (RFQ) proton accelerator (shown in Fig. 1), RF power supply and distributor, and beam transport. In the first half year of 2017 the Drift Tube Linac (DTL) is expected to be installed downstream the RFQ accelerator to upgrade the beam energy to the designed value of 13 MeV.



Figure 1: 3MeV RFQ accelerator at Tsinghua University.

Based on the proton and neutron beams, various applications mainly includes the development of the neutron detectors ( $B_4C$ -coated straw-tube and gadolinium-doped

Micro-Channel Plate (MCP)) and biological dosimeters, and neutron imaging. Furthermore, a proton irradiation station is being planned to provide the 13 MeV proton beam with a flux of  $10^8$ ~ $10^9$  p/cm<sup>2</sup>/s for the experimental simulation of the space radiation environment.

## OPERATION STATUS OF THE HIGH CURRENT 3MeV PROTON LINAC

The operation time of the CPHS facility in 2016 was ~300 hrs. The present main parameters together with the designed values of the proton beam are listed in Table 1. The RFQ accelerator is operated stably with the beam energy of 3 MeV, peak current of 26 mA, pulse length of 100  $\mu$ s and repetition rate of 20 Hz. The peak current is measured near the outside surface of the target station. The current of the proton beam at the entrance of the RFQ has decreased from 60 mA (year 2013) to 44 mA (year 2016).

Table 1: Main Parameters of the Proton Beam Passing into the Target Station

| Parameter                   | Designed Value | Present Value |
|-----------------------------|----------------|---------------|
| Beam Energy (MeV)           | 13             | 3             |
| Peak Current (mA)           | 50             | 26            |
| Beam Pulse Width ( $\mu$ s) | 500            | 100           |
| Repetition Rate (Hz)        | 50             | 20            |

Neutrons are produced by proton beam bombarding the 1.2 mm-thick Beryllium target. The Be target has been re-designed to be mounted on a 2 mm-thick aluminium plate since it had broken twice after only several-hour operation on the repetition rate of 50 Hz. The possible reason of the crack was evaluated to be the thermal stress under high repetition rate. The new target with Al plate mounted had worked well in 2014 with the repetition rate of 20 Hz. Increasing the repetition rate to 50 Hz to test the new target with the proton beam will be carried out in the future.

## MAINTENANCE AND UPGRADE OF THE 3MeV LINAC

The maintenance and upgrade of the CPHS linac are carried out as the following, among which the first five has been accomplished:

\* Work supported by National Natural Science Foundation of China (Project 11575098).

<sup>†</sup> wangxuewu@tsinghua.edu.cn

## DESIGN AND PROTOTYPING OF THE SPOKE CRYMODULE FOR ESS

P. Duthil<sup>†</sup>, D. Reynet, G. Olry, S. Braut, P. Duchesne, N. Gandolfo, E. Rampnoux, D. Longuevergne, M. Pierens, F. Chatelet, S. Bousson, Institut de Physique Nucléaire d'Orsay, UMR 8608 CNRS/IN2P3 – Univ. Paris Sud, BP1, 91406 Orsay- France  
C. Darve, N. Ellas, European Spallation Source, Lund, Sweden

### Abstract

A cryomodule integrating two superconducting radiofrequency double Spoke cavities and their power couplers is now being assembled at IPNO. It is the prototype version for the Spoke section which will be operated for the first time in a linear accelerator for the European Spallation Source. It will be the most powerful neutron source feeding multidisciplinary researches. This cryomodule provides the environment for operating the two  $\beta = 0.5$  cavities at full RF power in a saturated superfluid helium bath at a temperature of 2 K. For this operation, the prototype cryomodule includes all the interfaces with radiofrequency powering, cryogenics, vacuum systems, beam pipe and diagnostics. It will be tested by 2016 at IPNO by use of a test valve box which is also a prototype for the future cryogenic distribution system of the Spoke section, another contribution to ESS. Both prototypes will then be tested at full power in FREIA facilities at Uppsala University.

### THE EUROPEAN SPALLATION SOURCE

#### The ESS Linac

The European Spallation Source (ESS) [1] is now designed to be the most powerful neutron source dedicated to multidisciplinary researches. It is an intergovernmental research project, carried out by 17 European countries, which started to be built in 2014 in Lund, Sweden, and will be fully operational by 2025.

The ESS machine is based on a linear particles accelerator (linac) placed in a tunnel and which accelerates protons from a source to a tungsten target located on the ground surface. From the collisions of the protons onto this target, fast neutrons are produced and then moderated before feeding multiple physics experiment lines.

The ESS linac operates in a pulsed mode with a pulse duration of 2.86 ms and a repetition frequency of 14 Hz. It shall accelerate protons up to an energy of 2 GeV to produce a 5 MW beam with a peak current of 62.5 mA. For that purpose, it benefits from a 312 m long section integrating superconducting radiofrequency (SRF) accelerating cavities. Electromagnetic waves are produced by klystrons and distributed into the tunnel along a network of waveguides to the RF power couplers which radiate this wave into each cavity. The cavity then acts as an electromagnetic resonator and produces an accelerating electrostatic field phased in time with the protons bunches traveling within the high vacuum of the beam pipe. All SRF cavities are

made of bulk niobium and are operated in a superfluid helium bath at a temperature of about 2 K. This cryogenic environment is ensured by a surrounded dedicated horizontal cryostat, named cryomodule, and which also combines other functionalities and interfaces to run the cavities and transport the beam: magnetic shielding, support and alignment, RF powering, vacuum systems and beam interfaces.

Ordered by proton energy or by the ratio  $\beta$  of the speed of a particle (within the accelerating device) to the speed of light, this SRF linac section includes:

- 26 double Spoke type cavities with  $\beta = 0.50$  and paired in 13 cryomodules;
- 36 elliptical 6-cell type cavities with  $\beta = 0.67$  and grouped by 4 within 9 cryomodules;
- 84 elliptical 5-cell type cavities with  $\beta = 0.86$  and grouped by 4 within 21 cryomodules.

A cryogenic distribution system (CDS) runs all along the ESS linac tunnel to distribute or transform the needed cryofluids – helium at different thermodynamic states – produced by the cryoplant located at one end of the ESS machine. Consisting in a multichannel cryoline, this CDS also integrates 43 valve boxes aiming at managing the cryogenic distribution process of each cryomodule.

#### The Spoke Section

Between the Drifted Tube Linac (DTL) – which ends the warm section of the ESS linac – and the medium beta (elliptical cavities) linac (MBL), a 56 m long portion with 26 double Spoke SRF cavities shall increase the protons beam energy from 90 to 216 MeV. The Institut de Physique Nucléaire d'Orsay (IPNO) is responsible for the supply of most of this Spoke section pictured on Fig. 1: the 13 cryomodules and the cryodistribution system containing 13 valve boxes.

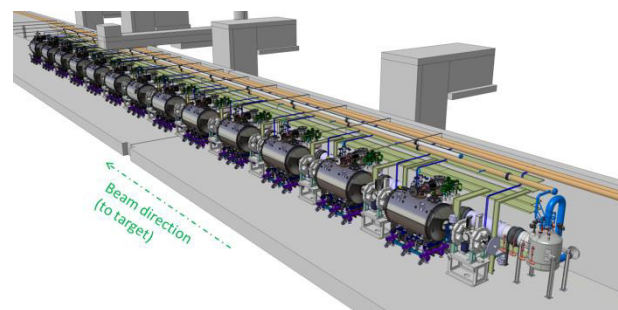


Figure 1: Spoke section of the ESS linac.

IPNO is also in charge of prototyping this section by designing, constructing one prototype cryomodule and one prototype valve box and testing them at IPNO. This valve box is also part of the facilities which will be

<sup>†</sup> duthil@ipno.in2p3.fr

# ANALYZING AND MATCHING STUDY OF MIXED HIGH INTENSITY HIGHLY CHARGED ION BEAMS\*

X.H. Zhang, Y.J. Yuan<sup>#</sup>, X.J. Yin, Y. Yang, L.T. Sun, H.W. Zhao, C.Qian  
Institute of Modern Physics, CAS

## Abstract

Electron cyclotron resonance (ECR) ion sources are widely used in heavy ion accelerators for their advantages in producing high quality intense beams of highly charged ions. However, it exists challenges in the design of the Q/A selection systems for mixed high intensity ion beams to reach sufficient Q/A resolution while controlling the beam emittance growth. Moreover, as the emittance of beam from ECR ion sources is coupled, the matching of phase space to post accelerator, for a wide range of ion beam species with different intensities, should be carefully studied. In this paper, the simulation and experimental results of the Q/A selection system at the LECR4 platform are shown. The formation of hollow cross section heavy ion beam at the end of the Q/A selector is revealed. A reasonable interpretation has been proposed, a modified design of the Q/A selection system has been committed for HIRFL-SSC linac injector. The features of the new design including beam simulations and experiment results are also presented.

## INTRODUCTION

The advances in electron cyclotron resonance (ECR) ion sources that are being achieved by producing high current beams of highly charged ions have made the design of the associated charge to mass ratio Q/A selection system more challenging. In the future, the total ion beam current extracted from an ECR ion source could reach several 10 mA. Serious space charge effect will reduce the resolution of the Q/A selector by increasing the beam size in the slit position and degrading the beam quality. Moreover, the coupled asymmetric beam extracted from the sextupole magnet field used to confine ECR plasma makes the analyzing more complicated. When the beam transmits through a Q/A selector line, the effects of aberrations and coupling in magnetic elements will be obvious, which will also deteriorate the beam quality and reduce the resolution of the system.

The Q/A selection system of LECR4 is designed taking account of all kinds of ion beams produced by the ion source, i.e. from proton to uranium ion beam. However, commissioning results [1] show that the beam quality of high intensity heavy ion beams is rather poor. Studies [2] have been carried out to investigate the possible causes. This study is focusing on the space charge effect on the Q/A selection system. Recent simulations and experimental results at the LECR4 platform are reported

and discussed in this paper. The research on LECR4 has provided basis for the design of a new Q/A selection system for LECR4. The features of the new design including beam experiments are also presented in this paper.

## EXPERIMENTS AND SIMULATIONS AT LECR4

### Experimental Setup

LECR4[3] is an ECR ion source to provide ion beams from Carbon to Uranium for HIRFL-SSC linac injector[4,5]. It uses unique liquid evaporation cooling method at room temperature coils to reach maximum 2.5 T magnetic field.

Fig. 1 shows the original layout of the Q/A selection system of LECR4. It mainly consists of a solenoid lens, a double focusing 90° analyzing magnet, two slits mounted for both the horizontal and the vertical directions, and beam diagnostic devices in a diagnostic chamber, including a faraday cup, a fluorescent target, and an Allison type emittance measurement device. The solenoid lens is directly attached to the extraction flange of the source body to provide an initial focusing and control the size of the beam into the analyzing magnet. Furthermore, the solenoid takes on the responsibility of the tuning flexibility of the system to deal with all kinds of ion species produced by the ion source.

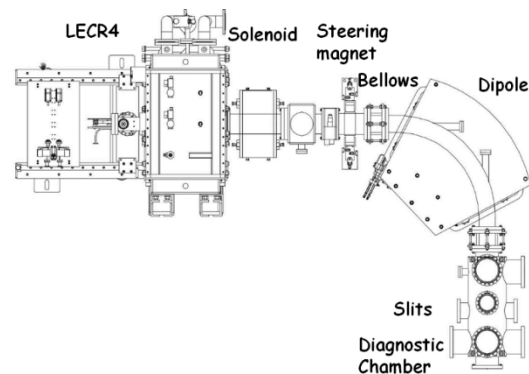


Figure 1: Layout of the multi-component A/Q selection system for LECR4.

### LECR4 Beam Emittance

In the original beam line design, nonlinear forces, such as space charge effect and aberrations in magnets [6], were not fully taken into account, resulting in bad transmissions for high current ion beams. Recent simulation results show that the second-order aberration

\*Work supported by the National Natural Science Foundation of China (No. 11575265, 11427904) and the "973" Program of China (No. 2014CB845501).

<sup>#</sup>yuanyj@impcas.ac.cn

# THE BEAM DELIVERY SYSTEM OF THE EUROPEAN SPALLATION SOURCE\*

H.D. Thomsen<sup>†</sup>, S.P. Møller, Dept. of Physics and Astronomy, Aarhus University, Aarhus, Denmark

## Abstract

The European Spallation Source (ESS) will apply a fast beam scanning system to redistribute the proton beam transversely across the spallation target surface. The system operates at sweep frequencies of tens of kHz and efficiently evens out the time-averaged beam intensity within a nominal beam footprint, thus reducing the level of beam-induced material damage. A modular design approach divides the raster action in each direction across 4 independent magnet-supply systems to distribute the magnetic load, ease the peak output power per modulator, and in general reduce the impact of single point of failures (SPOFs). The state of the magnet design and power supply topology will be discussed.

## INTRODUCTION

Several present and future accelerator projects at the intensity frontier feature an accelerator (linac or cyclotron) that delivers a MW-class beam to a fixed target for *e.g.* secondary beam production or reactors. Common to all such projects is the importance of the accelerator–target interface, where many challenges and compromises are to be dealt with, and the Accelerator-to-Target (A2T) section of the ESS is no exception. To be able to sustain the considerable beam power, the beam is here expanded to a substantial size to minimize the local power deposition and radiation-induced material degradation across the target shroud and accelerator vacuum windows, if relevant. The replacement frequency of such components and the capacity of their associated cooling systems can be reduced even more by applying schemes to produce transverse beam current profiles that are close to uniform with an extent that matches the edges of beam confinement regions, beyond which only fractions of beam are tolerated. These sophisticated Beam Delivery Systems (BDSs) include both a linear expansion (relying on magnetic quadrupoles) and a system to intentionally distort the time-averaged beam profiles by applying *e.g.* non-linear or AC dithering fields. Several facilities have considered such systems, as will be discussed. Given the considerable beam currents often involved, excessive uncontrolled primary beam losses may ensue, if these systems are not properly designed or the incoming beam is significantly different from the assumptions made in the design phase.

### Non-Linear Magnets

To flatten high-power ion beams using a system of non-linear magnetic lenses has long been studied [1], [2], [3], [4], [5], [6] and even applied at *e.g.* the NASA Space Radiation Laboratory, BNL [7], [8]. The scheme will be applied to

existing (J-PARC [9]) and future facilities (CSNS, C-ADS, IFMIF [10]). The systems include either pure multipole elements ( $O(2n)$  pole elements with  $n \geq 3$ , *i.e.* sextupoles, octupoles, *etc.*) or rely on more specialized combined function magnets, *e.g.* the so-called dipole pairs [1] or step-like field magnets [4] which are based on relatively similar magnet topologies. Considering *e.g.* a horizontally Gaussian beam profile with an elliptical phase space distribution  $(x, x')$ , a properly applied octupole magnetic field ( $B_y(x, y) \propto x^3$ ) will introduce a symmetric horizontal focusing force affecting in particular the beam tails, causing a characteristic S-shape in the phase space. Although the solution can provide close to uniform distributions by applying DC fields, there are several caveats.

**Overfocusing:** Unless compensated, the strong non-linear forces can severely overfocus halo particles, which may lead to excessive losses before the beam reaches its intended destination. Saturating the field strengths at large excursions, either by combined-function magnet design or introducing *e.g.* dodecapoles, can compensate for this [1].

**Lack of flexibility:** Non-linear magnets are usually designed with a narrow band of not only beam RMS sizes in mind, but also kurtosises, *i.e.* beam quality, something that can be very difficult to predict before the accelerator is constructed and commissioned. Combined-function magnets offering several degrees of freedom [11] can perhaps efficiently cover a span of kurtosises.

**Beam-magnet alignment:** In particular the pure non-linear magnets are very sensitive to beam-magnet displacement, giving rise to steering errors and beam profile artefacts, *e.g.* the characteristic “ears” near the profile edges, in case of octupoles [1].

**Aperture vs. field:** Designing the non-linear magnets also involves the trade-off between having a sufficient impact on the beam, while retaining sufficiently large apertures to avoid beam losses. This balance becomes increasingly difficult with an intense, rigid beam.

**Coupling:** To enable flattening of both the horizontal (H) and vertical (V) profile, dedicated H and V non-linear lenses should be applied at locations where the beam RMS size aspect ratio is large, ( $\sigma_x/\sigma_y \gg 1$  in the H multipole and vice versa) to avoid H–V coupling. The scheme thus requires magnetic elements between the two non-linear elements. Depending on the beam emittance and tuning accuracy, the beam waists cannot provide complete H–V decoupling, thus rendering tuning complicated.

\* Work supported by European Spallation Source ERIC

<sup>†</sup> heinetho@phys.au.dk

# EMITTANCE RECONSTRUCTION TECHNIQUES IN PRESENCE OF SPACE CHARGE APPLIED DURING THE LINAC4 BEAM COMMISSIONING

V. A. Dimov, J.B. Lallement, A. M. Lombardi, CERN, Geneva, Switzerland  
R. Gaur, RRCAT, Indore, India

## Abstract

The classical emittance reconstruction technique, based on analytic calculations using transfer matrices and beam profile measurements, is reliable only if the emittance is conserved and the space charge forces are negligible in the beamline between the reconstruction and measurement points. The effects of space charge forces prevent this method from giving sound results up to a relativistic beta of about 0.5 and make it inapplicable to the Linac4 commissioning at 50 and 100 MeV. To compensate for this drawback we have developed a dedicated technique, the forward method, which extends the classical method by combining it with an iterative process of multiparticle tracking including space charge forces. The forward method, complemented with a tomographic reconstruction routine, has been applied to transverse and longitudinal emittance reconstruction during the Linac4 beam commissioning. In this paper we describe the reconstruction process and its application during Linac4 beam commissioning.

## INTRODUCTION

The characterization of the beam emittance is essential during each commissioning stage of a linac to validate the settings and correct operation of the linac part being commissioned and predict the beam behaviour and potential beam losses downstream.

At Linac4, during the commissioning of the low energy part, a slit-grid emittance meter installed on a movable diagnostic bench [1] was used for the direct measurement of the transverse phase spaces. The bench was consecutively used for the beam measurements at 3MeV and 12MeV [2]. The longitudinal beam profiles were measured using a bunch shape monitor (BSM) [3] and longitudinal emittance was reconstructed from the measured profiles using forward method [4, 5].

At higher beam energies, the technical realization of a slit becomes challenging. Therefore, indirect emittance measurement methods based on reconstructing the emittance from profile measurements are preferred. The effects of space charge forces prevent the classical emittance reconstruction methods which depend on analytical calculations from giving sound results. Therefore, two methods, namely forward method and hybrid phase space tomography, were developed, validated and applied to the Linac4 commissioning for the emittance reconstruction in the presence of space charge. For the Linac4 50MeV and 100MeV commissioning stages, the diagnostic bench shown in Fig. 1 has been used. Transverse emittances were reconstructed at the entrance of the bench from the

measured profiles at three locations along the bench with secondary electron emission (SEM) grids. The quadrupole magnets at the entrance of the bench are essential for obtaining optimum beam sizes at the SEM grids for the reconstruction. The longitudinal emittance was reconstructed at the entrance of a cavity upstream of the bench by varying the cavity settings and measuring the longitudinal bunch profile with the BSM shown in Fig. 1.

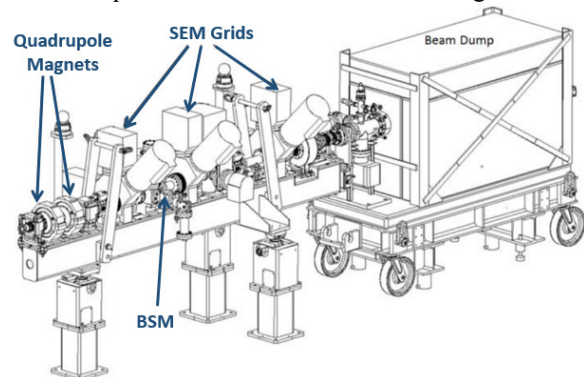


Figure 1: The Linac4 high energy diagnostic bench.

The 50MeV commissioning stage was completed in 2015 and the 100MeV commissioning stage was completed recently [6]. During each stage, the forward method and tomographic reconstruction were used to construct an estimate of the particle distribution in both transverse and longitudinal phase spaces.

The followings sections summarize the forward method with relevant references, discuss the tomographic reconstruction in detail and present the results of their applications to the measurement data.

## EMITTANCE RECONSTRUCTION IN STRONG SPACE CHARGE REGIME

The classical emittance reconstruction techniques, based on analytic calculations using transfer matrices and beam profile measurements are not reliable in strong space charge regime. Therefore, two methods are developed and applied during the Linac4 commissioning to estimate the emittance of the beam in the presence of space charge.

### The Forward Method

The forward method is a technique which aims at reconstructing the emittance of a particle beam from profile measurements in the presence of space charge. It was validated theoretically [7, 8] and experimentally [5] during the Linac4 commissioning.

# MODEL BENCHMARK WITH EXPERIMENT AT THE SNS LINAC

A. Shishlo<sup>†</sup>, A. Aleksandrov, Y. Liu, M. Plum, ORNL, Oak Ridge, TN 37831, USA

## Abstract

The history of attempts to perform a transverse matching in the Spallation Neutron Source (SNS) superconducting linac (SCL) is discussed. The SCL has 9 laser wire (LW) stations to perform non-destructive measurements of the transverse beam profiles. Any matching starts with the measurement of the initial Twiss parameters, which in the SNS case was done by using the first four LW stations at the beginning of the superconducting linac. For years the consistency between data from all LW stations could not be achieved. This problem was resolved only after significant improvements in accuracy of the phase scans of the SCL cavities, more precise analysis of all available scan data, better optics planning, and the initial longitudinal Twiss parameter measurements. The presented paper discusses in detail these developed procedures.

## INTRODUCTION

The SNS SCL is the world's first of the kind high power hadron superconducting linac. It accelerates H<sup>+</sup> ions from 186 MeV to 1 GeV with 81 six-cell niobium elliptical superconducting RF cavities [1]. There are two types of superconducting cavities in SNS: the first is optimized for relativistic beta of 0.61 (medium beta subsection), and the second is optimized for beta of 0.81 (high beta). The cavities are enclosed in 23 cryomodules with inside temperatures of 2 K. There are 3 and 4 cavities per module for the medium and high beta sections respectively. Between modules there are doublets of quadrupoles to provide the transverse focusing.

Commissioning of the superconducting linac started in July 2005, and in 2009 SNS reached 1 MW beam power. During the power ramp up, an unexpected beam loss in the SCL was encountered. Eventually, this beam loss was reduced to the acceptable level by empirically lowering the field gradients of the SCL quadrupoles without understanding the loss mechanism. That led to efforts by the accelerator physics group to understand and to control the beam sizes in the SNS superconducting linac. Later the mechanism of the unexpected beam loss was identified as the Intra Beam Stripping (IBSt) process [2,3]. This explained our success in the loss reduction, but it did not give us the model-based control over the beam sizes in the SCL. This paper describes our path in developing such a model-based SCL optics control.

In the present paper we are going to describe three basic components that allowed us to successfully benchmark the model against the measured SCL beam parameters. First, we developed a procedure to measure the initial transverse Twiss parameters with acceptable accuracy. Second, we speeded up the SCL RF cavity tuning process and improved the accuracy of the phase scan data analy-

sis. Finally, we developed an original method of measuring the longitudinal Twiss parameters based on the Beam Position Monitor signals.

## SNS SCL DIAGNOSTICS

In contrast to normal conducting linacs, the SNS superconducting linac is not allowed to have insertable destructive beam diagnostic devices to avoid surface contamination of the SCL cavities. Instead of wire scanners the SCL has 9 laser wire (LW) profile monitors [4]. As shown in Fig. 1, four of them are placed at the beginning of each of two (medium and high beta) sections, and the last one is at the end of SCL.

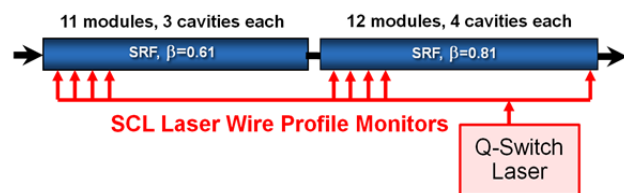


Figure 1: Positions of the 9 laser wire stations in the SNS SCL.

The LW system distributes the laser beam to intercept the H<sup>+</sup> ion beam, which removes the second electron. This creates neutral hydrogen, which will be eventually lost inside the SCL. The photo-detached electrons are collected, and their total charge is measured [4]. This signal is proportional to the density of the ion beam. By using a system of mirrors the laser beam can be moved in vertical and horizontal directions providing the ion beam profiles in both planes. The amount of beam loss created by the LW system is negligible, and it can be used even during 1 MW operations.

In addition to the LW system, the SCL has 32 stripline beam position monitors (BPMs) installed along the linac between cryomodules and in the cavity-free part of SCL. The BPMs measure the transverse positions of the beam, the arrival phases of the H<sup>+</sup> bunches, and the amplitudes of the 402.5 MHz harmonics (the bunch frequency) of the sum of all four stripline quadrant signals. This amplitude signal can be used for beam peak current measurements or for a longitudinal Twiss parameter analysis, as will be shown below.

The SNS superconducting linac also has a distributed system of Beam Loss Monitors (BLMs), but we are not going to discuss beam loss related issues in this paper.

## BEAM TRACKING MODELS

Several accelerator codes were used for the SCL data analysis. Two codes used in the first SCL transverse matching attempt [5] were a "Particle In Cell" (PIC) code IMPACT [6] and an "envelope" tracking Online Model (OM) from the SNS programming infrastructure XAL [7].

<sup>†</sup> shishlo@ornl.gov

# HPSIM - ADVANCED ONLINE MODELING FOR PROTON LINACS\*

L. J. Rybarczyk<sup>†</sup>, Los Alamos National Laboratory, Los Alamos, NM, 87545, USA

## Abstract

High-power proton linacs seek to operate with low and stable losses. This aspect is carefully evaluated with multi-particle beam dynamics codes during the design stage. However, it is just as important to evaluate the performance of the actual operating linac, which is typically more tedious and complicated when using these same design codes. To improve this situation, we have developed a high-performance, multi-particle online modeling tool, HPSim, with the goal of providing near real-time simulation results for our 800-MeV proton linac at Los Alamos. This presentation will cover the motivation, code features, benefits and applications.

## INTRODUCTION

High-power linacs, like the 800-MeV proton linac at the Los Alamos Neutron Science Center are designed and operated to achieve low and stable beam loss. During the accelerator design phase, envelope and multi-particle codes, such as TRACE 2-D & 3-D [1], PARMILA [2], TRACK [3], TRACEWIN [4], and others are used to create the linac layouts and evaluate them for losses. While the envelope codes are being used as online models for the operating machines, the multi-particle codes, until very recently [5], have not. This has been due in part to a combination of performance and computer resource issues associated with using these codes in a control room setting.

The typical multi-particle code, like those mentioned above and others, e.g. IMPACT [6], etc. used to successfully simulate proton beams in linacs, offer benefits and advantages not available from an envelope code. However, using these to simulate beam in an operating linac can be tedious and complicated. This is because all of the relevant beam and machine parameters and settings for a *single snapshot* of the operation must be transferred to the input format used by the code. Only then can a simulation be performed from which results can be compared to measurements under those same conditions.

Routine use of accurate online multi-particle simulations to setup, track and study performance of an operating linac would be beneficial. This is especially true for new and existing high-power linacs where detailed knowledge of the beam distribution along the linac can provide new insight into issues that produce beam spill. HPSim was developed for this purpose.

## MOTIVATION

The LANSCE accelerator utilizes both proton and H-beams and delivers them to several user facilities for basic

and applied research. The pulsed accelerator operates with a typical maximum beam duty factor of 120 Hz x 625  $\mu$ s for each species. Initially, the beams are accelerated to 750 keV using Cockcroft-Walton (C-W) style injectors. The high-current DC beams are subsequently bunched prior to injection into our 201.25-MHz 100-MeV drift tube linac (DTL) using two 201.25 MHz single-gap cavities. This scheme enables us to routinely achieve ~80% longitudinal capture of the standard proton and H-beams. However, this approach also results in significant longitudinal tails on each beam. These tails are clearly seen in the simulated longitudinal phase space of the proton beam at the entrance and exit of the DTL, as shown in Figure 1. To operate the DTL in a manner that produces the lowest beam spill along the entire side-coupled cavity linac (CCL) and further downstream, operations staff have found a new set of phase and amplitude set points for the DTL that are significantly different from design. The phase and amplitude set points of the DTL were empirically determined over years of high-power (800 kW) beam operation and are similar even under today's ~100 kW operation.

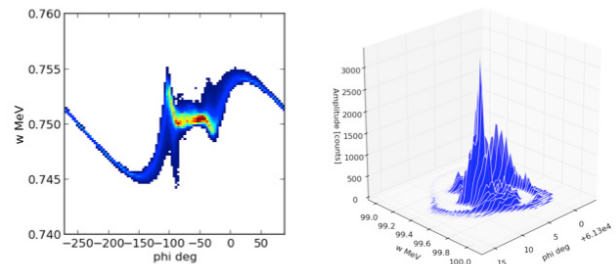


Figure 1: Simulated longitudinal phase space distributions for the LANSCE proton beam at the entrance (left) and exit (right) of the DTL.

The annual tune-up process for the LANSCE linac involves the typical physics-based approach of using envelope and previously established single- and multi-particle model results to determine good starting points for focusing magnets and accelerator modules along the linac. Once this phase is complete, the process becomes much more empirical and the operators resort to tweaking many of the newly established RF set points in order to further reduce beam loss along the accelerator. This is the same approach used at many other accelerator facilities as mentioned in a previous HB workshop [7].

Our first-hand experience, as well as those at other similar facilities, motivated us to develop HPSim. The existing envelope and single-particle models cannot provide the needed insight into the actual beam distribution expected from a particular set of accelerator operating set points. However, to be effective in an accelerator control room setting, the code needs to be fast and accurate with the ability to access the control system to minimize the

\* Work supported by the United States Department of Energy, National Nuclear Security Agency, under contract DE-AC52-06NA25396.  
<sup>†</sup>lrybarczyk@lanl.gov

# H- BEAM DYNAMICS STUDY OF A LEBT IN XIPAF PROJECT WITH THE WARP CODE

R. Tang, Q.Z. Xing, L. Du, Q.Z. Zhang, T.B. Du, H.Y. Zhang, X.L. Guan, X.W. Wang, C.X. Tang<sup>\*,†</sup>,  
 Key Laboratory of Particle & Radiation Imaging (Tsinghua University),  
 Ministry of Education, Beijing 100084, China  
 also at Laboratory for Advanced Radiation Sources and Application,  
 Tsinghua University, Beijing 100084, China  
 also at Department of Engineering Physics, Tsinghua University, Beijing 100084, China  
 Y. He, J. Li, NUTECH Co.Ltd, Beijing 100084,China

## Abstract

The 7 MeV H- linac injector of Xi'an Proton Application Facility (XiPAF) is composed of an ECR ion source, a Low Energy Beam Transport line (LEBT), a Radio Frequency Quadrupole accelerator (RFQ) and a Drift Tube Linac (DTL). The 1.7 m-long LEBT is used for matching a 40 μs pulse width 6 mA peak current beam to the entrance of the RFQ accelerator. The peak current and pulse-width of the 50 keV H- beam extracted from the ion source is 10 mA and 1 ms respectively. In the LEBT, an adjustable aperture is used for scraping the peak current of the beam to 6 mA, and an electric chopper is used for chopping the beam pulse width to 40 μs. These elements make the space charge compensation problem more complicated. A careful simulation of the space charge compensation problem of the H- beam has been done by considering the beam particles interacting with the residual gas with the help of WARP PIC code. To achieve the requirements of the LEBT in XiPAF, the type and pressure of the residual gas is given according to the simulation results.

## INTRODUCTION

Xi'an Proton Application Facility (XiPAF) is a new proton project which is located at Xi'an City, Shanxi Province of China. This facility is being constructed for single-event-effect experiments. It provides proton beam with the maximum energy of 230 MeV. The accelerator facility of XiPAF mainly contains a 7MeV H- linac injector and a proton synchrotron accelerator. The 7 MeV H- linac injector of Xi'an Proton Application Facility (XiPAF) is composed of an ECR ion source, a Low Energy Beam Transport line (LEBT), a Radio Frequency Quadrupole accelerator (RFQ) and a Drift Tube Linac (DTL). The H- beam current extracted from the ECR source is 10 mA. The space charge effect of this intense beam makes a huge impact on the beam transport. In general, the 50 keV H- beam ionizes the residual gas and traps the positive ions. This process named SCC (space charge compensation) decreases the space charge effect greatly. In the LEBT design of XiPAF, the degree of SCC is assumed as 85% [1]. With the help of WARP PIC code, the residual gas ionization and stripping process is added

into the H- beam dynamics simulation. This more accurate simulation is expected to provide guidance for the LEBT commissioning in the future.

## LEBT DESIGN

The actual length of the LEBT is about 1.7 m. With the beam waist as the entrance, the length of the beam dynamics simulation is 1.8 m. Figure 1 shows the layout of the LEBT. The LEBT is used to match the beam between the exit of the ion source and the entrance of the RFQ accelerator. Table 1 shows the symmetric beam parameters at the exit of the ion source and the acceptance of the RFQ accelerator. The Twiss parameters at the exit of the ion source are estimated to be  $\alpha=0$  and  $\beta=0.065$  mm/mrad.

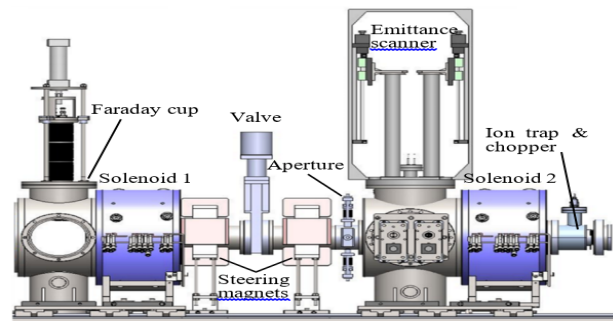


Figure 1: Layout of the Low Energy Beam Transport line (LEBT) of XiPAF.

Table 1: Beam Parameters Requirement

|                          | ECR exit          | RFQ entrance      |
|--------------------------|-------------------|-------------------|
| Particle species         | H-                | H-                |
| Particle energy          | 50 keV            | 50 keV            |
| Peak current             | 10 mA             | 6 mA              |
| Pulse width              | 1 ms              | 40 μs             |
| $\alpha$                 | 0                 | 1.052             |
| $\beta$                  | 0.065 mm/mrad     | 0.0494 mm/mrad    |
| Normalized RMS emittance | $0.2 \pi$ mm•mrad | $0.2 \pi$ mm•mrad |

\*work supported by the Major Research plan of the National Natural Science Foundation of China (Grant No. 91126003).

†tang.xuh@tsinghua.edu.cn

# STUDY ON SPACE CHARGE COMPENSATION OF LOW ENERGY HIGH INTENSITY ION BEAM IN PEKING UNIVERSITY\*

S. X. Peng<sup>1,†</sup>, A. L. Zhang<sup>1,2</sup>, H. T. Ren<sup>1</sup>, T. Zhang<sup>1</sup>, J. F. Zhang<sup>1</sup>, Y. Xu<sup>1</sup>, J. M. Wen<sup>1</sup>, W. B. Wu<sup>1</sup>, Z. Y. Guo<sup>1</sup>, J. E. Chen<sup>1,2</sup>

<sup>1</sup>State Key Laboratory of Nuclear Physics and Technology & Institute of Heavy Ion Physics, School of Physics, Peking University, Beijing, China

<sup>2</sup>University of Chinese Academy of Sciences, Beijing, China

## Abstract

To better understand the space charge compensation processes in low energy high intensity beam transportation, numerical simulation and experimental study on H<sup>+</sup> beam and H<sup>-</sup> beam were carried out at Peking University (PKU). The numerical simulation is done with a PIC-MCC model [1] whose computing framework was done with the 3D MATLAB PIC code bender [2], and the impacts among particles were done with Monte Carlo collision via null-collision method. Issues, such as beam loss caused by collisions in H<sup>+</sup>, H<sup>-</sup> beam and ion-electron instability related to decompensation and overcompensation in H<sup>-</sup> beam, are carefully treated in this model. The experiments were performed on PKU ion source test bench. Compensation gases were injected directly into the beam transportation region to modify the space charge compensation degree. The results obtained during the experiment are agree well with the numerical simulation ones for both H<sup>+</sup> beam [1] and H<sup>-</sup> beam [1]. Details will be presented in this paper.

## INTRODUCTION

The space charge compensation occurred by tapping opposite polarity of the particles could come from the secondary particles produced by gas ionization or supplied by specific device. For gas ionization, it takes time for a particle of the beam to produce a neutralizing particle on the gas. It is expressed as,

$$\tau = \frac{1}{\sigma_i n_g \beta_B c} \quad (1)$$

where  $\sigma_i$  is the ionization cross section of the incoming particles on the gas and  $n_g$  is the gas density in the beam line. The gas space charge compensation only applies to those beam whose pulse length is longer than  $\tau$ , for example CW beam or long-pulse beam. For those short pulsed beam, the opposite polarity of the particles should be initiatively provided and sustained by specific device without transient time limit, such as Electron Volume [3] and Gabor Lens [4]. In this paper, we will focus on the space charge effect and space charge compensation of CW beam and long-pulse beam. Study on space charge compensation can help us to understand the processes during the compensation and guide accelerator design. Experiment research as well as numerical simulation are complementary ways on this study. To simulate the pro-

cess of space charge compensation within an ion beam, the space charge effect should be treated by taking into account either through a linear analytical model or by treating the beam fully three-dimensional through particle-in-cell (PIC) methods. At PKU, a Monte Carlo collision (MCC) [5] package including the null collision method has been developed as an addition to the usual PIC charged particle scheme. This PIC-MCC code done with 2D MATLAB code has been used to simulate the space charge compensation of H<sup>+</sup> beam. The simulation results had a good agreement with the experimental ones when dealing with Ar compensating H<sup>+</sup> beam [1]. Recently, this PIC-MCC simulation code was improved to 3D model and had been used in the H<sup>-</sup> beam after considering the difference of positive and negative ion beams [2]. Again, the results obtained by H<sup>-</sup> beam experiment were coincident well with the numerical results. Space charge effect and space charge compensation, and experiment and simulation of space charge compensation will present in the paper.

## SPACE CHARGE EFFECT

Space charge is the most fundamental of the collective effects whose impact generally is proportional to the beam intensity. The defocusing force of space charge effect will lead to emittance growth ( $\Delta\epsilon_{rms}$ ) [5]. It can be expressed by the generalized perveance  $K$ ,

$$\Delta\epsilon_{rms} = \sqrt{\epsilon_{rms,final}^2 - \epsilon_{rms,start}^2} = \sqrt{\frac{\langle X^2 \rangle K \Delta W_{nl}}{8}} \quad (2)$$

Here  $X$  is the position of the ions in the beam,  $\Delta W_{nl}$  is the normalized non-linear field energy which mainly determined by the density distribution of the ion beam. The generalized perveance  $K$ , a dimensionless parameter, is defined as,

$$K = \frac{qI}{2\pi\epsilon_0 m_0 c^3 \beta^3 \gamma^3} \quad (3)$$

The perveance  $K$  refers to the magnitude of space-charge effects in a beam, and it will largely determine the particle trajectories in drift region. In equation (3),  $I$  is the density of the beam, while we approximate that  $\Delta W_{nl} \propto I$ , from equation (1) we get  $\Delta\epsilon_{rms} \propto I$ , which means the emittance growth is proportional to beam current.

Figure 1 showed the perveance  $K$  under different energy in several high current projects [6]. As shown in Fig. 1, in low energy region (100 keV) the perveance  $K$  is  $5 \times 10^{-3}$ , five orders higher than that in the high energy region (100 MeV). From equation (1) we know that  $\Delta\epsilon_{rms}$  is proportional to  $\sqrt{K}$ . This means the emittance

\*Work supported by the National Natural Science Foundation of China (11575013, 11305004)

†E-mail address: sxpeng@pku.edu.cn.

# SIMULATION OF SPACE-CHARGE COMPENSATION OF A LOW-ENERGY PROTON BEAM IN A DRIFT SECTION

Daniel Noll\*, Martin Droba, Oliver Meusel, Ulrich Ratzinger, Kathrin Schulte  
Institute for Applied Physics, Goethe University, Frankfurt am Main, Germany

## Abstract

Space-charge compensation provided by the accumulation of particles of opposing charge in the beam potential is an important effect occurring in magnetostatic low energy beam transport sections of high-intensity accelerators. An improved understanding of its effects might provide valuable input for the design of these beam lines.

One approach to model the compensation process are Particle-in-Cell (PIC) simulations including residual gas ionisation. In simulations of a drifting proton beam, using the PIC code *bender* [1], some features of thermal equilibrium for the compensation electrons were found. This makes it possible to predict their spatial distribution using the Poisson-Boltzmann equation and thus the influence on beam transport.

In this contribution, we will provide a comparison between the PIC simulations and the model as well as some ideas concerning the source of the (partial) thermalization.

## SIMULATION OF A DRIFT SECTION

The drift of a 120 keV, 100 mA proton beam over 50 cm through a system enclosed by repeller electrodes on  $-1.5$  kV and filled with Argon gas at  $1 \times 10^{-5}$  mbar was simulated. The code *bender*, the simulation model, the reasons for the choice of this system as well as the behaviour during compensation build-up were presented in previous contributions [1, 2].

Figure 1 depicts the charge densities of all simulated species – the beam protons, the residual gas ions ( $\text{Ar}^{1+}$ ) and the compensation electrons – in the steady-state of the simulation. The globally averaged compensation outside of the area affected by the repellers reaches  $\eta_{\text{part}} \approx 86.2\%$ . Beyond the mean effect of the compensation, a shift in the focus of the beam, which is also easily explained by a scaling of the current, some additional effects are present.

In the focus, the beam becomes hollow. As can be observed in the total charge density, the beam edge is not well compensated, especially in the focus point but also elsewhere in the system. Some electrons have enough energy to be able to form an area of negative charge density close to the beam edge. In most parts of the system, the residual gas ions are immediately expelled by the radial electric field. However, within the focus, the Argon ions accumulate to a density of approximately  $300 \mu\text{C m}^{-3}$  – surprising, since the radial electric fields should be largest in the focus.

Figure 2 shows the distribution of total particles energies  $H$  in arbitrarily selected places throughout the volume. For

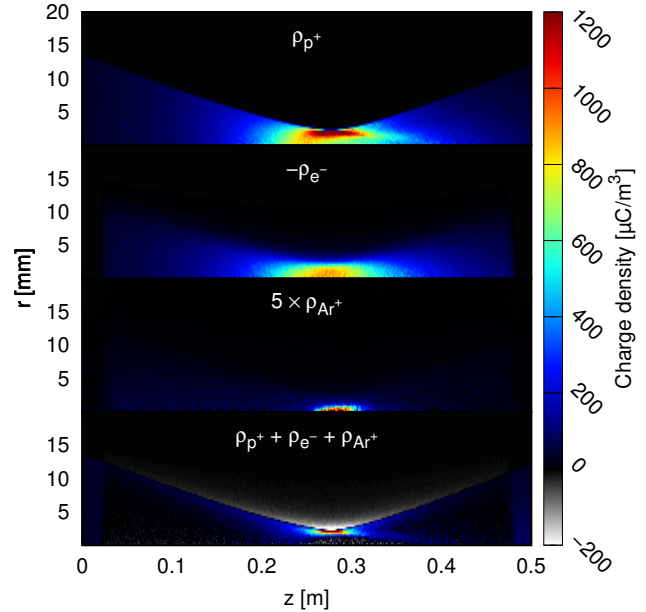


Figure 1: Charge densities for the different particle species in the simulation: beam protons, compensation electrons, residual gas ions and the netto charge density.

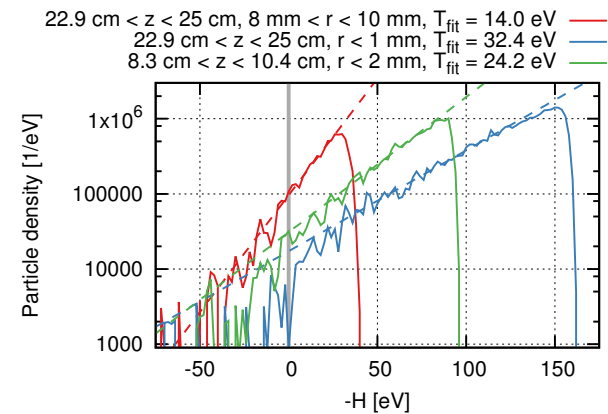


Figure 2: Distribution of total particle energy  $H$  (kinetic plus potential energy) at various arbitrarily chosen positions. For  $H < 0$ , the curves follow the dashed exponential curves. Positive  $H$  are underpopulated due to particle loss.

$H < 0$ , these follow an exponential dependence

$$\begin{aligned} H(r, v) &= H_0 \exp(-H / (k_b T)) \\ &= H_0 \exp\left(-p^2 / (2m_e k_b T) + e\varphi(r) / (k_b T)\right). \quad (1) \end{aligned}$$

For  $H \geq 0$ , particles are not confined and are gradually lost, leading to an underpopulation. The Boltzmann distribu-

\* noll@iap.uni-frankfurt.de

# REUSE RECYCLER: HIGH INTENSITY PROTON STACKING AT FERMILAB\*

P. Adamson<sup>†</sup>, Fermi National Accelerator Laboratory, Batavia, IL, USA

## Abstract

After a successful career as an antiproton storage and cooling ring, Recycler has been converted to a high intensity proton stacker for the Main Injector. We discuss the commissioning and operation of the Recycler in this new role, and the progress towards the 700 kW design goal.

## INTRODUCTION

Fermilab’s Recycler is a 3319.4 m circumference permanent magnet ring, installed in the Main Injector tunnel at Fermilab. It consists of strontium ferrite gradient magnets and in the straight sections strontium ferrite quadrupoles. It was designed as a storage ring for antiprotons, and with the use of electron cooling it was a key factor in the delivery of increased luminosity during the later years of the Tevatron operation.

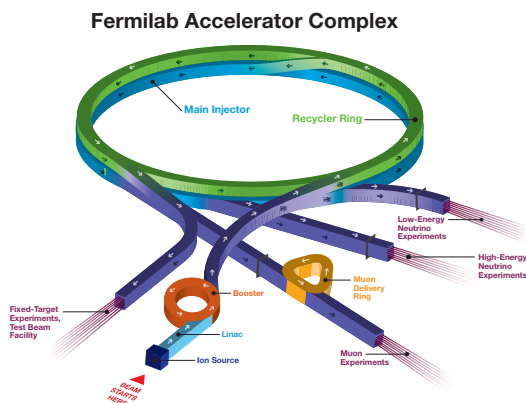


Figure 1: The Fermilab Accelerator complex in the NOvA era.

In a 16 month long shutdown, between May 2012 and September 2013, Recycler was converted for use as a proton stacker as part of the NOvA project [1]. The stochastic and electron cooling systems were removed, the section of ring used for electron cooling was rebuilt with a standard FODO lattice to match the rest of the ring, and the transfer lines used for antiproton transfer between Recycler and Main Injector were replaced with a new transfer line with larger acceptance. A new injection line to accept protons from the Booster was built, a 53 MHz rf system was installed, and new BPM cables and electronics capable of supporting 53 MHz operation was

\* Operated by Fermi Research Alliance, LLC under Contract No. De-AC02-07CH11359 with the United States Department of Energy.

<sup>†</sup> pa@fnal.gov

added. The Main Injector loss monitor system was modified to enable it to be continuously active (with Recycler used as a pre-stacker for Main Injector, high-intensity protons will be continuously present in the Main Injector tunnel.)

Recycler’s most challenging task is the slip-stacking and delivery of high intensity beam to the Main Injector for NuMI. The NOvA project [2] design goal is for a 700 kW proton beam ( $48.6 \times 10^{12}$  protons every 1.333 s.) In addition, Recycler stacks lower-intensity beam for transfer to Main Injector for resonant extraction to Switchyard 120 (the SeaQuest experiment, and the Fermilab Testbeam Facility), and beginning in 2017, it will rebunch protons into 2.5 MHz buckets for delivery to the Muon Campus (first Muon g-2, then  $\mu 2e$ .) In normal operation, roughly 10% of the time is devoted to Switchyard 120, so 630 kW would be delivered to the NuMI target at the design intensity.

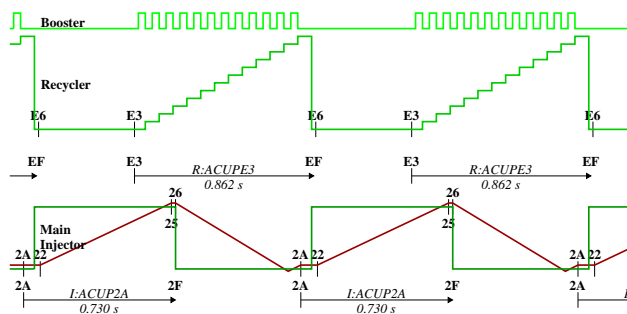


Figure 2: Relative timing of Booster, Recycler and Main Injector cycles for NOvA-era NuMI operation. Beam in each machine is shown in green, and Main Injector momentum in red. The start and end of cycle clock events for MI and Recycler are also shown.

The NOvA upgrade increases the beam power available at 120 GeV principally by reducing the cycle length. By moving the slip-stacking process from the Main Injector to the Recycler, the long front porch is eliminated, and the Main Injector can be kept ramping up and down at its maximum rate. As shown in Fig. 2, the Recycler starts stacking for the next NuMI pulse before the previous pulse has left the Main Injector.

## PERFORMANCE OF RECYCLER TO DATE

The NOvA ANU upgrades only provided the capability to transform the Recycler into a high intensity stacking ring. Significant work was required to realize this capability.

Figure 3 shows the NuMI beam power as a function of time since the end of the NOvA shutdown. During the 240 kW period at the start of the plot, the operational beam was

## THE OPERATION EXPERIENCE AT KOMAC\*

Yong-Sub Cho<sup>†</sup>, Kye-Ryung Kim, Kui Young Kim,  
Hyeok-Jung Kwon, Han-Sung Kim, Young-Gi Song

Korea Atomic Energy Research Institute, Korea Multi-purpose Accelerator Complex,  
Gyeongju, Gyeongbuk, Republic of Korea

### Abstract

A 100-MeV proton linac at the KOMAC (Korea Multi-purpose Accelerator Complex) is composed of a 50-keV microwave ion source, a 3-MeV four-vane-type RFQ, a 100-MeV DTL and 10 target stations for proton irradiation on samples from many application fields. The linac was commissioned in 2013 and the user service started in July 2013 with delivering proton beam to two target stations: one for a 20-MeV beam and the other for a 100-MeV beam. In 2015, the linac has been operated more than 2,800 hours with an availability of greater than 89%. The unscheduled downtime was about 73 hours, mainly due to troubles of ion source arcing and failures of pulsed high voltage power system. More than 2,100 samples from various fields such as materials science, bio-life, nano technology and nuclear science, were treated in 2015. Currently, a new target station for radioisotope production is under commissioning and a new target station for low flux irradiation experiments is being installed. Operational experiences of the 100-MeV linac during the past 3 years will be presented in the workshop.

### INTRODUCTION

KOMAC is located in Gyeongju, which was established as a branch of KAERI (Korea Atomic Energy Research Institute) in 2013. Among the gross area of the KOMAC site is 1,100 m × 400 m which is enough to house a 1-GeV proton accelerator, only 450 m × 400 m was developed for the 100-MeV linac as a 1<sup>st</sup> stage of the KOMAC as shown in Fig. 1 and the remaining area is reserved for future extension. An accelerator building, a beam application building, a utility building, power station and water treatment building are under operation [1]. The construction of the dormitory building will be finished in October, 2016 and the construction of the administration building starts in September, 2016.

After awarding the operation license, the operation of the 100-MeV linac started in 2013. Since then, two target stations have been opened for users. The operation statistics is reported in the following section. To meet the various and dedicated users' needs, a radioisotope production beam line was developed in 2015 and a low-flux beam line is under construction in 2016, which are described in detail. Finally the operational issues related to the accelerator components and user services are discussed in the paper.

\* Work supported by Ministry of Science, ICT & Future Planning of Korean Government.

<sup>†</sup> choys@kaeri.re.kr



Figure 1: KOMAC site.

### 100-MeV LINAC OPERATIONS

#### Accelerator

The main specifications of the 100-MeV linac depending on the energy of the beam line are summarized in Table 1. The characteristic of the linac is that it has two beam extraction points, one is at 20-MeV and the other is at 100-MeV. The designed beam duty up to 20-MeV is 24% and the other section up to 100-MeV is 8%. The accelerator layout is shown in Fig. 2. The ion source is a microwave ion source and magnetic LEBT (Low Energy Beam Transport) is used to match the beam to RFQ. A four-vane-type RFQ is used to accelerate the beam from 50-keV to 3-MeV. Total 11 DTL tanks are used to accelerate the beam from 3-MeV to 100-MeV. The operating frequency of RFQ and DTL is 350 MHz. There are total 9 klystrons to drive the 100-MeV linac. And total 4 modulators are used to drive 2 or 3 klystrons simultaneously. The 4 independent DTL tanks at 20-MeV section are driven by 1 klystron. The resonant frequencies of all the cavities such as RFQ, DTL and MEBT tanks are controlled by independent RCCS (Resonant frequency Control Cooling System).

Table 1: Specifications of the KOMAC Linac

| Parameters                | 20-MeV  | 100-MeV |
|---------------------------|---------|---------|
| Output energy [MeV]       | 20-MeV  | 100-MeV |
| Peak beam current [mA]    | 20      | 20      |
| Max. beam duty [%]        | 24      | 8       |
| Avg. beam current [mA]    | 0.1~4.8 | 0.1~1.6 |
| Pulse length [ms]         | 0.1~2   | 0.1~1.3 |
| Max. repetition rate [Hz] | 120     | 60      |
| Max. avg. beam power [kW] | 96      | 160     |

# INVESTIGATION TO IMPROVE EFFICIENCY AND AVAILABILITY IN CONTROL AND OPERATION OF SUPERCONDUCTING CAVITY AT ESS

Rihua Zeng, European Spallation Source ERIC  
Olof Troeng, Lund University, Sweden

## Abstract

The higher efficiency and higher availability (fault-tolerant oriented) of RF & Cavity system (with beam loading) to operate at, the more dynamic details needs to be identified, so as to have the abilities (a) to work at nonlinearities, (b) to work close to limitation, and (c) to change operation point quickly and correctly. Dynamic detail identifications rely heavily on high precision measuring and characterizing basic cavity parameters ( $Q_L$ , R/Q, dynamic detuning, phase and amplitude) and system behaviours under beam-RF-cavity interactions. It is especially challenging to characterize these dynamics under varying operating points or environment. Advanced technologies in LLRF and ICS providing real time/online characterizing will be the key enablers for addressing such challenges. However, to be successful, the deployment of these technologies must be embedded within local conditions taking into account available resources, existing hardware/software structures and operation modes. Several improvement approaches will be introduced. For example, 15% or more energy efficiency improvement at ESS will be obtained by reduction of power overhead and optimization of operation.

## INTRODUCTION

The European Spallation Source is a planned neutron source to be built in Lund, Sweden, with a start of neutron production in 2019. The performance goals are an average beam power at the target of 5 MW, with a 62.5 mA current and a pulse repetition rate and length of 14 Hz and 2.86 ms, respectively. It is to be built as a green plant, which places stringent demands on powers conservation and recycling of energy. This will be achieved by careful design and modern power recapture methods, such as using the cooling water to heat the surrounding municipalities. This also places stringent demands on the low level RF systems, especially as the plant at the same time has an operational goal of 95% availability and a comparably short time from start of final design to commissioning. Here we will describe some of the consequences these demands have on the RF, Cavity and LLRF system, and the proposed solutions and development projects that have started in order to reach this goal.

## ENERGY EFFICIENCY

Typically linear accelerators use klystrons as RF power amplifiers, as these can deliver the power to get necessary accelerating gradients in the cavities of the Linac. In feedback control mode, to facilitate the control of the phase and the amplitude of the fields in the cavities, the klystrons are typically run far below saturation in a linear

region of operation to leave some power overhead for regulation. Such overhead is not necessary if klystrons are operated in open loop. There are quite some electron machines (MAXIV, PSI, CLIC, etc.) in which klystrons are operated at their saturation point.

To better describe system efficiency, the power overhead in this paper is defined in a wide range: the difference between the maximum RF amplifier output and the power delivered to the beam, including necessary margin for error compensation and transient behaviour in feedback control, and also the power dissipation in RF distribution system. The operation points of klystron in traditional accelerators are often chosen at lower than 70% of saturation (where klystrons input-output power curve are much linear), to ensure adequate power overhead without considering high-order dynamic details. In JPARC, great effort has been put to figure out dynamic details of klystron and normal conducting cavities under heavy beam loading. As a reward for their effort, more of their klystrons are able to work at 85% of saturation level, reducing significantly power consumption. Advanced technologies in modern high performance hardware make these solutions possible, with great flexibility in configuration and short time in implementation.

Within the ESS project we will look into system dynamic details and try every effort to step further, so as to operate the power amplifiers at 90% of their saturation level, as shown in Figure 1.

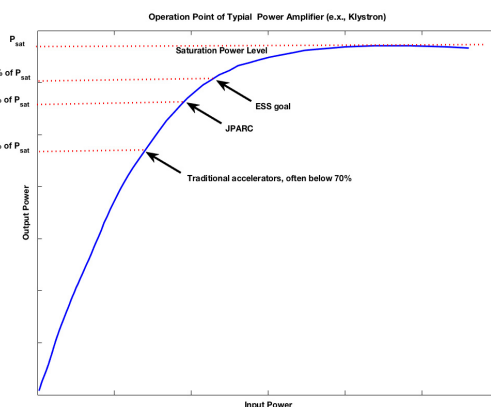


Figure 1: Operation points of klystron in closed loop in different facilities and ESS goal.

The higher efficiency point of power amplifiers we want to operate at, the more dynamic details we have to figure out for both cavity system and RF system. Dynamic detail identifications rely heavily on high precision measuring and characterizing basic cavity parameters ( $Q_L$ , R/Q, dynamic detuning, phase and amplitude) and system behaviours under beam-RF-cavity interactions. It

## THE PATH TO 1 MW: BEAM LOSS CONTROL IN THE J-PARC 3-GeV RCS

H. Hotchi<sup>#</sup>, H. Harada, S. Kato, M. Kinsho, K. Okabe, P.K. Saha, Y. Shobuda, F. Tamura, N. Tani, Y. Watanabe, K. Yamamoto, M. Yamamoto, and M. Yoshimoto  
J-PARC Center, Japan Atomic Energy Agency, Tokai, Naka, Ibaraki, 319-1195 Japan

### Abstract

The J-PARC 3-GeV RCS started a 1-MW beam test in October 2014, and successfully achieved a 1-MW beam acceleration in January 2015. Since then, a large fraction of our effort has been concentrated on reducing and managing beam losses. In this paper, recent progresses of 1-MW beam tuning are presented with particular emphasis on our approaches to beam loss issues.

### INTRODUCTION

The J-PARC 3-GeV rapid cycling synchrotron (RCS) is the world's highest class of high-power pulsed proton driver aiming for a 1-MW output beam power. As shown in Fig. 1, a 400-MeV  $H^-$  beam from the injector linac is delivered to the RCS injection point, where it is multi-turn charge-exchange injected through a  $340\text{-}\mu\text{g}/\text{cm}^2$ -thick carbon foil over a period of 0.5 ms. RCS accelerates the injected protons up to 3 GeV with a repetition rate of 25 Hz. Most of the 25-Hz pulses are transported to the material and life science experimental facility (MLF), while only 4 pulses every several seconds are delivered to the following 50-GeV main ring synchrotron (MR).

Recently injector linac upgrades were completed, by which the injection energy was upgraded from 181 MeV to the design value of 400 MeV in 2013, and then the injection peak current was increased from 30 mA to the design value of 50 mA in 2014. Via these series of the injector linac upgrades, RCS now has all the hardware parameters to realize its design performance.

Figure 2 shows the history of the RCS beam operation. RCS was beam commissioned in October 2007 [1] and made available for the user program in December 2008 with an output beam power of 4 kW. Since then, the RCS beam power ramp-up has steadily proceeded following progressions in beam tuning and hardware improvements [2, 3]. The output beam power for the routine user program has been increased to 500 kW to date, though it is temporarily limited to 200 kW at present due to a malfunction of the neutron production target at MLF. In addition to such a routine user operation, RCS has intermittently been continuing high-intensity beam tests toward realizing the design output beam power of 1 MW. As shown by red bars in Fig. 2, RCS started a 1-MW beam test in October 2014 right after completing the injector linac upgrades, and successfully achieved a 1-MW beam acceleration in January 2015.

The most important issue in realizing such a MW-class high-power routine beam operation is to keep machine

activations within a permissible level, that is, to preserve a better hands-on-maintenance environment. Thus, a large fraction of our effort has been concentrated on reducing and managing beam losses. This paper presents recent progresses of 1-MW beam tuning especially focusing on our approaches to beam loss issues.

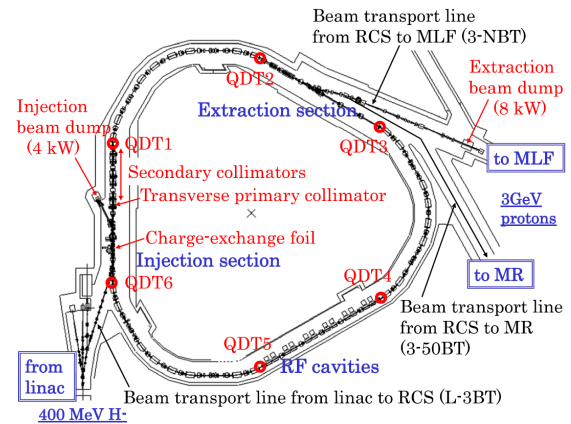


Figure 1: Layout of the J-PARC 3-GeV RCS.

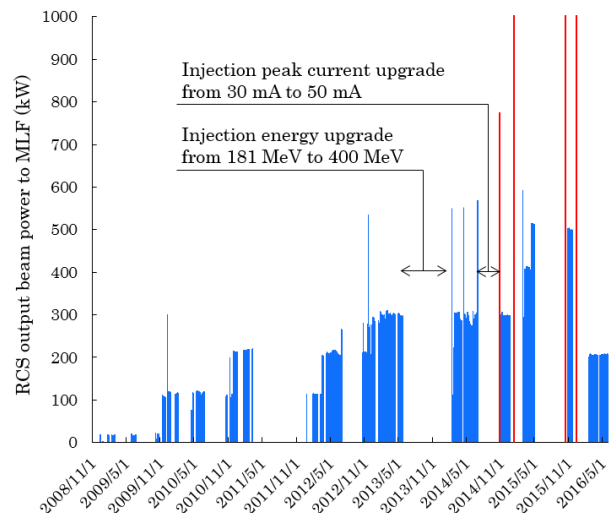


Figure 2: History of the RCS beam power since the start-up of the user program in December 2008.

### RESULTS OF THE INITIAL STAGE OF THE 1-MW BEAM TEST

#### *Longitudinal Beam Loss and its Mitigation*

As already reported in the last HB workshop [3], the first 1-MW beam test was conducted in October 2014. In this trial, the beam acceleration of up to 770 kW was

# TYOLOGY OF SPACE CHARGE RESONANCES

Ingo Hofmann\*, Technische Universität Darmstadt, Darmstadt, Germany  
 also at GSI Helmholtzzentrum für Schwerionenforschung GmbH, Darmstadt, Germany  
 also at Goethe Universität, Frankfurt am Main, Germany

## Abstract

The existence of structural space charge resonant effects in otherwise linear periodic focusing systems is well-known, but referred to in a variety of languages and contexts. We show here that for short bunched beams a “classification” in two major groups is possible, e.g. parametric resonances or instabilities on the one hand and single particle type space charge resonances on the other hand. The primary feature of distinction is that for the former the driving space charge force initially exists on the noise level (rms or higher order mismatch) only and gets amplified parametrically, hence an entirely coherent response; for the latter the driving space charge multipole is part of the initial density profile and the coherent response is weak. In the extreme limit of KV beams only parametric resonances (instabilities) exist, and in principle in all orders. For waterbag or Gaussian distributions we find half-integer parametric resonances only up to fourth order, but evidence for single particle resonances in all orders up to tenth have been identified.

## INTRODUCTION

With advancing demands on the control of space charge effects for beam dynamics of both linear and circular high intensity accelerators the appearance of purely space charge driven resonances merits careful consideration. The present study considers this space charge case in an otherwise linear periodic focusing lattice. It is based on a recent analysis of the so-called ninety degree and other structural space charge driven stopbands, where it was found that a distinction between single particle type resonant effects and instabilities - here also called parametric resonances - is fundamental [1].

The analytical basis for resonant space charge phenomena in periodic focusing was given by a perturbational Vlasov analysis of structural instabilities of different order for a Kapchinskij-Vladimirskij (KV) distribution of a coasting beam [2]. Our present examples show that this earlier work - though derived for the special case of a 2d KV beam, and under the constraints of a perturbation theory, is still highly relevant and a key to differentiating types of resonant behaviour.

Experimental investigation of this stop-band was undertaken only in 2009, in a dedicated experiment at the UNILAC high intensity heavy ion linear accelerator [3]. This experiment gave evidence of a fourth order resonance as suggested already in an earlier simulation study for a periodic lattice [4], and no indication of a simultaneously occurring envelope instability was found. However, a recent study has shown that the matter is more complex and not independent

of the length of the system and the initial mismatch [1]. In particular, the claim of Ref. [5] that the envelope mode is suppressed by the appearance of a fourth order resonance is not supported by our findings. Likewise, we cannot confirm a more recent interpretation that the envelope mode is induced by a mismatch induced by the fourth order resonance [6], which ignores the independence of these modes.

Note that our examples are related to short bunches, where the synchrotron period is not very different from betatron periods; in circular accelerators the synchrotron period is usually very long, which requires special consideration due to possibly different mixing effects. The suggested typology is, however, still applicable.

Resonances driven by space charge in combination with emittance exchange - so-called non-equipartitioned beams [7, 8] - are not part of the present study. They are driven by beam anisotropy rather than the periodic focusing, which leads to a related typology including single particle resonances and anisotropy driven instabilities.

## RESONANT PARTICLES AND COHERENT MODES

### Single Particle Resonances

The commonly considered resonances in accelerators are based on external forces periodically acting on particles. The origin of these forces usually are systematic and error multipoles of magnets, which provide the driving terms for the resonance.

In a linear lattice with non-uniform space charge density similar driving terms can be given, if one expands the space charge potential in so-called space charge “pseudo-multipoles”, which particles cannot distinguish from external forces provided that the space charge terms are well-matched and follow the lattice periodicity.

Resonances in such well-matched beams will be called “single-particle” or “incoherent resonances” reflecting the fact that coherent motion does not affect the resonance condition. Using linac notation the corresponding resonance condition in the  $x - x'$ -plane (similar in the other planes) can be written as

$$mk_x = 360^0, \quad (1)$$

with  $k_x \equiv k_{0,x} - \Delta k_{x,inc}$  the phase advance with space charge, and  $k_{0,x}$  without. Note that applied to circular accelerators, these quantities would have to relate to a periodic structure cell. Here, we assume  $\Delta k_{x,inc} (> 0)$  is an rms average of incoherent tune shifts and ignore possible spreads depending on amplitudes.

\* i.hofmann@gsi.de

# RESONANCES AND ENVELOPE INSTABILITY IN HIGH INTENSITY LINEAR ACCELERATORS

Dong-O Jeon<sup>†</sup>, Ji-Ho Jang, Hyunchang Jin, Institute for Basic Science, Daejeon, S. Korea

## Abstract

Understanding of space charge effects has grown and recent studies have led to the findings of space charge resonances in high intensity linear accelerators. Lately the sixth order resonance of high intensity linear accelerators was reported, along with the in-depth studies on the interplay of the fourth order resonance and the envelope instability. Experiment studies on space charge resonances were reported. This paper reviews the resonances of high intensity linear accelerators such as the  $4\sigma = 360^\circ$ , and the  $6\sigma = 720^\circ$  resonances, along with the envelope instability.

## INTRODUCTION

For high intensity beams, the envelope instability [1, 2] has been long known and the high intensity linac designers have kept  $\sigma_0 < 90^\circ$  to avoid the envelope instability. However in 2009 researchers found that the space charge fourth order  $4\sigma=360^\circ$  resonance was excited rather than the envelope instability [3] and was verified experimentally [4, 5]. Here  $\sigma(\sigma_0)$  is the depressed (zero-current) phase advance per cell. These works led to further studies about the fourth order resonance and the envelope instability such as [6]. In 2015 it was reported that the envelope instability grows out of the mismatch induced by the fourth order resonance for a linear accelerator with a constant  $\sigma_0$  lattice [7]. Recently a space charge sixth order  $6\sigma=720^\circ$  resonance was found in the high intensity linear accelerators [8].

Space charge coupling resonances were measured in the linear accelerators [9-10, 5] and in the circular accelerators for example in [11].

Recent study showed that the envelope instability can be suppressed or excited after the development of the fourth order resonance by controlling the  $\sigma$  or  $\sigma_0$  of the linac lattice [12].

This paper reviews the space charge resonances in high intensity linear accelerators; their simulation studies and the experiment studies, and the interplay of the fourth order resonance and the envelope instability.

## THE FOURTH ORDER SPACE CHARGE RESONANCE

The space charge fourth order  $4\sigma=360^\circ$  resonance was found and reported in 2009 [3]. It was observed that the fourth order resonance dominates over the envelope instability. Various studies were done to confirm that it was a resonance including the resonance crossing studies and the frequency analysis. It was shown that the resonance

takes effect only for  $90^\circ - \Delta\sigma \leq \sigma \leq 90^\circ$  with a stopband  $\Delta\sigma$ . No fourth order resonance effect is found beyond  $90^\circ$ .

Figure 1 shows the four resonance islands of this resonance populated with beam particles. And Fig. 2 shows pronounced peaks at the tune of  $1/4$  ( $90^\circ/360^\circ$ ) for the  $\sigma=85^\circ$  and  $\sigma=75^\circ$  lattices. For the lattice with  $\sigma=92^\circ$ , one does not observe the peak at  $1/4$ . The lattices were designed to maintain a constant  $\sigma$  depressed phase advance per cell.

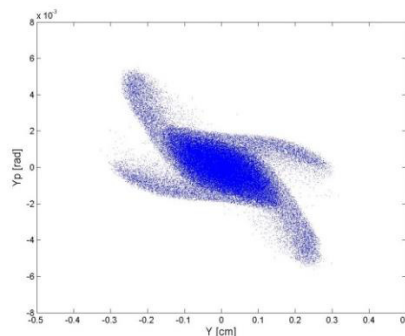


Figure 1: Beam distributions after the development of the fourth order resonance for the  $\sigma = 85^\circ$  lattice (Courtesy of [3]).

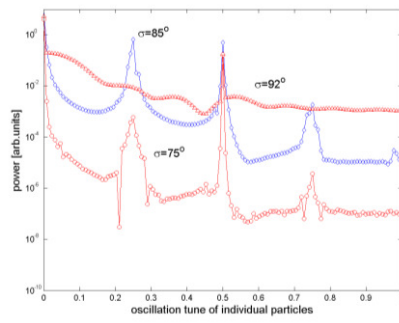


Figure 2: Plot of the FFT power spectrum of the rms beam size for the  $\sigma=85^\circ$  and  $\sigma=75^\circ$  lattices. One can see the pronounced peak at  $1/4$  ( $90^\circ/360^\circ$ ) due to the resonance. (Courtesy of [3])

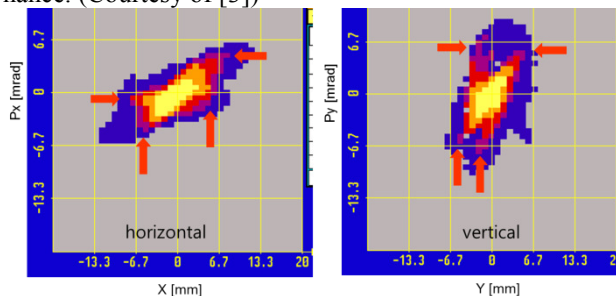


Figure 3: Measured x and y emittance for the lattice with  $\sigma_0=100^\circ$  of the GSI UNILAC. Clear evidence of the fourth order resonance is observed. (Courtesy of [4])

<sup>†</sup> jeond@ibs.re.kr

# USING AN ELECTRON COOLER FOR SPACE CHARGE COMPENSATION IN THE GSI SYNCHROTRON SIS18\*

W. D. Stem<sup>†</sup>, O. Boine-Frankenheim<sup>1</sup>, TEMF, TU Darmstadt, Darmstadt, Germany  
<sup>1</sup>also at GSI, Darmstadt, Germany

## Abstract

For the future operation of the SIS18 as a booster synchrotron for the FAIR SIS100, space charge and beam lifetime are expected to be the main intensity limitations. Intensity is limited in part by the space-charge-induced incoherent tune shift in bunched beams. A co-propagating, low energy electron lens can compensate for this tune shift by applying opposing space-charge fields in the ion beam. In this paper, we study the effect of using the existing electron cooler at the SIS18 as a space charge compensation device. We anticipate beta beating may arise due to the singular localized focusing error, and explore the possibility of adding additional lenses to reduce this error. We also study the effect of electron lenses on the coherent (collective) and incoherent (single-particle) stopbands. Furthermore, we estimate the lifetime of partially stripped heavy-ions due to charge exchange process in the lens.

## INTRODUCTION

The future Facility for Antiproton and Ion Research (FAIR) project will include several scientific experiments that require high-intensity (more than  $10^{11}$  ions) primary beams to produce sufficiently high-intensity secondary beams. The incoherent tune shift due to space charge is one of the main intensity-limiting factors standing in the way of this goal. This tune shift, in terms of ion beam parameters, is given by

$$\Delta Q_y^{SC} \approx \frac{NZ^2 r_p}{2\pi A \epsilon_y \beta_0^2 \gamma_0^3 B_f}, \quad (1)$$

where  $N$  is the number of particles,  $Z$  and  $A$  are the charge and mass number of the ion beam, respectively,  $r_p$  is the classical proton radius,  $\epsilon_y$  is the four-times rms beam emittance,  $\gamma_0$  and  $\beta_0$  are the relativistic factors of the ion beam, and  $B_f$  is the bunching factor.

Many authors estimate a maximum attainable space charge tune shift of 0.2-0.4 [1, 2]. The FAIR reference ion,  $U^{28+}$ , will reach a space charge tune shift of 0.25 horizontally and 0.45 vertically at its injection energy. It is clear that a tune shift mitigation process is necessary to obtain the target intensities.

Electron lenses have been studied as a way to compensate for this tune shift [2–5]. Electron lenses are low energy co- or counter-propagating electron beams that provide a localized, amplitude-dependent space charge kick to the ion

beam. The tune shift due to co-propagating electron lens with density  $n_e$  over interaction length  $L_e$  is given by

$$\Delta Q_y^e = -\frac{Z}{A} \frac{\beta_y r_p n_e L_e}{2\gamma_0 \beta_0^2} (1 - \beta_0 \beta_e), \quad (2)$$

where  $\beta_y$  is the beta function in the electron lens and  $\beta_e$  is the relativistic factor for the electron beam. The electron density in the cooler  $n_e$  is given by

$$n_e = \frac{I_e}{e\pi a^2 \beta_e c}, \quad (3)$$

for electron current  $I_e$ , electron charge  $e$ , speed of light  $c$ , and rms electron beam radius  $a$ . For an electron lens to work as designed, the ion beam must be centered inside the electron beam,  $\beta_0 \neq \beta_e$  to prevent cooling, the transverse density profiles of the two beams should match, and the electron beam must be pulsed to match the longitudinal density profile of the bunched ion beam.

## CHALLENGES

There are numerous challenges one must face when designing an electron lens. Among these are resonances, instabilities, and charge exchange. This paper discusses how we are addressing each of these problems in the SIS18, and how each help to answer the ultimate question: how many electron lenses are necessary for space-charge compensation.

### *Resonances and Instabilities*

The localized focusing structure of the electron lens has an impact on both the coherent (betatron) and incoherent (single particle) stopbands. Equation (2) acts not only on the incoherent tune but also the collective tune of the ion beam. Furthermore, half-integer resonance stopbands due to single particle closed orbit instabilities are determined by the stability criterion [6, 7]. Fig. 1 plots a stability diagram that represents the combined effect of a single electron lens on both the incoherent and coherent tunes of the ion beam. In this simplified case, the electron lens fully compensates for an ion beam that has a space charge tune shift of 0.1 in both planes. The incoherent tune shifts to the standard working point of the SIS18 ( $Q_x = 4.2$ ,  $Q_y = 3.3$ ), while the coherent tune, unaffected by the incoherent space charge tune shift, also shifts by 0.1 in both planes. The result is a compensated beam with a coherent tune offset. Since the instabilities only act on single particle orbits, Fig. 1 represents an example of stable compensation.

By doing an experimental tune scan, it will be possible to empirically see these instabilities. The results should provide information on how much tune shift each lens should

\* Work supported by BMBF contract FKZ:05P15RDRBA

<sup>†</sup> stem@temf.tu-darmstadt.de

## SPACE CHARGE EFFECTS IN FFAG \*

M. Haj Tahar, F. Méot , BNL, Upton, Long Island, New York, USA

### Abstract

Understanding space charge effects in FFAG is crucial in order to assess their potential for high power applications. This paper shows that, to carry out parametric studies of these effects in FFAG, the average field index of the focusing and defocusing magnets are the natural parametrization. Using several classes of particle distribution functions, we investigate the effects of space charge forces on the non-linear beam dynamics and provide stability diagrams for an FFAG-like lattice. The method developed in this study is mainly applicable to systems with slowly varying parameters, i.e slow acceleration.

### INTRODUCTION

Since the early 1990s, cyclotrons and linacs have been proposed to address the mission of coupling a high power proton accelerator with a spallation target in an Accelerator Driven Subcritical Reactor (ADSR) application. However, due to the recent revival of interest in using FFAG accelerators, the question then arises as to what sort of improvement can the FFAG technology bring. In an effort to demonstrate the high beam power capability of FFAG, studies of the collective effects such as the space charge effects have been undertaken and plans for high intensity experiments are ongoing [1]. Benchmarking work has also been undertaken to validate the simulation results. The following study is in major part induced by the successful benchmarking work so far [2].

### AVERAGE FIELD INDEX OF THE FOCUSING/DEFOCUSING MAGNET

In a FFAG accelerator, it is not possible to define a single closed orbit. Instead, the beam moves outwards, and therefore, all parameters are likely to change with the energy of the reference particle. For that reason, it is particularly misleading to replace the equation of motion with a transfer matrix since the betatron amplitude functions continuously change with the energy. For instance, in a scaling FFAG where the tunes are to remain constant,  $\beta_{x,y} \propto R$  where  $R$  is the radius of the closed orbit [3].

In order to carry out parametric study of space charge effects in non-linear FFAG lattices, the idea is to vary the strength of the applied forces on the beam. For that reason, an extension of the mean field index  $k$  as defined by Symon [4], is to introduce its azimuthal variation by defining the mean field index of the focusing ( $F$ ), defocusing ( $D$ ) magnets and the drift (*drift*) in the following way:

$$k_i = \frac{R}{B_i} \frac{dB_i}{dR} \quad ; \quad i = F, D, \text{drift} \quad (1)$$

where  $B_i$  is the vertical component of the magnetic field in the median plane of the FFAG that is averaged over the width of the element. Since the drift space between the magnets is likely to contain the fringe fields, it may be important to assign a mean field index to it to determine its effect on the beam dynamics. However, in the ideal case,  $k_{drift} = 0$ , which we will assume in the following for simplification, yet without loss of generality. Now, assuming that the  $k$  values have no radial dependence, Eq. (1) can be integrated and the magnetic field expressed in cylindrical coordinates:

$$B(R, \theta) = B_{F0} \times \left(\frac{R}{R_0}\right)^{k_F} \times F_F(\theta) + B_{D0} \times \left(\frac{R}{R_0}\right)^{k_D} \times F_D(\theta) \quad (2)$$

where  $F_F$  and  $F_D$  are the fringe field factors that describe the azimuthal variation of the field in the F and D magnets respectively. It is important to note that the field is a separable function in radial and azimuthal coordinates since the fringe fields merge to zero in the drift space between the magnets as can be seen in Fig. 1 below. Also, note that if  $k_F = k_D$ , the field writes in the standard form of a scaling FFAG. The lattice considered for this study is a radial sector KURRI-like DFD triplet [1]. Now assuming that all orbits

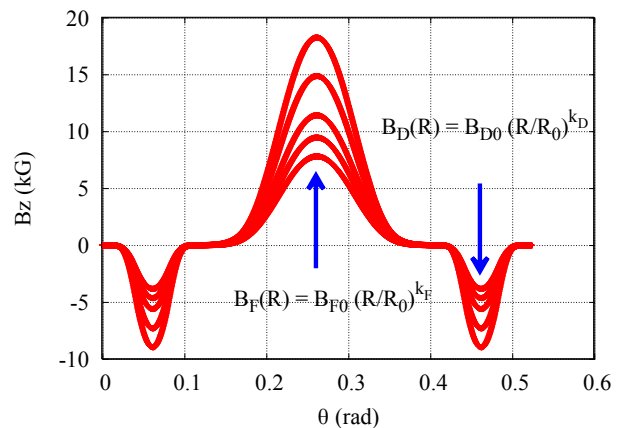


Figure 1: Magnetic field along several closed orbits.

are similar, i.e assuming a linear motion around the closed orbits in which only the path length and the field index may change with the radius, it can be shown that the square number of betatron oscillations in the transverse plane is a linear combination of the  $k_i$  values [3]. However, this result is not valid in the general case as shown in [3]: by using the Bogoliubov-Krilov-Mitropolsky (BKM)'s method of averages [5], one can compute approximately the frequencies of the betatron oscillations and their dependence on the average field index of the F and D magnets. To the first order

\* Work supported by Brookhaven Science Associates, LLC under Contract No. DE-AC02-98CH10886 with the U.S. Department of Energy.

# USE OF RF QUADRUPOLE STRUCTURES TO ENHANCE STABILITY IN ACCELERATOR RINGS

M. Schenk<sup>1\*</sup>, A. Grudiev, K. Li, K. Papke, CERN, CH-1211 Geneva, Switzerland  
<sup>1</sup>also at EPFL, CH-1015 Lausanne, Switzerland

## Abstract

The beams required for the high luminosity upgrade of the Large Hadron Collider (HL-LHC) at CERN call for efficient mechanisms to suppress transverse collective instabilities. In addition to octupole magnets installed for the purpose of Landau damping, we propose to use radio frequency (rf) quadrupole structures to considerably enhance the aforementioned stabilising effect. By means of the PyHEADTAIL macroparticle tracking code, the stabilising mechanism introduced by an rf quadrupole is studied and discussed. As a specific example, the performance of an rf quadrupole system in presence of magnetic octupoles is demonstrated for HL-LHC. Furthermore, potential performance limitations such as the excitation of synchro-betatron resonances are pointed out. Finally, efforts towards possible measurements with the CERN Super Proton Synchrotron (SPS) are discussed aiming at studying the underlying stabilising mechanisms experimentally.

## INTRODUCTION

To push the limits of the Large Hadron Collider (LHC) [1] and its future upgrade HL-LHC [2] towards higher luminosities, the machine must be able to handle beams with significantly increased brightnesses and intensities. Amongst others, these parameters are limited by the presence of transverse collective instabilities induced by the transverse beam coupling impedance of the accelerator structure. A successful stabilising mechanism for the so-called slow head-tail instabilities is the effect of Landau damping [3]. It is present when there is a spread in the betatron frequency, or tune, of the particles in the beam as discussed in detail e.g. in [4] and references therein. This so-called incoherent tune spread is a result of non-linearities in the machine. Partially, they are of parasitical nature, i.e. originating from non-linear space-charge forces, non-linearities in the magnetic focusing systems, beam-beam interactions at collision, etc. In addition, they are often introduced by design through dedicated non-linear elements for better control and efficiency. Magnetic octupoles are commonly used for the latter purpose. They change the betatron tunes of a particle depending on its transverse actions. In LHC for instance, families of 84 focusing and 84 defocusing, 0.32 m long superconducting magnetic octupoles are installed and successfully used to suppress a variety of instabilities [5, 6]. Nevertheless, LHC operation in 2012 at an energy of 4 TeV and a bunch spacing of 50 ns, as well as in 2015 at 6.5 TeV and 25 ns has shown that these Landau octupoles (LO) need to be powered close to their maximum strength in order to guarantee stable

beams [7]. With the HL-LHC upgrade, the bunch intensity will be increased from  $1.15 \cdot 10^{11}$  p<sup>+</sup>/b to  $2.2 \cdot 10^{11}$  p<sup>+</sup>/b which will potentially lead to more violent instabilities. At the same time, the normalised transverse emittances will be reduced from 3 μm (LHC operational) to 2.5 μm, and the beam energy will be increased from 6.5 TeV to 7 TeV, thus rendering the LO less effective.

An rf quadrupole operating in a transverse magnetic quadrupolar mode TM<sub>210</sub> was proposed as a more efficient device for introducing a non-vanishing betatron tune spread in the beams of a high energy particle accelerator like (HL-)LHC [8]. A first numerical proof-of-principle study was presented in [9]. The quadrupolar focusing strength of such a device has a harmonic dependence on the longitudinal position of the particles in the bunch. As a result, the betatron tunes of a particle are changed as a function of its longitudinal position. Since in high energy hadron colliders, the longitudinal emittance is much larger than the transverse ones, the rf quadrupole is able to generate a betatron tune spread more efficiently than magnetic octupoles.

The publication is structured as follows. Firstly, the working principle of an rf quadrupole as well as the PyHEADTAIL macroparticle tracking code are introduced. Thereafter, the applicability of an rf quadrupole for HL-LHC as well as the excitation of synchro-betatron resonances are discussed. Finally, experimental studies of the concerned stabilising mechanism are proposed for the SPS.

## THEORY

### Radio Frequency Quadrupole

A bunch of electrically charged particles of momentum  $p$  traverses an rf quadrupole along the  $z$ -axis. Given that the thin-lens approximation holds, a particle  $i$  located at position  $z_i$  measured with respect to the zero crossing of the main rf wave ( $z = 0$ ) experiences both transverse and longitudinal kicks

$$\Delta p_{\perp}^i = pk_2 (y_i \mathbf{u}_y - x_i \mathbf{u}_x) \cos \left[ \frac{\omega z_i}{\beta c} + \varphi_0 \right], \quad (1)$$

$$\Delta p_{\parallel}^i = \frac{\omega pk_2}{2\beta c} (x_i^2 - y_i^2) \sin \left[ \frac{\omega z_i}{\beta c} + \varphi_0 \right]. \quad (2)$$

$x_i$  and  $y_i$  are the transverse coordinates of the particle,  $\omega$  denotes the rf quadrupole angular frequency,  $\mathbf{u}_{x,y}$  are the unit vectors along the  $x$  and  $y$  coordinates respectively, and  $\varphi_0$  is a constant phase offset of the rf quadrupole wave with respect to  $z = 0$ . It has been added for reasons of generality.  $\beta$  and  $c$  denote the relativistic beta and the speed of light respectively.  $k_2$  is the amplitude of the normalised integrated

\* michael.schenk@cern.ch

# EARLY TESTS AND SIMULATION OF QUASI-INTEGRABLE OCTUPOLE LATTICES AT THE UNIVERSITY OF MARYLAND ELECTRON RING \*

Kiersten Ruisard<sup>†</sup>, Heidi Baumgartner, Brian Beaudoin, Irving Haber, David Matthews, Timothy Koeth  
<sup>1</sup> Institute for Research in Electronics and Applied Physics, University of Maryland, College Park, USA

## Abstract

Nonlinear quasi-integrable optics is a promising development on the horizon of high-intensity ring design. Large amplitude-dependent tune spreads, driven by strong nonlinear magnet inserts, lead to decoherence from incoherent tune resonances. This reduces intensity-driven beam loss while quasi-integrability ensures contained orbits. The experimental program at the University of Maryland Electron Ring (UMER) will explore the performance of a strong octupole lattice at a range of operating points. Early measurements use a distributed octupole lattice, consisting of several small octupole inserts. We vary lattice tune to change the quasi-integrable condition as well as probe behavior near different resonant conditions. Simulation results show there should be invariant conservation under carefully chosen conditions. We discuss the effect of steering errors on the lattice performance and on-going efforts to reduce these errors. We also discuss plans for a single-channel insert.

## INTRODUCTION

Beam resonances that drive particle losses and beam halo present a significant challenge for high intensity accelerators, limiting beam current due to risk of damage and/or activation. While Landau damping can control resonant effects, the addition of weak nonlinearities to a linear lattice can introduce resonant islands and chaotic phase space orbits, which reduce dynamic aperture and lead to destructive particle loss. Theory predicts that lattices with one or two invariants and sufficiently strong nonlinear elements should suppress tune and envelope resonances without loss of stable phase space area [1].

In [1], the small-angle Hamiltonian for transverse motion of a particle in an external linear focusing system is given by

$$H_N = \frac{1}{2} (p_x^2 + p_y^2 + K(s) (x^2 + y^2)) + V(x, y, s) \quad (1)$$

where  $V(x, y, s)$  is a generic nonlinear term. In the normalized frame, the Hamiltonian becomes

$$H_N = \frac{1}{2} (p_{x,N}^2 + p_{y,N}^2 + x_N^2 + y_N^2) + \kappa U(x_N, y_N, s) \quad (2)$$

where  $x_N = \frac{x}{\sqrt{\beta(s)}}$  and  $p_N = p\sqrt{\beta(s)} - \frac{\alpha x}{\sqrt{\beta(s)}}$ .

\* Work and travel supported by NSF GRFP, NSF Accelerator Science Program, DOE-HEP and UMD Graduate School ICSSA award.

<sup>†</sup> kruisard@umd.edu

In order for  $U(x_N, y_N)$  to be an invariant quantity (and therefore for  $H_N$  to be conserved),  $\beta_x = \beta_y$  inside the nonlinear element and the nonlinear element strength parameter  $\kappa(s)$  depends on  $\beta(s)$ . In particular, for an octupole element  $\kappa \propto \frac{1}{\beta(s)^3}$ .

For an elliptic nonlinear magnet, the transverse motion of a particle will be fully integrable with two conserved invariants, the normalized Hamiltonian and an additional quadratic term. The theory of the integrable lattice will be tested at the IOTA ring, currently under construction at Fermilab [2, 3]. The proposed lattice consists of a transversely symmetric ( $\beta_x = \beta_y$ ) beam in an axially varying nonlinear insert, linked by linear sections of  $n\pi$  phase advance that provide external focusing and image the beam between nonlinear sections, for pseudo-continuous motion of particles through the nonlinear insert. This lattice is illustrated in Fig. 1.

The goal of the nonlinear optics program at UMER is to test a quasi-integrable octupole lattice, experimentally demonstrating increased transverse stability and halo mitigation, predicted in [4]. While IOTA aims to test a fully integrable nonlinear solution, UMER does not have the precision necessary to verify integrability [2]. The strength of UMER lies in its flexibility to accommodate variable space charge beams with flexible focusing schemes. For the quasi-integrable lattice, the conserved  $H_N$  will result in chaotic but bounded motion, while still providing large amplitude-dependent tune spreads to reduce resonant behavior.

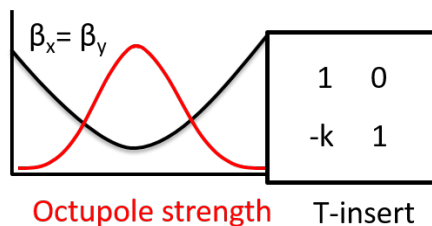


Figure 1: Ideal nonlinear lattice composed of  $\beta_x = \beta_y$  channel and ideal thin lens transfer matrix.

This paper will discuss preliminary testing of a distributed octupole lattice, conducted in parallel with preparations for the more robust single-channel design.

## EXPERIMENTAL SETUP

UMER is a 10 keV, 11.52 meter circumference ring designed for the study of high intensity beam dynamics. The

ISBN 978-3-95450-178-6

# SPACE CHARGE EFFECTS AND MITIGATION IN THE CERN PS BOOSTER, IN VIEW OF THE UPGRADE

E. Benedetto, F. Schmidt, CERN, Geneva, Switzerland  
 V. Forte, CERN and University Blaise Pascal, Clermont-Ferrand, France  
 M. Cieslak-Kowalska, CERN and EPFL, Lausanne, Switzerland

## Abstract

The CERN PS Booster (PSB) is presently running with a space charge tune spread larger than 0.5 at injection. Since the High Luminosity LHC (HL-LHC) will require beams with twice the intensity and brightness of today, the LHC Injector Upgrade (LIU) Project is putting in place an upgrade program for all the injector chain and, in particular, it relies on the important assumption that the PS Booster can successfully produce these beams after the implementation of the 160 MeV H- injection from Linac4. This contribution describes the studies (measurements and simulations) that have been carried out to confirm that the PSB can indeed perform as needed in terms of beam brightness for the future HL-LHC runs. The importance of the mitigation measures already in place, such as the correction of the half-integer line, and the effects of non-linear resonances on the beam are also discussed.

## INTRODUCTION

The PSB is the first synchrotron in the LHC proton injector chain and it is where the beam brightness is defined. The future increase of the PSB injection energy from 50 MeV to 160 MeV with Linac4 gives a factor  $(\beta\gamma^2)^{160\text{MeV}}/(\beta\gamma^2)^{50\text{MeV}} = 2.04$  reduction of the space charge tune spread for the present beams. The baseline of LIU is to keep the same tune spread at the PSB injection energy and to inject twice as many protons in a given emittance [1]. In the first part of the paper we summarize the studies that are leading to the beam brightness predictions for the upgrade to 160 MeV, additional details in [2,3]. The simulations, compared with measurements at 50 MeV, are done with PTC-Orbit [4,5]. In the second part we discuss the mitigation measures in place against space charge for both the present situation and the upgrade. Finally we discuss our first attempt to include non-linear errors in our model.

## BEAM BRIGHTNESS

### Present Machine, 50 MeV p+ Injection

Measurements of LHC beams in the PSB show that, after optimization of the injection settings, the points of the emittance as a function of intensity lay on a straight line [6, 7], indicating that we are running at constant brightness. The brightness here is defined as  $(E_x+E_y)/2/N_p$ , where  $E_x$ ,  $E_y$  are the normalized rms transverse emittances and  $N_p$  is the number of protons.

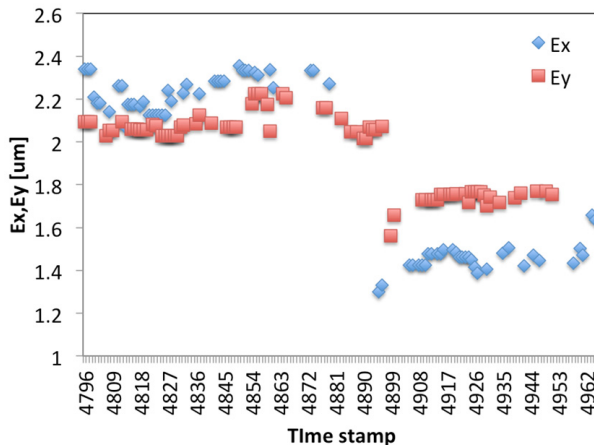


Figure 1: Measured horizontal and vertical rms normalized emittance, averaged over the 4 PSB rings, for  $Q_x=4.28$  ( $<496$ ) and after the change to  $Q_x=4.42$  ( $>496$ ). The vertical tune is fixed at 4.45.

Moreover, in operation we see an important reduction of the horizontal emittance, when the working point is moved from  $Q_x=4.28$  to  $Q_x=4.42$ , as shown in Fig. 1.

In the present PS Booster, the beams emittances are determined by space charge effects and by the multi-turn injection process itself.

In order to prove that the emittances strongly depend on the distance of the working point from the integer lines, we launched PTC-Orbit simulations with a simple model that does not include the proton multi-turn injection process, but only looks at the evolution of an initially matched beam, in a pure linear lattice.

Figure 2 shows the emittance evolution versus time when starting from an initial Gaussian beam of  $1.5 \mu\text{m}$ , for two working points similar to the ones used in operation. We find good qualitative agreement with the measurements. In particular, the horizontal emittance is strongly reduced when going to a larger working point. In this case the vertical emittance is also slightly increasing, since the vertical tune is smaller.

For what concerns the longitudinal plane, the beam is injected in coasting mode and then the voltage of the two RF cavities,  $h=1$  and  $h=2$  (in anti-phase) is raised to  $V=8\text{kV}$  within 7 ms in an accelerating bucket. This is an important ingredient in the space charge simulations because the bunching factor is going down from 1 to 0.4, thus the line density is increasing. Figure 3 shows the initial and final profiles, from simulations.

# STRIPLINE BEAM POSITION MONITORS WITH IMPROVED FREQUENCY RESPONSE AND THEIR COUPLING IMPEDANCES

Y. Shobuda, J-PARC Center, JAEA, Ibaraki, JAPAN,  
 Y. H. Chin, K. Takata, T. Toyama, KEK, Tsukuba, Ibaraki, JAPAN  
 K. G. Nakamura, Kyoto University, Kyoto, JAPAN

## Abstract

In J-PARC MR, there is a concern that electron cloud instabilities may appear and limit the beam current at future higher power operations. For the case, we have developed a wider-band beam position monitor by deforming the electrode shapes. The modification of the electrode can be done without significant enhancement of the beam coupling impedance. For typical electrode shapes, we show the coupling impedances as well as the frequency responses of the electrodes.

## INTRODUCTION

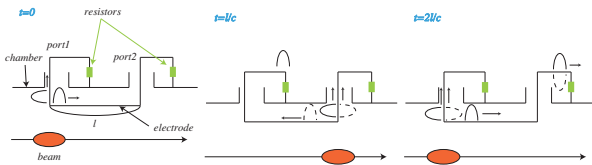


Figure 1: Flow chart of the induced pulses at a BPM.

Stripline beam position monitors (BPMs) are widely used for measurements of beam position signals in study of beam instabilities. The electrode is placed inside of the chamber. Figure 1 schematically shows the principle of the working of the BPMs.

Based on two-dimensional theory, the frequency response of the BPM is analytically given by the transfer function  $F(\omega)$  as [1]

$$F(\omega) = i\omega \int_0^{2l/c} \frac{1}{2} k\left(\frac{ct}{2}\right) e^{-i\omega t} dt = \frac{i\omega}{c} \int_0^l k(z) e^{-i\frac{2\omega}{c}z} dz, \quad (1)$$

where  $i$  is imaginary unit,  $\omega$  is angular frequency,  $k(z)$  is the coupling function to the fields at point  $z$ ,  $l$  is the electrode length and the velocity of the beam is approximated by the speed of light  $c$ .

For the electrode in a shape of rectangle, the transfer function is calculated as

$$F(\omega) = k_0 \frac{(1 - e^{-i\omega \frac{2l}{c}})}{2}, \quad (2)$$

by extracting the  $z$ -dependence from the coupling function  $k(z) = k_0$ . The distinctive feature of this function is that the absolute value has sharp notches with its interval:  $f_n = nc/2l$ , where  $n$  is integer (see the red lines in Fig.2).

The origin of these notches can be qualitatively understood as follows. As Fig.1 shows, when a beam arrives at the front-end of the electrode ( $t = 0$ ), the beam excites two currents with opposite polarities. One current flows to the downstream with the beam, while the other does to the upstream side and enters the port1.

When the beam reaches the back-end of the electrode ( $t = l/c$ ), new currents with opposite polarities (the dashed-pulse) are additionally excited there. The total signal to the port 2 is cancelled by superposing the currents (the solid and the dashed pulses at  $t = l/c$ ).

When successive pulse trains come with their interval  $2l/c$ , the subsequent pulse (the solid pulse at  $2l/c$ ) compensates the prior signal (the dashed pulse) created by the predecessor pulse as in the figure at  $t = 2l/c$ . Finally, all beam-induced signals with the frequency:  $f_n$  cannot be detected at all outside the chamber.

## THE IDEAL ELECTRODE SHAPE

To avoid the demerit of the rectangular electrode, no pair of image currents should be generated by the leaving pulse. It is enabled by narrowing the electrode toward downstream and carefully reclining the electrode to the chamber, to preserve the characteristic impedance  $Z_c$  of the electrode.

In 1970's Linnecar suggested an exponential electrode for better frequency characteristic [2]. When the coupling function  $k(z)$  is given by

$$k(z) = k_0 e^{-\frac{az}{l}}, \quad (3)$$

the transfer function  $F(\omega)$  is calculated as

$$F(\omega) = k_0 \frac{i\omega l (1 - e^{-a - i\frac{2\omega l}{c}})}{c(a + \frac{i2\omega l}{c})}, \quad (4)$$

where  $a$  is a positive dimensionless parameter defining the degree of the exponential tapering of the electrode. The blue line in the left figure of Fig.2 shows the transfer functions for the Linnecar's exponential electrode with  $a = 2.63$  and  $l = 190$  mm. We can find that the notches appearing in the red line (rectangle electrode) diminish in the blue line, while Linnecar's exponential electrode theoretically keeps oscillating at high frequency as

$$F(\omega) \sim \frac{k_0}{2} (1 - e^{-a - i\frac{2\omega l}{c}}). \quad (5)$$

As Eq.(1) shows, the transfer function  $F(\omega)$  can be interpreted as the Fourier transform of the step function, which

## BEAM COMMISSIONING OF C-ADS LINAC INSTRUMENTATION\*

Y.F. Sui<sup>#</sup>, J.S. Cao, H.Z. Ma, L.D. Yu, Y. Zhao, J. He, X.Y. Zhao, S.J. Wei, Q. Ye, J.H. Yue, L. Wang  
 Key Laboratory of Particle Acceleration Physics and Technology, IHEP, Chinese Academy of Sciences,  
 Beijing, 100049, China

### Abstract

The China Accelerator Driven Subcritical system (C-ADS) linac, which is composed of an ECR ion source, a low energy beam transport line (LEBT), a radio frequency quadrupole accelerator (RFQ), a medium energy beam transport line (MEBT) and cryomodules with SRF cavities to boost the energy up to 10 MeV. The injector linac will be equipped with beam diagnostics to measure the beam position, the transverse profile and emittance, the beam phase as well as beam current and beam losses. Though many are conventional design, they can provide efficient operation of drive linac. This paper gives an overview and detail in beam commissioning of C-ADS linac beam instrumentation.

### INTRODUCTION

The Chinese ADS project is aimed to solve the nuclear waste problem and the resource problem for nuclear power plants in China. With its long-term plan lasting until 2030th, the project will be carried out in 3 phases: Phase I of R&D facility, Phase II of experiment facility and Phase III of industry demonstration facility. The driver linac of the CADS consists of two injectors to

ensure its high reliability. Each of the two injectors will be a hot-spare of the other. Although the two injectors that are installed in the final tunnel will be identical, two different design schemes, named injector I and II respectively are being pursued in parallel by the Institute of High Energy of Physics (IHEP) and the Institute of Modern Physics (IMP) [1]. This paper aims to introduce the instrumentation beam commissioning of the injector I. The Injector I ion source is based on ECR technology. The beam will be extracted with an energy of 35 keV. The ion source will be followed by a Low Energy Beam Transportline (LEBT), which consists of 2 solenoids, a fast chopper system and a set of beam diagnostics including CTs and faraday cup. A Radio Frequency Quadrupole (RFQ) will accelerate the beam up to 3.2 MeV and will be followed by the first Medium Energy Beam Transport line (MEBT1), fully instrumented and also equipped. The next section is two cryogenic modules named CM1 and CM2 with seven cold beam position monitors in each, which accelerate beam up to about 10 MeV. The last section is the second Medium Energy Beam Transport line (MEBT2). The drift tubes between magnets provide the gap for diagnostics.

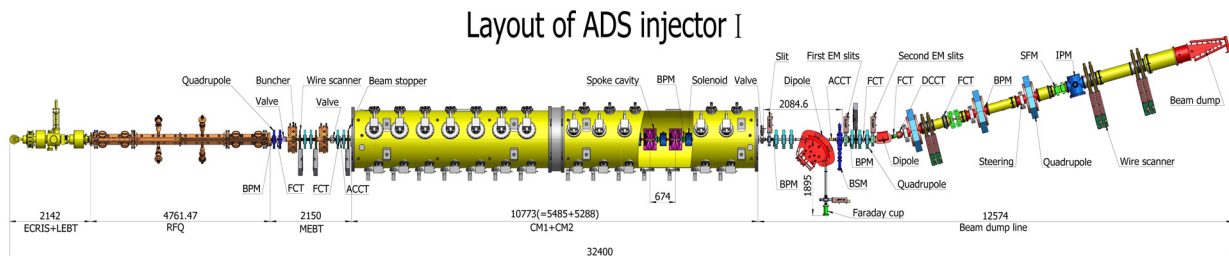


Figure 1: Beam instrumentation layout in C-ADS linac.

### INSTRUMENTATION OF INJECTOR I

The injector I linac is equipped with beam diagnostics to measure the beam position, the transverse profile, the beam emittance, the beam energy as well as beam current and beam losses. This will provide efficient operation of drive linac and ensure the beam loss at a low level. A list of the different type of monitors using in the injector I linac is presented in Table 1.

According to the geometry of pick-ups, three type of BPMs are hired to measure the beam position in the injector I linac. There are 25 BPMs of which 14 is cold BPM installed in two cryostats. Measurement of the particle beam position of CADS injector I proton linac is an essential part of beam diagnostics. The BPMs could

provide information about both the center of mass position and the beam phase that can be used to detect energy on line by using the time-of-flight (TOF) method [2]. The sum signal of BPM could be used for beam loss measurement which can be detected by a Differential Beam Current Monitor (DBCM) measuring beam current difference at two locations along the accelerator, especially for the beam energy is lower than 10MeV [3].

For the beam profile monitor in injector I, four wire scanners using solid material as a probe inside the beam to sample the charge at different location is installed in MEBT1 and the start of MEBT2. Three pairs of wire scanner is installed downstream of the first SFM (step-like field magnet). For the beam profile is expanded quickly, one wire scanner can only measure one direction beam dimension. Although the double slits is for emittance

\*Work supported by China ADS Project (XDA03020000) and the National Natural Science Foundation of China (NO. 11205172, NO. 11475204)  
<sup>#</sup>syf@ihep.ac.cn

# MEASUREMENTS OF BEAM PULSE INDUCED MECHANICAL STRAIN INSIDE THE SNS\* TARGET MODULE

W. Blokland<sup>†</sup>, M. Dayton, Y. Liu, B. Riemer, M. Wendel, D. Winder, Oak Ridge National Laboratory, Oak Ridge, USA

## Abstract

Because several of the SNS targets have had a shorter lifetime than desired, a new target has been instrumented with strain sensors to further our understanding of the proton beam's mechanical impact. The high radiation and electrically noisy environment led us to pick multi-mode fiber optical strain sensors over other types of strain sensors. Special care was taken to minimize the impact of the sensors on the target's lifetime. We also placed accelerometers outside the target to try correlating the outside measurements with the internal measurements. Remote manipulators performed the final part of the installation, as even residual radiation is too high for humans to come close to the target's final location. The initial set of optical sensors on the first instrumented target lasted just long enough to give us measurements from different proton beam intensities. A second set of more rad-hard sensors, installed in the following target, lasted much longer, to give us considerably more data. We are developing our own rad-hard, single-mode fiber optic sensors. This paper describes the design, installation, data-acquisition system, the results of the strain sensors, and future plans.

## INTRODUCTION

The Spallation Neutron Source uses neutron scattering to study the structure and properties of materials and macromolecular and biological systems. Proton beam pulses of less than 1  $\mu$ s long, up to 24  $\mu$ C, hit a stainless steel vessel filled with mercury at 60 Hz for a total power of up to 1.4 MW to generate the neutrons. The beam creates an initial pressure field of up to  $\sim$ 34 MPa that leads to tension and cavitation of the mercury as the pressure wave interacts with the target vessel.

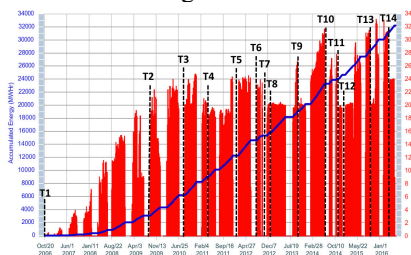


Figure 1: The SNS production runs.

The reliability of the target vessel is critical for minimizing interruptions to the operation schedule. It was initially thought that the lifetime of a target would be limited by the erosion of the target wall, due to the cavita-

\* ORNL is managed by UT-Battelle, LLC, under contract DE-AC05-00OR22725 for the U.S. Department of Energy. This research was supported by the DOE Office of Science, Basic Energy Science, Scientific User Facilities.

<sup>†</sup> blokland@ornl.gov

tion of the mercury during the proton beam impact, and by reaching the SNS administrative radiation damage limit of the vessel's steel at about 5000 MWHrs.

However, at higher proton beam powers, we did start seeing target failures before the radiation damage limit. Four out of seven premature target failures were due to weld failures from fatigue, while two were due to cavitation erosion, and one could not be determined. Figure 1 shows the quick succession of installation of targets 10, 11, and 12.

We decided to measure the strain on the actual target vessel wall to better understand the limitations to the target lifetime: Do the pulses induce a higher strain on the target than expected and does the repetition rate of the beam hit a resonance? Once we have a strain measurement system in place, we can see if certain mitigation methods are effective. In particular, we are interested in how effective injecting gas bubbles is at reducing the pressure wave. Also, we know that during operation an internal baffle erodes and a partial, non-critical, crack occurs. We hope that with a long-lasting strain sensor, we can find the point in time when this crack occurs.

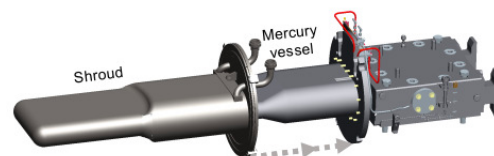


Figure 2: The target layout showing the shroud sliding over the mercury vessel.

The pulse-induced strain on liquid metal targets has been measured previously for the SNS target at LANL [1] and for displacement measurements of the J-PARC target [2], but not for the actual SNS target during beam impact. The SNS target has a double containment design, see Figure 2, and the outer shroud is structurally independent from the inner mercury vessel. Therefore, measurements on the outer surface, as done at J-PARC, will not give meaningful results. Based on the experience from the LANL experiment, we selected commercially available fiber optic strain sensors [3]. These sensors are small enough to fit in the interstitial space between the shroud and mercury vessel, have enough bandwidth (100kHz) to see the pressure wave, and do not suffer from electromagnetic noise from the beam and surrounding equipment. The optical sensors work on the Fabry-Perot interferometer principle, where one measures the phase shift of the light reflecting in the cavity as the length of the cavity changes along with the material, in our case the vessel wall, to which it is attached.

## R&D ON MICRO-LOSS MONITORS FOR HIGH INTENSITY LINACS LIKE LIPAc

J. Marroncle\*, P. Abbon, A. Marchix, CEA Saclay, DRF/DSM/IRFU, Gif sur Yvette, France  
M. Pomorski, CEA Saclay, DRT/LIST/DM2I/LCD, Gif sur Yvette, France

### Abstract

Before approaching the micro-loss monitor concept, we propose to present the high intensity Linac for which the R&D program was done, LIPAc (Linear IFMIF Prototype Accelerator). This later is the feasibility accelerator demonstrator for the International Fusion Materials Irradiation Facility (IFMIF). IFMIF aims at providing a very intense neutron source ( $10^{18}$  neutron/m<sup>2</sup>/s) to test materials for the future fusion reactors. This challenging accelerator LIPAc (1.125 MW deuteron beam) is in installation progress at Rokkasho (Japan).

Then, we will focus on the feasibility study of the beam optimization inside the SRF Linac part. Commissioning of such high beam intensity has to be done with a different approach based on detection of micro-losses, CVD diamonds, set inside the cryomodule linac. This is mandatory to keep beam losses below 1W/m for hands-on maintenance purposes.

### INTRODUCTION

This paper deals with the R&D on  $\mu$ LoM (micro-Loss Monitor) which was attempted for beam fine tuning of high intensity Linac while maintaining losses below 1W/m for maintenance hands-on purpose. Beam dynamics team working on the Linear IFMIF prototype Accelerator, LIPAc, warned about the feasibility for fulfilling this requirements with the foreseen diagnostics. Thus, they proposed to introduce the new concept of beam micro-losses and required monitors for measuring them.

After a swift introduction to LIPAc and its commissioning plans, this R&D program devoted to  $\mu$ LoM will be presented. Firstly micro-loss concept will be defined, emphasizing their importance for beam optimization. Therefore the step by step study will be investigated like, counting rate estimates and their potential background contributions, experimental neutron tests for rate validation and a proposition for signal processing before to conclude.

### IFMIF CONTEXT

The International Fusion Materials Irradiation Facility (IFMIF) [1], a project involving Japan and Europe in the framework of the "Broader Approach", aims at producing an intense flux of neutrons, in order to characterize materials envisaged for future fusion reactors. This neutron source will be a combination of two deuteron beam accelerators (125 mA – 40 MeV cw) and a liquid lithium target. Therefore, these two 5 MW accelerators impinging the Li

target will produce a huge neutron flux ( $10^{18}$  neutrons/m<sup>2</sup>/s). Downstream, dedicated cells will be implemented to test the material sample responses submitted to mechanical and thermal stresses in these very harsh conditions. Shielding structures are optimized in order to roughly reproduce the neutron energy spectrum expected in fusion reactors.

IFMIF project has to face to many challenges, thus an intermediate phase of validation was decided which consists to design and built an accelerator prototype, a 1/3-scaled Li loop target and parts of test cells.

The prototype accelerator LIPAc (Linear IFMIF Prototype Accelerator) is a 1-scaled IFMIF accelerator up to the first Superconducting Radio Frequency Linac (SRF), delivering 9 MeV deuteron beam at 125 mA cw. A high beam transport line will be installed to lead safely the beam toward a high power beam dump able to handle 1.1 MW. This accelerator is in commissioning and assembling progress at Rokkasho (Japan).

### GENERAL COMMISSIONING PLANS

LIPAc accelerator components have been mainly designed and manufactured in Europe by European Institutions (CEA Saclay, CIEMAT Madrid, INFN Legnaro and SCK-CEN) under F4E management, who is also responsible of other activities. LIPAc building was constructed by QST (National institutes for Quantum and Radiological Science and Technology), who takes also in charge the supply of conventional facilities, the control system, the protection and the timing system.

The accelerating components (Fig. 1) are the injector delivering a deuteron beam at 100 keV (A), the RFQ (175 MHz) to bunch and accelerate up to 5MeV (B) and the superconductive Linac increasing the energy up to 9 MeV (C). These components are connected through beam transport lines (LEBT, MEBT, HEBT) tuned and qualified by various diagnostic monitors [2] and the beam is absorbed into the HPBD (High Power Beam Dump) (phase D) to stop safely the 1.1 MW beam power.

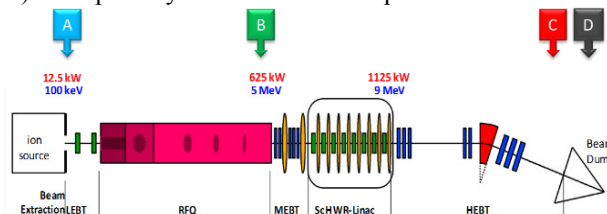


Figure 1: commission plan with the 4 phases.

\* Jacques.marroncle@cea.fr

# NEW ARRANGEMENT OF COLLIMATORS OF J-PARC MAIN RING

M. J. Shirakata<sup>†</sup>, S. Igarashi, K. Ishii, Y. Sato, and J. Takano  
 J-PARC/KEK, Tokai/Tsukuba, Ibaraki, Japan

## Abstract

The beam collimation system of J-PARC main ring has been prepared in order to localize the beam loss into the specified area, especially during the injection period. At the first time, it was constructed as a scraper-catcher system in horizontal and vertical planes which consisted of one halo-scraper and two scattered protons catchers, whose the maximum beam loss capacity was designed to be 450 W in the beam injection straight of the ring. In 2012, the scraper was replaced by two collimators with a movable L-type jaw for both planes. Two catchers remained at the same places, and they were used as collimators. This large change of design concept of main ring collimation system was required in order to increase the beam loss capacity more than 3 kW. The system worked well but unexpected loss spots still remained in the following arc and straight sections. The four-axis collimator was developed with movable jaw in horizontal, vertical directions adding tilt functions which has high cleaning efficiency. We have four four-axis collimators, two two-axis collimators, and two original catchers. The most effective arrangement of collimators was investigated in this report.

## INTRODUCTION

The Japan Proton Accelerator Research Complex (J-PARC) is a multi-purpose accelerator facility in Tokai village of Ibaraki, Japan [1]. The 3 GeV beam from the rapid cycling synchrotron (RCS) is utilized in muon and many neutron beam lines. The main ring (MR) has been providing 30 GeV beam to the neutrino and hadron experiments since early 2009. The recent beam power has achieved 416 kW for the T2K neutrino oscillation experiment, which corresponds to  $2.15 \times 10^{14}$  protons per 2.48 s cycle [2]. We have about  $2.7 \times 10^{13}$  protons per bunch. It is important to localize the beam losses for the maintenance, and to handle the beam loss amount for the machine protection. In order to localize the beam losses, MR has the beam collimation system to remove the halo component from the circulating beam.

## ORIGINAL DESIGN

The beam collimation system of J-PARC MR has been updated since 2011. The first collimation system started as a single scraper-catchers system which was an ordinary one for the ring accelerators for horizontal and vertical planes. As there are 216 quadrupole magnets in MR, the ring is addressed from address 001 to 216 by using their sequential number. We call as the insertion-A (INS-A) from QDX216 to QDX016 which corresponds to address 001 to 016. The beam collimation system was installed in

INS-A as shown in Fig.1, where QFRs and QDRs indicated the focusing and defocusing quadrupole magnets with address numbers, respectively. It consisted of one halo-scraper, catcher-1, and catcher-2 which were often called as Col-1, Col-2, and Col-3. STR means a steering magnet. The scraper was installed in address 007, catchers were installed in address 008 and 010. The designed beam loss capacity was 450 W but we prepared the 1 kW capable system to have a leeway in an actual beam operation. The original collimation system was designed for the tune  $(\nu_x, \nu_y) = (22.41, 20.80)$  which was called as a mid-tune in 2006. The actual operating point was set to  $(22.40, 20.75)$  until May 2016.

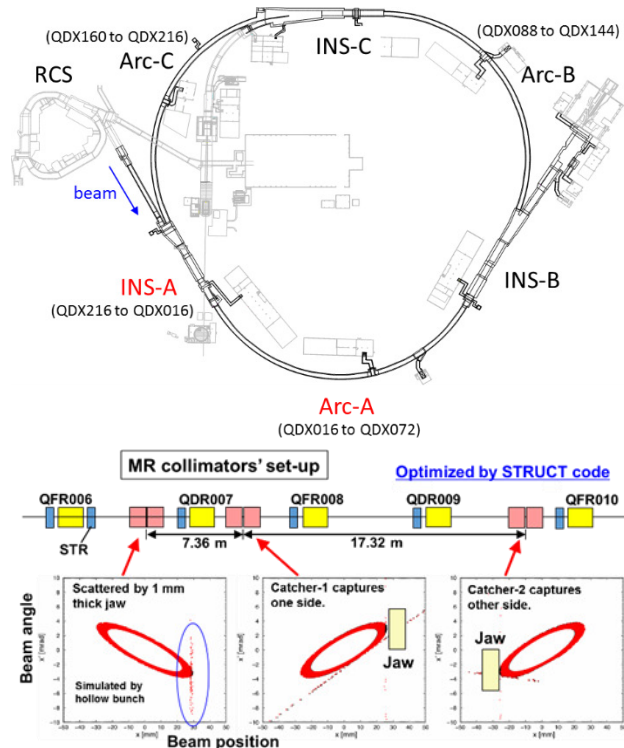


Figure 1: Schematic view of J-PARC MR and a layout of the original beam collimation system.

The scraper and catchers have a same radiation shield system. They have two cubic iron shields placed next to each other on beam line. Upstream shield can move to horizontal direction, and the other can move to vertical direction. Their movable range is  $\pm 12$  mm. Vacuum pipe which has scraper jaws or catcher jaws moves with the radiation shield. The vacuum pipe has a transverse position shift ability at the jaw positions by double bellows prepared at the middle and both ends. The beam loss distribution during the fast extraction (FX) operation in the circumference as a function of MR address number is

<sup>†</sup> masashi.shirakata@kek.jp

# PATH TO BEAM LOSS REDUCTION IN THE SNS LINAC USING MEASUREMENTS, SIMULATION AND COLLIMATION

A. Aleksandrov, A. Shishlo

Oak Ridge National Laboratory, Oak Ridge, TN 37830 USA

## Abstract

The SNS linac operation at its design average power currently is not limited by uncontrolled beam loss. However, further reduction of the beam loss remains an important aspect of the SNS linac tune up and operation. Even small “acceptable” beam loss leads to long term degradation of the accelerator equipment. The current state of model-based tuning at SNS leaves an unacceptably large residual beam loss level and has to be followed by an empirical, sometimes random, adjustment of many parameters to reduce the loss. This talk will discuss a set of coordinated efforts to develop tools for large dynamic range measurements, simulation and collimation in order to facilitate low loss linac tuning.

## INTRODUCTION

The SNS linac has demonstrated successful operation at the design average beam power of 1.4 MW with acceptable uncontrolled beam loss [1]. However, beam loss mechanisms study and mitigation methods development remains to be on top of the accelerator physics and beam instrumentation tasks list for the following reasons:

- The “acceptable” uncontrolled beam loss is typically defined by the possibility of hands-on maintenance on the accelerator equipment, which corresponds to a dose rate of <100 mRem/hour at 30 cm from the beam pipe, a few hours after beam shutdown. The actual residual activation of the SNS linac is typically lower than that but the long term damaging effect to the equipment in the tunnel from the prompt radiation is important as well. The observed slow degradation of the plastic cable insulation and water hose materials is certainly due to irradiation. Degradation of the superconducting cavities performance is observed as well and in many cases can be correlated to elevated beam loss in the vicinity. Further beam loss reduction is certainly beneficial for long term stable operation.
- The last step in the process of low-loss linac set up involves manual tweaking of many parameters. This step is poorly documented and can be done by only few experienced people. It can be time consuming in case of a significant change of the linac configuration. A knowledge based set up procedure is highly desirable
- The SNS power upgrade and the Second Target Station plans envision doubling the average beam power and adding another beam pulse flavor. This will require cutting the fractional beam loss at least

by half to keep the prompt radiation and activation levels on the same level.

- Model-based methods of beam loss control are crucial for future high power linacs. The SNS linac is an ideal test bench for beam instrumentation and loss mitigation methods development.

Reduction of the beam loss in the SNS Super Conducting Linac (SCL) using knowledge of beam dynamics rather than blind tweaking is our first goal. This paper describes the tools and methods we think will be required to achieve this goal.

## BEAM LOSS IN SCL

The main mechanism of beam loss in SCL is believed to be the intra-bunch stripping [2]. The rate of loss is proportional to the bunch density therefore increasing the transverse and longitudinal bunch core sizes is an effective way of beam loss reduction. A low loss SCL optics configuration with enlarged bunch size was found empirically and is still in use for high power operation. Only recently a reliable model of RMS beam dynamics in SCL was established [3], which shows not perfectly RMS matched beam for the current optics. The mismatch causes the beam size maximum and minimum to deviate from the average. The increased bunch size maximum prevents further enlargement of the average size; the decreased bunch minimum size creates local bunch density peaks with larger loss rate. We expect to reduce the intra-beam stripping losses using the model to find a better matched optics. However, any further attempt to increase the average RMS bunch size will be limited by the beam halo touching the beam pipe. The current ratio of the beam pipe aperture to the maximum loss limited transverse bunch size is about  $76\text{mm}/7\text{mm} \approx 11$ , indicating presence of a significant halo. As a result, having an accurate control of the RMS bunch size is not enough for decreasing the intra-beam stripping - the halo also needs to be controlled.

The exact origin of the halo is not known but we can tell for sure that at least part of it comes from the injector. The easiest method of reducing this part is collimation (or scraping) of the large amplitude particles in the MEBT (a 2.5MeV transport line between the RFQ and the linac).

It is also possible the halo is formed during acceleration in the warm linac due to effect of the space charge. Matching the bunch RMS Twiss parameters to the lattice is believed to mitigate this effect. If the perfect match is not possible or the halo is formed even in the RMS matched beam then the minimum loss is achieved as a compromise between matching the RMS parameters to

# SIMULATIONS AND DETECTOR TECHNOLOGIES FOR THE BEAM LOSS MONITORING SYSTEM AT THE ESS LINAC

I. Dolenc Kittelmann\*, T. Shea, ESS, Lund, Sweden

## Abstract

The European Spallation Source (ESS), which is currently under construction, will be a neutron source based on 5 MW, 2 GeV superconducting proton linac. Among other beam instrumentation systems, this high intensity linac requires a Beam Loss Monitoring (BLM) system. An important function of the BLM system is to protect the linac from beam-induced damage by detecting unacceptably high beam loss and promptly inhibiting beam production. In addition to protection functionality, the system is expected to provide the means to monitor the beam losses during all modes of operation with the aim to avoid excessive machine activation. This paper focuses on the plans and recent results of the beam loss studies based on Monte Carlo (MC) simulations in order to refine the ESS BLM detector requirements by providing the estimations on expected particle fluxes and their spectra at detector locations. Furthermore, the planned detector technologies for the ESS BLM system will be presented.

## INTRODUCTION

The ESS is a material science facility, which is currently being built in Lund, Sweden and will provide neutron beams for neutron-based research [1]. The neutron production will be based on bombardment of a tungsten target with a proton beam of 5 MW average power. A linear accelerator (linac) [2] will be used to accelerate protons up to 2 GeV and transport them towards the target through a sequence of a normal conducting (NC) and superconducting (SC) accelerating structures (Fig. 1).

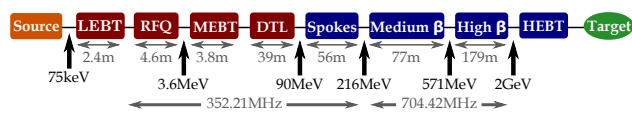


Figure 1: The ESS linac layout. Red color represents the NC and blue the SC parts of the linac.

Rapid startup and reliable operation of the linac requires a certain suite of beam instrumentation. As part of this suite, the BLM system will detect high beam losses potentially harmful to the linac components and inhibit beam production before damage occurs. Additionally, the system provides information about the particle rates during all linac modes of operation in order to enable tuning and keep the machine activation low enough for hands-on maintenance.

## ESS BLM DETECTOR TECHNOLOGIES

The ESS BLM system will employ 3 types of detectors. In the SC parts of the ESS linac, parallel plate gas ionization

chambers (ICs) developed for the LHC BLM system [3] will be used (Ionization Chamber based BLM – ICBLM). These were chosen due to their availability as part of a joint procurement with CERN and other facilities. Background due the RF cavities must be taken into account when using ICs in a linac. This background is mainly due to the electron field emission from cavity walls resulting in bremsstrahlung photons created on the cavity or beam pipe materials [4]. The background levels are difficult to predict numerically as they depend on the quality of the cavities, beam loading, operation conditions and time. It is planned to asses this experimentally at the ESS RF test stand in Uppsala with the spoke cavities and at the CEA Saclay with the elliptical cavities. Nevertheless, simplified energy spectra estimations show that photons with energies up to tens of MeV can be expected [5]. With a characteristic cut-off value for the photons of ~2 MeV for the LHC ICs [3], background sampling and subtraction is needed for the ICBLM system. In addition to the primary IC-based system, some Cherenkov radiation detectors may also be deployed. These offer inherent rejection of the RF cavity background.

BLM detectors are planned also in the MEBT and DTL sections of the NC ESS linac. Here the particle fields outside the tanks and beam pipe are expected to be dominated by the neutrons and photons. With RF cavity background still a possible source of photons in these sections, a neutron sensitive detector should be considered. Special micromegas detectors are in development [6] by the micromegas team from the CEA Saclay, designed to be sensitive to fast neutrons, but not to thermal neutrons, X-rays or  $\gamma$ -rays.

## ESS BLM SIMULATIONS

MC simulations for tracking of the lost protons are needed in order to address several points crucial for the design of a BLM system, namely: system response time limit, detector locations and dynamic range of the system. In addition to this, they provide a tool for determination of the initial machine protection threshold settings used during the startup period. Furthermore, the MC simulations serve to estimate the anticipated response of the system during the fault studies that will verify the BLM system response. The focus of this chapter are the aforementioned first three simulation tasks, while the last two are not discussed here.

Most of the results presented here are focused on the NC linac, and will provide a basis for the nBLM specifications. The anticipated neutron and photons spectra at the detector locations are required to finalize the micromegas detector design. Previous efforts focused primarily on the SC linac; thus some preliminary results valid for the ICBLM already exist.

\* irena.dolenckittelmann@esss.se

# DESIGN AND BEAM DYNAMICS STUDIES OF A MULTI-ION LINAC INJECTOR FOR THE JLEIC ION COMPLEX\*

P.N. Ostroumov<sup>#</sup>, A.S. Plastun, B. Mustapha and Z.A. Conway  
ANL, Argonne, IL 60439, U.S.A

## Abstract

The electron-ion collider (JLEIC) being proposed at JLab requires a new ion accelerator complex which includes a linac capable of delivering any ion beam from hydrogen to lead to the booster. We are currently developing a linac which consists of several ion sources, a normal conducting (NC) front end, up to 5 MeV/u, and a SC section for energies > 5 MeV/u. This design work is focused on the beam dynamics and electrodynamics studies performed to design efficient and cost-effective accelerating structures for both the NC and SC sections of the linac. Currently, we are considering two separate RFQs for the heavy-ion and light-ion beams including polarized beams, and different types of NC accelerating structures downstream of the RFQ. Quarter-wave and half-wave resonators can be effectively used in the SC section.

## INTRODUCTION

Recently, we have proposed a pulsed multi-ion linac with a normal conducting (NC) front-end up to 5 MeV/u and a superconducting (SC) section for higher energies as an injector for the JLab electron-ion collider (JLEIC) [1]. Separate radio-frequency quadrupole (RFQ) sections for heavy ( $A/Z \leq 7$ ) and light ( $A/Z \leq 2$ ) ions (polarized or non-polarized) and high-performance superconducting quarter-wave and half-wave coaxial resonators make the injector linac capable of effectively accelerating any ion species from hydrogen (up to 135 MeV) to lead (up to 44 MeV/u). This linac can be used for other purposes during the idle time of the booster ring; for example, isotope production.

## LINAC LAYOUT

A block-diagram of the injector linac is shown in Figure 1 and the basic design parameters are listed in Table 1. The JLEIC ion linac will use both heavy and light ion sources including polarized  $H^+$ ,  $^2H^+$ ,  $^3He^{2+}$ ,  $^7Li^{3+}$  ion sources. The emittance of polarized beams is usually larger than the emittance of heavy-ion beams. For this reason, we propose to build two separate RFQs.

### RFQ

Both RFQs operate at 100 MHz and accelerate ions up to 500 keV/u. Both of them produce low longitudinal

emittance while the light-ion RFQ has larger transverse acceptance which is required for polarized light-ion beams.

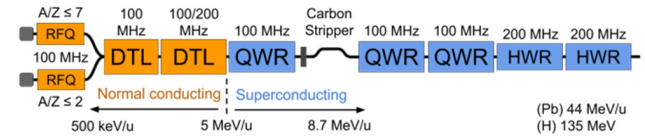


Figure 1: A schematic drawing of the JLEIC ion linac.

Table 1: Main Parameters of the Linac

| Parameter                             | Value       | Units |
|---------------------------------------|-------------|-------|
| Ion species                           | $H^+$ to Pb |       |
| Fundamental frequency                 | 100         | MHz   |
| Kinetic energy of protons & lead ions | 135&44      | MeV/u |
| Maximum pulse current                 |             |       |
| Light ions ( $A/q \leq 2$ )           | 2           | mA    |
| Heavy ions ( $A/q > 2$ )              | 0.5         | mA    |
| Pulse repetition rate                 | up to 10    | Hz    |
| Pulse length                          |             |       |
| Light ions ( $A/q \leq 2$ )           | 0.5         | ms    |
| Heavy ions ( $A/q > 2$ )              | 0.25        | ms    |
| Maximum pulsed beam power             | 260         | kW    |
| # of QWR cryomodules                  | 3           |       |
| # of HWR cryomodules                  | 2           |       |
| Total length                          | ~55         | m     |

A higher injection energy into the light-ion RFQ allows us to mitigate beam space charge effects. Parameters of the RFQs are presented in Table 2. There are several possible electromagnetic and mechanical designs for the RFQ resonator such as a four-rod structure, a compact 4-vane RFQ resonator with magnetic coupling windows [2, 3] and the so-called “4-ladder” structure [4].

### DTL

The drift tube accelerating section (DTL) is conceived to accelerate any ion species up to 5 MeV/u for injection into the superconducting part of the linac. We are considering either IH-DTL with triplet focusing [5, 6] or a spatially-periodic radio-frequency quadrupole focusing structure (see Figure 2) [7]. Both accelerating structures are highly efficient in this energy range, especially in pulsed

\*This work was supported by the U.S. Department of Energy, Office of Nuclear Physics, under Contract DE-AC02-06CH11357. This research used resources of ANL’s ATLAS facility, which is a DOE Office of Science User Facility.

<sup>#</sup>ostroumov@anl.gov

# A NEW RFQ MODEL AND SYMPLECTIC MULTI-PARTICLE TRACKING IN THE IMPACT CODE SUITE\*

J. Qiang<sup>†</sup>, Lawrence Berkeley National Laboratory, Berkeley, USA  
Z. Wang, H. P. Li, Peking University, Beijing, China

## Abstract

The IMPACT code suite is a self-consistent parallel three-dimensional beam dynamics simulation toolbox that combines the magnetic optics method and the parallel particle-in-cell method. It has been widely used to study high intensity/high brightness beams in many accelerators. In this paper, we will report on recent improvements to the code such as the capability to model RFQ in time domain and symplectic multi-particle tracking with a gridless spectral solver for space-charge simulation.

## INTRODUCTION

The IMPACT code suite is a parallel three-dimensional multi-particle tracking code to simulate charged particle beam dynamics in high intensity/high brightness accelerators. It includes a time-dependent code, IMPACT-T [1] and a longitudinal position dependent code, IMPACT [2]. Both codes use a particle-in-cell (PIC) method to self-consistently model the space-charge effects in the simulation. It has been used to model high intensity proton/ion linac, high brightness photoinjector, electron linac, proton synchrotron and other accelerators.

## A NEW RFQ MODEL

The popular RFQ design code Parmteqm uses position as an independent variable and has a two-dimensional space-charge solver [3]. These approximations might introduce significant errors at lower energy for high intensity proton/ion beams. A new RFQ model is added into the IMPACT-T code with a three-dimensional space-charge solver including space charge effects within the bunch and the effects from neighboring bunches. In the RFQ model, eight term expression was implemented to account for the external accelerating/focusing effects. All coefficients can be obtained from the Parmteqm output file PARIOUT.OUT. Normally, an RFQ consists of different types of cells including radial matching section (RMS) cells, normal cells, and transition cells (including  $m = 1$  cell and fringe cell). Inside the normal cells, the potential expression is given by

$$U(r, \theta, z) = \frac{V}{2} \{ A_{01} \left(\frac{r}{r_0}\right)^2 \cos(2\theta) + A_{03} \left(\frac{r}{r_0}\right)^6 \cos(6\theta) \\ + [A_{10} I_0(kr) + A_{12} I_4(kr) \cos(4\theta)] \cos(kz) \\ + [A_{21} I_2(2kr) \cos(2\theta) + A_{23} I_6(2kr) \cos(6\theta)] \cos(2kz) \\ + [A_{30} I_0(3kr) + A_{32} I_4(3kr) \cos(4\theta)] \cos(3kz) \} \quad (1)$$

\* Work supported by the U.S. Department of Energy under Contract No. DE-AC02-05CH11231.

<sup>†</sup> jqiang@lbl.gov

In the above equation,  $0 \leq z \leq L$ , where  $L$  is the length of a cell. In the sine and cosine terms,  $k = \pi/L$ ; in the modified Bessel function  $I_{2m}(nkr)$  terms,  $k$  varies linearly over the cell. In the fringe cell and the RMS cells, the potential expression is given by

$$U(r, \theta, z) = \frac{V}{2} \frac{6A_{01}}{k^2 r_0^2} (I_2(kr) \cos(kz) + \frac{1}{27} I_2(3kr) \cos(3kz)) \cos(2\theta) \quad (2)$$

where  $k = \pi/(2L)$ ,  $L$  is length of transition cell. In the transition cell, the potential expression is given by

$$U(r, \theta, z) = \frac{V}{2} \left[ \left(\frac{r}{r_0}\right)^2 \cos(2\theta) - A_{10} I_0(kr) \cos(kz) - A_{30} I_0(3kr) \cos(3kz) \right] \quad (3)$$

where  $k = \pi/(2L)$ ,  $L$  is the length of the transition cell. In all of these expressions, the  $A_{01}, \dots, A_{32}$  coefficients values can be calculated by linear interpolation at each  $z$  (defining  $z = 0$  at the interface).

As an illustration of this new model, we simulated a charged proton beam with 5 mA current at 2.1 MeV transporting through an RFQ designed for the PIP-II project. The final beam phase distributions at the RFQ exit from the IMPACT-T simulation, from the Toutatis [4] simulation, and from the ParmteqM simulation are shown in Fig. 1. It is seen that the IMPACT-T results agree with the Toutatis and the Parmteqm simulation results quite well.

## SYMPLECTIC MULTI-PARTICLE TRACKING WITH A GRIDLESS SPECTRAL METHOD

In the accelerator beam dynamics simulation, for a multi-particle system with  $N_p$  charged particles subject to both space-charge self fields and external fields, the approximate Hamiltonian of the system can be written as:

$$H = \sum_i \mathbf{p}_i^2/2 + \frac{1}{2} \sum_i \sum_{j, j \neq i} q\phi(\mathbf{r}_i, \mathbf{r}_j) + \sum_i q\psi(\mathbf{r}_i) \quad (4)$$

where  $H(\mathbf{r}_1, \mathbf{r}_2, \dots, \mathbf{p}_1, \mathbf{p}_2, \dots, s)$  denotes the Hamiltonian of the system,  $\phi$  is the space-charge Coulomb interaction potential among the charged particles (with appropriate boundary conditions),  $\psi$  denotes the potential associated with the external fields.  $\mathbf{r}_i$  denotes the canonical spatial coordinates of particle  $i$ , and  $\mathbf{p}_i$  the normalized canonical momentum coordinates of the particle  $i$ . The equations governing the motion of individual particle  $i$  follows the Hamilton's equa-

# BEAM ENERGY LOSS IN A BETA=0.09 SRF HWR CAVITY FOR 100 mA PROTON ACCELERATION\*

F. Zhu<sup>#</sup>, H.T.X. Zhong, S.W. Quan, F. Wang, K.X. Liu

Institute of Heavy Ion Physics & State Key Laboratory of Nuclear Physics and Technology,  
Peking University, Beijing, 100871, China

## Abstract

There's presently a growing demand for cw high current proton and deuteron linear accelerators based on superconducting technology to better support various fields of science. Up to now, high order modes (HOMs) studies induced by ion beams with current higher than 10mA and even 100 mA accelerated by low  $\beta$  non-elliptical Superconducting rf (SRF) cavities are very few. One of the main HOM related issues of the SRF linac is the HOM-induced power. HOM power is the important part of beam energy loss which is used to estimate the cryogenic losses. In this paper, we compare the beam energy loss induced by 100 mA beam passing through a  $\beta=0.09$  HWR SRF cavity calculated from time domain solver and frequency domain cavity eigenmodes spectrum method.

## INTRODUCTION

Compared to normal conducting accelerator, rf Superconducting accelerator has more advantages and the potential to accelerate super high current (for example 100 mA) cw ion beam. The beam pipes can be larger and the operation cost could be much less. Such high current SRF cavities have been adopted by some future facilities. For example, IFMIF has two 125 mA deuteron accelerators [1] and BISOL [2] recently proposed a 50 mA deuteron accelerator as a driver. Peking University (PKU) is developing a  $\beta = 0.09$  HWR SRF prototype cavity for BISOL deuteron acceleration or for 100 mA proton beam acceleration.

Compared to elliptical SRF cavities, quarter wave resonators (QWRs) or half wave resonators (HWRs) have much sparse high order modes. The modes are a little far from the accelerating mode and not easily activated. Normally the effect of the HOMs of QWRs or HWRs can be neglected and the studies of HOMs of HWRs are very few. But for 100 mA beam, whether the beam energy loss induced by the HOMs can be negligible or not still needs study.

All modes contribute to the additional cryogenic load. Cavity loss factor calculation is very important for the total cryo-losses estimation for the SRF cavities. In this paper, we will describe our efforts to characterize the beam-induced power in the  $\beta=0.09$  HWR cavity for 100 mA beam acceleration, and present the results of calculations made by two independent methods (in time domain and frequency domain) so as to achieve reliable results.

\*Work supported by National Basic Research Project  
(No. 2014CB845504)

<sup>#</sup>zhufeng7726@pku.edu.cn

## TIME DOMAIN ANALYSIS

The power deposited by the beam consisting of bunches following through the cavity with the bunch repetition rate  $f_{\text{rep}}$  is

$$P = k_{//} I q = k_{//} q^2 f_{\text{rep}} = k_{//} I^2 / f_{\text{rep}} \quad (1)$$

Where  $I = q f_{\text{rep}}$  is the average beam current,  $q$  is the bunch charge, and  $k_{//}$  is the beam energy loss factor.

The time domain calculation of beam energy loss factors is very common and well developed for elliptical cavities and for relativistic beams. Code ABCI can calculate the loss factor of symmetric structure and for relativistic beams [3]. CST can calculate the loss factor of 3D structure, but normally also for relativistic beams. When simulating non-relativistic beams passing through a cavity, one needs to take into account the static Coulomb forces. CST Studio direct wake field solver was used to calculate wake potentials. The total wake potential includes both static (Coulomb forces) and dynamic (beam-cavity interaction) parts. Because static component is not perfectly symmetrical to the bunch centre, the convolution of the bunch profile with the wake potential gives the wrong result for the loss factor. The remedy is to run two consecutive simulations with slightly different pipe lengths, and then the static components of the wake potential will change proportionally to the length while the dynamic part remains the same [4]. Thus, from these two solutions it is possible to subtract the static part and find the wake potential caused by beam-cavity interactions only. We used this method to calculate the wake potentials and further the loss factor for the high current taper type  $\beta=0.09$  HWR cavity [5]. The structure geometry is illustrated in Figure 1.

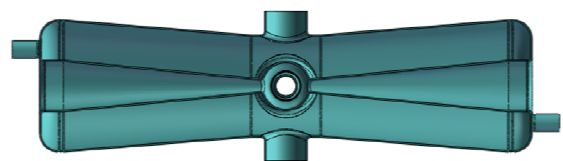


Figure 1: The 162.5 MHz, high current  $\beta=0.09$  HWR cavity designed by Peking University.

Frequencies of HOMs excited by a non-relativistic beam bunch, passing through an SRF structure, depend on the characteristic size of the EM field distribution on the wall of the beam pipe at the cavity entrance, which is of the order of the beam pipe radius [6]. The beam pipe radius of the HWR cavity is 40 mm, frequencies below 7.5 GHz are present in the bunch field spectrum. It means

# AN ADVANCED PROCEDURE FOR LONGITUDINAL BEAM MATCHING FOR SC CW HEAVY ION LINAC WITH VARIABLE OUTPUT ENERGY

Stepan Yaramyshev<sup>1\*</sup>, Kurt Aulenbacher<sup>2,3</sup>, Winfried Barth<sup>1,2</sup>, Viktor Gettmann<sup>1,2</sup>,  
 Manuel Heilmann<sup>1,4</sup>, Sascha Mickat<sup>1,2</sup>, Maksym Miski-Oglu<sup>1,2</sup>

<sup>1</sup>GSI Helmholtzzentrum für Schwerionenforschung, Darmstadt, Germany

<sup>2</sup>HIM, Helmholtz Institute Mainz, Germany

<sup>3</sup>IKP, Johannes Gutenberg-University Mainz, Germany

<sup>4</sup>IAP, Goethe-University Frankfurt am Main, Germany

## Abstract

A multi-stage program for the development of a heavy ion superconducting (SC) continuous wave (CW) linac is in progress at HIM (Mainz, Germany), GSI (Darmstadt, Germany) and IAP (Frankfurt, Germany). The main beam acceleration is provided by up to nine multi-gap CH cavities. Due to variable beam energy, which could be provided by each cavity separate, a longitudinal beam matching to each cavity is extremely important. The linac should provide the beam for physics experiments, smoothly varying the output particle energy from 3.5 to 7.3 MeV/u, simultaneously keeping high beam quality. A dedicated algorithm for such a complicate matching, providing for the optimum machine settings (voltage and RF phase for each cavity), has been developed. The description of method and the obtained results are discussed in this paper.

## INTRODUCTION

The High Charge State Injector (HLI) in combination with the Universal Linear Accelerator (UNILAC) serves as a powerful high duty factor (up to 25%) accelerator, providing heavy ion beams for the experiment program at GSI [1,2]. Operation of the new GSI Facility for Antiproton and Ion Research at Darmstadt (FAIR) foresees the UNILAC as a heavy ion high intensity injector for the synchrotron SIS18. Therefore beam time availability for Super-Heavy Elements research (SHE) is decreased [3]. To keep the SHE program at GSI on a high competitive level, the development of a heavy ion superconducting (SC) continuous wave (CW) linac is in progress (Fig. 1). Such a machine will provide for significantly higher beam intensities and an increased rate of SHE production [4].

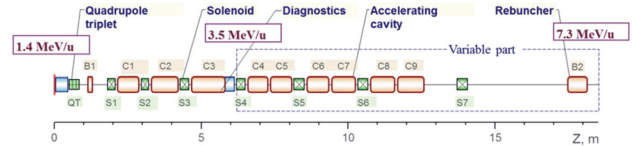


Figure 1: The conceptual layout for SC part of the CW linac at GSI.

## SC CW DEMONSTRATOR

The multi-cavity advanced SC Demonstrator is recently under construction at GSI [5-7]. The existing HLI serves as injector and provides heavy ion beams with an energy of 1.4 MeV/u, delivered with a dedicated transport line to the demonstrator cave (Fig. 2).

Besides the room temperature focusing magnetic quadrupoles (triplet and 2 doublets), the setup comprises two rebuncher cavities, beam diagnostics and cold-warm junction of the cryostat. Adequately chosen gradients of the quadrupole lenses make the input beam at the Demonstrator entrance axially symmetric in 4D transverse phase plane for easier further focusing by the solenoids. The rebuncher cavities, operated at 108 MHz, provide for the required longitudinal matching. Therefore the beam 6D matching to the demonstrator is accomplished [8].

The commissioning of the CW-Demonstrator, consisting of two superconducting solenoids and the superconducting CH-cavity, has already started in 2016 [9].

After successful testing of the first cryostat, the construction of an extended cryomodule, which is foreseen to comprise two shorter CH cavities is planned to be tested until end of 2017. Two identical short CH cavities are already ordered; delivery to GSI is expected until summer 2017. The schematic layout of the machine is shown on Fig. 3.

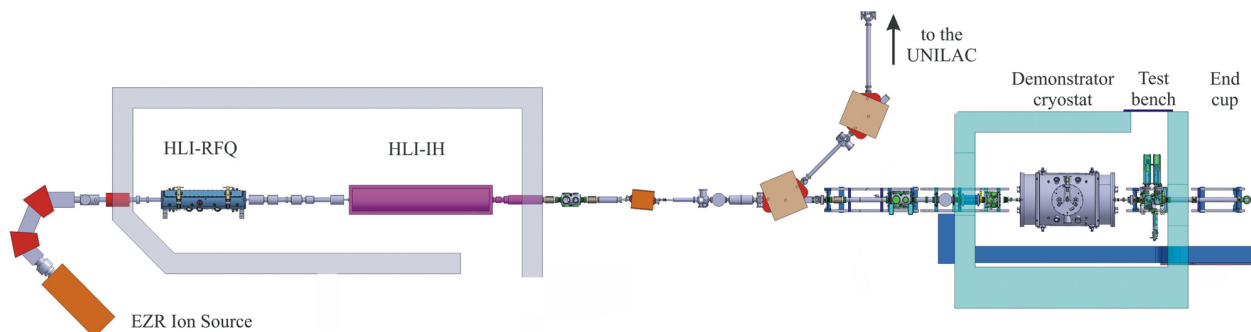


Figure 2: Recent schematic layout of the SC Demonstrator at GSI.

\* S.Yaramyshev@gsi.de

## SUMMARY OF WORKING GROUP A

Wolfram Fischer, BNL, Upton, NY, USA  
 Giuliano Franchetti, GSI, Darmstadt, Germany  
 Yong Ho Chin, KEK, Ibaraki, Japan

The working group A, Beam Dynamics in Rings, was structured with the following 6 sections:

- 1) Collective effects (4 talks),
- 2) Space charge - beam-beam (4 talks);
- 3) Code development and benchmarking (4 talks);
- 4) New machines / New Concepts (4 talks);
- 5) Theory (4 talks);
- 6) Emerging talents (6 talks).

A few highlight are given below.

### COLLECTIVE EFFECTS

**Elias Metral, CERN** has presented a status of the collective effect at CERN [1]. The talk concluded that in a machine like LHC, not all the effect can be understood separately. Instead all the possible interplay between the several phenomena need to be analyzed in detail, these effects should include: beam-coupling impedance (collimators, crab cavities); linear and nonlinear chromaticity; Landau octupoles; transverse damper; space charge; beam-beam; electron cloud; linear coupling; tune separation between transverse planes; tune split between the two beams; transverse beam separation between the two beams; noise effects.

**Giovanni Rumolo, CERN** reviewed the state of the art of the electron cloud effects in the LHC and SPS [2]. The comprehensive talk showed that because of intensive measurements and new simulation tools, a deeper knowledge of the electron cloud in the different CERN accelerators has been reached. For the present 25 ns beam parameters PS and SPS can deliver the required beams within the original specifications. The LHC still suffers from electron clouds. Scrubbing mitigates the electron cloud, and allows for LHC operation, but it is not known up to which point one can rely on scrubbing. Future parameter studies include: in PS e-cloud instabilities should be prevented by transverse feedback system; SPS relies on scrubbing, and relevant chambers will be a-C coated; the HL-LHC will also require studies on scrubbing.

### SPACE CHARGE – BEAM-BEAM

**Hannes Bartosik, CERN** has presented a study of the beam loss in LEIR for high intensity bunched beams [3]. The intensity limitation at LEIR are found experimentally to happen during and after the RF capture. It has been identified that the mechanism driving the beam loss is the interplay of space tune-spread with betatron resonances. It is also found that the vertical emittance is enlarged after RF capture. The mitigation of the beam loss happens by reducing the bunching factor and thereby the space charge

tune-spread, and by reducing the excitation of chromatic sextupoles (resonance reduction). These steps have provided a significant reduction of beam loss in LEIR. Plans to further increase the intensity aim at increasing the repetition rate to 10 Hz, the development of a new optics that reduces the strength of low order resonances.

**Shinji Machida, STFC** presented a study on the effect of space charge on the multi-turn extraction scheme presently running at CERN [4]. The study is motivated by the experimental studies reported in [5, 6], where it appears that the fixed-points in the four islands drift outwards in the phase space when the beam intensity is increased. Simulation studies tracking beam in free space have highlighted that the effect of space charge on the fixed-points is reverted (they move inward in phase space when increasing the beam intensity). The study shows that the effect of the image charge created by the pipe plays the crucial role for unraveling the reverted pattern of the fixed-points. The talk has presented the slope of the fixed-point/intensity for each beam-let when the boundary is included.

### CODE DEVELOPMENT AND BENCHMARKING

**Frank Schmidt, CERN** has presented a code-code benchmarking based on previous HB work [7]. For several codes that implement frozen or PIC space charge algorithm, a comparison of emittance growth over  $10^5$  turns is made. The physics case is the periodic crossing of one SIS18 resonance. The result of the benchmarking showed that the codes MICROMAP, SIMSONS, MADX and SYNERGIA agree well especially considering the differences in space charge calculation methods, and lattice modeling. In the talk it was shown that code-experiment benchmarking has been performed using the PS experiment data showing a good agreement also for a storage time of half million turns.

**Oliver Boine-Frankenheim, GSI** has presented a new development in PIC solvers [8]. The issue of simplicity in particle tracking, which uses PIC is of relevance for long term tracking. In fact, artificial emittance growth is the result of un-physical modeling of the beam dynamics. The talk has presented a review of the methods for avoiding grid heating and artificial noise. A test example using a spectral solver has shown that artificial emittance growth due to grid heating can be avoided. This removes artificial emittance growth at the expenses of heavier computational load. Also Ji Qiang [9] has discussed in WGB a similar integration scheme.